NATIONAL AERONAUTICS AND SPACE ADMINISTRATION

Technical Memorandum 33-452

Volume I

Deep Space Network Support of the Manned Space Flight Network for Apollo

1962–1968

F. M. Flanagan
P. S. Goodwin
N. A. Renzetti

JET PROPULSION LABORATORY
CALIFORNIA INSTITUTE OF TECHNOLOGY
PASADENA, CALIFORNIA

July 15, 1970

NATIONAL AERONAUTICS AND SPACE ADMINISTRATION

Technical Memorandum 33-452

Volume I

Deep Space Network Support of the Manned Space Flight Network for Apollo

1962–1968

F. M. Flanagan
P. S. Goodwin
N. A. Renzetti

JET PROPULSION LABORATORY
CALIFORNIA INSTITUTE OF TECHNOLOGY
PASADENA, CALIFORNIA

July 15, 1970

Prepared Under Contract No. NAS 7-100
National Aeronautics and Space Administration

Preface

The work described in this report was performed by the engineering and operations personnel of the Tracking and Data Acquisition organization of the Jet Propulsion Laboratory. From the beginning of the space program through 1968, the network has had as its primary mission the support of unmanned lunar and planetary missions. A secondary mission has been to support, through the Manned Space Flight Network, manned lunar exploration: primarily *Apollo*. Since 1969, the primary mission has been defined as that of unmanned deep space missions to planetary and interplanetary space.

Volume I is concerned primarily with the design, engineering, and implementation phases of support to the Manned Space Flight Network and flight support from the initial qualifying flights up to the successful manned lunar orbiting flight of *Apollo 8*. Succeeding volumes will record support of *Apollo* missions starting with *Apollo 9*.

Acknowledgment

The authors express their gratitude to the many contributors whose skill in designing, implementing, and operating the equipment described in this report contributed significantly to the success of the Deep Space Network in support of the *Apollo* program. Special recognition is therefore given to them.

The authors especially thank the following individuals who contributed articles, reports, etc., used in the preparation of this report:

W. Baumgartner
M. Brockman
R. C. Bunce
C. W. Cole
E. K. Davis
H. Donnelly
W. J. Kinder
P. L. Lindley
V. Lobb
W. F. McAndrew
A. Nicula
L. W. Randolph
E. Rechtin
J. Roudebush
F. Schiffman
C. P. Wiggins
J. H. Wilcher
H. Younger

Furthermore, the authors wish to acknowledge the contributions of Mr. W. P. Varson of the Goddard Space Flight Center and Mr. P. H. Vavra of the Manned Spacecraft Center for their untiring efforts in behalf of a compatible telecommunications system design for Project *Apollo.*

They also wish to express their gratitude to Messrs. A. C. Belcher and L. M. Robinson of the Office of Tracking and Data Acquisition at NASA headquarters for their significant contributions in obtaining support for the efforts described in this document.

Contents

Contents (contd)

Contents (contd)

Contents (contd)

Tables

Contents (contd)

Tables (contd)

Figures

Contents (contd)

Figures (contd)

Figures (contd)

Figures (contd)

Figures (contd)

Abstract

This document summarizes the development, engineering, and implementation activities of the NASA Deep Space Network (DSN) at the Jet Propulsion Laboratory in support of NASA's Manned Space Flight Network (MSFN), managed by the Goddard Space Flight Center, for Project *Apollo* from 1960 through 1968.

In the field of *Apollo* telecommunications, the state of the art of the unified S-band system is traced through the development at JPL of the receiver/exciter and ranging subsystems implemented in both the DSN and MSFN.

A detailed account is presented of the operational support the DSN provided to the MSFN from *Apollo 4* to the historical moon orbiting flight of *Apollo 8* during Christmas of 1968.

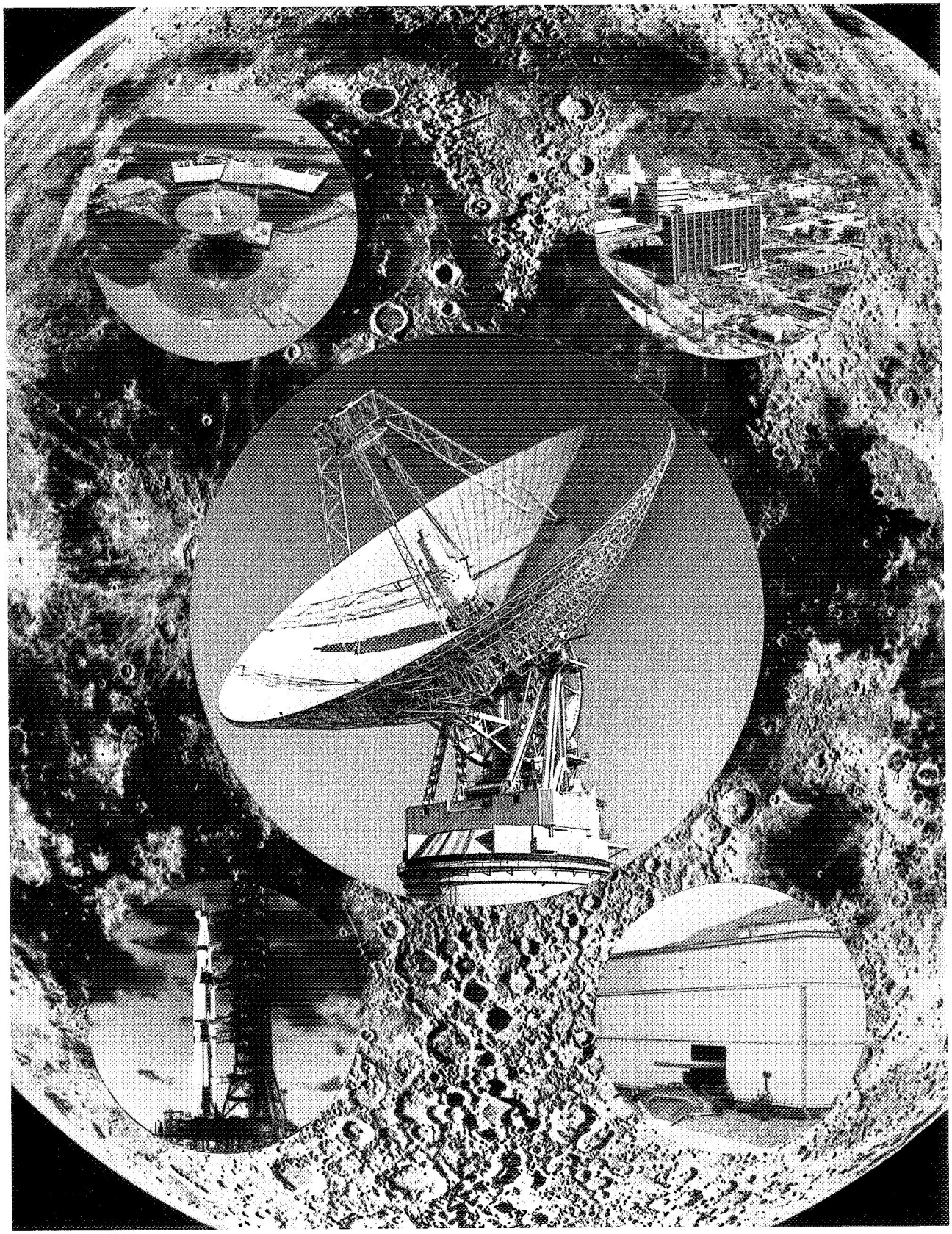

Deep Space Network Support of the Manned Space Flight Network for *Apollo*

1962–1968

I. Introduction

This report provides an account of the Jet Propulsion Laboratory (JPL) activities in the development of the National Aeronautics and Space Administration (NASA) unified S-band (USB) RF system for the *Apollo* program. The report covers the design, development, and implementation effort that was provided by JPL in support of the Manned Space Flight Network (MSFN) and Project *Apollo*.

When President John F. Kennedy established manned lunar landing as a national goal in May 1961, JPL was already involved in unmanned lunar exploration projects. The first of these projects was *Ranger*, which demonstrated the accuracy and feasibility of precise radio guidance to the moon, and the value of continuous telecommunications between a distant spacecraft and a network of earth-based communications stations.

It was the *Ranger VII* spacecraft that provided scientists with their first close view of the lunar surface and clues to its character. The spacecraft was guided to its selected area and its multiple television cameras were activated 15 min prior to impact. The television signals were transmitted to earth where the final display showed the impact area in detail never before seen so clearly by man.

The *Ranger* Project was followed by the Langley Research Center *Lunar Orbiter* and the JPL *Surveyor* projects. All three contributed valuable knowledge about the moon and its environment, which was needed in making many of the decisions for *Apollo*.

The JPL network of earth-based communications stations began in 1958 with the establishment of the first 85-ft antenna Deep Space Station at Goldstone in the Mojave Desert approximately 40 mi from Barstow, Calif. (Fig. 1). The Deep Space Network (DSN) was formally established when two additional 85-ft antenna Deep Space Stations became operational at Woomera, Australia (Fig. 2) in December 1960, and at Johannesburg, South Africa (Fig. 3) in June 1961. In addition to the 85-ft antenna, Johannesburg also had a mobile tracking station with a 10-ft-diam antenna and several trailers (Fig. 4) with equipment to effect initial acquisition of the spacecraft, making it possible to lock in the less-maneuverable 85-ft antenna more quickly after the spacecraft was above the horizon. By July 1964, a Ground Communication Facility (GCF) and a Space Flight Operations Facility (SFOF), located at JPL, completed

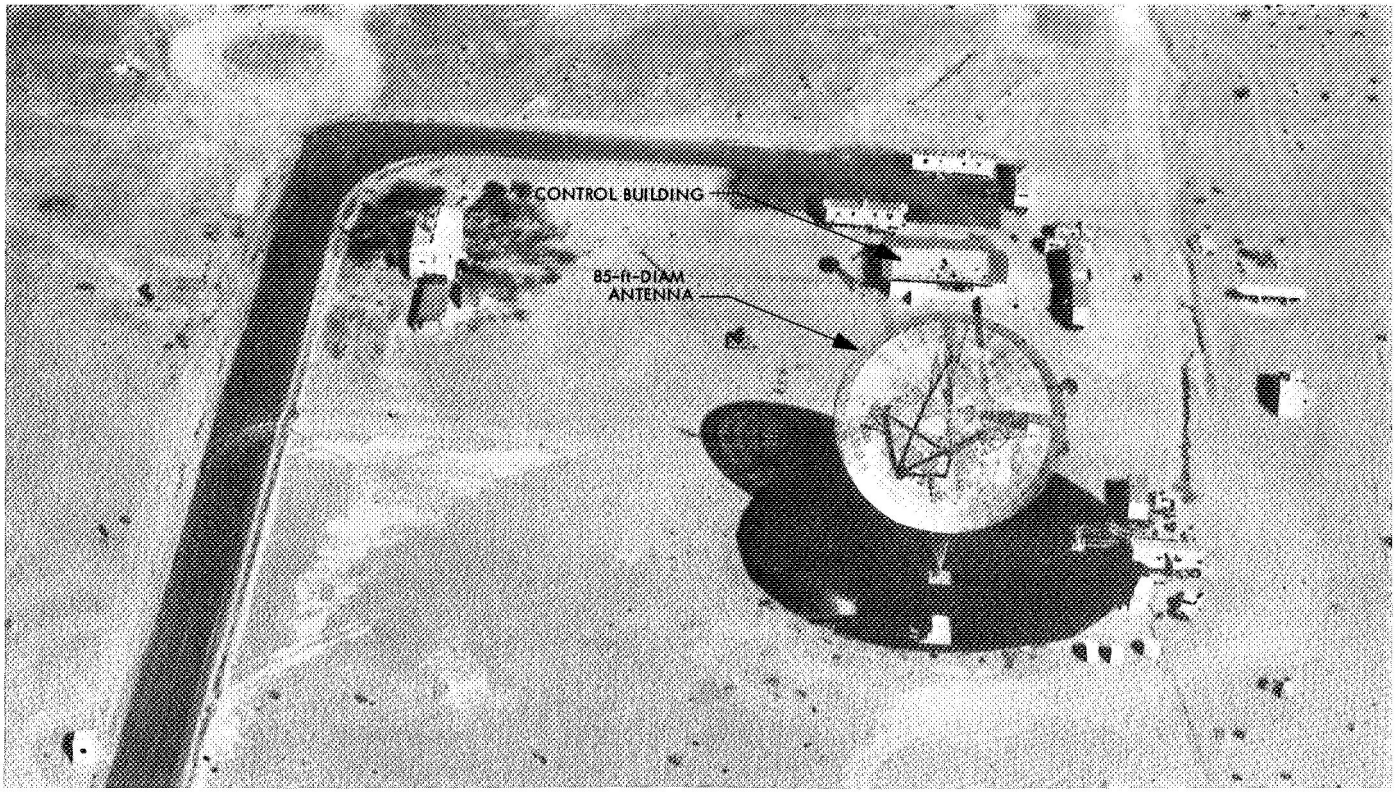

Fig. 1. The original DSN station (Pioneer site)

the requirements to provide an integrated capability designed to track lunar or planetary probes in deep space.

Present (1970) DSN stations and their locations are as follows:

Designation	Location
Pioneer	Goldstone, Calif.
Echo	Goldstone, Calif.
Mars	Goldstone, Calif.
Woomera	Island Lagoon, Australia
Tidbinbilla	Canberra, Australia
Johannesburg	Johannesburg, S. Africa
Robledo	Madrid, Spain
Cebreros	Madrid, Spain
Cape Kennedy	Cape Kennedy, Fla.

The sites for these Deep Space Stations were chosen so that three prime stations would be separated by approximately 120 deg in longitude and would be located between 40°N and 30°S lat. This assured contact with spacecraft vehicles in deep space by at least one station at all times—this despite the rotation of the earth. All of the stations are equipped with steerable-dish antennas 85 ft in diameter except Mars, which has a 210-ft-diam antenna that is designed to receive radio signals from millions of miles in space. Because of the extreme sensitivity of the equipment, the stations are located in natural depressions or valleys to decrease interference from local radio stations and other electromagnetic sources.

The *Apollo* program developed the need for: (1) expansion in the geographical coverage provided by *Mercury/Gemini* network, (2) larger antennas to maintain radio communications in the vicinity of the moon, and (3) simultaneous transmission of voice, engineering science, video, and telemetry data. The MSFN network of 85- and 30-ft antennas was established to meet the geographic requirements. The most significant electronics system addition to the network was the USB system. This single system replaced the multiple antennas and RF links previously used for the *Mercury* and *Gemini* spacecraft. The USB allowed simultaneous modulation of voice and telemetry data on the same RF carrier used

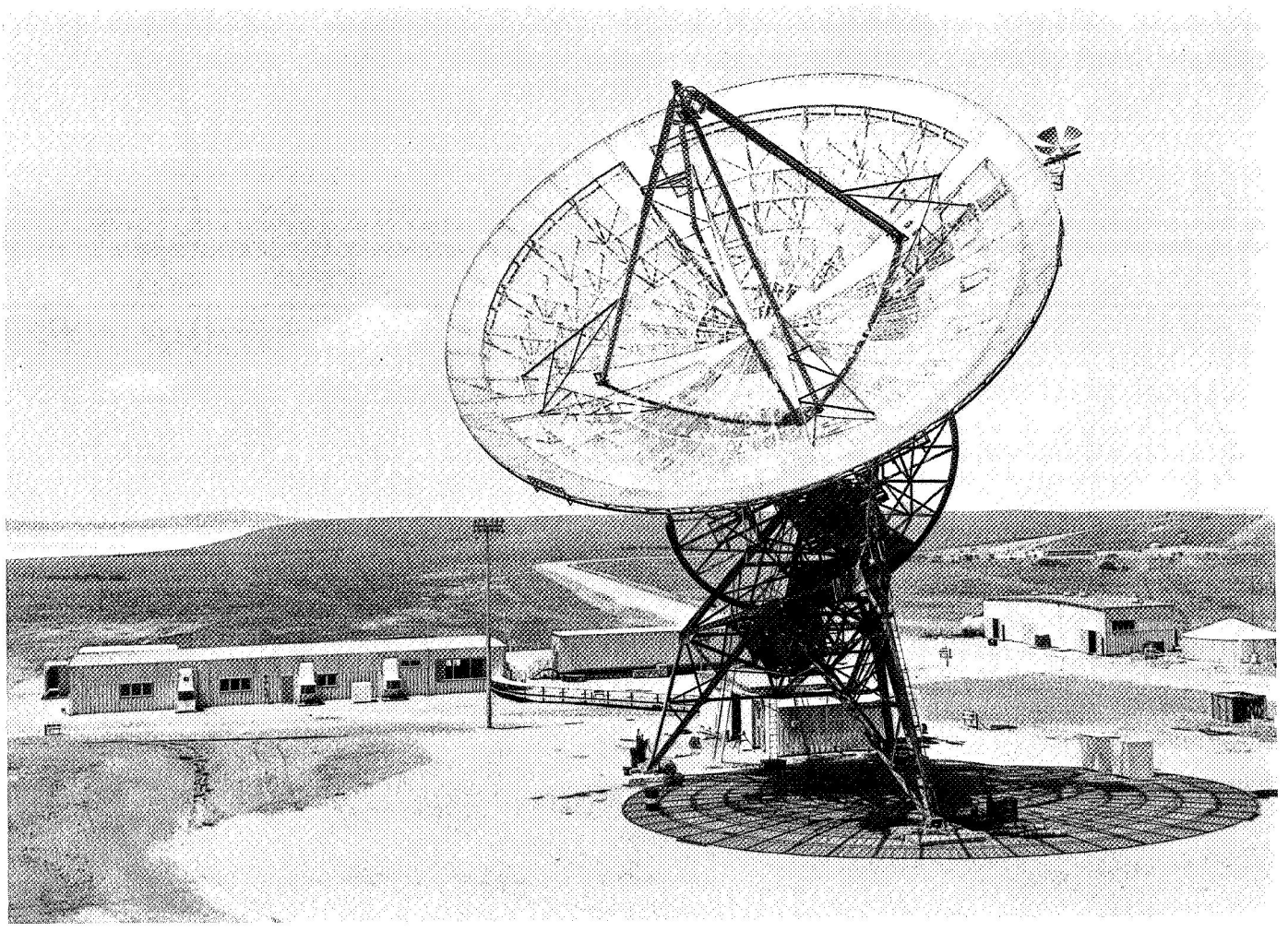

Fig. 2. Deep Space Network station at Woomera, Australia

for the tracking function and provided the performance improvement needed for lunar-distance communications.

In October 1962, the Associate Director of the Manned Spacecraft Center (MSC), in a memorandum to the Director of Office of Tracking and Data Acquisition (OTDA), requested the use of JPL facilities in support of Project *Apollo*. In its request, MSC stated:

> The *Apollo* mission schedule calls for flights well beyond the capability of the current Manned Space Flight Network. It is anticipated that there will be requirements for metric tracking data (position and velocity vector), voice, telemetry, and possibly an up-data link, all at lunar distances.
>
> The MSC desires to make use of the facilities of Jet Propulsion Laboratories, both current and planned, to assist in meeting these requirements....

The National Aeronautics and Space Administration/ OTDA assigned to the Goddard Space Flight Center (GSFC) MSFN the task of the primary *Apollo* support role in a letter to the Director of JPL, requesting "... JPL assistance in the planning and implementation of ground instrumentation for the lunar missions of the *Apollo* program. Due to the JPL experience ... in connection with the *Ranger* and *Mariner* programs, ... JPL possesses a particularly valuable competence in the area of ground instrumentation for lunar missions, whether manned or unmanned."

The added network complexity required for participation in the *Apollo* program is reflected in expansion and modification in the following four areas:

(1) Implementation of additional stations, including those on ships and aircraft, needed to provide the required near-space coverage, all capable of employing the USB system.

(2) Incorporation of additional data-handling capability for more effective mission control.

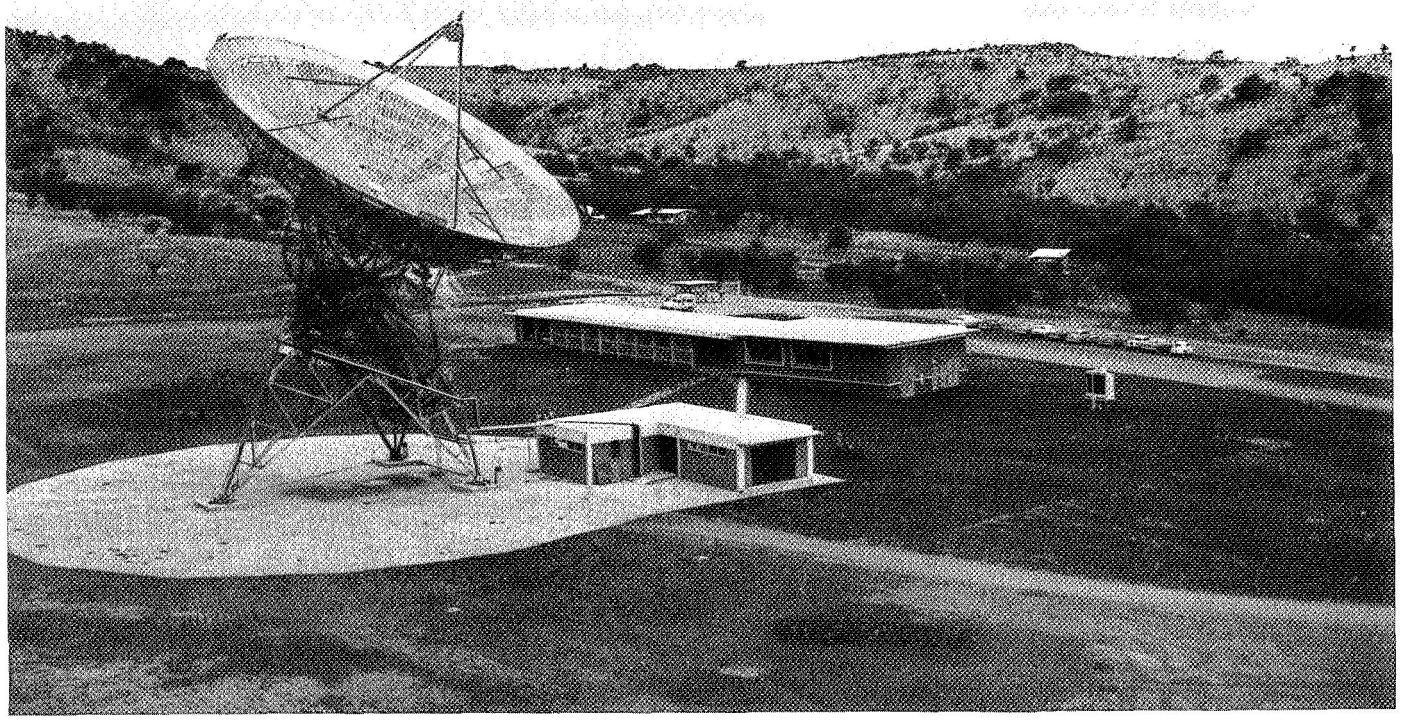

Fig. 3. Deep Space Station at Johannesburg, South Africa

(3) Expansion of network communications capabilities, including the use of commercial satellites, for more reliable communications.

(4) Incorporation of the USB system and the implementation of 85-ft-diam antennas at three sites and 30-ft-diam antennas at 11 sites to extend network capability to provide its services out to lunar distances.

(5) Incorporation of the JPL/DSN to provide capacity for communications over the great distances of lunar flight.

For the *Apollo* program, the network was required to maintain contact with as many as three vehicles at one time. Network participation was required for earth-orbital and for lunar missions beginning with the check-out of all *Apollo* vehicles in earth orbit before injection into a translunar trajectory.

II. Role of JPL in Project *Apollo*

A. Background Information

The role of JPL in Project *Apollo* began in December 1960. The Director of JPL was invited by NASA to attend the first meeting of a newly formed NASA liaison group, known as the *Apollo* Technical Liaison Group, Instrumentation and Communication. The members of this new group represented the Space Task Group (STG), Marshall Space Flight Center, Lewis Research Center, Langley Research Center, and the Flight Research Center. Dr. Eberhardt Rechtin, then the Deep Space Instrumentation Facility (DSIF) program director, attended the meeting representing the Director of JPL.

The first meeting of this group was held at the STG, Langley Field, Va., on January 6, 1961. Mr. Ralph Sawyer, of the STG, opened the meeting by giving the purpose of the Technical Liaison Group which he outlined as effecting systematic liaison in various technical

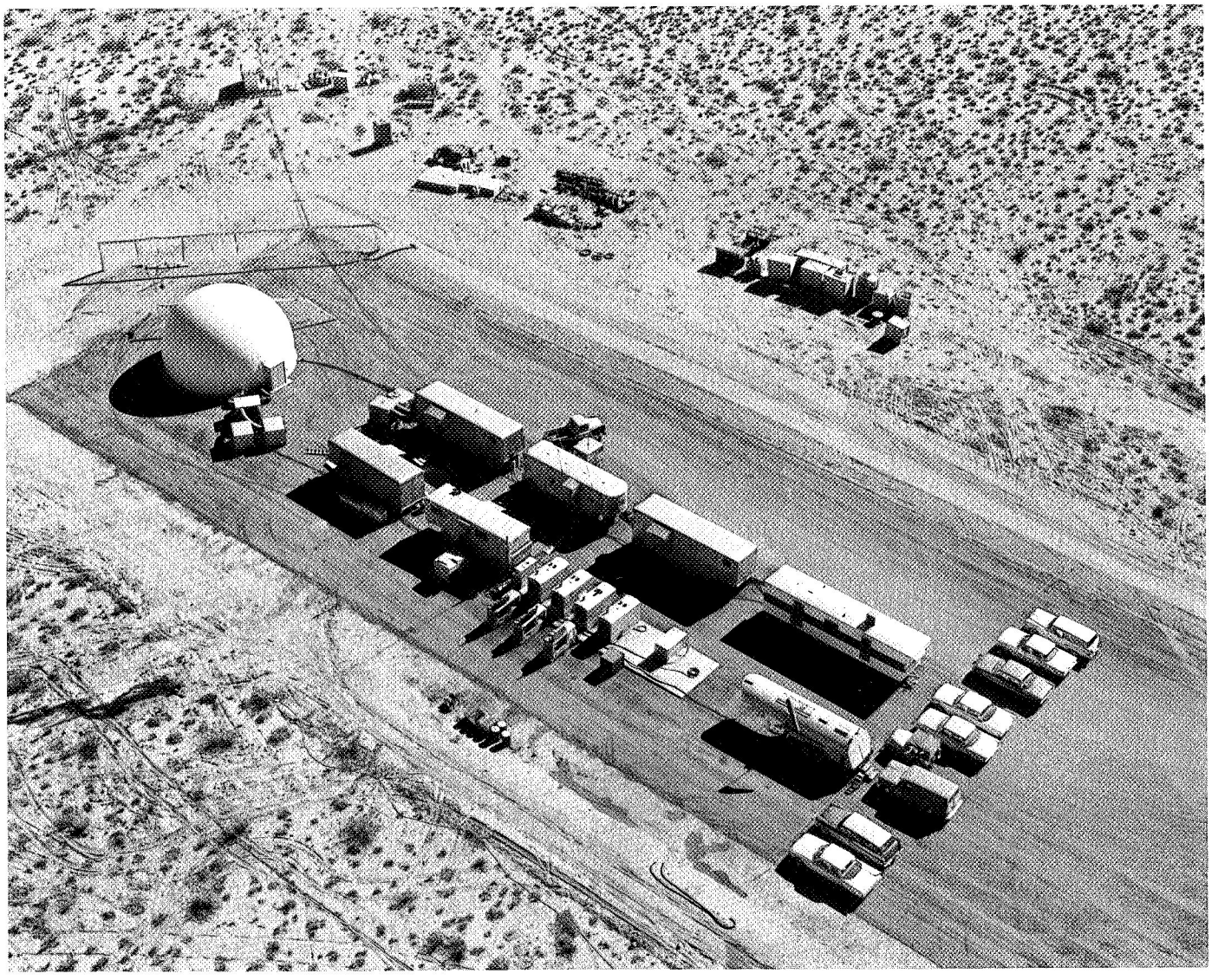

Fig. 4. Mobile tracking station at Johannesburg, South Africa

areas between the several NASA organizations involved in work related to the *Apollo* Project. The objectives and scope of this group were to:

(1) Provide an up-to-date summary of activities then under way that were pertinent to Project *Apollo*, in the specific technical areas at the various NASA centers.

(2) Provide regularly a summary of results of research and study investigations pertinent to Project *Apollo* to ensure their use in the implementation of the project.

(3) Provide a means of reporting *Apollo* contractors' activities to group members.

(4) Provide a mechanism for bringing expert technical consideration to technical problems as they arose.

(5) Point out areas where research activity was needed in support of the project for consideration by the NASA centers.

(6) Assist in monitoring contractor studies through participation of individual panel members for consideration of particular problems, and as geographically convenient.

(7) Develop requirements for flight tests resulting from consideration of research and study activity.

(8) Provide regular overall assessments of progress in the given technical areas as related to the project.

In addition, Mr. Sawyer reviewed the *Apollo* guidelines related to command and communications. Each member of the group was given a copy of the Space Task Group *Apollo* Systems Study work statement, which contained the guidelines set forth for command and communications. A proposed set of working guidelines was drawn up, emphasizing that the primary objective of the group, during the study phase, was to determine the optimum system or the criteria which would result in the most optimum system.

1. General considerations. General considerations in regard to the spacecraft instrumentation and communication during the study phase included the following:

(1) Maximum use of ground sites that were presently available or planned, and recommendations for additional ground stations or modification to existing stations for maximum use.

(2) Use of the same equipment for various phases of flight and for multiple purposes wherever possible.

(3) Maximum use of the crew.

(4) Use of modular construction for replacement by the crew.

(5) Progressive failure concept, brought about by multiple use of equipment; for example, providing for telemetry transmission on another system (possibly a tracking beacon), which would allow at least degraded information to be transmitted.

(6) Power management by providing for manually manipulating the power output and/or narrowing the information bandwidth.

2. Tracking considerations. Tracking considerations in regard to the spacecraft included the following:

(1) Determination of the required accuracy and rate of metric tracking data for the several mission phases.

(2) Adequacy of existing installations and their deployment to provide such data; required additions to equipment at those sites as well as new sites, including ships and recommended positional systems for those ships.

(3) Determination of tracking beacon requirements with an allowance for the use of the same beacons during the various phases of flight.

(4) Determination of the effect of ionization on tracking during the *Apollo* reentry flight.

3. Near-earth communications. Near-earth communications (voice, telemetry, etc.) considerations in regard to the spacecraft included the following:

(1) Determination of ground station locations to meet the requirements of launch, abort, earth orbit, reentry, and landing phases of flight.

(2) Determination of onboard requirements and communication systems suitable for the *Apollo* mission with an effort to utilize the same equipment as used for deep space.

(3) Analysis of the communication requirements during reentry; if communications are necessary during this time, an investigation of the best ways of meeting minimum requirements in the presence of ionization.

(4) Determination of antenna requirements.

4. Deep space communications. Deep space communications (voice, telemetry, etc.) considerations included the following:

(1) Determination of detailed information to be transmitted and information rates required for telemetry.

(2) Thorough investigation of the suitability of existing and expected ground facilities, especially the DSN, with consideration of the need for modifications or additions to various sites and the need for additional sites. (Past studies were to be used to the fullest extent possible.)

(3) Investigation of modulation techniques appropriate to the signal and noise relationships of the space environment with emphasis on power requirements, reliability, and weight.

(4) Investigation of the need for television transmission and its feasibility; determination of the hardware required, such as frame rate, power, and bandwidth.

(5) Determination of requirements and characteristics for the *Apollo* communications systems.

(6) Investigation of all antenna requirements.

The overall *Apollo* program was reviewed, including broad objectives, various elements of the study phase, the *Saturn* development flight test, schedules, tentative

Apollo research and development spacecraft schedules for *Saturn C-1*, and other flight tests. Figures and memoranda containing this information were provided to group members.

The Jet Propulsion Laboratory agreed to the proposed maximum use of existing and planned ground sites. It was pointed out that the DSN locations had been selected so that additional equipment could be moved into the area without appreciable interference with existing equipments. If NASA was considering additional stations, the DSN locations could be kept in mind because logistic support and communications would be readily available. Also, in regard to possible overseas sites, intergovernment agreements had already been made and were thought to be broad enough to cover the *Apollo* program. The position of the DSN in the *Apollo* program was not yet determined. Although the use of JPL facilities for tracking and communications during the *Apollo* flight to and from the moon appeared quite reasonable on technical grounds, it was also apparent that neither the STG nor JPL intended their actions in the technical liaison groups to be interpreted as commitments. In addition, JPL had neither instructions nor funding from NASA headquarters for participation in a manned lunar flight program. This was pointed out solely so that there would be no misunderstanding that the technical interests shown by JPL implied the availability of time and equipment of the DSN to the *Apollo* program. The DSN was saturated with commitments to the *Ranger, Surveyor,* and *Mariner* programs. Although JPL intended to obtain additional antennas to relieve the saturation problem, neither the use of these antennas nor the manpower necessary to run them could be guaranteed at that time.

The Jet Propulsion Laboratory was principally interested in the deep space communication aspects of the *Apollo* instrumentation and communication problem. Using directional antennas aboard the spacecraft and the existing DSN, it was thought practical to consider real-time television for most of the flights. In the *Surveyor* application, an antenna approximately 4 ft in diameter, a transmitter of 5 W, and ground stations of 100°K system temperature were capable of high quality picture transmission at a rate of 1/*s* from the moon. Transmission bandwidth was about 220 kHz. The power consumption for the receiver and transmitter was 100 W. Frequency modulation transmission had the advantages of simplicity and reliability. Digital communications appeared useful for narrowband telemetry but of no great advantage to the voice and television links, which have high signal-to-noise ratios.

Because of JPL experience with large 85-ft antennas, high-speed data transmission, and successful deep space spacecraft such as *Pioneer, Ranger,* and *Mariner,* the members of the *Apollo* Instrumentation and Communications Group unanimously recommended that JPL participate in all future activities of the *Apollo* Technical Liaison Group, Instrumentation and Communication.

B. Capability of DSN for *Apollo* Support

Late in May 1961, Dr. R. R. Gilruth stated in a letter to the Director of JPL that a bidders' conference would be held on August 1, 1961. Since the JPL/DSN would be used in tracking and communicating with the *Apollo* spacecraft, it was necessary to supply the prospective bidders with complete information concerning the following:

(1) System description and capabilities.

(2) Development scheduling.

(3) Site locations.

(4) Network computation facilities.

(5) Intersite communication capability.

It was requested that this information be provided in the form of a report to be submitted before July 15, 1961, so that it could be included as part of the bid package.

The task of coordinating the preparation of the report fell to Mr. Paul S. Goodwin, the DSN *Apollo* manager. With the cooperation of various JPL engineering personnel, the report was completed on July 3, and printed copies were mailed to STG on July 14, 1961.

In 1961, the DSN had two 85-ft antenna stations, Pioneer and Echo, located at Goldstone, Calif. Construction of the Pioneer station had been started while JPL was under contract to Army Ordnance, in 1958. Shortly after its establishment, NASA negotiated a lease with the Army for the 68-mi^2 area of the Camp Irwin military reservation on which the station was being built. The Pioneer station was completed in time to track the *Pioneer III* spacecraft in December 1958. In 1960, the Echo station was built approximately 6.5 mi southeast of the Pioneer station.

At that time both of these stations were operating in the L-band frequency range (890–960 MHz) and were

capable of maintaining radio contact with spacecraft up to a distance of 400,000 mi from earth.

It was during this time that the Federal Communications Commission requested that NASA vacate the L-band frequency range by January 1963 (later changed to April 1964), because it would be needed for a commercially operable communication system that was being developed by the American Telephone & Telegraph Company. In place of the L-band, NASA was allocated the S-band frequency range of 2110–2120 MHz for earth-to-spacecraft and 2270–2360 MHz for spacecraft-to-earth communication. Engineers at JPL had started a design study for an S-band radio system in early 1961. The performance characteristics of the new S-band radio system would have to be comparable to those of the L-band radio system. In May 1964, the first S-band radio system was operational at the Pioneer station. By July 1964, the L-band radio system at Johannesburg, South Africa had been converted to operate in both the L- and S-bands.

C. History of S-Band

Changing from an operational L-band radio system to a completely new S-band radio system within such a short time required a prompt but thorough analysis of existing equipment.

To provide the DSN with a 2000/2300 MHz transmit/receive capability and at the same time maintain the 890–960 MHz capability, an L- to S-band conversion plan had to be worked out that would be satisfactory from both the Deep Space Station and spacecraft point of view. Therefore, the following ground rules were developed:

(1) The spacecraft-to-earth frequency had to lie in the 2290–2300 MHz band.

(2) The nongovernment frequency band of 1800–2200 MHz had to be avoided if possible.

(3) The conversion plan was to favor a simplified transponder redesign without over-complicating the ground RF system.

(4) The transmitted and received frequencies were to be separated by at least 6% but not more than 10%.

(5) A 10-MHz bandwidth for ranging and telemetry was required.

1. Flight transponder. Design work was initiated on an S-band transponder on the basis of the successful L-band flight transponder. The JPL Telecommunications Division, with the assistance of the Military Electronics Division of Motorola, Inc., was able to design an S-band transponder using eight of twelve L-band transponder modules. Block diagrams of the L-band and S-band transponders are shown in Figs. 5 and 6, respectively.

Of major concern was the need for a more powerful power amplifier. Whereas the L-band transponder could transmit a 0.25-W output, the new S-band transponder required from 3- to 25-W output. At that time, there were several power amplifier possibilities: (1) klystrons (rejected because their magnetic fields were incompatible with scientific requirements), (2) amplitrons (potentially the most efficient but rejected because of nonlinear amplification characteristic), (3) traveling wave tubes, and (4) the relatively new tube-cavity amplifier. In the end, both the traveling wave tube and tube-cavity amplifier were incorporated into the transponder design.

Once the power amplifier problem was resolved, the S-band transponder was in relatively good shape. All components had been tested successfully, both in the laboratory and in helicopter flight tests. Acquisition experiments were performed in the laboratory at signal levels corresponding to nominal Mars communication distance. In the helicopter tests, the acquisition procedure averaged about 2 min, and the preflight calibrations indicated good consistency, with a deviation of approximately 3 m rms.

2. Receiver/exciter. In May 1961, JPL awarded a contract to Hallamore Electronics to design, fabricate, test, and install a prototype S-band receiver/exciter. The prime objective of the prototype was to accomplish an RF system frequency translation from L- to S-band that would eventually be incorporated into each Deep Space Station. The performance characteristics of the new S-band radio system had to be equal to those of the L-band radio system. The Hallamore prototype was to be delivered to JPL in May 1962. However, because of numerous technical and design problems, Hallamore was unable to complete the task within the specified time.

The JPL Source Evaluation Board held a meeting to select another contractor who could start with the available components and develop the necessary circuits and assemblies, and produce units in quantity. The Military Electronics Division of Motorola, Inc., was selected be-

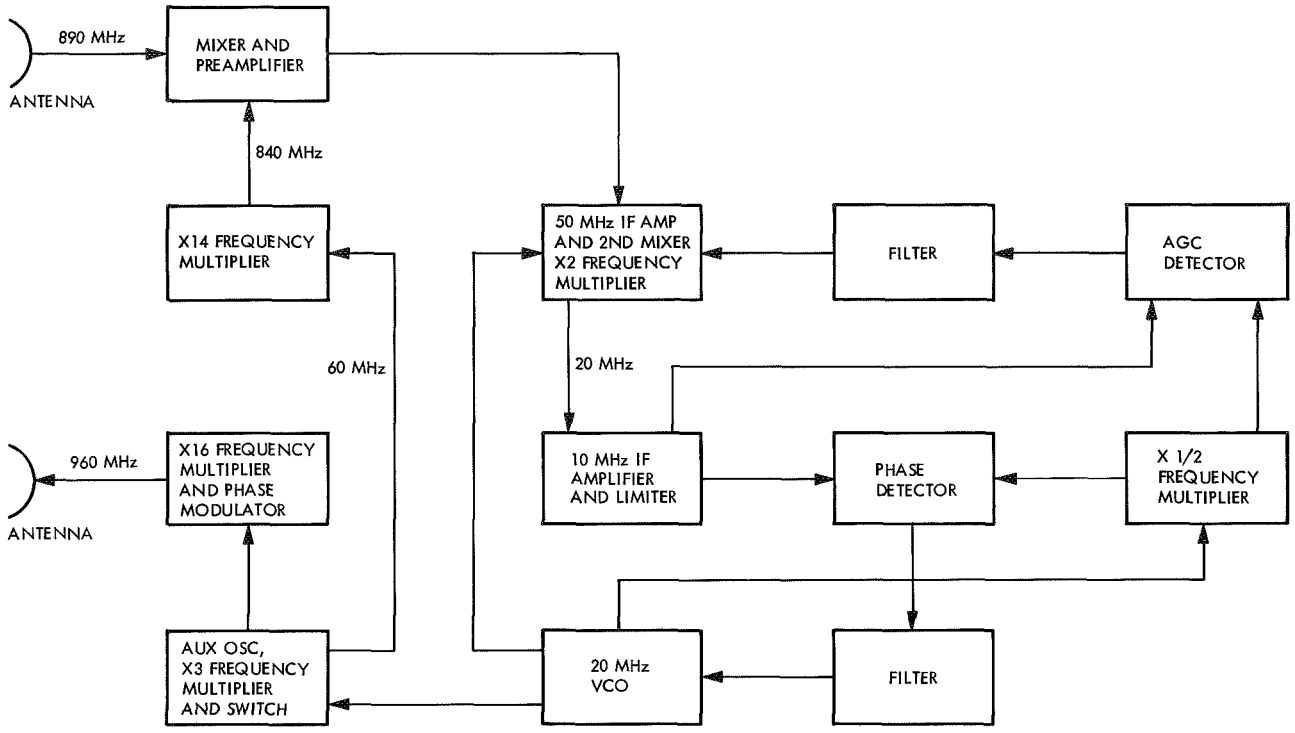

Fig. 5. Block diagram of L-band transponder

cause of its experience and background in assisting JPL in the development of the flight transponder. With NASA approval, JPL awarded the contract to Motorola, which had proposed to package the receiver/exciter in much the same manner as it was packaging the flight transponder. Motorola was to have at least one working example of each critical circuit available with its test data by November 1962, for a design review by JPL engineering.

3. Combined effort. At the design review meeting, it was obvious that the receiver/exciter development was seriously behind schedule. Motorola had not been able to develop the necessary circuits within the time allowed because JPL/Hallamore had not been able to turn over any completed components, assemblies, or data. As a result, JPL decided to consolidate the development efforts for both the flight transponder and receiver/exciter. In December 1962, a new section known as the RF Systems Development Section was formed in the Telecommunications Division under the leadership of Mr. Lee W. Randolph, former head of the Spacecraft Radio Development Group, and composed of personnel from DSIF Engineering and the Spacecraft Telemetry and Command Section. After much study and research, this new section decided that it would be wise to use common assemblies wherever possible in the flight transponder, ground support equipment, and the portable spacecraft test equipment. It was also decided at that time that Motorola should immediately fabricate an appropriate set of components so that JPL engineers could assemble the critical parts of the prototype receiver/exciter ground equipment.

A new ground communication equipment block diagram, prepared by Mr. Randolph and his group, utilized three-quarters of the assemblies, including all critical assemblies, from the flight transponder. As a result of the new block diagram, only minor changes were required in the equipment specifications and in the Motorola contract.

In addition to accelerating the probable S-band operation, the consolidation resulted in several other advantages, including the following:

(1) A common production line for all equipment was established.

(2) Life-test data on more equipment of the same type would be advantageous to other JPL flight projects.

(3) Compatibility of equipment was assured.

(4) Immediate procurement was possible for critical components.

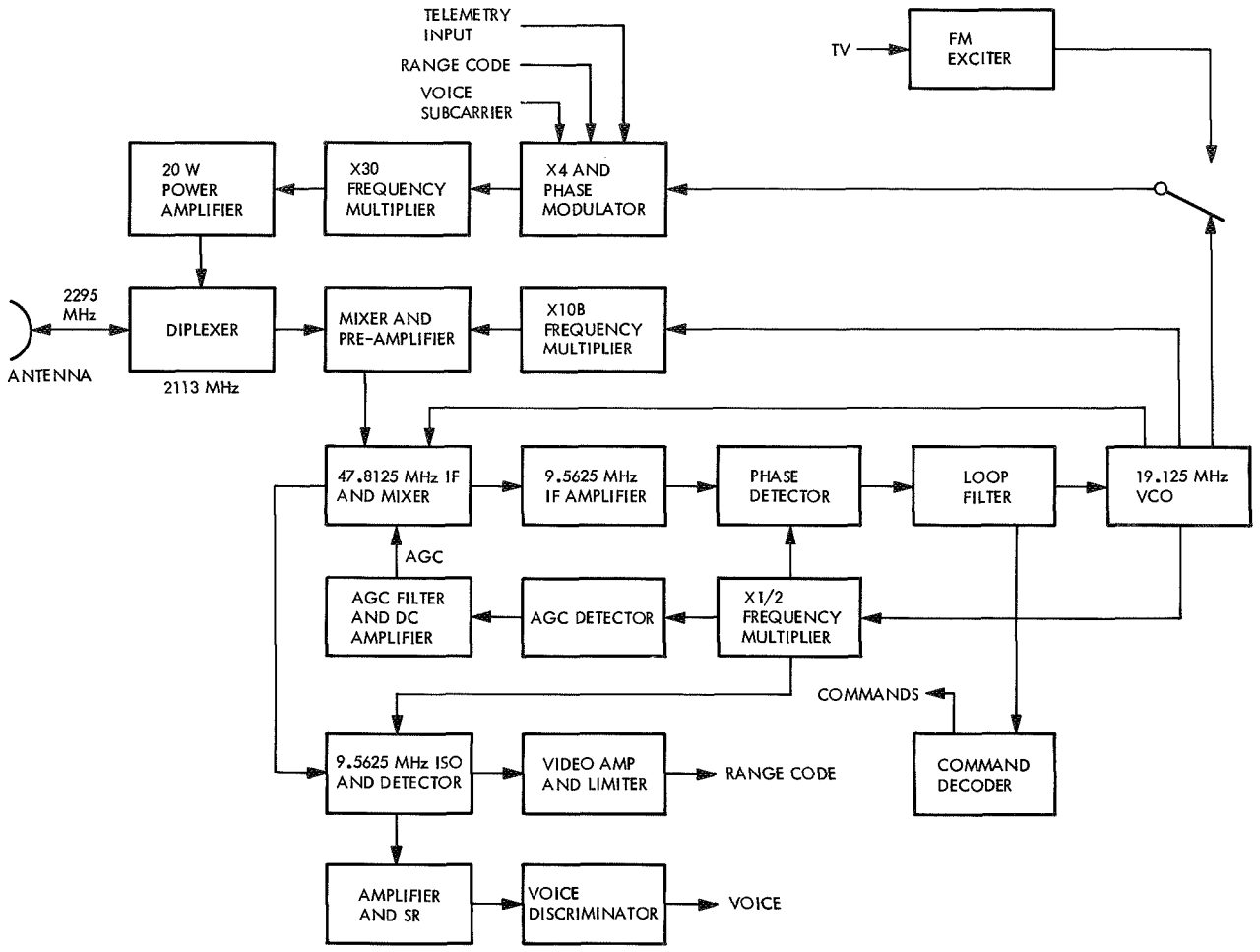

Fig. 6. Unified S-band transponder

Under the direct guidance of JPL engineering, Motorola began delivery of the ground-based receiver/exciter assemblies from its transponder development project to JPL in 1963.

Meanwhile, JPL had awarded a time and material contract to the Resdel Engineering Corp. to provide the facilities and personnel required to assemble the first three receiver/exciter subsystems from the assemblies supplied by Motorola. In addition, Resdel was to prepare the necessary engineering drawings, specifications, and test data required for the production of the subsystem. Thus, the first three S-band receiver/exciter subsystems for the JPL Deep Space Network were manufactured by JPL and Resdel.

With complete engineering documentation available, a cost-plus-fixed-fee contract was awarded to Motorola in January 1964, for the manufacture of seven S-band receiver/exciter subsystems for the DSN.

4. The JPL ranging system. The JPL ranging system that was being developed in 1962 was an extension of the two-way doppler technique, but also made use of the cross-correlation properties of certain binary waveforms to measure the range to interplanetary spacecraft unambiguously. As shown in Fig. 7, the ground transmitter signal was phase-modulated by a long pseudo-random binary waveform. At the spacecraft, it was transponded back to the ground station, where the signal was cross-correlated in a tracking receiver against a local model of the original signal. When maximum correlation was achieved, the phase difference between the transmitter code and the receiver code was a measure of the range to the spacecraft. By means of automatic phase control of the clock that drove the receiver code generator, the range measurement was continuously updated.

The ranging modulation was a periodic binary waveform in which the autocorrelation function was nearly zero for phase shifts different by one or more digit periods. Figure 8 illustrates a typical short-length code and its autocorrelation function.

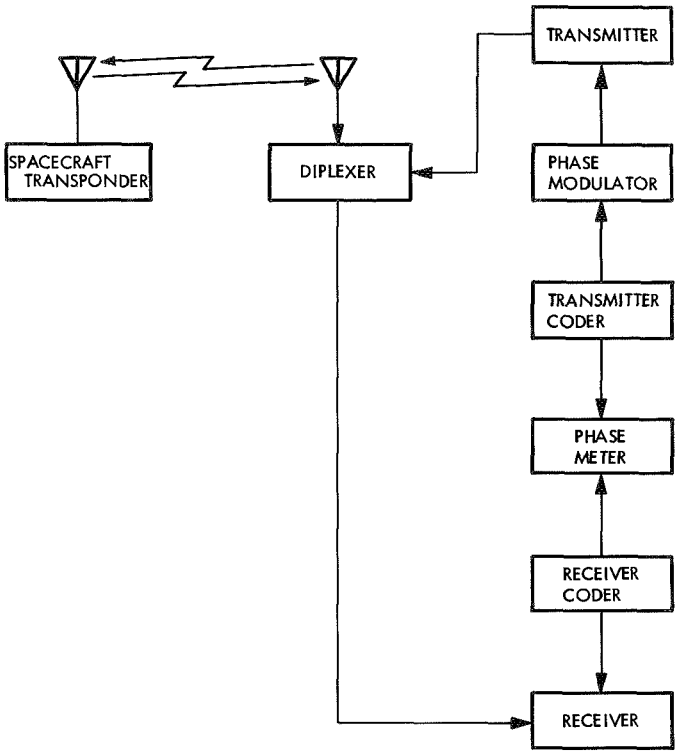

Fig. 7. Basic ranging system

In these systems, the digit period was approximately 1 μs. Because relative displacement of the transmitted and received codes could be measured to within a one-half-digit period, a range measure to a resolution of 75 m could be made. In the system that was developed, both the clock signal and the transmitted RF carrier were coherently derived. By comparing the relative phase shift between both the transmitted and received codes and the transmitted and received RF carriers, an improvement in resolution by a factor of approximately 72 m was achieved. The resolution was constant and independent of the range to the spacecraft. The overall accuracy capability of this system was better than 15 m. Because this measurement technique was actually a measurement of propagation delay, the ultimate system accuracy was dependent on knowledge of the velocity of light through the transmission medium.

Two different ways of using this ranging technique were developed. In the first, the ranging signal was passively reflected from the celestial object that was being tracked. This technique had been successfully used for tracking the *Courier* satellite, the Project *Echo* satellite, and the planet Venus.

The second method used a simple modification to the basic transponder whereby the ranging modulation was coherently demodulated in a wideband auxiliary IF channel, filtered, amplified, and used to modulate the spacecraft-to-earth carrier (Fig. 9). This "turnaround"

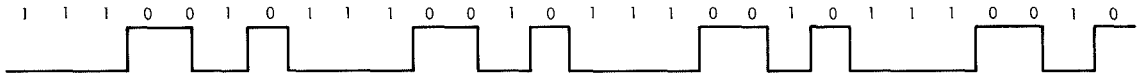

MAXIMUM LENGTH SHIFT REGISTER SEQUENCE
AND CORRESPONDING RANGING CODE

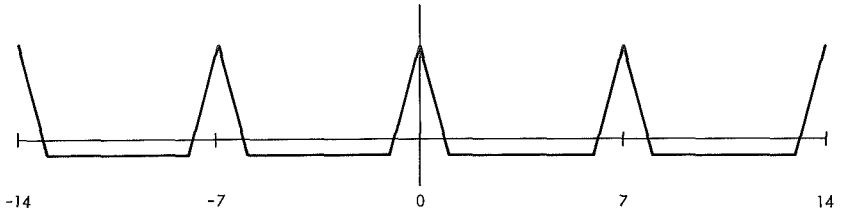

Fig. 8. Pseudo-random sequence

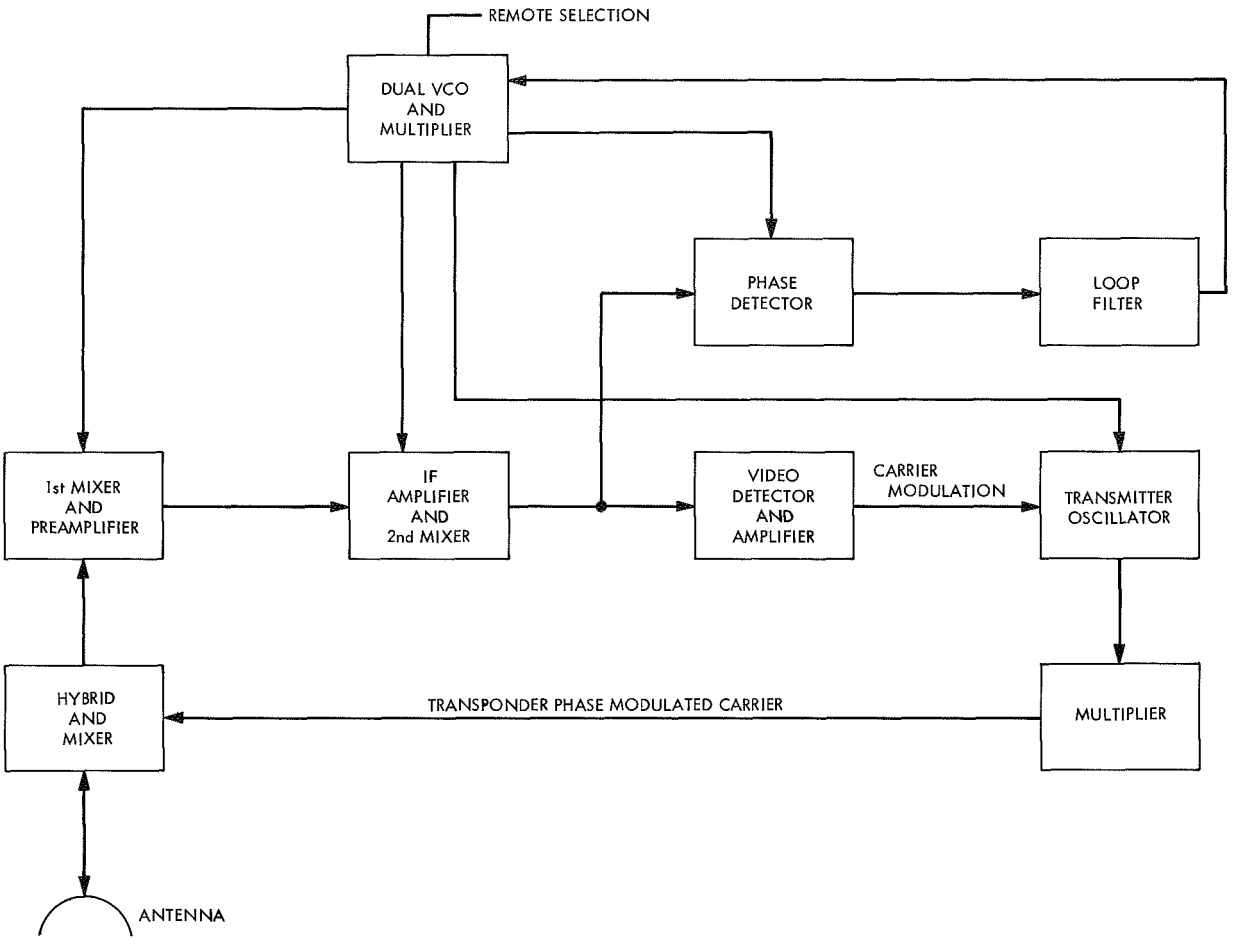

Fig. 9. Block diagram of turnaround ranging transponder

system was developed specifically for ranging to lunar distances using 5–10 W of S-band spacecraft power.

III. The JPL S-Band RF Receiver/Exciter and Ranging Subsystems at the Time of NASA Adoption

A. Background Information

The decision by NASA headquarters in November 1963 to adopt the unified S-band system for both the *Apollo* earth orbital and lunar missions resulted in the NASA Office of Tracking and Data Acquisition directing JPL to provide the MSFN with 39 receiver/exciter, and Mark I ranging subsystems in addition to test transmitter/transponder sets. At that time, the first of three RF subsystems was being produced by the combined efforts of both JPL and Resdel Engineering from modules supplied by the Military Electronics Division of Motorola, Inc., for use in the DSN.

To meet NASA requirements, JPL awarded a contract to Motorola's Military Electronics Division to produce seven additional receiver/exciter subsystems, designated as block I subsystems. Of these, four were tuned to the 2290–2300 MHz frequency range used by the DSN and were incorporated into the Goldstone duplicate standard. The remaining three, tuned to the *Apollo* allocated frequency range of 2270–2290 MHz, were delivered to the MSFN.

The first 10 Mark I ranging subsystems were assembled by JPL engineers from assemblies and subassemblies fabricated by various vendors. An additional 38 subsystems were produced by General Electric, Oklahoma City, Okla., under a contract with JPL, for both DSN and MSFN use.

The first 25 test transmitter/transponder sets were produced by the Philco Western Development Laboratory under a contract with JPL.

The receiver/exciter subsystem, the Mark I ranging subsystem, and the test transmitter/transponder set are discussed in this section in terms of the early block I configuration.

B. The JPL S-Band RF Subsystem

1. Subsystem description. The S-band RF subsystem, consisting of a receiver, transmitter, and antenna microwave subsystems operating in conjunction with an acquisition aid subsystem in the Goldstone duplicate standard 1964 model, is the earth-based portion of a two-way, phase-coherent, precision tracking and communications system capable of providing command, telemetry, and position tracking for deep-space vehicles on a single band of radio frequencies. Because the tracking and communications were accomplished on a single band of radio frequencies, the system soon became known as a *unified* RF system. Earlier RF systems had required the use of separate transmitting and receiving stations operating on different radio frequencies to accomplish tracking and communications. The subsystem measures two angles (local hour angle and declination), radial velocity, and range to the space vehicle as well as providing an efficient and reliable two-way communication capability.

The DSN tracking stations equipped with the USB system were located approximately 120 deg apart in longitude and between 40°N and 30°S lat, so that a spacecraft more than 10,000 mi from earth would in general be under continuous surveillance (Fig. 10).

The JPL S-band subsystem provides a dual-channel reception capability and can be operated in various configurations of antennas, low-noise amplifiers, and receivers for acquisition and tracking and/or listening modes. Design of the subsystem is such that state-of-the-art improvements can be incorporated quickly, easily, and economically.

The design characteristics of the complete RF subsystem are summarized in Table 1 and a block diagram of the receiver subsystem is shown in Fig. 11.

2. Receiver/exciter subsystem. The receiver/exciter subsystem consists of 11 cabinets (Fig. 12), with 8 cabinets installed in the control room and 3 mounted in the antenna structure; the control room cabinets are identified in the figure as C1–C8.

The general functions of the control room cabinets are as follows:

Cabinet	Function
C1	Exciter control and system monitoring
C2	Receiver 1 control, range receiver control, and system monitoring
C3	Receiver 2 control and system monitoring
C4	Exciter, doppler extractor, and range receiver
C5	Receiver 1, angle receivers, and receiver 1 telemetry
C6, C7	Test instrumentation and isolation amplifiers
C8	Receiver 2, acquisition aid angle receivers and receiver 2 telemetry

The general functions of the antenna-mounted cabinets are as follows:

Cabinet	Function
1AC1	Test transmitter, test transponder, and test instrumentation
1AC2	The high frequency portion of the exciter, receivers, and the angle receivers
1AC3	Receivers 1 and 2 input switching circuit

The receiver/exciter subsystem contains eight major functional elements; the elements and their functional capabilities are described in the paragraphs that follow.

a. Reference receiver 1. Reference receiver 1 is a narrowband phase-coherent, double-conversion superheterodyne type that receives signals in the 2290–2300 MHz range from the antenna microwave subsystem. It includes the following basic functional capabilities:

(1) Automatically tracks the signal level, frequency, and phase of the received carrier.

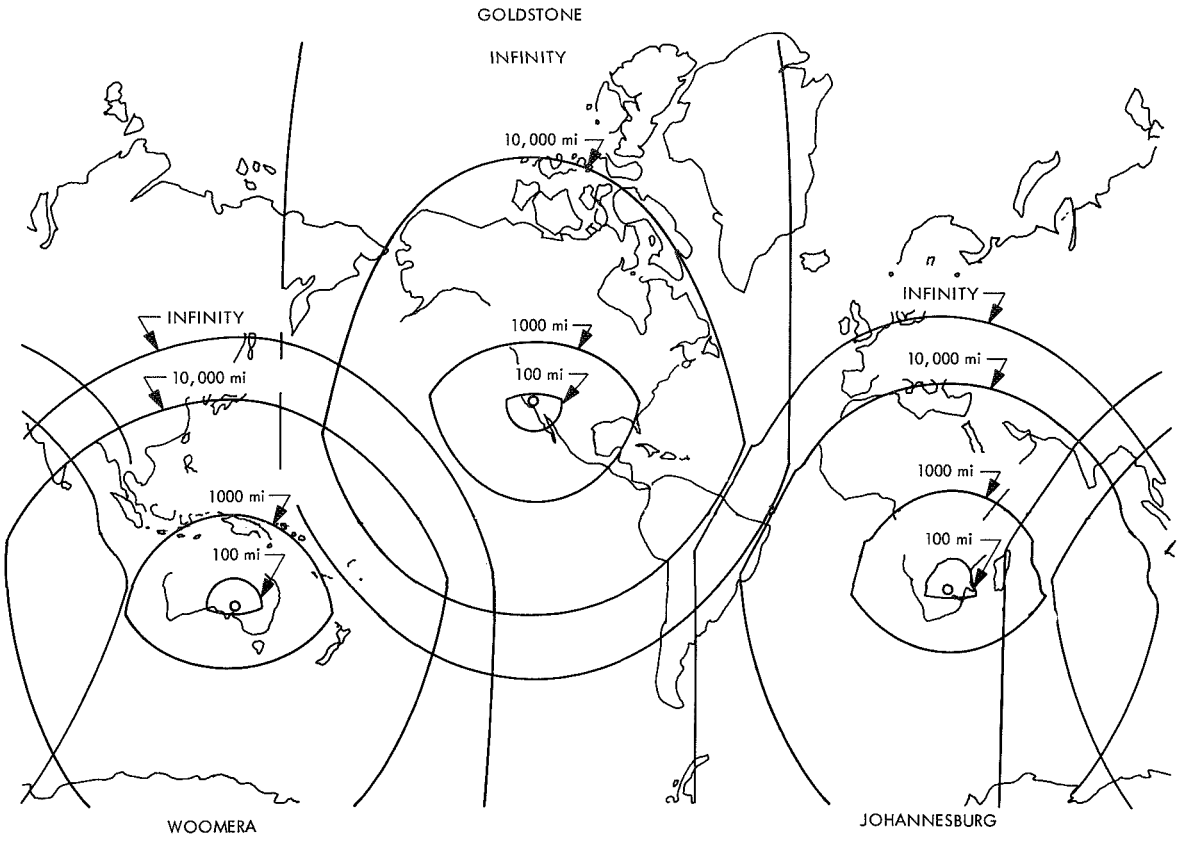

Fig. 10. Coverage of original DSN 85-ft antennas

(2) Provides gain control and reference signals to the reference angle channel receiver.

(3) Provides outputs for telemetry, doppler extraction, and the range clock receiver.

(4) Provides RF switches, control circuits, and performance monitoring.

(5) Provides a method (open-loop operation) for accurately setting the receiver local oscillator frequency.

b. Receiver 1 telemetry. Receiver 1 telemetry operates in conjunction with reference receiver 1 and provides selectable bandwidth filtering for telemetry demodulation. It provides the telemetry output as demodulated subcarrier(s) or as a modulation spectrum centered at 10 MHz for further information processing.

c. Reference receiver 2. Reference receiver 2 is similar to reference receiver 1 and provides the same basic functional capabilities, except as follows:

(1) It is capable of operating on either the same or a different frequency from reference receiver 1.

(2) It provides (during operation with the acquisition aid subsystem) gain control and reference signals to the acquisition angle channel receiver.

d. Receiver 2 telemetry. Receiver 2 telemetry operates in conjunction with reference receiver 2 and performs the same basic functions as receiver 1 telemetry.

e. Reference angle channel receiver. The reference angle receiver is a double-conversion, superheterodyne type that receives two angular error RF signals in the 2290–2300 MHz range from the antenna microwave subsystem and accepts gain control and reference signals from reference receiver 1. It detects the angular error RF signals during phase-coherent operation to provide dc error signals in local hour angle and declination angle to the antenna servo in the antenna mechanical subsystem.

f. Acquisition angle channel receiver. The acquisition angle channel receiver is a double-conversion, superheterodyne type that receives two angular error RF signals in the 2290–2300 MHz range from the acquisition aid antenna and accepts gain control and reference

Table 1. Summary of JPL S-band RF subsystem characteristics

Item	Characteristic	
Antenna microwave subsystem		
Cassegrain feed and microwave circuitry	Tracking–Transmit	
(1) Type	Receive	Transmit
(2) Gain	53 +1.0, −0.5 dB	51 ±1.0 dB
(3) Loss	0.16 ±0.03 dB	0.4 ±0.1 dB
(4) Polarization	Right-hand circular	Right-hand circular
(5) Ellipticity	0.7 ±0.3 dB	1 ±0.5 dB
(6) Effective noise temperature	27 ±3°K (including losses)	
(7) Beamwidth	0.36 ±0.03°K	0.45 ±0.03°K
Low-noise amplifier		
(1) Type	Parametric	Maser
(2) Gain	20 dB	30 dB
(3) Bandwidth	17 ±7 MHz (3 dB)	11 MHz (1 dB)
(4) Effective noise temperature	165 +30, −15°K	15 MHz (3 dB) 16 ±2°K
(5) Input signal level range	−70 dBmW to threshold	−80 dBmW to threshold
Receiver subsystem		
Type	Phase-coherent double conversion superheterodyne	
Effective noise temperature (antenna at or near zenith)		
(1) SCM[a] and reference receiver	2700 ±300°K	
(2) SCM, TWM,[b] and reference receiver	55 ±10°K	
(3) SCM, parametric amplifier, and reference receiver	270 ±50°K	
Input signal level	−70 dBmW to threshold	
Frequency		
(1) Range	2290 to 2300 MHz	
(2) Nominal	2295 MHz	

Item	Characteristic
Receiver subsystem (contd)	
Noise bandwidth (2 β_L)	Threshold bandwidth
(1) RF	12 Hz +0, −20% 48 Hz +0, −20% 152 Hz +0, −20%
(2) Range receiver	0.8 Hz +0, −20% 4.0 Hz +0, −20% 12.0 Hz +0, −20%
Detected telemetry	
(1) Modulation	Phase modulation
(2) Bandwidth (1 dB)	Selectable 2.2 kHz, 10 kHz, 210 MHz, and 0.7 MHz
(3) Output level	0 dBmW (one subcarrier at 1 rad rms modulation index under strong signal conditions)
(4) Output impedance	50 Ω
10-MHz IF output for telemetry	
(1) Modulation	Amplitude, frequency, or phase
(2) Bandwidth (3 dB)	6.5 MHz
(3) Output level	0 dBmW (noncoherent reception), −22 dBmW (coherent reception)
(4) Output impedance	50 Ω
Precision doppler	
Accuracy	0.2 Hz rms at carrier frequency (uncorrelated error for 1-min sample spacing)
Angle error detection	
(1) Gain tracking	Differential ±2-dB max
(2) Phase tracking	Differential ±15-deg max
Transmitter subsystem	
Frequency control	Phase stable, crystal-controlled oscillator: frequency synthesized from an atomic frequency standard
Stability	
(1) Frequency	$1:11^{11}$ for 20 min $5:10^{11}$ for 10 h
(2) Phase	5 deg rms [noise error in bandwidth (2 β_L) of 12 Hz]

[a]SCM = S-band cassegrain-monopulse.

[b]TWM = traveling-wave maser.

Table 1 (contd)

Item	Characteristic		
Transmitter subsystem (contd)			
Frequency			
(1) Range	2110 to 2120 MHz		
(2) Normal	2113 MHz		
Power output	10 kW		
Modulation			
(1) Type	Phase		
(2) Command			
(a) Bandwidth	dc to 100 kHz		
(b) Sensitivity	3 rad peak/V peak		
(c) Input impedance	50 Ω		
(3) Range			
(a) Bandwidth	dc to 2 MHz		
(b) Sensitivity	5 rad peak/V peak		
(c) Input impedance	50 Ω		
RF threshold signal levels			
	Threshold bandwidth, +0, −20%		
Antenna at or near zenith	12 Hz	48 Hz	152 Hz
(1) SCM and reference receiver	−154 ±1.0 dBmW	−148 ±1.0 dBmW	−143 ±1.0 dBmW
(2) SCM, TWM, and reference receiver	−170.8 +1.4, −1.2 dBmW	164.8 +1.4, −1.2 dBmW	−159.8 +1.4, −1.2 dBmW
(3) SCM, parametric amplifier, and reference receiver	−163.9 +1.4, −1.2 dBmW	157.9 +1.4, −1.2 dBmW	−152.9 +1.4, −1.2 dBmW

signals from reference receiver 2. It detects the angular error RF signals during phase-coherent operation to provide dc error signals in local hour angle and declination angle to the antenna servo in the antenna mechanical subsystem.

g. Doppler extractor. The doppler extractor operates in conjunction with either reference receiver 1 or 2 by selection. It includes the following basic functional capabilities:

(1) Accepts reference frequencies from the transmitter subsystem that are coherently related to the transmitted carrier frequency.

(2) Accepts the 10-MHz reference and a frequency coherently related to the receiver voltage-controlled local oscillator (VCO) from either reference receiver 1 or 2.

(3) Accepts a stable 1-MHz bias signal from the frequency and timing standard subsystem.

(4) Processes the signals in items (1), (2), and (3) to provide continuously the two-way doppler frequency at the received carrier frequency. In addition, it adds the 1-MHz bias signal to this two-way doppler frequency to provide biased UHF doppler to the tracking data handling subsystem.

(5) Provides signals to the range clock receiver, which contains unbiased two-way RF doppler frequency information at one-fourth the received carrier frequency.

(6) Provides a transmitter-derived clock frequency to the range clock receiver. The clock frequency is coherently related to the transmitter carrier frequency.

h. Range clock receiver. The range clock receiver operates in conjunction with either reference receiver 1 or 2, the doppler extractor, and the ranging subsystem. It includes the following basic functional capabilities:

(1) Accepts the received range code modulation spectrum centered at 10 MHz from either reference receiver 1 or 2 by selection.

(2) Accepts the range decoding signal (from the ranging subsystem), which, during closed-loop ranging, is correlated with the received range code modulation to provide continuously the doppler-shifted clock frequency to the receiver clock phase-coherent tracking loop.

(3) Provides the clock frequency (coherently related to the transmitter frequency) to the range encoder in the ranging subsystem.

(4) Provides the clock frequency to the range decoder (in the ranging subsystem) via a phase-coherent clock transfer tracking loop. The input to the clock transfer loop can be switched between the transmitter-derived clock frequency and the doppler-shifted received clock frequency.

(5) Processes the transmitter-derived clock frequency and the doppler-shifted received clock frequency

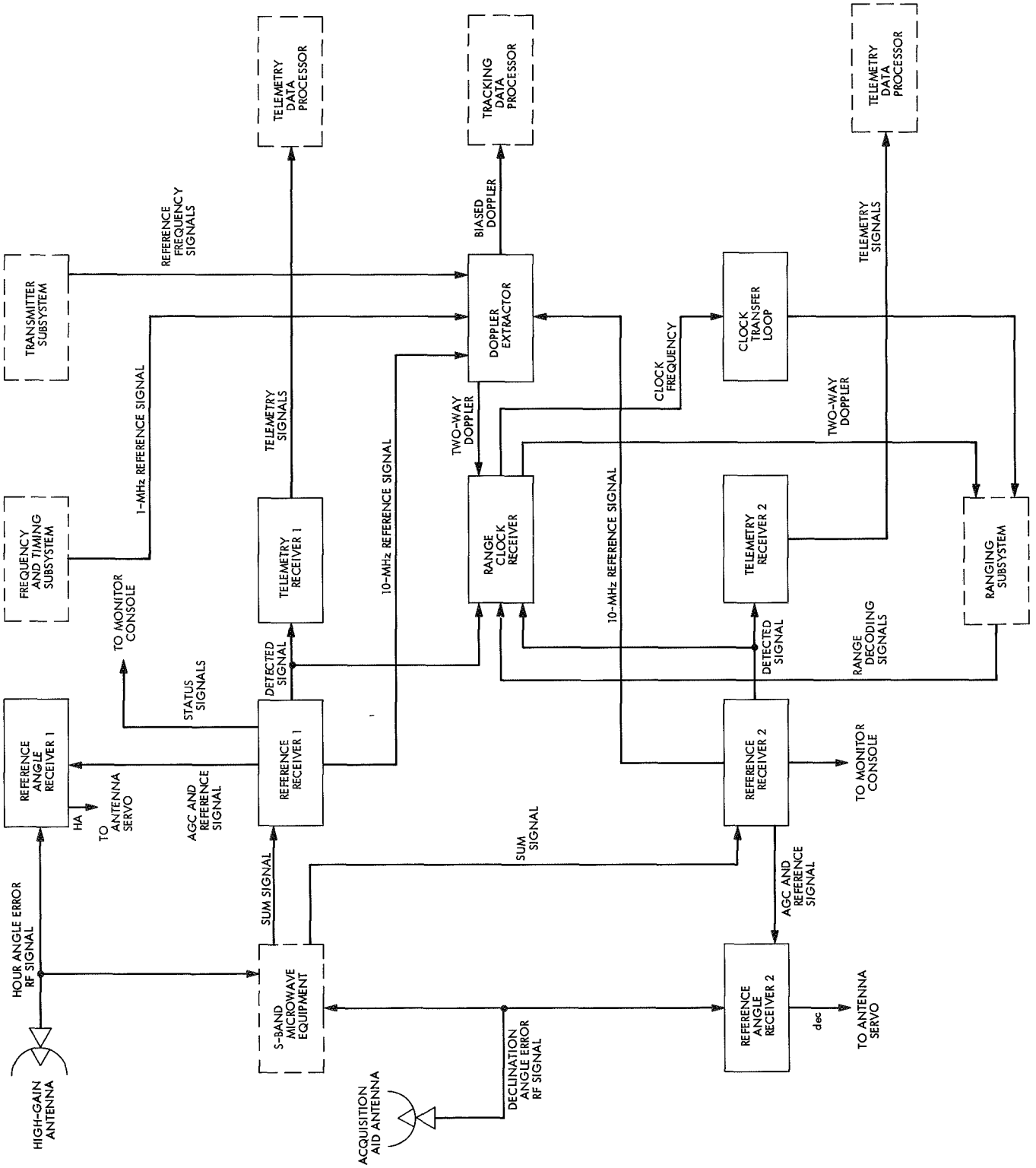

Fig. 11. Block diagram of S-band receiver subsystem

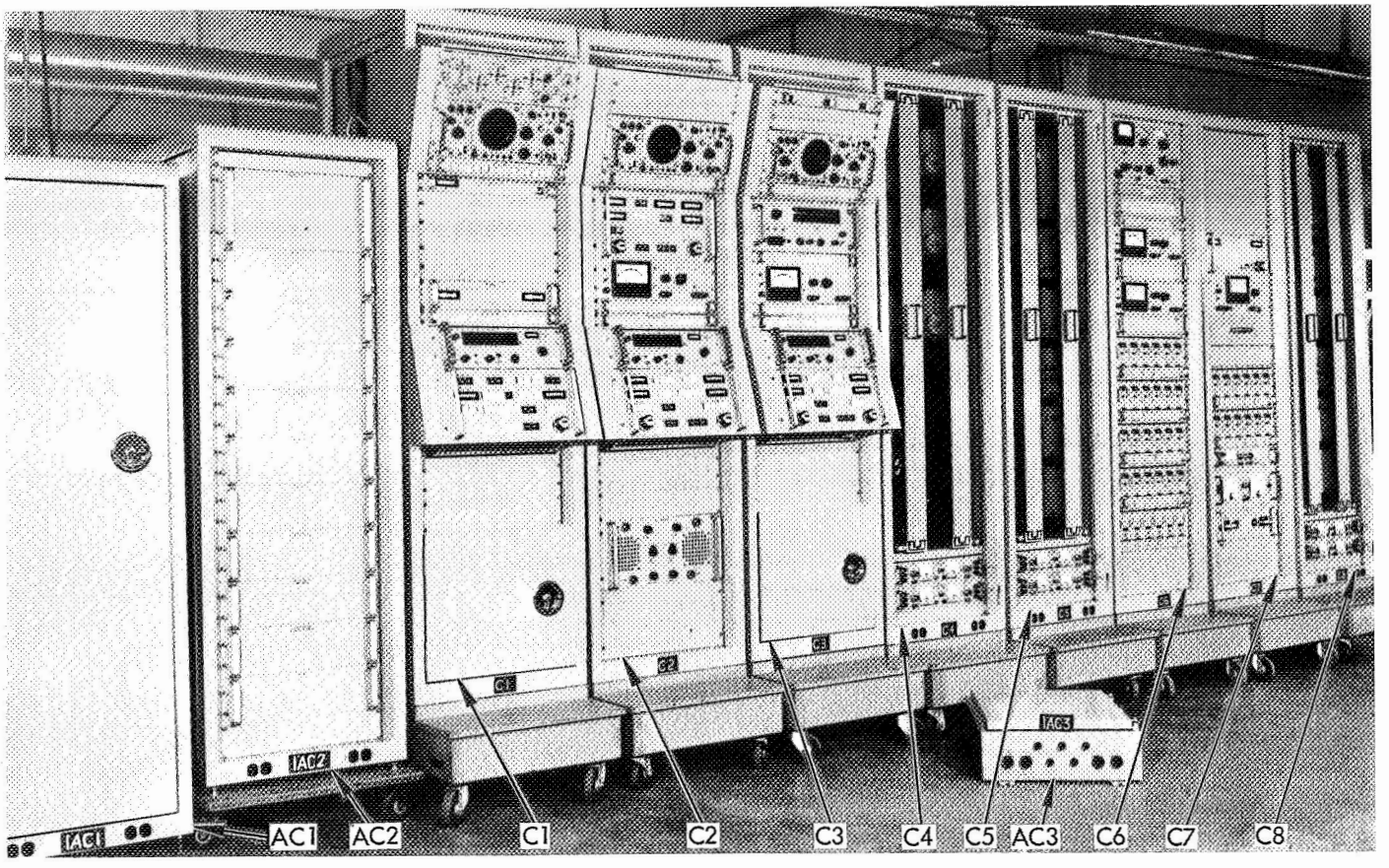

Fig. 12. Receiver/exciter subsystem

continuously to provide two-way clock doppler shift to the ranging subsystem.

(6) Processes the RF signals from the doppler extractor continuously to provide two-way RF doppler shift to the ranging subsystem.

Performance data of a typical receiver/exciter subsystem are tabulated in Table 2. Data for which values are not tabulated are shown graphically in Figs. 13–20.

3. Test transmitter–transponder. Specialized RF test equipment is used with the receiver/exciter subsystem and is contained in two primary subassemblies—the test transmitter and the test transponder. These two subassemblies, with associated equipment, provide the capability of: (1) accurate signal level calibration of the DSN receiver, and (2) simulation of the spacecraft-to-ground link to two-way link between the spacecraft and ground.

One set of these two subassemblies is mounted in the antenna racks of the receiver/exciter subsystem and, when the set is connected by a hard line to this subsystem, one- and two-way tests over cable can be performed. Another set is mounted in the collimation tower for similar tests over an air link. In addition, the test transponder can be installed in an aircraft for acquisition tests, doppler and range measurements, and operator training.

A complete set of equipment for the test transmitter–transponder consists of: test transmitter, test transponder, Harrison Labs 129/802B power supply, Hewlett-Packard 431B power meter, and interconnecting cables.

a. Test transponder. The test transponder (Fig. 21) consists of a fully coherent transponder, transmitter, and associated microwave components as shown in Fig. 22. The transmitter has the capability of being driven by a fixed frequency auxiliary oscillator in a noncoherent mode or by the receiver VCO in a coherent mode. In addition, the VCO output is available to drive the test transmitter in a two-way coherent mode with the test

Table 2. Typical receiver/exciter subsystem test data

Item	Test	Specification
Exciter		
Power, dB	+33.1	+33, +3, −0
RF bandwidth (−3 dB), Hz	13.5	10.1 *min*
Test output, dB	+3.4	+7, +3, −1
Spurious outputs, dB	−31	−30 min
Modulation		
(1) Command		
(a) Sensitivity, rad/V	3.16	3.0 +0.3, −0
(b) Bandwidth, kHz	3440	100 min
(2) Ranging		
(a) Sensitivity, rad/V	5.2	5.0 +0.5, −0
(b) Bandwidth, Hz	2.8	2 min
(c) Null, dB	41	30 min
(3) Incidental AM[a]	1.1	2 max
Synthesizer loop response	(See Fig. 13)	
Phase jitter exciter and receiver in 2 β_{LO} = 12 Hz, deg		
(1) Receiver 1	1.8	5 rms
(2) Receiver 2	2.8	5 rms
Receiver		
	Receiver 1 / Receiver 2	
Noise figure, dB		
(1) Reference channel	9.8 / 9.7	10.6 max
(2) Hour angle channel	8.8 / 8.9	10.6 max
(3) Declination channel	9.1 / 9.0	10.6 max
Image rejection	60.0 / 61.3	45 min
AGC[b] characteristic response	(See Fig. 14)	
Threshold, dBmW		
(1) (2 β_{LO} = 12 Hz)	−156 / −153	−154 ±1
(2) (2 β_{LO} = 48 Hz)	−149 / −147	−148 ±1
(3) (2 β_{LO} = 152 Hz)	−145 / −146	−143 ±1
RF loop response	(See Fig. 15)	
AGC loop response	(See Fig. 16)	

Item	Test		Specification
Receiver (contd)			
	Receiver 1	Receiver 2	
Angle channels			
(1) Phase tracking, deg	±10	±9	±15 max
(2) Gain tracking, dB	±1.7	±1.95	±2 *max*
Doppler tracking rate 30-deg phase error −100 dBmW, Hz/s			
(1) (2 β_{LO} = 12 Hz)	97.6	124	100
(2) (2 β_{LO} = 48 Hz)	790	944	920
(3) (2 β_{LO} = 152 Hz)	4852	5640	5000
Telemetry			
(1) Predetected bandwidth, Hz			
(a) Channel A (−3 dB)	5.60	5.38	6 min
(b) S + N to N[c]	(See Fig. 17)		
(c) Channel B	3.70	4.04	2.8 min
(−1 dB),	432	443	420 min
	24	26	20 min
	5.3	4.6	4.5 min
(2) Detected			
(a) Bandwidth (−1 dB), Hz	715	780	710 min
(b) Output level, dBmW	−4	−2.1	0 ±2 dB
(c) S + N to N	(See Fig. 18)		
Biased doppler			
(1) Bandwidth, Hz	1.69	—	1.5 min
	0.433		0.5
(2) Output level, V	1.54	—	1.29 ±0.29 rms
(3) Phase jitter, deg	1.4	1.5	8 rms max
RF doppler			
(1) Bandwidth (−2 dB), Hz			
(a) 0-deg output	197.9	—	200 min
(b) 90-deg output	360	—	200 min
(2) Phase jitter, deg	1.8	1.9	2 rms max
CCTL[d] response	(See Fig. 19)		
Range receiver			
(1) Loop response	(See Fig. 20)		
(2) Noise bias, V	0.15	—	0.2 max
(3) Phase jitter, deg	1.4	1.3	5.0 rms

[a]AM = amplitude modulation. [b]AGC = automatic gain control. [c]S + N to N = output signal plus noise-to-noise ratios. [d]CCTL = clock code transfer loop.

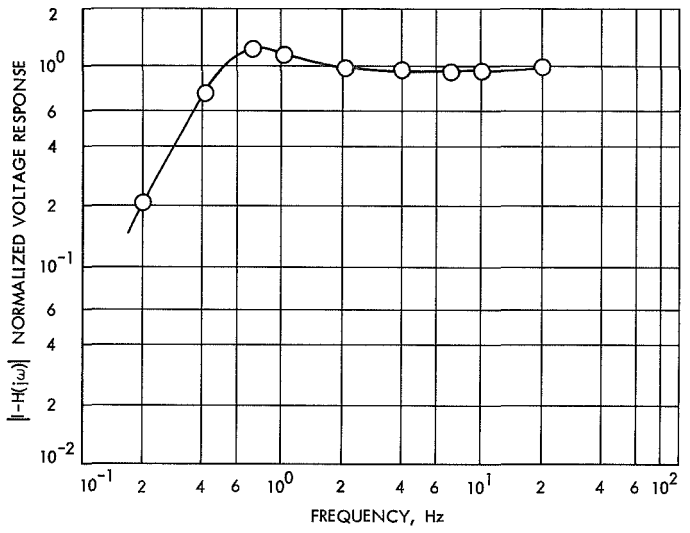

Fig. 13. Synthesizer loop frequency response

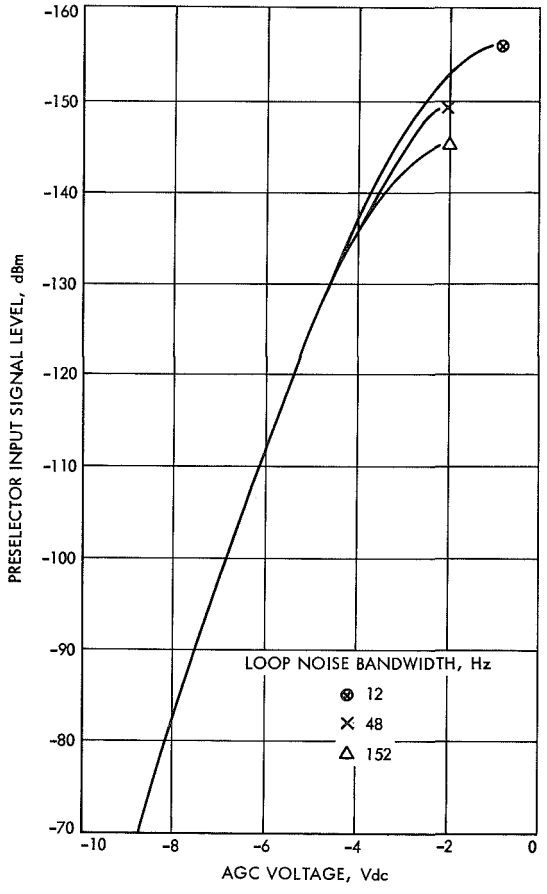

Fig. 14. Automatic gain control characteristics

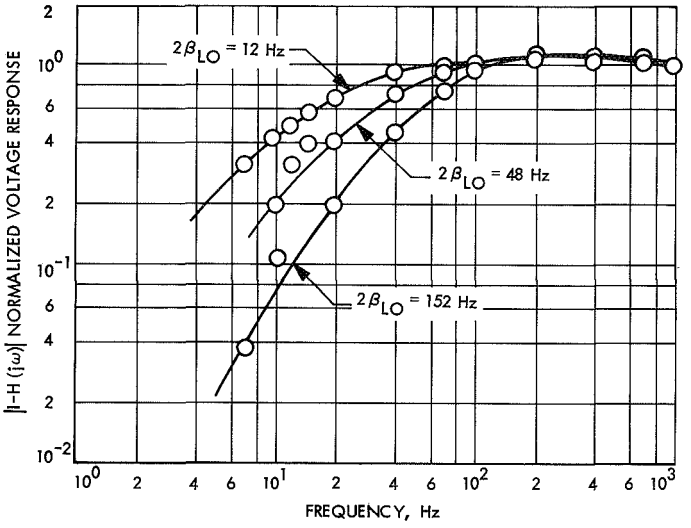

Fig. 15. Radio frequency loop frequency response

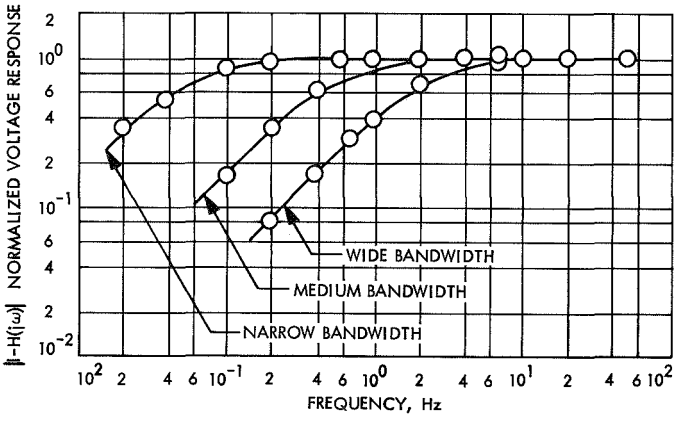

Fig. 16. Automatic gain control loop frequency response

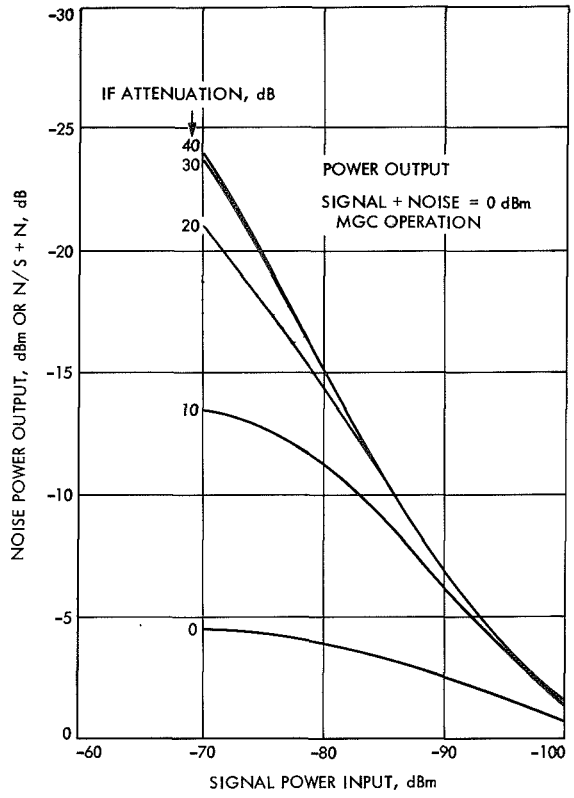

Fig. 17. Wideband telemetry output signal plus noise-to-noise ratios

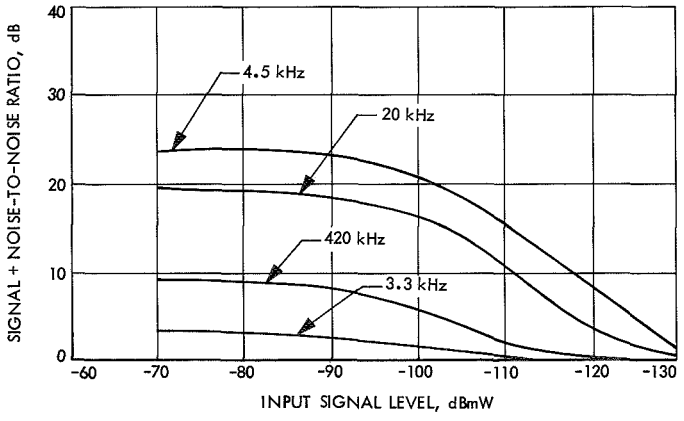

Fig. 18. Narrowband telemetry output signal plus noise-to-noise ratios

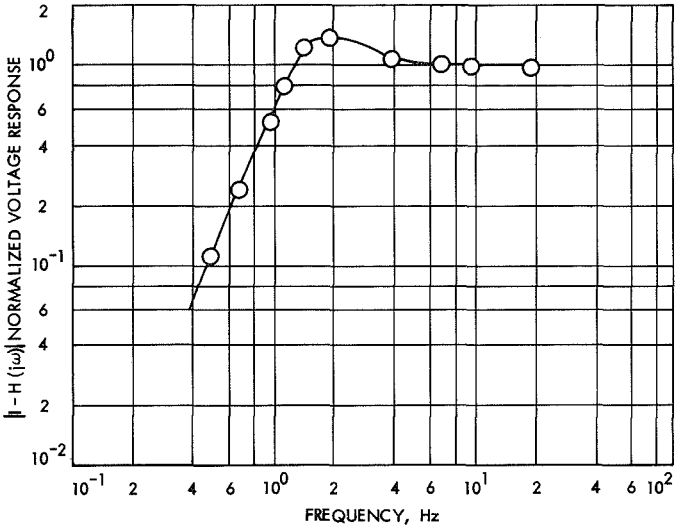

Fig. 19. Code clock transfer loop frequency response

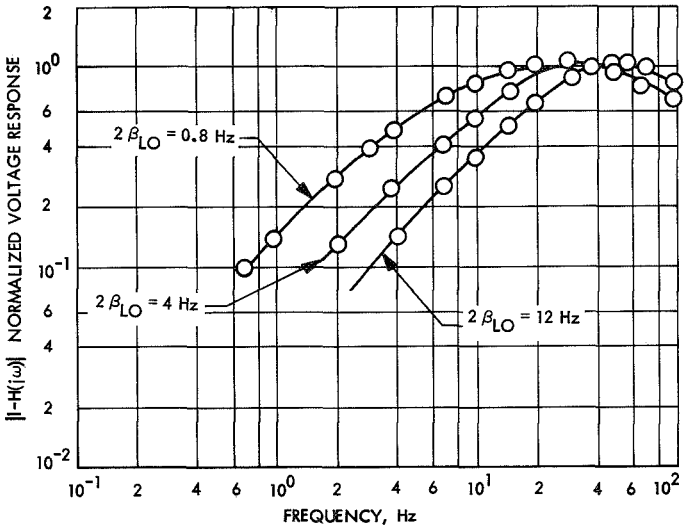

Fig. 20. Range receiver loop frequency response

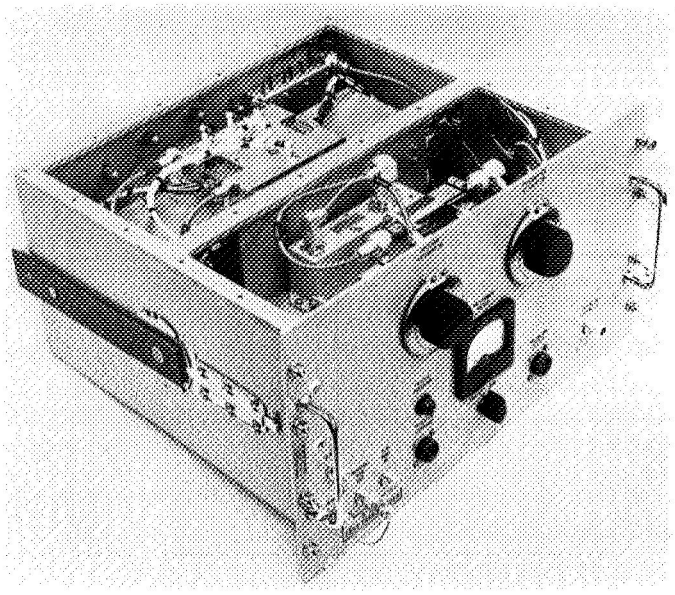

Fig. 21. Test transponder

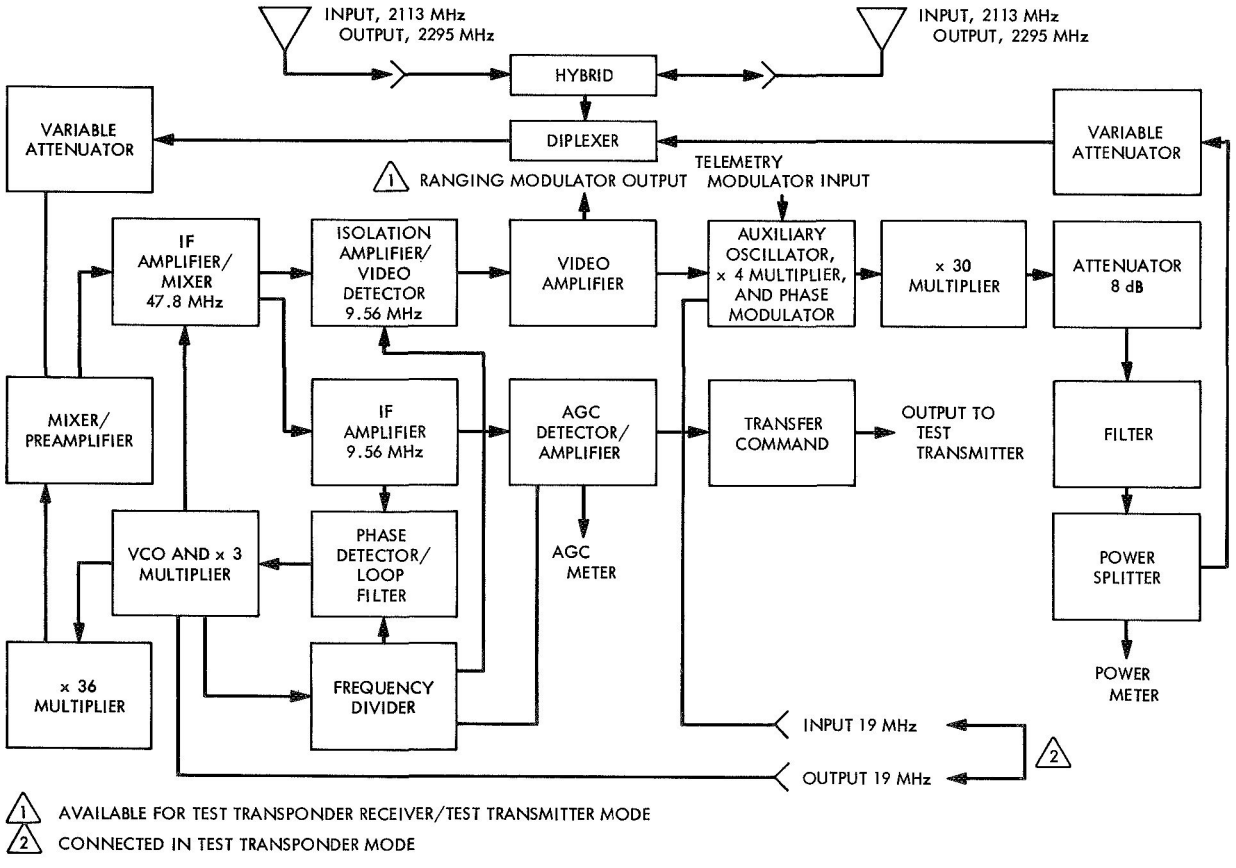

Fig. 22. Functional block diagram of test transponder

transponder receiver. Turnaround ranging capability is also provided.

The transponder in the test transponder subassembly is similar to the one used on the *Mariner C* spacecraft. Frequency agility is attained by omission of the 4500-Hz noise bandwidth predetection filter, thus eliminating the necessity of changing the filter each time the frequency is changed to another channel. The penalty of this design is that the threshold is limited by the capability of the receiver to perform under the high levels of noise in the predetection noise bandwidth of approximately 1 MHz. The degradation in performance in this configuration can be seen in the comparison of the automatic gain control (AGC) curves of a *Mariner C* transponder receiver and the test transponder receiver (Fig. 23). The threshold, however, is adequate for the range of signal levels used in test, which are primarily strong signals. Performance characteristics of the test transponder are listed in Table 3.

b. Test transmitter. The test transmitter (Fig. 24) provides a stable, accurately calibrated signal source. The signal is generated by one of the two selectable VCOs (Fig. 25) and is then multiplied 120 times by solid-state amplifiers and multipliers to give the required S-band output. This circuitry is the same as the transmitter portion of the test transponder. Accurately calibrated step and variable attenuators, and a power monitor at a high power level permit precise control of the output power level. The power is then split by a hybrid to provide outputs at both the front and rear panels. Shielded compartments, extensive use of filters, and power decoupling keep leakage to a minimum.

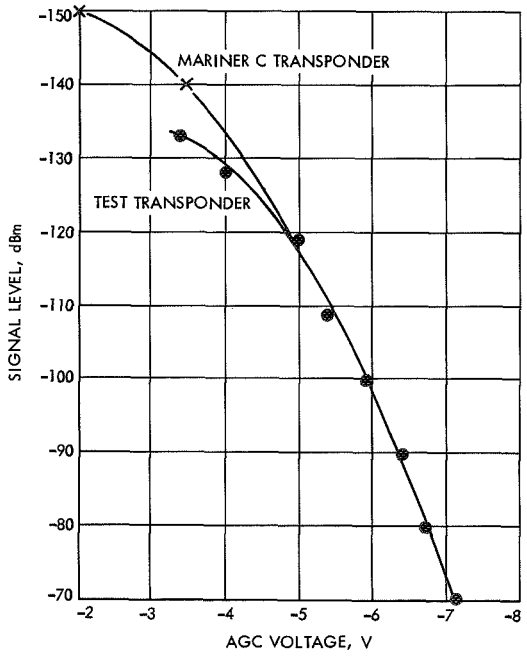

Fig. 23. Automatic gain control characteristics of test transponder

Table 3. Test transponder performance characteristics

Item	Characteristic
Receiver	
Frequency	2113.3125 MHz (nominal), *operational from* 2110 to 2120 MHz
Tracking capability	±3 parts/10^5
Noise figure	<11 dB without variable attenuator
Input signal range	−50 dBmW to threshold
RF loop	
Design noise bandwidth (2 β_{LO}) in predetection, noise-to-signal ratio = 23.5 dB	20 Hz
AGC loop	
Design noise bandwidth	<2 Hz
Loop filter time constant	23 s
Intermediate frequencies	47.8 and 9.56 MHz (nominal)
VCO stability, phase frequency (at constant temperature)	<9-deg peak in 2 β_{LO} = 20 Hz 1 parts/10^6, long term
Ranging channel	
Bandwidth (−3 dB) video out	100 Hz to 1.65 MHz (min)
Video response	140 ns rise and fall (max)
Transmitter	
Frequency	2295 MHz (nominal)
Output power	−20 to −120 dBmW
Phase stability	<9-deg peak in 2 β_{LO} = 20 Hz
Frequency stability	
Auxiliary oscillator	1 parts/10^6, long term
Modulation	
Type	Phase
Deviation	Variable to 2.5 rad
Sensitivity	
Telemetry	1 rad peak/V peak
Ranging	2 rad peak/V peak

Provision for modulation is made through front panel connectors for both telemetry and ranging.

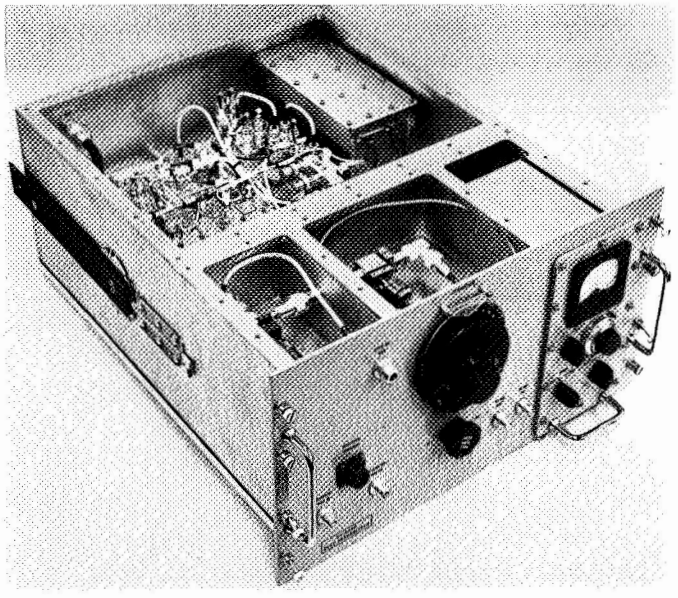

Fig. 24. Test transmitter

The VCO contains a variable voltage source to control its frequency. A front panel switch is available to select either VCO 1 or 2.

Table 4 lists the performance characteristics of the test transmitter.

C. Mark I Ranging Subsystem

1. Subsystem description. The Mark I ranging subsystem is a special-purpose version of the JPL Mod II ranging equipment that had demonstrated a high degree of success and reliability. The Mark I ranging subsystem implements precision ranging on either a reflecting satellite (such as an *Echo*-type balloon) or a turnaround spacecraft transponder. Two sets of codes, one long and one short, are provided. The long code, which permits ranging on lunar and circumlunar missions, has a maximum unambiguous range of 800,000 km. It can also be used for ranges in excess of that distance if the (precisely known) error equal to its maximum capacity is added to the range readout. The short code, which permits somewhat more rapid acquisition, is quite useful for some tests and has a maximum unambiguous range of 10,000 km.

2. General principles. The Mark I ranging subsystem measures the round-trip propagation time of a signal from a ground transmitter to a spacecraft transponder and back to a ground receiver. The accuracy and resolution is independent of the velocity of the spacecraft relative to either the ground transmitter or the ground receiver.

The measurement is made continuously and can be sampled on demand. The unit of measurement is called the range unit, which has the dimension of time. The range unit is defined and determined by the frequency of the transmitter S-band carrier and is otherwise invariant. Specifically, the range unit is independent of any doppler shift on the signal received from the spacecraft.

The major signal paths associated with the ranging function are shown in Fig. 26. The digital ranging equipment, known as the ranging subsystem, although not a part of the receiver/exciter subsystem, is shown in the diagram to simplify the description.

A pseudo-random noise code spectrum containing a clock component is applied from the ranging subsystem as phase modulation (code x clock) to the exciter. The resulting modulated carrier is transmitted to the spacecraft, turned around, and retransmitted to the ground receiver. Within the receiver reference loop, the carrier containing the received code x clock modulation is translated to an IF of 10 MHz and applied to the ranging receiver.

Within this receiver, the received code x clock is correlated with a locally generated code from the ranging subsystem. The correlation process is functionally subtractive, yielding an output of clock signal alone; the amplitude of the clock signal is proportional to the degree of correlation. This signal is tracked by a receiver phase-lock loop, and its amplitude is detected to appear as a dc *correlation indication.* This indication is then routed back to the ranging subsystem as a primary information input.

The ranging receiver also supplies clock frequency reference and clock doppler signals, whereas the reference loop supplies a UHF range doppler signal (at one-fourth the S-band doppler value or D/4), for use by the ranging subsystem.

Using these various inputs, the ranging subsystem programs an acquisition sequence from which data proportional to the range of the spacecraft are obtained.

Upon completion of the acquisition program, the ranging subsystem delivers updated range information

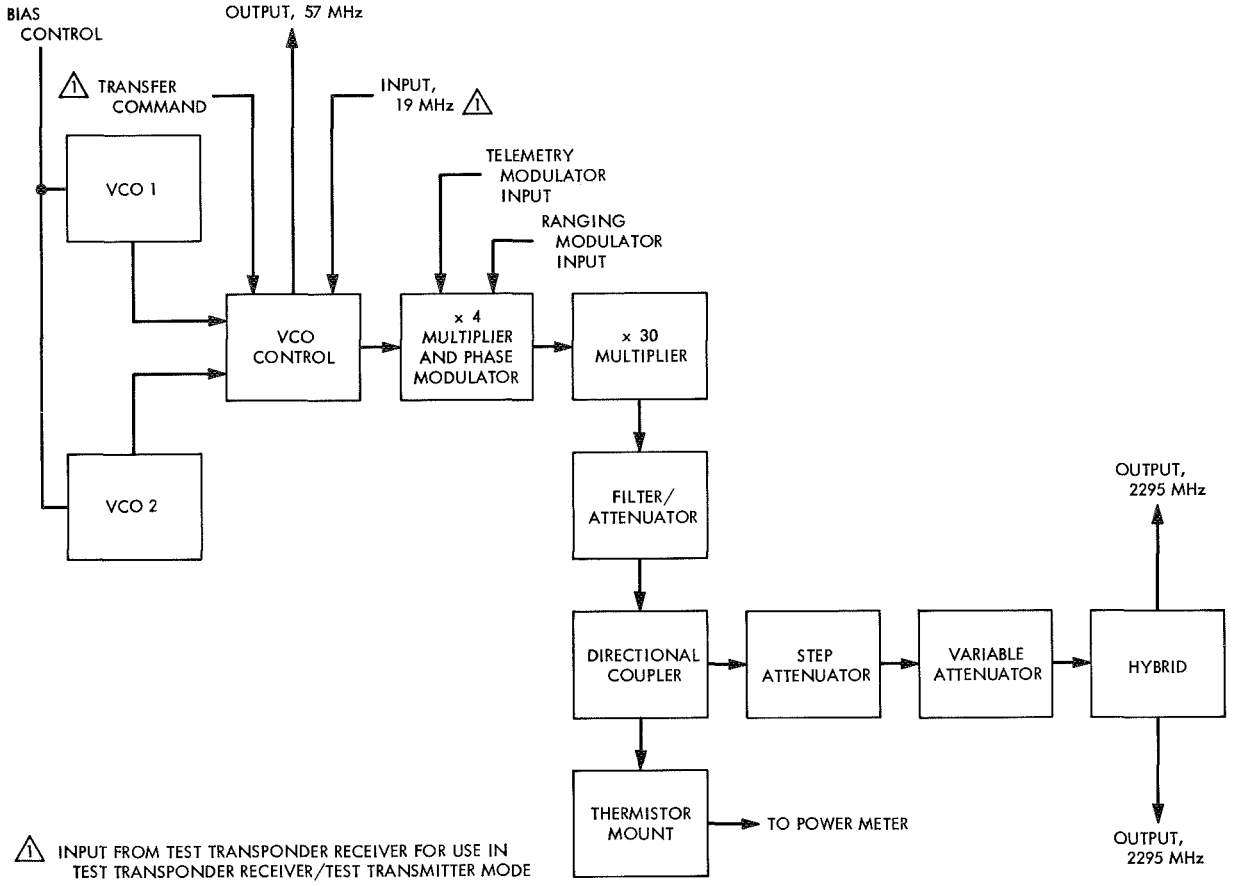

Fig. 25. Functional block diagram of test transmitter

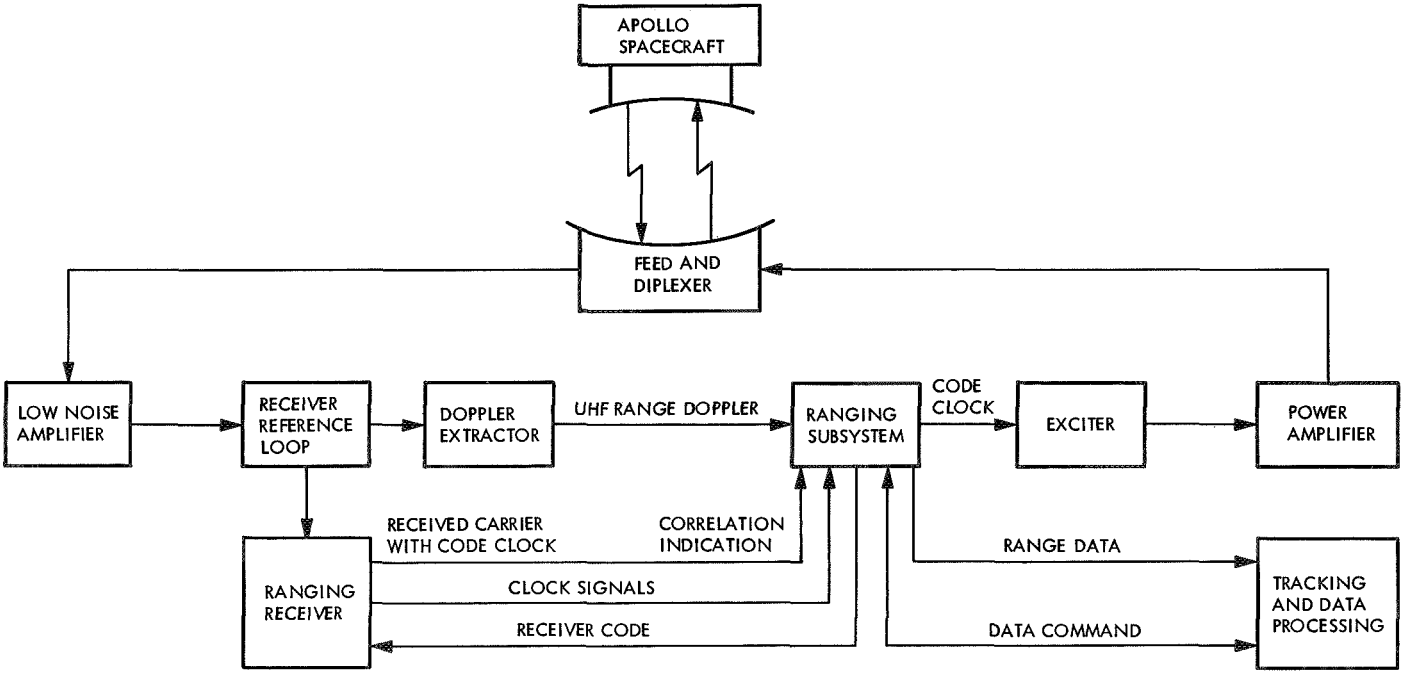

Fig. 26. Ranging function

Table 4. Test transmitter performance characteristics

Item	Characteristic
Frequency	2295 MHz (nominal)
Bandwidth	>15 MHz
Power output	−45 to −195 dBmW
Power output accuracy	Settable to ±0.5 dB of absolute
Phase stability	<9-deg peak in 2 β_{LO} = 20 Hz
VCO	
Frequency	19.125 MHz (nominal)
Tuning range	±3 parts/10^5 with a single VCO crystal
Frequency stability (at constant temperature)	1 parts/10^6, long term
Output monitor	3 times VCO frequency
Modulation	
Type	Phase
Deviation	Variable to 2.5 rad
Sensitivity	1 rad peak/V peak telemetry
	2 rad peak/V peak ranging
Stability	±5 % from 0 to 50°C
Bandwidth	1.8 MHz (min)
Radiation level	Less than −150 dBmW as detected by a tuned dipole 1 m from test transmitter
Spurious signal level	At least 40 dB below CW signal level

to the tracking and data processing subsystem upon command from that subsystem.

The subsystems directly involved in the determination and readout of range data are the S-band exciter and transmitter, the S-band receiver, the tracking data processor, and the Mark I ranging subsystem.

a. Basics of pseudo-random-code ranging. The basic nature of pseudo-random-code ranging is probably best explained by starting with a basic, though inadequate, concept and increasing its complexity as shortcomings become apparent. To this end, a series of what in German are called *gedanken-experimente,* or thought experiments, are conducted in this presentation.

Range measurement on a stationary reflecting target. By assuming a reflecting target rather than a transponder, and by stipulating that it be anchored in space, as shown in Fig. 27, its range may be determined in the most straightforward manner.

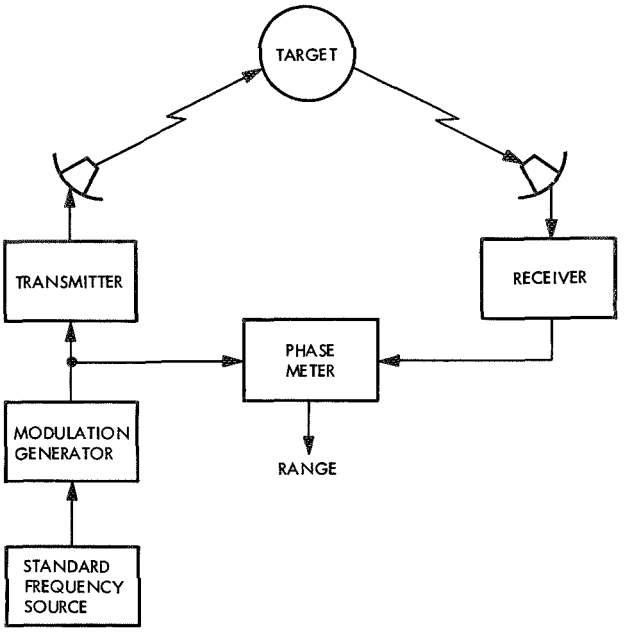

Fig. 27. Continuous wave radar ranging system

This example envisions a standard frequency source that serves to modulate an S-band carrier with periodic single pulses. The reflected modulation signal is detected in a receiver and, by means of a phase meter of some sort, the phase difference between modulation transmission and reception is determined. It will be found that the period of the pulse modulation (i.e., the interval between single-pulse transmissions) must be greater than the round-trip transit time. Otherwise, there will be ambiguities of integral pulse periods. Conventional pulse radar works in this way.

Range changing measurement on a moving reflecting target. Assuming the reflecting target is permitted to move, the concern is to detect the resultant changes in range. As the target moves, the phase meter reading changes, increasing as the target moves away.

Resolution of range measurements. The resolution of the range increment detection and the initial range determination depend on the precision of the phase meter. By designing the phase meter as a digital device as shown in Fig. 28, it was possible to attain almost any desired resolution, which will then be invariant.

The transmitter is shown to be modulated at a much higher frequency which, in turn, is continuously compared with the received frequency in a doppler detector consisting of a mixing device and a counting device; the

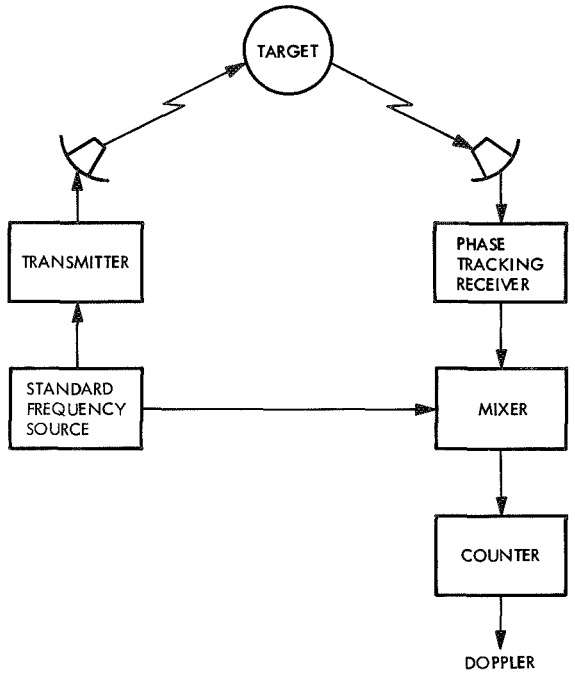

Fig. 28. Doppler measurement by coherent continuous wave radar

shorter the period of the modulating pulses, the finer the resolution of measurement.

The general ranging principle. In general, ranging consists of filling the uplink and downlink path with uniformly transmitted cycles of known period, determining the number of cycles in space at the start of ranging acquisition, and subsequently adding or subtracting cycles in accordance with motion of the target.

b. Determination of fractional cycle of initial range. Again, considering the target anchored in space, by subdividing the transmitter local oscillator frequency, a transmitter clock signal is derived that serves as one input to a clock doppler detector and also drives a transmitter coder that generates a continuous code (101010...) two bits in length, referred to as transmitter clock code. This then modulates the transmitter coherently with the carrier, as shown in Fig. 29.

A receiver clock signal is derived from the received modulation and fed to the other input of the clock doppler detector. In the absence of doppler (since the target is stationary), the received clock code will be delayed with respect to the transmitted clock code by some unknown integral number n of clock code periods τ, plus a delay d equal to some unknown function of τ. In other words, total round-trip delay $= n\tau + d$.

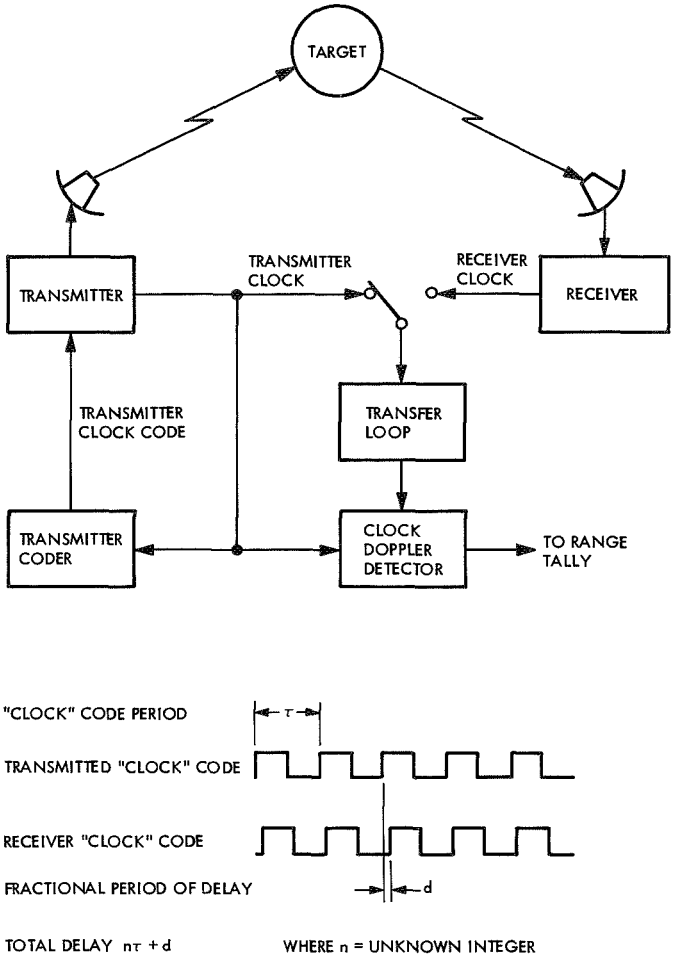

Fig. 29. Determination of fractional cycle

A clock transfer loop is then provided to help determine the value of d and concern about the number n is postponed until later.

A range tally is provided in the form of a digital accumulating register, in which range numbers, in range units, are tallied in accordance with outputs from the clock doppler detector.

At the start of range acquisition, the input to the transfer loop is switch-connected to the transmitter. The inputs to the clock doppler detector are then identical and there is no output. The range tally is set to zero range units.

The transfer loop is now switched to the receiver. As the transfer loop tracks into the phase without loss of lock, the doppler detector keeps track and causes tallying of range numbers in accordance with what appears to

be a slight spacecraft motion. This then corrects what would otherwise have been an error in range corresponding to the fractional clock-cycle delay d.

c. Determination of incremental cycles of range. Assuming, again, that the target is moving, the resultant increments in range will be detected, clock cycle by clock cycle, in the clock doppler detector and will be continually tallied in the range tally.

d. The complete ranging equation. The determination of total range at time t is based on the relation

$$R_t = R_0 + \int_0^t \dot{R} dt$$

where R_0 is the range at some reference time t_0 and the integral is the sum of range increments since that time. The mechanization of the ranging system is quite analogous to solving this integral equation.

First, the integration is performed by determining the incremental range throughout the time required for acquisition and the subsequent time of tracking. This is accomplished by continual tallying of range units corresponding to doppler cycles which, in turn, are derived from comparison of received carrier submultiple with transmitted carrier submultiple.

Secondly, the constant of integration R_0 is established by determining the fixed range at the start of ranging acquisition. This is accomplished by tallying range units corresponding to the time offset (or delay) between transmission and reception of a given point in the ranging code at the start of range acquisition. This, in turn, comprises the determination of the fractional clock-cycle delay d (already accomplished) and the determination of the integral number of clock cycles n (next step):

$$R_0 = d + n_0 \tau$$

The operations required to determine R_0 are referred to as range acquisition and are the only operations requiring the use of the pseudo-random codes.

e. Modulation pattern desiderate. For the purpose of precisely determining the number of clock cycles n, a modulation pattern having the following four characteristics is desired:

(1) A detectable overall periodicity greater than the maximum anticipated round-trip time. This is required to prevent ambiguous results, and means, in effect, that the measuring tape should be longer than the distance to be measured.

(2) A detectable, fixed, high-frequency periodicity within the overall modulation pattern. This is required for the sake of high resolution or precision of measurement. The clock code period of slightly over 2 μs, which has been discussed previously, will serve this requirement.

(3) The characteristic of two-level autocorrelation. This means that the overall pattern is required to be such that if the pattern is compared with the same pattern displaced by integral numbers of bits, the two patterns will match exactly in one relative position, and they will fail to match to the same degree in all other relative positions. The firm requirement here is that there be only one relative position that yields maximum correlation. If it is possible to have all other relative positions yield uniformly low correlation, the correlation detection is, of course, greatly simplified because it becomes a binary (or true–false) problem, rather than one of precise measurement.

(4) The characteristic of being essentially balanced (i.e., of having as many ones as zeros in it). While this is not an absolute requirement, balanced use of power in the carrier sidebands makes for higher efficiency and better system design.

f. Ranging codes. The problem is solved by the use of a pseudo-random binary sequence continually generated in the form of ones and zeros in digital equipment.

Figure 30 shows two cycles of such a sequence having 15 binary digits per cycle. Also shown is the rectangular waveform of a ranging code derived from the sequence where one is represented by a low level and zero by a high level.

To see whether and how this code satisfies the requirement for two-level autocorrelation, consider it matched against a second code, identical to that shown, but displaced by any number of digits other than 0, 15, or a multiple of 15. It will be found that the measure of correlation (i.e., of digit-by-digit matching) is uniformly low. It is high when the two codes are in phase, which occurs every 15 displacements in this example.

The resolution obtainable from a code as such is inversely proportional to the digit period. The maximum

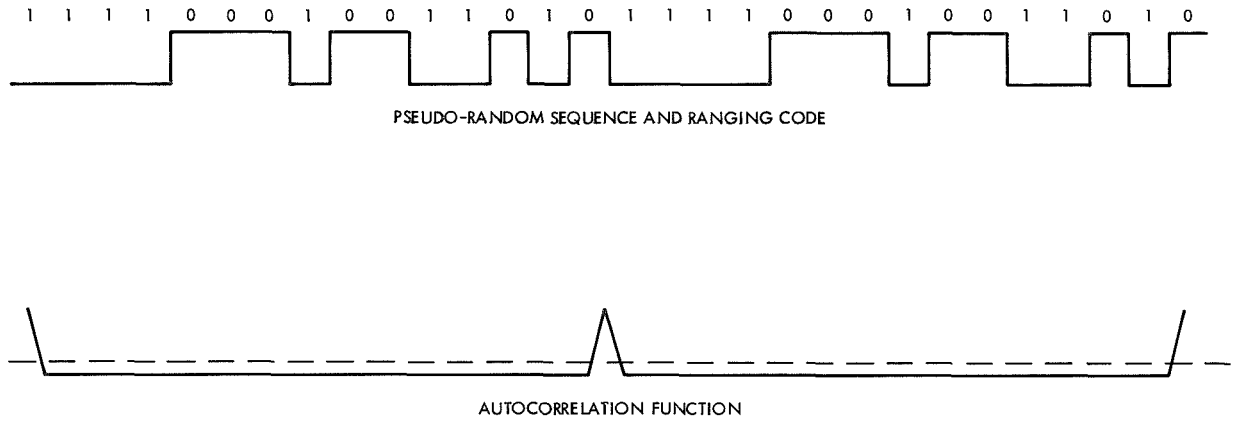

Fig. 30. Pseudo-random binary sequence and ranging code waveform

round-trip time that can be determined without ambiguity corresponds to the total length of the code (here, 15-digit periods).

In Fig. 31, a transmitter coder has been provided to generate the repetitive pseudo-random ranging code to be used to biphase modulate the transmitted S-band carrier.

A receiver coder has been provided to generate the same code as the transmitter coder, with additional features whereby this code can be matched to the received code in the receiver. It must, therefore, be time-movable by bits with respect to the received code or, in a way, with respect to the transmitted code. A reference must, of course, be provided for this receiver code shifting. Thus, when the transfer loop is still connected to the transmitter and the range tally reset to zero at the start of acquisition, the receiver coder is code-synchronized to the transmitter coder, as shown schematically by a switch.

g. The overall code and code components. With respect to the overall code to be used, a bit period 1/992,000 s, or slightly more than 1 μs, was chosen. This corresponds roughly to 300 m of round-trip distance or to 150 m of one-way range. It is intended that the Mark I reach to 800×10^6 m, requiring then a code of no less than 800/150, or $5\frac{1}{3} \times 10^6$ bits. Such a code can be generated directly, but its acquisition requires $5\frac{1}{3} \times 10^6$ correlation readings to determine the proper match.

It is possible, on the other hand, to generate such a long code by combining, bit by bit, several repetitive shorter subcodes or code components cleverly chosen. These components must meet the same requirements as the total code.

Provided their lengths in bits have no common factors, the length in bits of the total code is the product of the lengths in bits of the individual components, or 5,456,682 bits.

Furthermore, it is possible to acquire the total code by acquiring the components individually in turn. This reduces the number of correlation readings required from the previously suggested $5\frac{1}{3} \times 10^6$ to 232. It must be noted that the 2-bit *CL* component was not acquired by digital means in the Mark I, but rather by the process of locking up the clock loop in the ranging receiver.

Therefore, the transmitter code contains the five components *CL*, *X*, *A*, *B*, and *C*, combined bit by bit in accordance with a certain Boolean logical relationship. The receiver code as generated by the Mark I itself contained only the components *X*, *A*, *B*, and *C*.

h. The double-loop ranging receiver. Figure 32 shows a schematic diagram of a part of the ranging receiver. Here the *CL* component is designated as clock; the components *X*, *A*, *B*, and *C* in combination are designated as code; and the combination of all five components as code *X* clock. The code generator shown is the receiver coder of the Mark I. Its code output, matched against the received code *X* clock in a balanced detector, provides a clock output whose average amplitude is a measure of the degree of correlation between the received code and the receiver code.

The inner phase-locked loop, or clock loop, is initially locked up to the incoming clock component that it subsequently tracks, whether or not there is any code present.

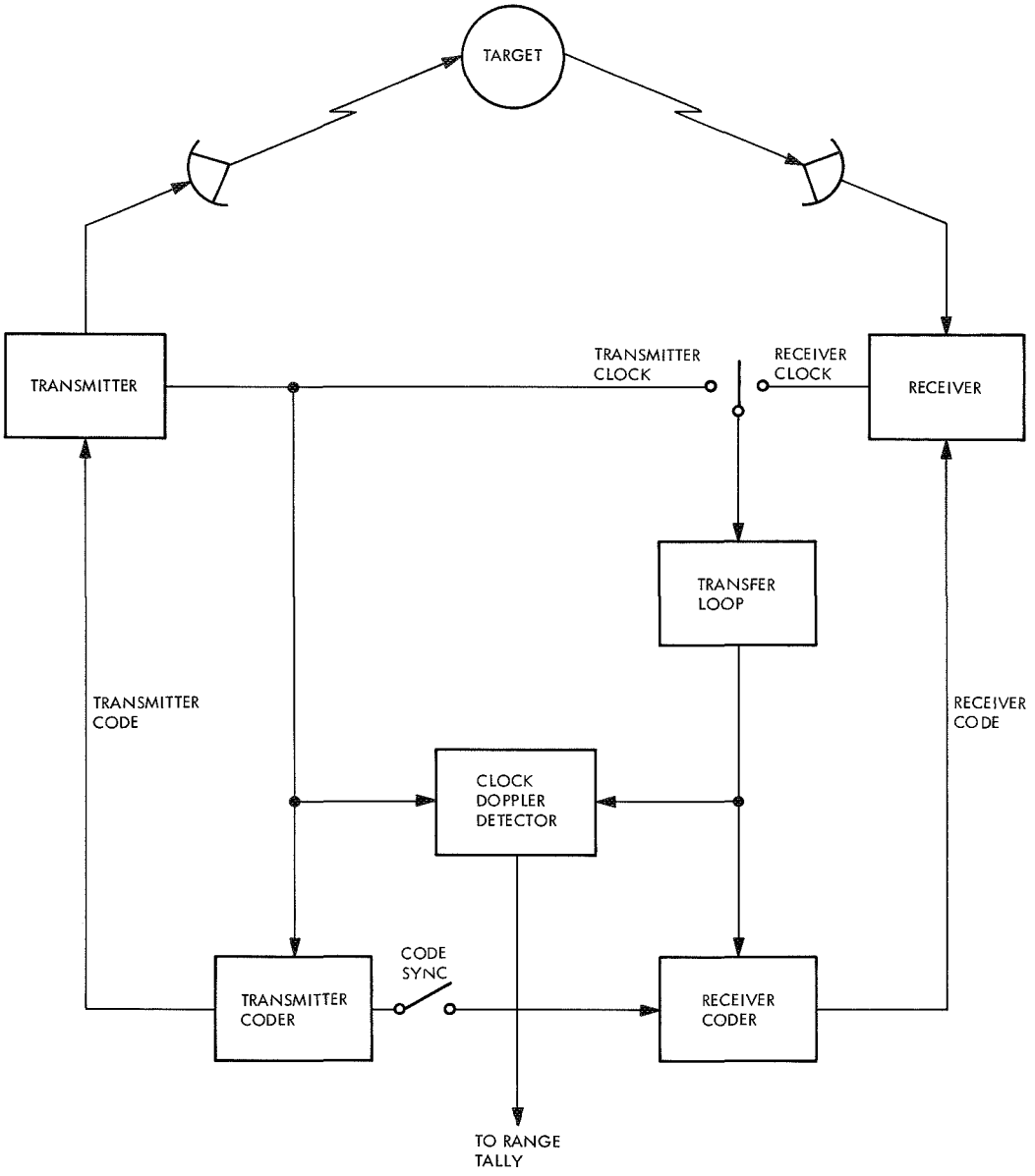

Fig. 31. Phase modulation of S-band carrier

The outer, or code loop, is held in gear by the locked state of the clock loop. It serves no other purpose than to match the received code to the receiver code.

i. Code correlation: determination of integral cycles of initial range. This matching is accomplished by digitally shifting the components of the receiver code and measuring the correlation indication at each relative shift position until a maximum is obtained.

The total ultimate shift of the receiver code from its initial phase is a measure of the initial range at the start of acquisition or, more correctly, a measure of $R_0 - d$ (both R_0 and d in units of time).

Each shift of each component in the process of acquisition is noted by adding the appropriate number of range units into the range tally whenever such a shift is made. This in no way interferes with the adding (or subtracting) of the previously mentioned clock doppler tallies, as required by target motion, which can occur simultaneously.

j. Resolution of measurement. The resolution of measurement is indicated earlier as being 1 clock doppler

cycle, for ease of presentation. Since this represents 2-bit periods of about 1 μs each, it corresponds roughly to 2 μs, or 600 m of round-trip distance, or 300 m of range. Actually, clock doppler tallies are made every quarter cycle, for a resolution of about 0.5 μs, or 75 m of range.

Once acquisition has been accomplished, the Mark I automatically switches from tallying every ¼ clock doppler cycle to tallying every sixteenth S-band doppler cycle. This improves the resolution by a factor of 72 to 1 range unit, or approximately 1 m.

k. Modulation change from code to clock. At the same time, or any time thereafter, it is possible to disable the full code modulation and modulate the carrier instead, with the 2-bit clock component only. There is, as previously indicated, no further need for the code; the clock component alone is responsible for keeping the clock loop in lock. The advantage of changing from full code to clock code lies in the fact that this not only cuts down on the required sideband power, but also limits the spectral distribution of ranging frequencies to two single spectral lines: 496 kHz above and below the carrier frequency.

3. Performance characteristics. To summarize, the performance parameters of the Mark I are as follows:

(1) Maximum unambiguous range of 800,000 km, or twice the distance to the moon.

(2) Resolution of 1 range unit, which is defined as

$$\frac{221 \text{ light-s}}{30 \times \text{transmitted frequency}}$$

and is of the order of 1 m.

Overall system inaccuracies of no more than 15 m were attributable to drifts and instabilities in ground and space loops.

Minimum range acquisition time was 1.6 s at strong signal levels and might possibly go as high as 30 s at lunar distances in the MSFN configuration.

Range data output was in binary range units and could be effected once per second.

4. Functional description. The subsystem (Fig. 33) is contained in one equipment rack of standard size and shape and comprises the following functional units:

(1) Transmitter coder.

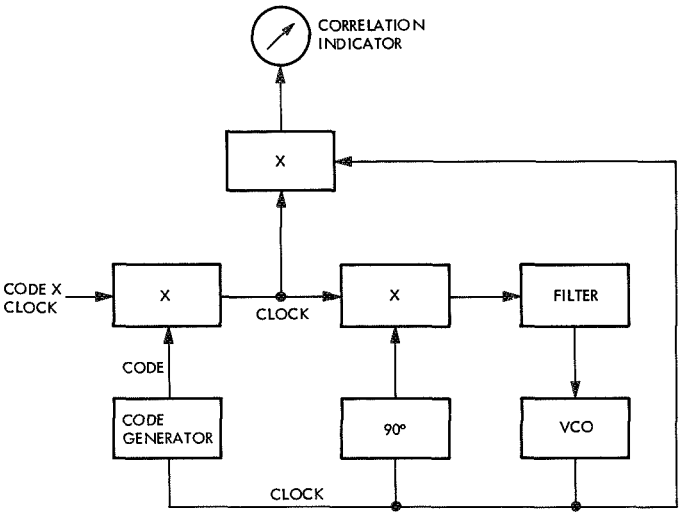

Fig. 32. Double-loop code tracking system

(2) Receiver coder.

(3) Timer.

(4) Number generator.

(5) Range tally.

(6) Readout register.

(7) Output buffer.

(8) Doppler-input buffer and doppler simulator.

(9) Program unit.

(10) Acquisition unit.

Most of these units consist of digital modules and modular assemblies. Other commercial units that form part of the subsystem are an analog-to-digital converter, a counter–timer, and a rack-mounted oscilloscope. Several special circuit modules are custom-designed. The design philosophy called for integrated subsystem completeness without dependence on auxiliary facilities or equipment for checkout, calibration, or troubleshooting.

a. Transmitter and receiver coders. The length of the pseudo-random binary digital code used for ranging determines the maximum unambiguous range that can be measured. The code is synthesized from several code components to minimize the steps, and hence the time, required for code acquisition. By choosing the components in accordance with certain mathematical criteria to feature two-level autocorrelation, the components are made individually acquirable. Complete code acquisition

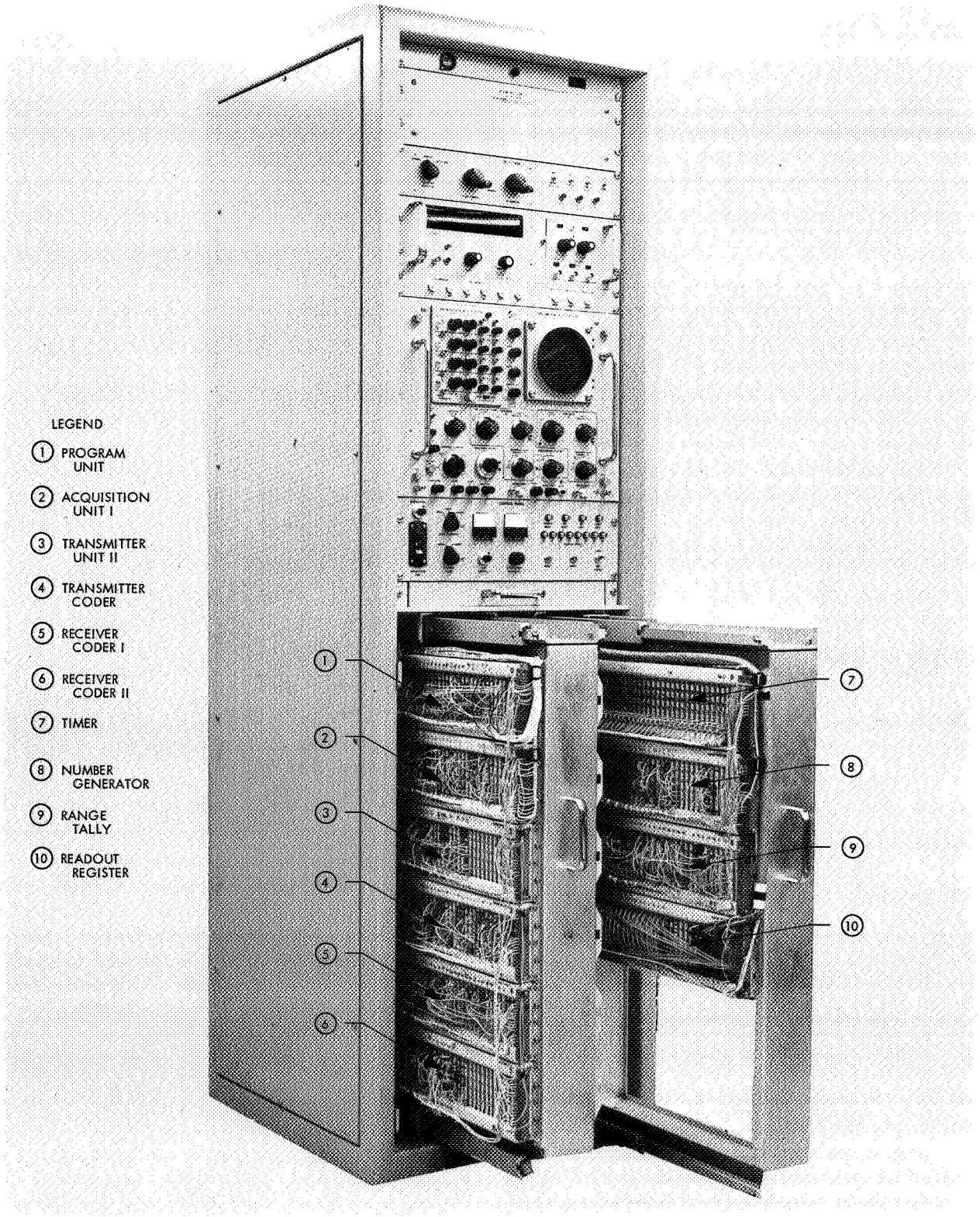

Fig. 33. Mark I ranging subsystem

is the immediate result of having acquired all the components. The subsystem acquires an individual code component by phase shifting that component in the receiver coder, one bit at a time, while automatically monitoring the resultant degree of correlation between the code fed to the receiver and the code modulation returned from the spacecraft.

The pseudo-random binary digital codes, which modulate the ground-to-spacecraft carrier and detect the ranging modulation on the spacecraft-to-ground carrier, are generated in the transmitter coder *XC* and receiver coder *RC*, respectively. The codes are made up of several components, suitably combined. The code components themselves are identical in the *XC* and *RC*. In Table 5, lower-case letters designate the components generated in the *XC;* upper-case letters designate those generated in the *RC*. The subscripts n and s are used to designate components used only in the normal or short (test) code, respectively.

All code components, except those of length 11, are generated in maximum-length shift registers. This is made possible by the fact that they contain $(2^n - 1)$ bits. The length-11 code components are direct-logic-generated Legendre sequences. Components of lengths 7 and 15 are generated in the same shift registers as components of lengths 63 and 127, respectively, suitably shortened by manual switch selection.

A word detector, provided for each code component in the *XC* and in the *RC*, generates a pulse each time that the component is repeated. A word coincidence detector, provided in the *XC* and in the *RC*, generates a pulse (w and W, respectively) each time the entire code is repeated. During a ranging operation the time delay between w and W is determined by means of a counter–timer, which provides a visual readout of the range for monitoring purposes.

Transmitter coder. A fifth code component, designated *cl* (clock), of 2-bit length, is generated in the *XC* only. The code components of the *XC* are combined in the Boolean logical form:

$$x \cdot cl + \bar{x} \cdot [(a \cdot b + b \cdot c + a \cdot c) \oplus cl]$$

The resultant code, in the form of a rectangular wave, is fed to the RF transmitter.

Table 5. Ranging subsystem code components

Selected range	Bit length of code component	Component designation in XC	Component designation in RC
Normal or short	11	x	X
Normal or short	31	a	A
Normal	63	b_n	B_n
Short	7	b_s	B_s
Normal	127	c_n	C_n
Short	15	c_s	C_s

Receiver coder. The four code components of the *RC* are combined in accordance with the respective acquisition mode of the ranging subsystem as follows:

(1) Acquisition mode 1. Code $X \cdot A$. This code serves to acquire components x and a of the modulation code on the returned signal.

(2) Acquisition mode 2. Code $X \cdot B$. This mode serves to acquire component b.

(3) Acquisition mode 3. Code $X \cdot C$. This mode serves to acquire component c.

(4) Acquisition mode 4. Code $X \cdot (A \cdot B + B \cdot C + A \cdot C)$. This mode is used for ranging, acquisition having been completed.

The respective resultant code, in the form of a rectangular wave, is fed to the RF receiver.

Means are provided to synchronize the code components in the *RC* to those in the *XC*, preceding ranging acquisition. Means are also provided to shift the *RC* code components individually with respect to their counterparts in the *XC*, one bit at a time. A "shift-left" command causes one bit of the selected code component to be skipped once, shortening the component. Conversely, a "shift-right" command causes one bit of the selected code component to be repeated once, lengthening the component. The 1-bit offset with respect to the component's counterpart in the *XC*, resulting from such a shift, is then maintained.

b. Timer. The timer is a 1-MHz 31-stage open-ended shift register. Each stage consists of a digital dynamic module, providing both direct and complemented ouputs with sufficient power to drive 20- and 40-gate loads, respectively, throughout the subsystem.

An input pulse is provided to the timer every 31 μs by the length-31 code component word detector of the transmitter coder. The "minor machine cycle" of the subsystem is defined as this 31-μs period. A two-stage binary counter, also run by this pulse, defines the 124-μs "major machine cycle" and its four minor phases.

c. Range tally. From the user's viewpoint, the range tally may be considered the heart of the ranging subsystem, since it is in this unit that the output information is synthesized. The range tally stores the current range number in series-binary form in a 31-μs, 31-bit circulating register, consisting of a magnetostrictive delay line and three binary adders-subtractors which, for brevity, will simply be called adders. The three sequential adders add algebraically the range numbers corresponding to the indicated changes in range or corrections as follows:

(1) Chinese-number adder. This adds the equivalent of the appropriate Chinese number[1] each time a 1-bit shift is made of a receiver-code component with respect to its transmitter-code component counterpart. This adder is used only during ranging code acquisition.

(2) Doppler-number adder. This adds the equivalent of the appropriate doppler cycle incremental count as it occurs, (viz., ¼-cycle increments of "clock" doppler or 16-cycle increments of RF doppler, depending on the system's mode of operation).

(3) Modulo-number adder. The greatest range number required of the ranging subsystem is that corresponding to the maximum unambiguous range which, in turn, is given by the product of the four code component lengths in bits. This modulo number is permanently available as an output of the Chinese-number generator. Whenever the accumulated range number exceeds the modulo number, the latter is subtracted from the accumulated range number total. Likewise, whenever the range number goes negative, a modulo number is added. These functions are performed in the modulo-number adder. The range tally is cleared (i.e., reset to zero) when the transmitter and receiver coders are synchronized, under program control.

[1]Stewart, B. M., *Theory of Numbers*, pp. 130–131. The MacMillan Co., New York, 1952. (See also "Chinese-Number Generator," in *The Deep Space Instrumentation Facility*, Space Programs Summary 37-21, Vol. III, pp. 17–18. Jet Propulsion Laboratory, Pasadena, Calif., May 31, 1963.)

d. Readout register. The readout register is a static shift register consisting of 31 flip-flops. A readout command pulse is received from the data handling system. This is translated into a 31-μs gate which, in turn, causes the range number currently circulating in the range tally storage to feed into and fill the readout register. The contents of the register remain static until the next readout command.

e. Output buffer. The output buffer consists of relays that are controlled by the ranging subsystem and sensed by other subsystems, specifically the RF receiver and the data handling subsystems. The former group of relays perform various operational and interlock functions. The latter group are the data output relays, which are driven, one-for-one, by the flip-flops of the readout register. Their configuration can then be sampled by the data handling system at intervals of one or more integral seconds. The output is thus in range units in binary (or octal) form, from which it may be converted into decimal measures of time or distance.

f. Program unit. The program unit controls the sequential operation of the ranging subsystem. In that this subsystem is a special-purpose machine, the program is permanently wired and is not readily subject to change as, for instance, from one mission to another.

The program unit provides a reset state and seven sequential program states, numbered p1, p2 ··· p7. In connection with the program unit, there are two operational pushbuttons on the control panel (viz, RESET and START). Actuation of the reset button causes the program unit to enter the reset state in which the unit is cleared and readout from the subsystem is disabled. Actuation of the start button is required for entry into state p1, with the additional provision that the selected S-band receiver and the ranging clock loop be in lock. Figure 34 shows a functional block diagram of the program unit. It shows the various program states, the condition for entry into each state, and the activities which the various portions of the ranging complex are called upon to perform in each state.

Once the start button has been pushed and the subsystem enters state p1, it goes through the other program states sequentially and automatically as the respective state-entry conditions are fulfilled. Finally, the program unit enters state p7, which is the tracking and ranging state. In this state the readout register is enabled, since valid range numbers are then available. If, at any time

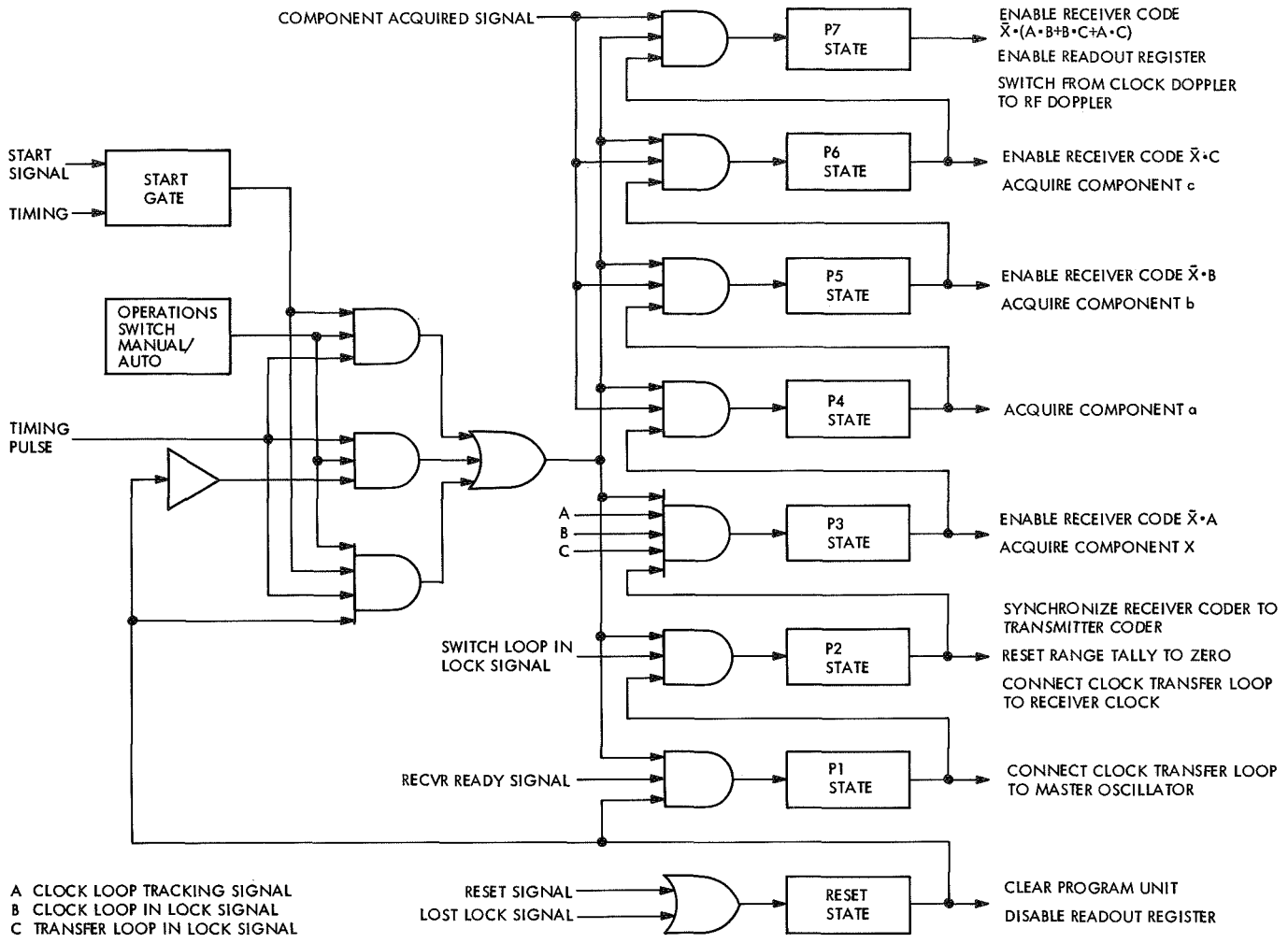

Fig. 34. Mark I ranging subsystem program unit

during acquisition or tracking RF lock is lost, the program unit immediately returns into the reset state.

Time synchronization of the program states is provided by a step pulse which, in the automatic mode of operation, is generated once each major machine cycle, or every 124 μs. Only at that time is it possible to step from one program state to the next.

A manual mode of operation is also provided for checkout, test, and troubleshooting purposes. In this mode the start button must be pushed not only to step from the reset state into state p1, but also to step from any other program state into the next in sequence.

Upon entry into states p3, p4, p5, and p6, an acquire pulse is generated that serves to initiate the acquisition subroutine for acquiring code components $x, a, b,$ and c, respectively. This subroutine is under the control of the acquisition unit. At the end of each component acquisition, a component acquired signal is received from the acquisition unit; this returns control to the program unit and permits it to advance into the next successive program state.

Once every major machine cycle (124 s) the program unit generates a convert command that is transmitted to the voltage digitizer. This causes the voltage digitizer to generate a digital sampling of the receiver code correlation voltage as of that moment.

g. Acquisition unit. The acquisition unit (Fig. 35) performs, without assistance from any other unit of the subsystem, the complete acquisition of a given component of the received code. A particular component

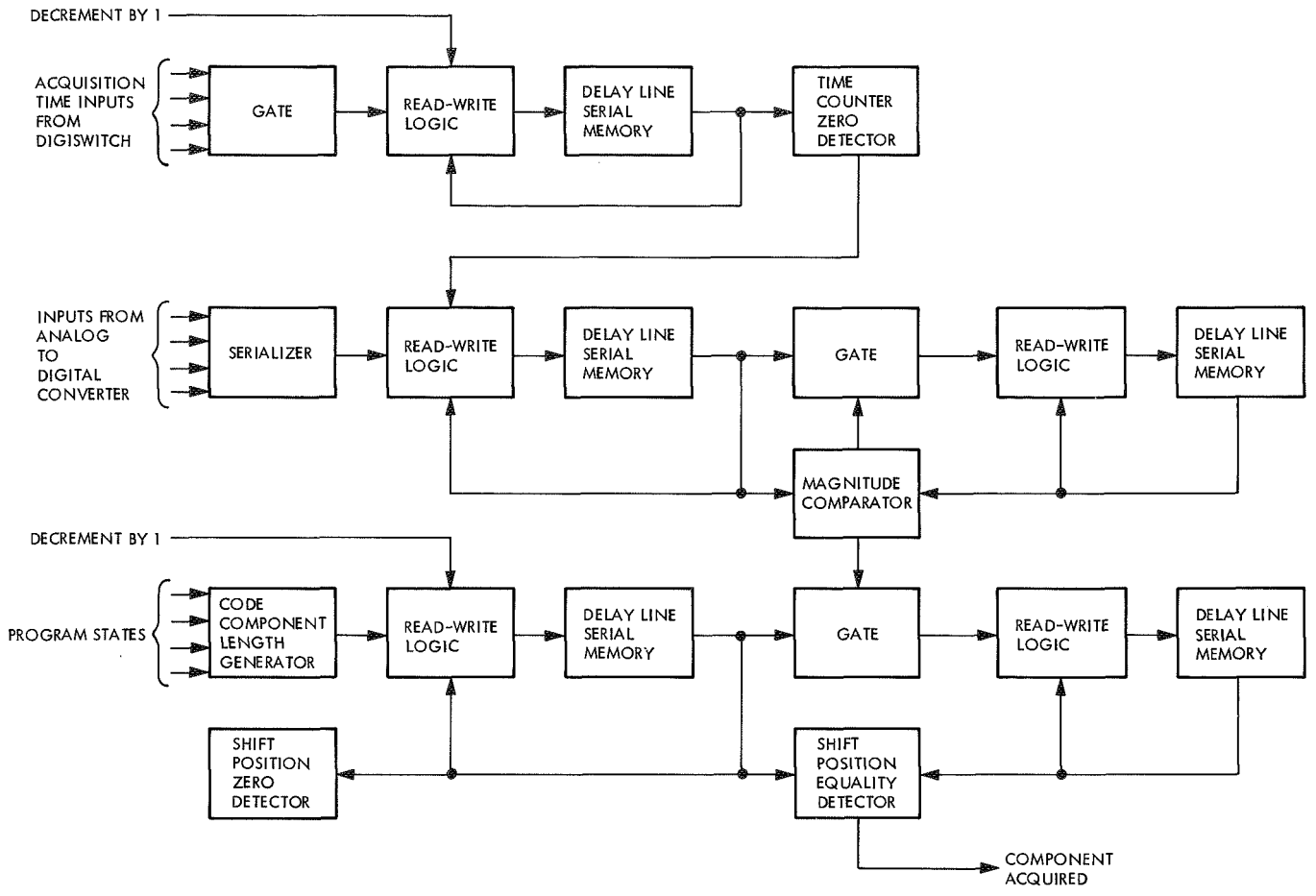

Fig. 35. Mark I ranging subsystem acquisition unit

acquisition is initiated by the program unit, as mentioned earlier.

The acquisition unit causes the receiver coder to shift the receiver code component one bit at a time, until all shift positions have been examined. After each shift the correlation voltage from the receiver is sampled and digitized a predetermined number of times. These samples are summed, yielding a finite time integral of the correlation voltage which, in turn, is an analog measure of the degree of correlation in phase between the received code component and the receiver code component. The shift position that yields the largest time integral is determined, and the receiver code component in question is then again shifted into that relative position. The particular code component has then been acquired, and control is returned to the program unit.

The digitizing of the correlation voltage is performed, on periodic command (every 124 μs) from the program unit, by a commercial analog-to-digital converter, the output of which is 10 binary bits plus sign bit.

The number of samples to be taken is a function of the received signal strength (i.e., signal-to-noise ratio). This must be determined by the operator prior to ranging acquisition. A multiposition Digiswitch on the control panel is then set to a suitable number of samplings. The switch settings permit a choice of from 1 to 2^{10} samplings per shift position.

The particular code component to be acquired is determined by the program state. Thus, components x, a, b, and c are acquired in program states p3, p4, p5, and p6, respectively. The binary number equivalent to the bit length of the component is initially gated into the shift-position counter. This number is then decremented by one each time the receiver code component is shifted. Thus, when this counter is in its zero state, the code component has been shifted through all positions and is back to its original position.

The number of samples to be taken for each shift position is, as mentioned earlier, determined by the manual setting of the Digiswitch. The binary number corresponding to the setting is stored in the time counter. For every sampling (i.e., once per 124-μs major machine cycle), this number is decremented by one. A zero detector senses when the counter reaches zero and initiates the next receiver-code-component shift command. After any code-component shift a certain amount of time must be allowed before the new RF steady-state condition can be reliably determined. The time counter is again used to provide this alternative function; the counter is preset with a number corresponding to the necessary time. Again, this counter is decremented by one every major machine cycle. The zero detector in this case initiates the start of the correlation-voltage integration.

The integrator sums the digitized correlation-voltage samples by adding each new sample to the previous content of the circulating register. When all the samples have been added, the register holds the correlation integral for that particular shift position.

The high-correlation storage is loaded with the first correlation integral obtained for a given code component. Each succeeding correlation integral is compared with the one currently in the high-correlation storage. If the new value is the larger of the two, it is made to replace the old one in the high-correlation storage and, simultaneously, the number currently in the shift-position counter is copied into the shift-position storage. Thus, when the integration has been performed in all shift positions of the code component, the number in the shift-position storage corresponds to the shift position that produced the largest correlation integral.

The shift-position counter is then loaded with the code-length number for the second time, the code component is shifted, and the position count decremented until the count is equal to the number in the shift-position storage. The code component has then been acquired, and the output of the equality detector signals the program unit to proceed into the next program state.

IV. Evolution of the NASA Receiver/Exciter/Ranging Subsystem for Use by the MSFN

A. Background Information

The NASA receiver/exciter /ranging (RER) subsystem, employed in the USB system, evolved in three stages from the original JPL block I S-band subsystem described in Section III. As design changes and improvements were made to meet the MSFN *Apollo* requirements, the subsystems reflecting these changes were designated as the blocks II, IIB, and IIIC configurations. Subsections B, C, and D of this section describe the changes that took place in these configuration blocks that led to the S-band RF subsystem delivered to the MSFN.

B. Block II RER Subsystem

1. Subsystem description. The block II MSFN receiver/exciter subsystem (Fig. 36) was similar in design to the block I described in Section III except as follows:

(1) Bandwidths were increased in the RF loop, AGC loop, range clock receiver, and telemetry channel to meet the *Apollo* mission requirements.

(2) Rapid receive/transmit frequency switchover capability was provided by multiple VCOs in both the receivers and exciters; the VCOs provided selection of any one of four MSFN operating frequencies.

(3) The VCOs provided increased tracking range capability ($\pm 9.0/10^5$).

(4) Both reference channel receivers (1 and 2) provided a 50-MHz output with AGC for FM reception.

(5) The range clock receiver and code clock transfer loop each accommodated the two-way phase coherent frequencies in the MSFN (or DSN) band with a single VCO.

(6) Phase adjustment was included to provide the same input signal phase to the range clock receiver from either reference receiver 1 or 2.

(7) Semiautomatic RF acquisition capability was provided to achieve rapid two-way RF carrier lock with the spacecraft.

(8) The S-band receive frequency test signal was coherently derived from the exciter frequency.

New modules to accomplish these changes were incorporated into all MSFN receiver/exciter subsystems.

2. Block II range receiver modification. In the block I receiver/exciter subsystem, the VCOs in the range receiver and code clock transfer loops had crystals at the

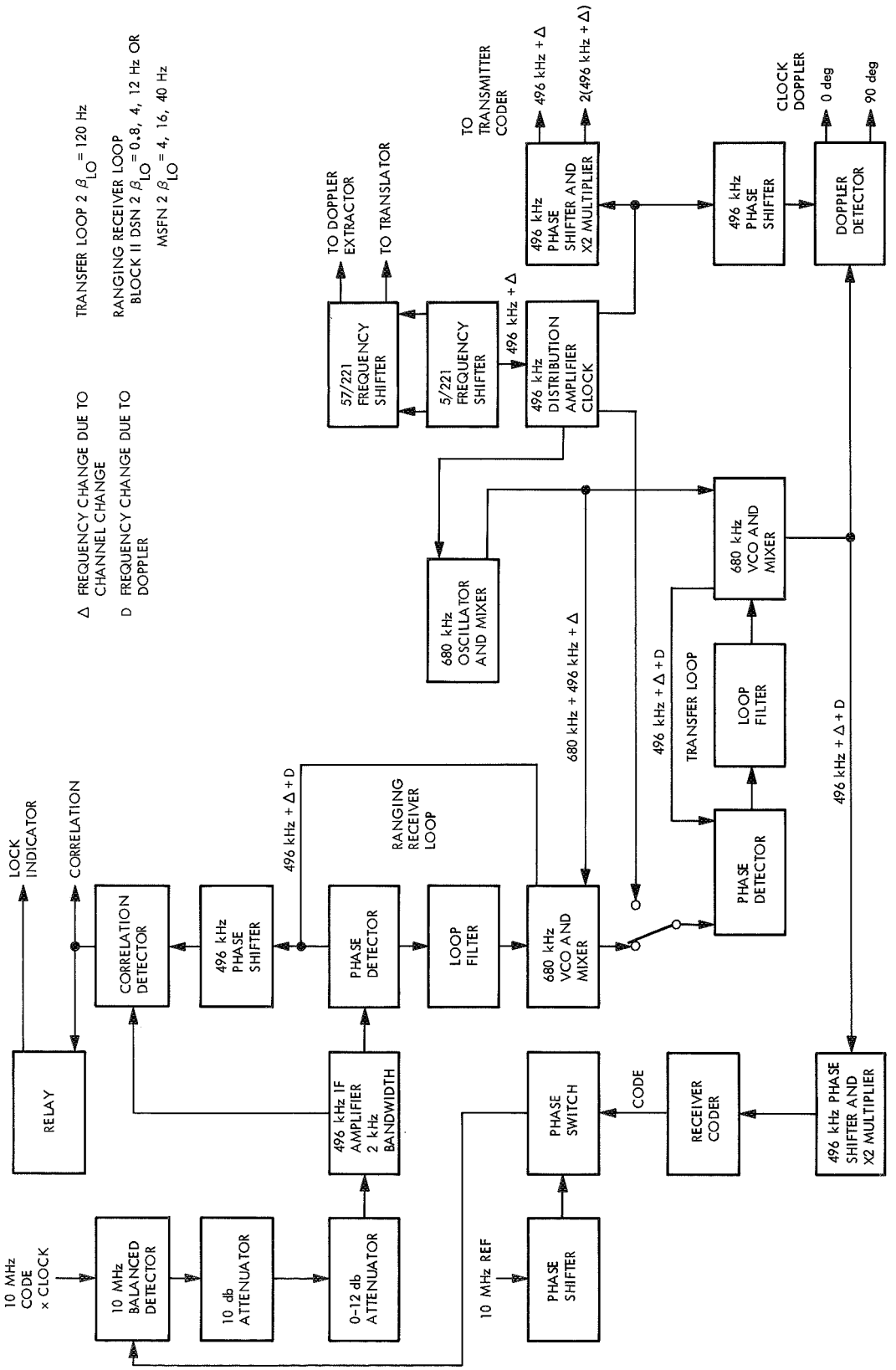

Fig. 36. Block diagram of block II ranging receiver

clock frequency. Because the clock frequency was related to the S-band exciter frequency f_t by the factor of 5/221 (f_t/96), it was necessary to replace the crystal in the range receiver and transfer loop VCOs each time the exciter channel was changed. The necessity for changing VCO crystals was eliminated in the block II subsystems by the injection of a reference signal into these loop VCOs (Fig. 37). The VCO output frequency (clock) is the difference between the reference signal and the 680-kHz VCO signal.

The reference frequency for the VCO units, generated within a 680-kHz oscillator/mixer, contain an internal 680-kHz crystal-controlled oscillator and a balanced mixer. The 680-kHz signal is summed with the clock signal generated from the exciter VCO, and, since the clock signal is changed as the exciter VCO is transferred from one channel to another, the reference signal frequency also follows the exciter frequency changes. The range receiver VCO output frequency, therefore, maintains its coherent relationship with the exciter VCO without the necessity of a crystal change.

Figure 38 shows a graph of the VCO characteristics within a typical 680-kHz VCO/mixer unit. Figure 39 shows the conversion bandpass characteristics between the 1.17-MHz reference input terminal and the 497-kHz output terminals on a typical VCO/mixer unit. The reference input frequency range, for an equivalent deviation of $\pm$10 MHz at the exciter S-band frequency (which covers the coherent MSFN and the DSN bands), is approximately $\pm$2.5 kHz. Measurements of the VCO stability of the oscillator/mixer configuration indicate comparable performance with the Goldstone duplicate standard receiver/exciter system. There is no measurable degradation in phase stability resulting from the use of the oscillator/mixer technique. In addition, evaluation of this technique indicated that there was no measurable leakage of the reference clock signal from the exciter into the receiver range and code clock transfer loops.

C. Block IIB Subsystem

1. Subsystem description. The block IIB design work started in July 1966 and resulted in a modification that provided the capability of operating the subsystem on either the DSN or MSFN channel by using a fixed frequency clock. On October 20, 1966, a contract was awarded to Motorola's Military Electronic Division for 50 range receiver modification kits. Each modification kit contained one each of the following:

Item	Contents
57/221 frequency shifter	—
496/1000 frequency shifter	—
Ranging loop filter modification pack	Parts, minor assemblies, and testing and inspection procedures for modifying block I subassemblies to block IIB
Correlation J-box modification pack	
System modification pack	Parts and minor assemblies to modify the subsystem cabinets rather than the subassemblies; required a complete subsystem test upon completion of modification

2. Block IIB ranging receiver modification. The fixed clock and reference frequency establishes a relatively constant delay in the range receiver. Except for doppler offset, the detected ranging receiver clock frequency is constant, thereby minimizing the effect of the predetection filter. A fixed clock frequency of 496 kHz was selected to be compatible with most of the existing hardware. The clock signal is derived by multiplying a 1-MHz signal output from the tracking station standard by a factor of 496/1000 (Fig. 40).

The subassembly that performs the 5/221 multiplication in the block II system to obtain the clock signal also generated two other coherent signals. These two signals drove a 57/221 frequency shifter subassembly to provide reference signals for the coherent translator and doppler extractor portions of RF system. Because the 5/221 output was not required when the fixed clock frequency was used, a new 57/221 frequency shifter was designed to replace both the 5/221 and 57/221 frequency shifters employed in the block II configuration.

The new 57/221 frequency shifter was developed to derive reference signals coherently related to the exciter VCO frequency by a factor of 57/221. These reference signals are required for the doppler extractor and the coherent translator.

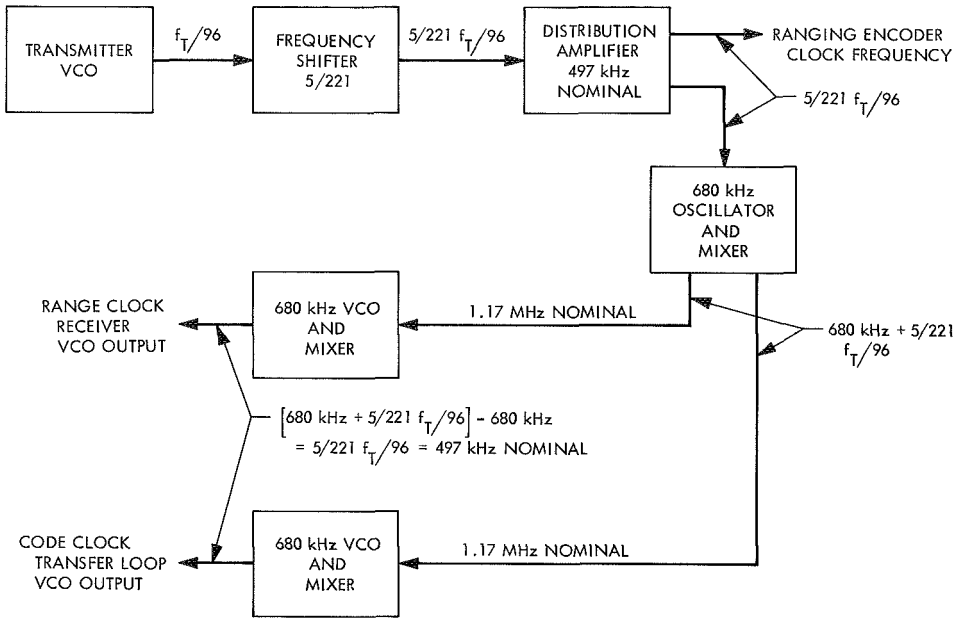

Fig. 37. Block diagram of range and code clock loop

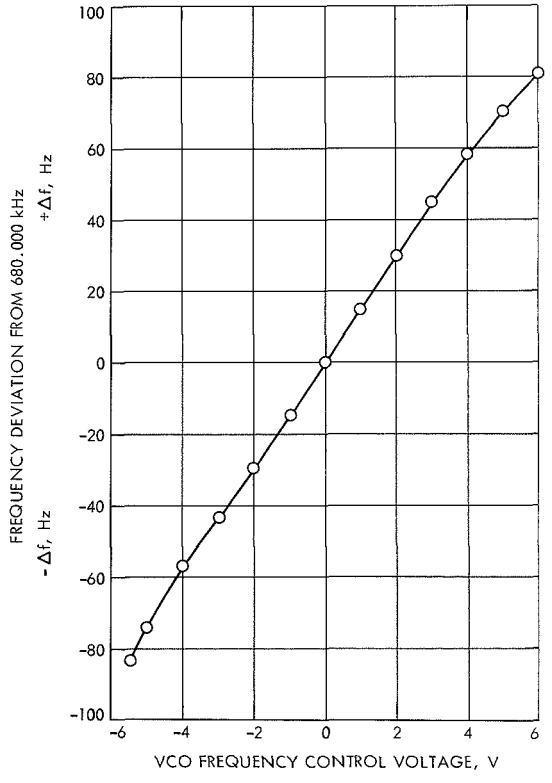

Fig. 38. Voltage-controlled oscillator frequency vs control voltage

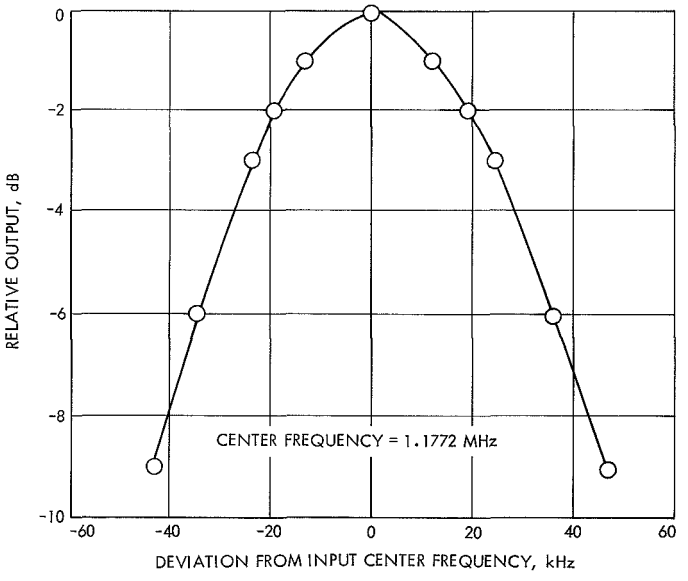

Fig. 39. Conversion bandpass characteristics, 680-kHz VCO/mixer

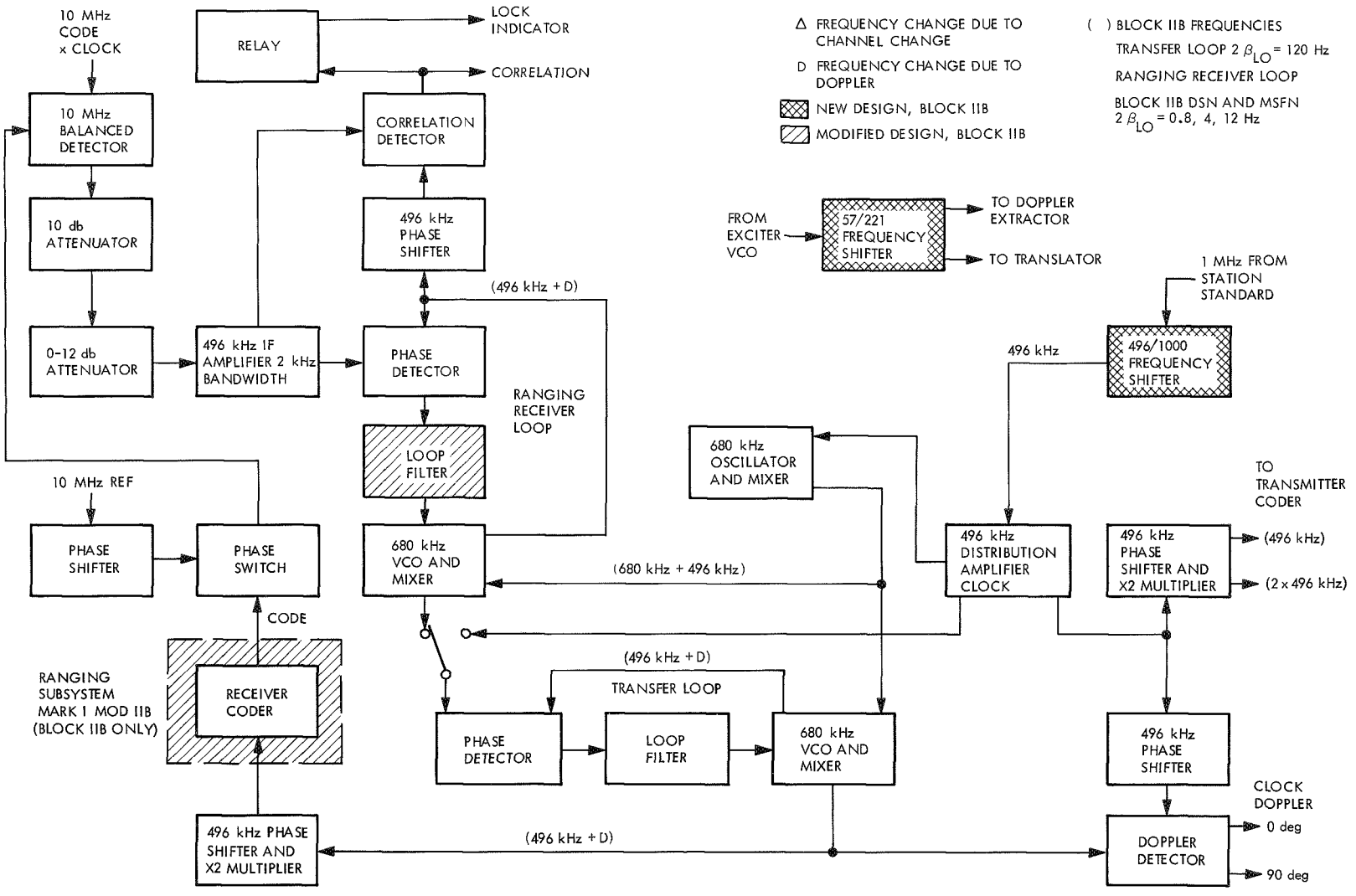

Fig. 40. Block diagram of block IIB ranging receiver

Basic to the operation of the frequency shifter is the type of synchronized oscillators used to perform the division processes. Although schematically the oscillators appear to be similar to the conventional type, their operation is entirely different.

In the conventional type, the natural frequency (tuned circuit resonant frequency) is the desired frequency. It is difficult to force the circuit to oscillate at frequencies higher or lower than its natural frequency by an external signal and, therefore, it can be synchronized only over a narrow frequency range. During the development of the 57/221 frequency shifter, it was found that this type of oscillator would not perform the high-division ratios over the required frequency range. Another characteristic of the conventional locked oscillator is its relatively large degree of phase instability. Since the natural frequency of the oscillator is the desired frequency, synchronization is maintained by supporting this natural oscillation with the incoming signal. This does not occur at precisely the same phase in each cycle, and phase instability occurs. In addition, oscillator drift with temperature change causes loss of synchronization unless compensation is added.

To meet the requirements of the block IIB 57/221 frequency shifter design, it was necessary to investigate other means of synchronizing an oscillator circuit. The use of avalanche breakdown as a method of synchronizing was explored.

The avalanche-type locked oscillator depends on the breakdown point as well as its tuned circuit to establish the output frequency, making it more easily controlled by an external signal.

Control of the output frequency is relatively independent of the collector tuned circuit. Consequently, it is not necessary to pull the naural oscillator frequency when changing the frequency of the input synchronizing signal. The avalanche oscillator, therefore, inherently has a much larger lock range than the conventional type. Measurements of two divide-by-five circuits (28.35–5.67 MHz), one of each type, show the lock range for the avalanche oscillator to be more than four times that of the conventional oscillator. The conventional type was optimized for lock range before performing the measurements.

Controlling the synchronism of the oscillator by avalanche breakdown, rather than supporting the natural frequency of the oscillator, gives a more positive lock. This has been demonstrated in phase instability measurements made on both types. To accomplish this, two identical avalanche divide-by-five circuits (28.35–5.67 MHz) were compared, using a 5.67-MHz phase detector. The two divide-by-five circuits were driven by the same signal generator to eliminate the instability of the source. Then an avalanche and a conventional divider were compared in the same manner. The measurements indicated that the phase instability contributed by the conventional locked oscillator divider circuit is approximately four times as great as that contributed by the avalanche type. The contribution of the avalanche oscillator in the second measurement is negligible, so this measurement represents approximately the instability of the conventional locked oscillator.

Because of the method of synchronization, the avalanche oscillator demonstrated several advantages over the conventional locked oscillator. The advantages are that it:

(1) Maintains synchronism over a greater frequency range.

(2) Has less inherent phase instability.

(3) Is less sensitive to temperature changes.

A block diagram of the 496/1000 frequency shifter, which generates the fixed 496-kHz clock signal, is shown in Fig. 41. A 1-MHz signal is divided into two paths. One path connects the 1-MHz amplified signal to one input of a balanced mixer. The second path is used to synchronize an oscillator whose output is tuned to 200 kHz. Two similar divide-by-five stages follow, generating an 8-kHz signal that is applied to the second input of the balanced mixer. The 992-kHz difference frequency at the mixer output is selected by a crystal bandpass filter. After two successive stages of amplification, the 994-kHz signal is used to synchronize a divide-by-two oscillator circuit generating the desired 496-kHz signal.

3. ***Mark IA ranging subsystem.*** The fixed ranging clock frequency of the block IIB receiver/exciter caused a noninteger ratio to exist between the clock and RF doppler frequency. The doppler counting logic of the Mark I was therefore changed to allow the RF doppler to be tallied correctly and the subsystem redesignated as the Mark IA.

Figure 42 illustrates the method of doppler counting used in the Mark I ranging configuration. Both the clock and RF doppler signals pass through an input buffer to

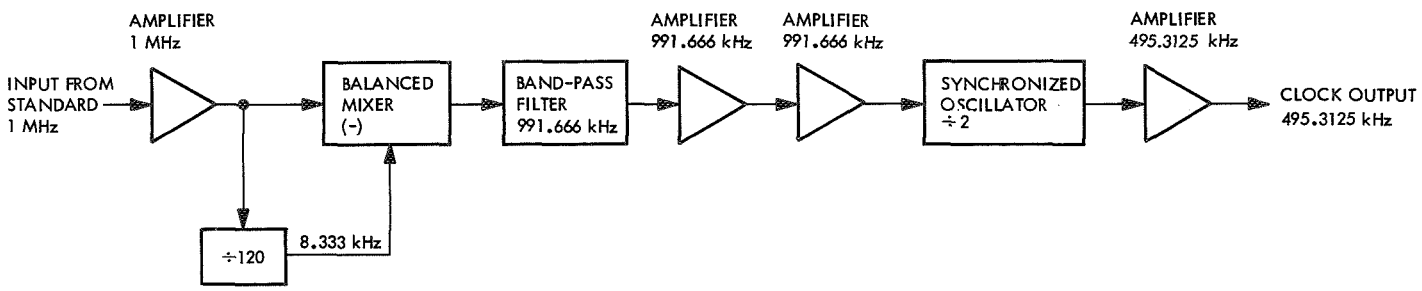

Fig. 41. Block diagram of 496/1000 frequency multiplier

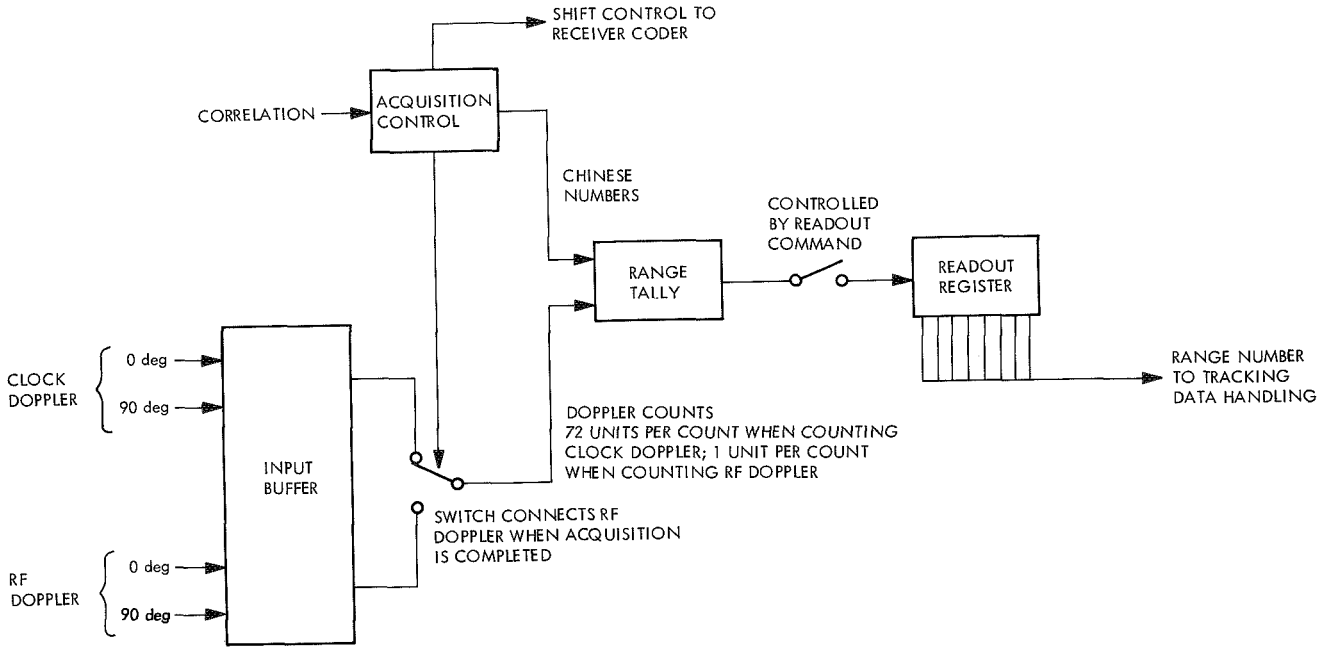

Fig. 42. Mark I doppler tally

the range tally. The doppler selector routes the clock doppler to the range tally during code acquisition, and RF doppler to the range tally during the tracking portion of the ranging operation. The clock and RF doppler counts are related to each other by a fixed ratio: 72 RF doppler counts = 72 range units (RU) = 1 clock doppler count. The length of the range unit in light-time units is dependent upon the ranging clock frequency, which, in turn, is derived from the transmitter frequency F_t, and is:

$$1\,RU = \frac{1}{2 \times 288 \frac{5}{221} \times \frac{f_t}{96}} \text{ light s, one-way range}$$

In the block IIB configuration, the ranging clock frequency is fixed at 496 kHz. The range unit is, therefore, a constant length, and is

$$1\,RU = \frac{1}{2 \times 288 \times 496\,\text{kHz}} = 3.5002 \text{ light s, one-way range or approximately } 1.049 \text{ m}$$

Figure 43 illustrates the manner in which the clock and RF doppler are counted in the Mark IA configuration. The range tally retains the Chinese number and clock doppler tallying functions. The RF doppler tallying is done by a new subassembly called the doppler unit that contains the RF doppler input buffer, fine range accumulator, and range number adder.

The range tally stores the portion of the total range that resulted from code shifting and clock doppler counting, and the doppler unit stores the range change that

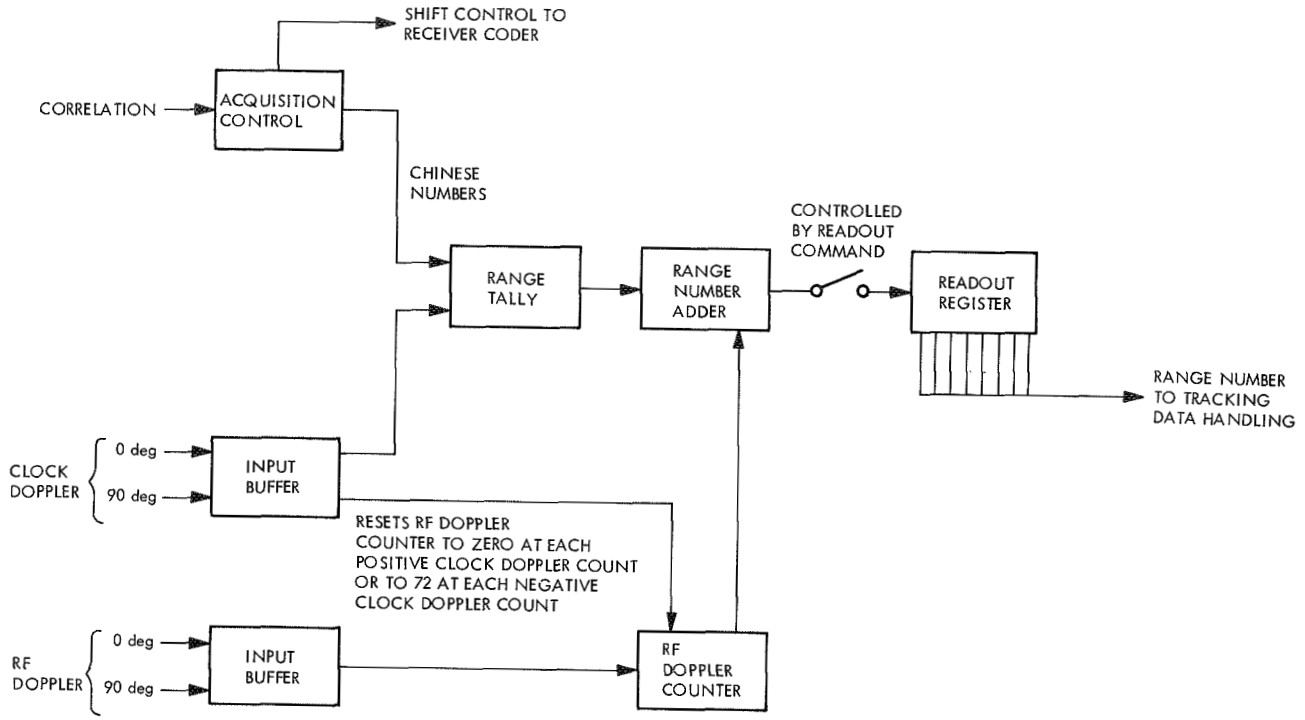

Fig. 43. Mark IA doppler tally

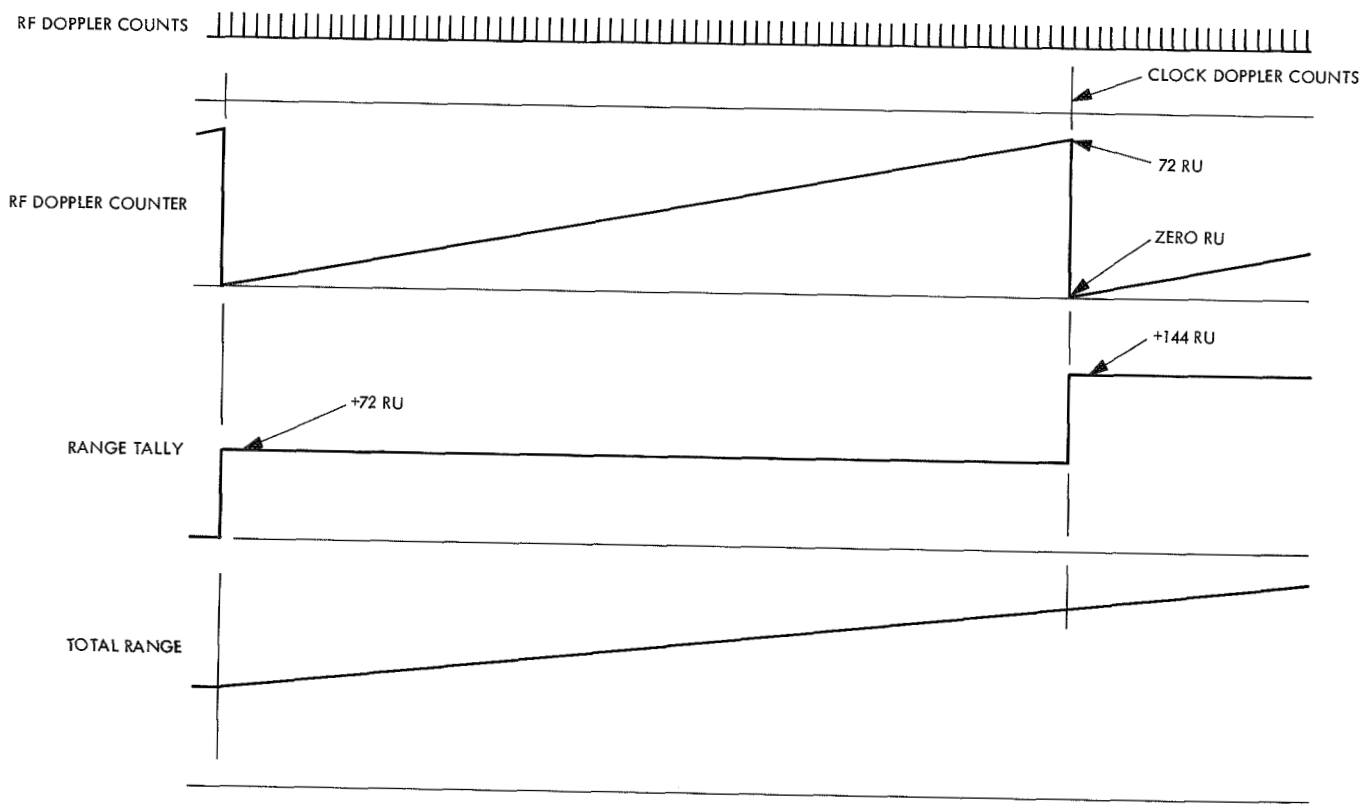

Fig. 44. Timing diagram

occurred since the last clock doppler count. The doppler unit counts the number of range units of RF doppler between clock doppler counts (Fig. 44). When the range to the spacecraft is increasing, a clock doppler count causes 72 range units to be added to the range tally, and the doppler unit to be reset to zero. The RF doppler counts then accumulate in the doppler unit until the next clock doppler count resets it to zero. If the range to the spacecraft is decreasing, a clock doppler count causes 72 range units to be subtracted from the range tally, and the doppler unit to be set to 72. The range number adder sums the outputs of the range tally and the doppler unit to provide an output that is the total range.

D. Block IIIC Subsystem

1. Subsystem description. The degree of similarity between the MSFN and the DSN versions of the S-band RER subsystem stimulated interest in a block III version that would be capable of operating in either the MSFN or the DSN frequency band with the proper performance characteristics. Several configurations (A, B, and C), with varying flexibility and changeover time, were proposed as a block III modification to the block II RER subsystems. The C configuration was adopted, and block IIIC modification kits were produced by the Philco Western Development Laboratory under JPL contract for use with all MSFN and DSN RER subsystems (Fig. 45).

The following are the five major changes introduced into the RER subsystem by the block IIIC modification:

a. Wider RF bandwidth. The MSFN and DSN frequency assignments are in adjacent bands. The total required transmitter channel bandwidth is in excess of 20 MHz, whereas that of the receiver channels is in excess of 30 MHz. Block II systems had an RF bandwidth of only about 15 MHz, centered near the middle of their respective channel assignments. The subassemblies having a significant effect on the RF bandwidth (preselectors and $\times 32$ multipliers) were discarded from the block II equipment, and replaced by the new wideband equivalents (preselectors, $\times 4$, and $\times 8$ multipliers) supplied in the III-C kits.

b. Increased communication channels. The communication channel nominal frequencies of the subsystems were established by crystals contained within receiver and exciter multiple VCOs. Each VCO contained four crystals. When a desired channel crystal was not present in a particular in-system VCO, the VCO required removal, and an appropriate replacement (containing the desired crystal) substituted. This substitution was not a necessity in the MSFN equipment; only four channels (maximum) were required. However, the DSN assignment had 26 channels, and VCOs had to be substituted from time to time for particular missions.

The block III-C modification supplied VCOs containing crystals for the MSFN channels for use in the DSN stations and, conversely, supplied VCOs containing crystals for four designated DSN channels for MSFN use.

c. Increased number of closed-loop bandwidths. The DSN program commitments required that the RF equipment be capable of exceedingly weak signal performance. This led to narrow phase-lock-loop overall bandwidths (12, 48, and 152 Hz) and an associated narrow predetection bandwidth (2 kHz). On the other hand, the MSFN stations normally received strong signal carriers with large frequency variations caused by high doppler rates. These conditions required wide phase-lock-loop bandwidths (50, 200, and 700 Hz) and an associated wide predetection bandwidth (7 kHz).

Because the receiver loop filters in the block IIB configuration all contained time-constant components, which established one or the other of the above sets of bandwidths, it was not necessary to supply complete new filters in the modification kits. Only parts and minor assemblies were required for installation in the field. Similarly, it was not necessary to discard the entire 10 MHz IF amplifier subassembly containing the predetection filter. It was only necessary to remove this filter and replace it with a broadband transformer in the field.

The parts to accomplish these field modifications were supplied in the modification kit "mod packs." To obtain the required predetection bandwidths, the modification kits also contained the new subassembly designated the "10 MC (MHz) filter amplifier." This subassembly, as mentioned, contained selectable predetection filters compatible with the two mentioned sets of bandwidths. Within the subsystem, this subassembly replaced a variable attenuator. The attenuator function was replaced by close tolerance adjustments within the dual filter amplifier subassembly and were performed as part of the factory alignment procedure.

d. Common AGC loop bandwidth. It had been determined that only one set of AGC loop time-constants

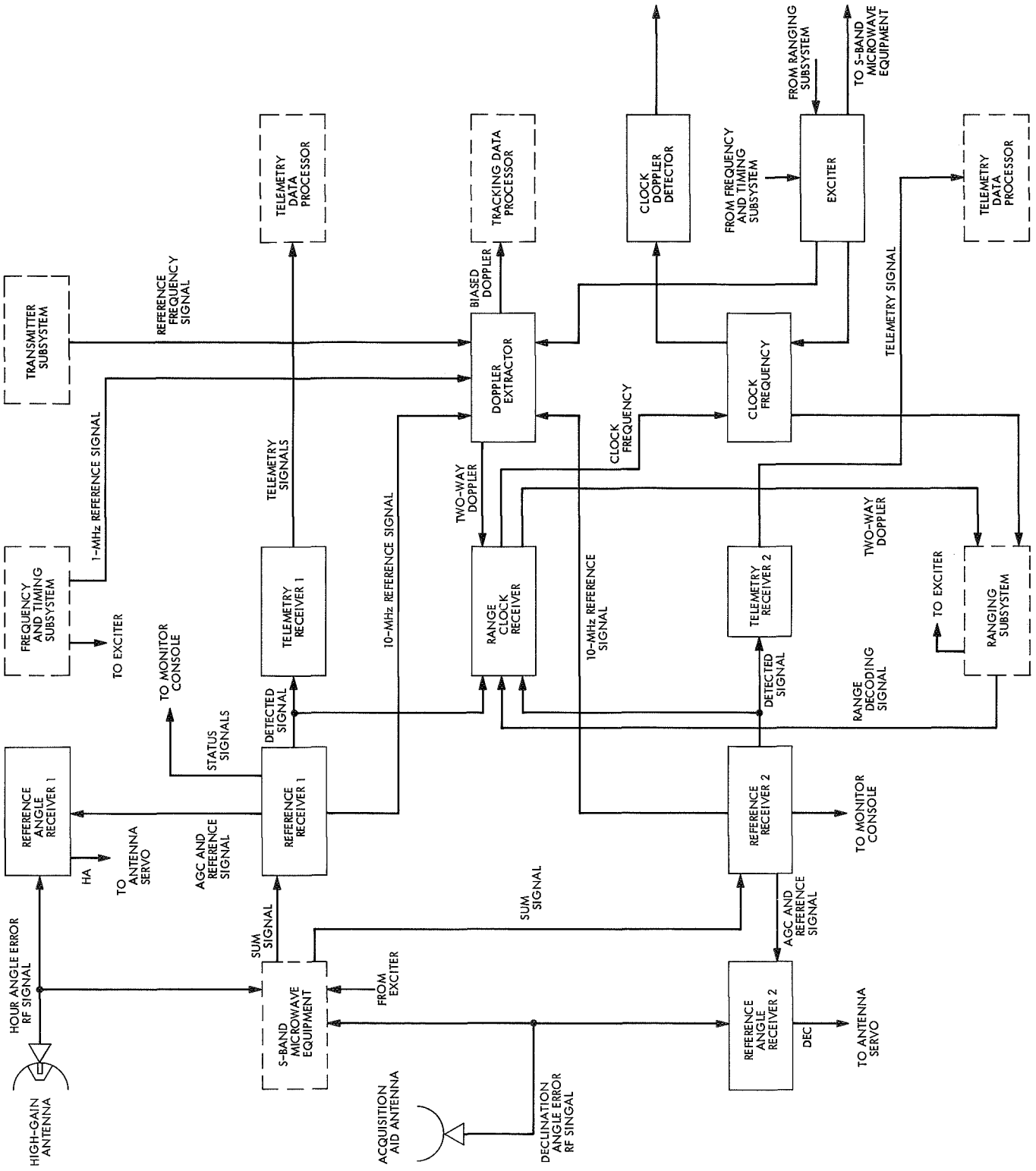

Fig. 45. Block diagram of block IIIC receiver/exciter subsystem

would be necessary in the block III MSFN/DSN configuration. The AGC loop filters required field modification to establish the time constants. Modification packs to accomplish this were part of each modification kit.

c. Switchover capability, MSFN/DSN. In addition to the aforementioned items, certain wires, cables, and miscellaneous hardware such as attenuators, plates, and brackets were required to modify equipment within the subsystem racks. These miscellaneous items completed the integration of each subsystem to the block III-C configuration.

2. Exciter tuning range. The ×32 frequency multiplier and UHF buffer amplifier of block II RER was capable of delivering the required drive level to the power amplifier over either the DSN or MSFN 10-MHz bands but not over the combined 20-MHz band. In block IIIC (Fig. 46), the ×32 frequency multiplier has been replaced with a design that has an adequate bandwidth to cover both the DSN and MSFN frequency bands. This is accomplished in two subassemblies, an ×4 and an ×8 frequency multiplier. The 27.5 dBmW minimum output level of the block IIIC multiplier chain provides adequate drive to obtain the 20-MHz bandwidth from the block II UHF buffer amplifier.

The ×4 frequency multiplier subassembly consists of two cascaded low-level balanced diode doublers separated by an isolation amplifier and followed by four stages of amplification. A coaxial commercial bandpass filter is installed between the first two of the four cascaded amplifiers to provide rejection of harmonics of the input frequency other than the ×4.

The ×8 frequency multiplier uses some of the latest techniques in step recovery diode frequency multiplication. The ×8 frequency multiplier was developed for use in the local oscillator and transmitter exciter multiplier chains. To achieve this modification with a minimum amount of change, the physical design of the unit was made compatible with the available mounting space in the system. The block II multiplier chains included an ×32 module. In the modified chain, this multiplication is accomplished in two steps: a solid state ×4 and amplifier module, and a step-recovery diode ×8 unit. A multiplication factor of 8 was chosen to achieve the power output required consistent with the input power

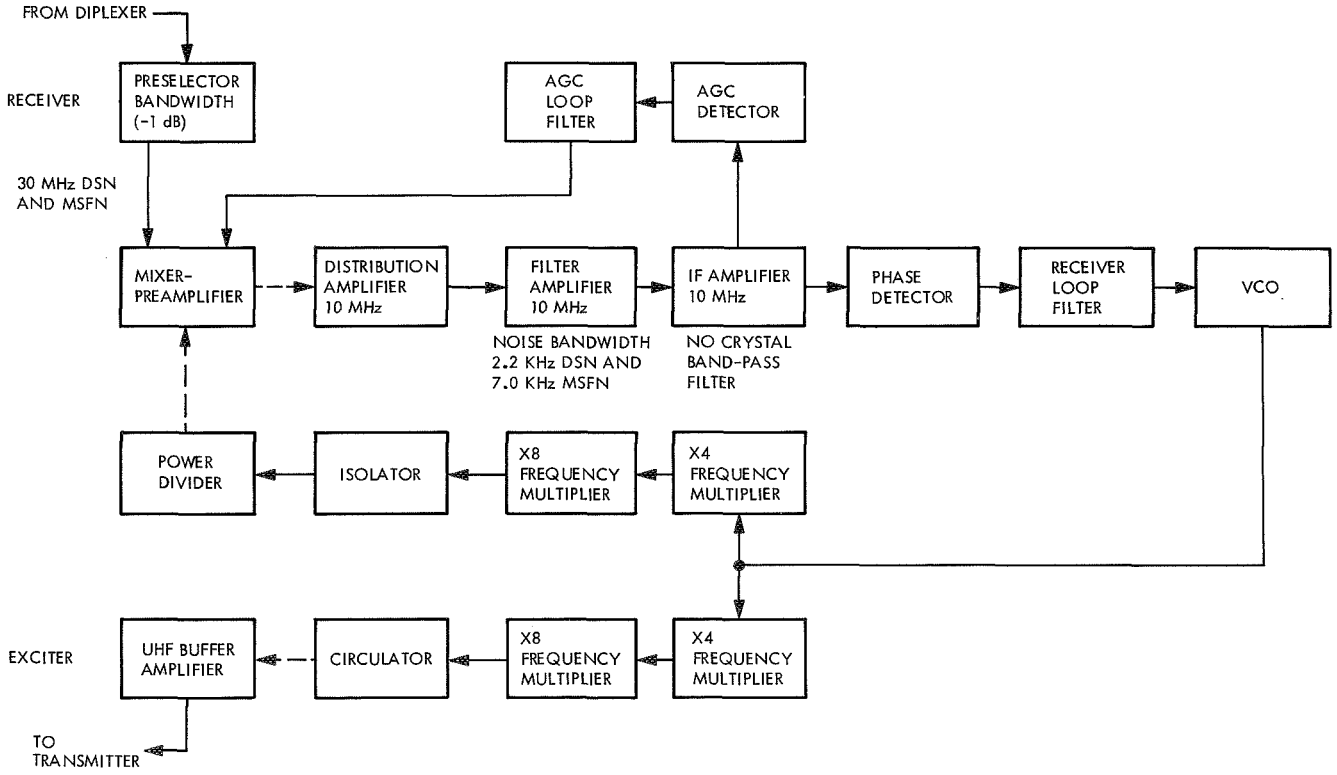

Fig. 46. Block diagram of block IIIC DSN and MSFN exciter/tuning range

capability of the available diodes. This also places the input frequency in the VHF region of 260 to 280 MHz where sufficiently high levels of power can be generated with transistor circuits. An added advantage of an ×8 unit is the fact that the nearest sideband at the output is 260 to 280 MHz away from the center of the output bandpass. This allows sufficient suppression of undesired sidebands to tolerable levels with a minimum number of output filtering stages. Considerable effort was exerted towards making the design as simple as possible without compromising performance so that the unit would be easily reproducible and require a minimum amount of testing time.

Performance characteristics of the unit are presented in Table 6.

The tuning range of the multiplier is sufficiently wide (1900–2300 MHz) to allow the use of the same unit for both exciter and local oscillator application by applying the appropriate input signal and tuning the output cavities to the corresponding output signal.

3. Receiver tuning range. The problem of adequate tuning range in the receiver local oscillator for both DSN and MSFN combined bands was resolved in block IIIC by replacing the local oscillator multiplier chain with the same design used in the exciter. The use of a second coaxial filter in the ×4 multiplier subassembly at the output of the final power amplifier provides the additional attenuation of sidebands that is required. With this design, it is no longer necessary to provide a filter at the S-band output of the local oscillator multiplier.

Table 6. Performance characteristics of ×8 frequency multiplier

Parameter	Exciter ×8 (f_o = 2110 MHz)	Local oscillator ×8 (f_o = 2235 MHz)
Input power, dBmW	36	33
Output power, dBmW	27	24
Bandwidth (−1 dB), MHz	40	40
Input impedance, Ω	50	50
Spurious signal level below desired signal, dB		
Sixth harmonic	>40	>40
Seventh harmonic	>40	>40
Ninth harmonic	>40	>40
Tenth harmonic	>40	>40

Adequate tuning range at the receiver input is obtained by replacing the existing preselector with one that covers the combined DSN and MSFN bands.

4. Reference receiver predetection and loop noise bandwidths. The block IIIC configuration contains the predetection and loop noise bandwidths of both the DSN and MSFN block II subsystems. Selection is made independently for each receiver with the switches on the acquisition control panel.

To provide both DSN and MSFN predetection filter bandwidths, a new 10-MHz filter amplifier subassembly was added to the RER subsystem ahead of the 10-MHz IF amplifier. Because both the DSN and MSFN predetection crystal filters are located in the 10-MHz filter amplifier subassembly, the crystal filter in the 10-MHz IF amplifier was removed from the block II configuration.

A new receiver loop filter module was incorporated into the block IIIC configuration containing the time constants for both the three DSN and the three MSFN loop noise bandwidths.

5. Receiver AGC loop noise bandwidth. Three loop time constants (380, 34, and 4 s), which adequately cover the DSN and MSFN requirements, were selected. These bandwidths are common to both systems and no selection is required.

6. Range receiver predetection and loop noise bandwidths. As in the AGC loop, a design common to the DSN and MSFN was selected for the ranging receiver.

The 496-kHz fixed-clock frequency was used in both the DSN and MSFN block IIB design. To obtain a completely common system, which was the purpose of the block IIIC design, the three block II DSN loop noise bandwidths were used for both the block IIB DSN and MSFN receivers. This eliminated the need for including both the three DSN and the three MSFN bandwidths and the capability of selecting either set of three. The DSN noise bandwidths (0.8, 4, and 12 Hz) are adequate to meet the requirements of both the DSN and MSFN.

7. Solution to phase jitter problem in MSFN range receiver. The block IIB receiver/exciter/ranging subsystem was modified to operate with a fixed ranging clock frequency. This modification, however, caused a phase jitter problem in the range receiver clock and clock code transfer loops during ranging code acquisition and range tracking. The prototype receiver/exciter/ranging subsystem located at JPL was converted to the MSFN configuration and tested to determine the source of the interference. Periodic phase jitter with an amplitude of 20 deg peak-to-peak (3.3 deg *rms*) was noted during code acquisition (in program states p3 and p4) and during range tracking (in program state p7). The frequency of the phase jitter was measured and found to be equal to the difference between the 10.496 MHz that is derived from the atomic frequency standard and the 10.496 MHz that is derived from the 20-MHz oscillator.

An increase in the phase jitter in the range clock loop raised the noise power level in the range receiver, thereby increasing the acquisition error probability for a given signal-power-to-noise-power ratio. It also increased the scatter of the individual points in the range data about the mean or average value.

Figure 47 shows that one of the inputs to the balanced detector was a 10.496-MHz signal from the reference receiver. The 496-kHz portion of this signal was the ranging clock frequency derived by multiplying the 1.0-MHz signal from the atomic frequency standard by 496/1000. The other input to the balanced detector was the local model of the ranging code modulated on a 10-MHz carrier by the phase switch. This local model of the code contained square-wave components of the code, including a 496-kHz component and also the harmonics that related to the length of the code. When one of the harmonic frequencies of the code length occurred at a frequency near 10.496 MHz, it was combined with the received ranging signal in the balanced detector to produce periodic phase jitter on the 496-MHz output of the phase detector.

The ranging subsystem used the A code component in program states p3, p4, and p7 to generate the XA and $X(AB + BC + AC)$ code component combinations, respectively. The length of the A code was 31 bits. At a clock frequency of 496 kHz, the bit frequency was 992 kHz, and the repetition rate of the code was 32.000 kHz. The 328th harmonic of this frequency was 10.496 MHz, the frequency of the clock component of the received ranging signal. The A component of the code did not appear separately in the code transmitted to the phase switch; however, it was present at the input to the code combiner, and influenced the digital clock and the dc power during the combining operation. A slight phase and amplitude distortion appeared on the code output of the ranging subsystem.

The XA code, generated in program states p3 and p4, also generated a harmonic frequency of 10.496 MHz. The XA code had a length of 11×31 bits. At a bit frequency of 992 kHz, the code repetition rate was 2.90909 kHz, which is a submultiple of 10.496 MHz.

The power in these interference signals was quite small; however, if it was as large as 76 dB below the power level of the ranging code, the interference signal power would be equal to the incoming ranging signal power.

The solution to the problem was to change the ranging clock frequency to place the harmonic products of the ranging code length outside the bandwidth of the range receiver by replacing the 496/1000 frequency multiplier that had been incorporated during the block IIB modification with a 495.833/1000 frequency multiplier (Fig. 48).

E. Functional Description of the MSFN Receiver/Exciter/Ranging Subsystem

Within the control room facilities of the MSFN, the USB concept is extremely evident in the RER subsystem, which acts as the link between the microwave equipment, the low-frequency RF, metric data processing, and the dc-actuated equipment. Information and reference signals from 10 different external subsystems interface with this subsystem which is, in essence, the focal point of the USB.

The RER subsystems are employed throughout the MSFN in both single and dual configurations. The dual configuration provides two complete RER subsystems for redundancy and multiple vehicle operation. In describing the major functional capabilities of the RER, the single configuration will be used for simplicity.

1. Functional description of USB system. The design of the USB system is based on the coherent doppler and pseudo-random range system developed by JPL in which a single carrier frequency is utilized in each direction

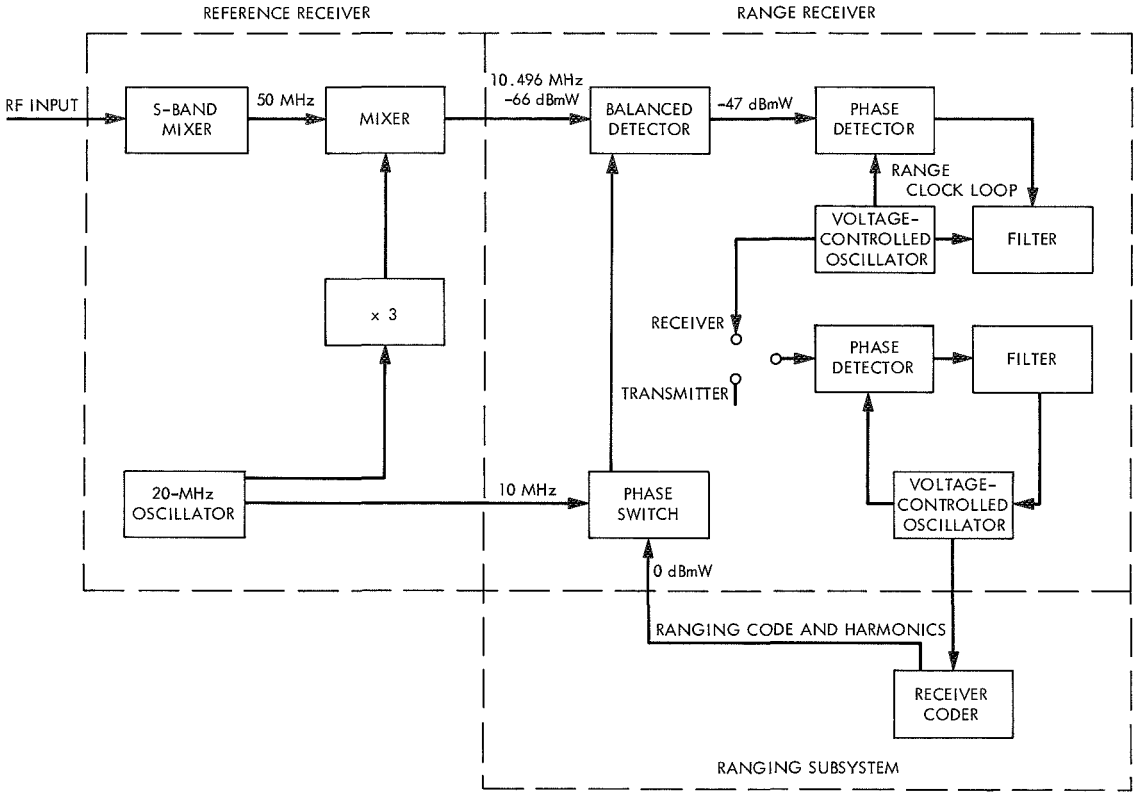

Fig. 47. Simplified block diagram of ranging subsystem

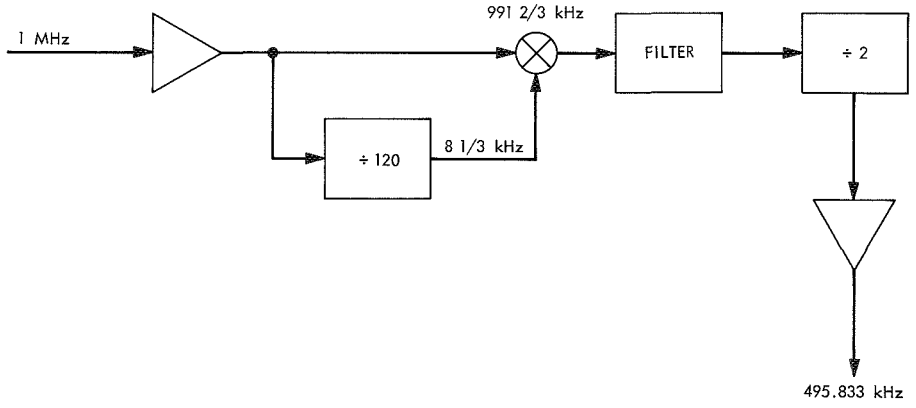

Fig. 48. Frequency multiplier, 495.833-kHz

for the transmission of all tracking and communications data between the spacecraft and the ground (Fig. 49). The voice and update data are modulated onto subcarriers and then combined with the ranging data, and this composite information is used to phase-modulate the transmitted carrier frequency. The received and transmitted carrier frequencies are coherently related, to allow measurement of the carrier doppler frequency by the ground station for determination of the radial velocity of the spacecraft.

In a transponder aboard the spacecraft, the subcarriers are extracted from the carrier and detected to produce the voice and command information. The binary ranging signals, which are modulated directly onto the uplink carrier, are detected by the wideband phase detector, and the resulting video signal is modulated onto the transponder downlink carrier.

The voice and telemetry data transmitted from the spacecraft are modulated onto subcarriers, combined

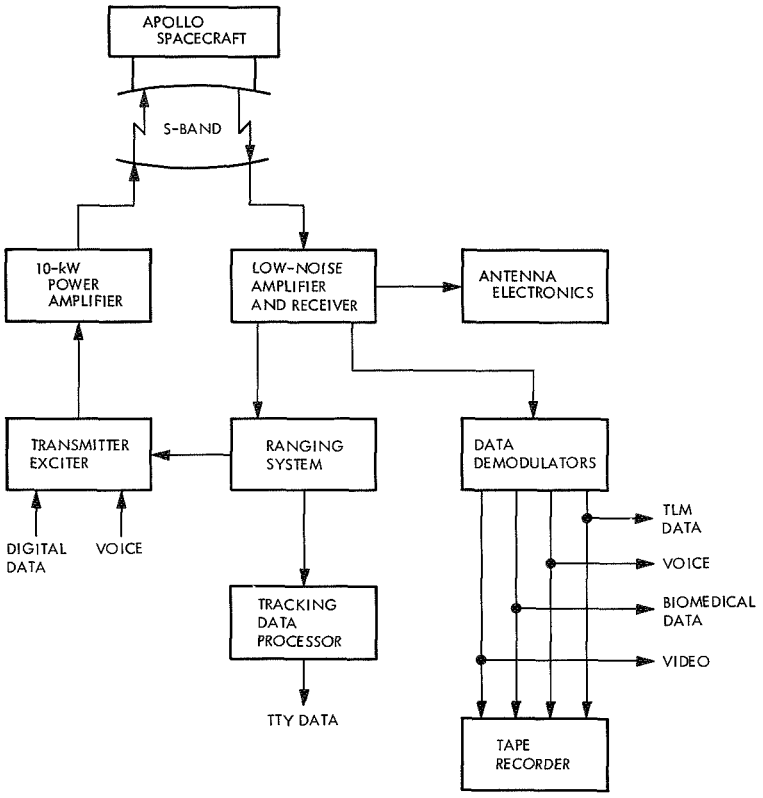

Fig. 49. Simplified block diagram of *Apollo* unified S-band system

with the video ranging signals, and used to phase-modulate the downlink carrier frequency. Transponder transmitter can also be frequency-modulated for the transmission of television information or recorded data instead of ranging signals, but on the command service module (CSM) a separate transmitter is used.

The basic USB system has the ability to provide tracking and communications data for two spacecraft simultaneously, provided they are within the beamwidth of the single antenna. Two sets of frequencies separated by approximately 5 MHz are used for this purpose. In addition to the primary mode of communications, the USB system has the capability of receiving data on two other frequencies that are used primarily for the transmission of data from the spacecraft.

The receivers have the following general capabilities:

(1) Accepting RF signals that contain angle-of-arrival error, carrier frequency and phase, range code modulation, and telemetry modulation information.

(2) Coherently detecting frequency and phase of the received signal carrier, and continuously providing the two-way doppler frequency shift that occurs at the received carrier frequency during round-trip transmission to the spacecraft for precise measurement of velocity.

(3) Detecting angle-error RF signals to provide dc error signals, which are unambiguous in polarity and approximately linearly related in magnitude to the angular error between the angle of arrival of the received RF signal and the RF axis of the antenna to provide automatic correction of antenna angle at acquisition and during flyby.

(4) Demodulating the range code and clock, and in conjunction with the ranging subsystem, continuously providing the two-way phase (time) delay experienced by the range code during round-trip transmission to and from the spacecraft for precise measurement of range.

(5) Demodulating telemetry modulation and providing telemetry subcarrier or telemetry modulation spectrum information.

(6) Providing an absolute level measurement of the received signal carrier power.

The fundamental S-band two-way carrier path is diagrammed in simplified form in Fig. 50. Excitation from the exciter is applied to the power amplifier and the output is transmitted to the spacecraft where the uplink carrier is received, transponded, and retransmitted as the downlink carrier, which is received by the ground station antenna and feed, passed through the diplexer, and amplified by the parametric amplifier output is applied to the receiver.

The receivers and exciter interconnect with the doppler and ranging equipment to perform the listed functions. In the paragraphs that follow, the mechanization of these major functional capabilities is discussed in greater detail.

2. *Doppler extraction function.* The RER subsystem provides a signal whose frequency is proportional to the doppler shift occurring on the two-way transponded carrier. The doppler shift is a result of spacecraft motion with respect to the ground equipment.

Assume the exciter output carrier frequency at S-band (between 2100 and 2110 MHz) is designated F_T. The frequency F_T has a precision based upon the accuracy of a 1.0-MHz reference supplied by the timing and frequency reference assembly (Fig. 51).

The output frequency is amplified and transmitted to the spacecraft, where it is coherently transponded by the ratio 240/221, and then retransmitted to the ground station. On the ground the received signal is preamplified by the low noise amplifier and appears at the receiver input as the frequency:

$$(240/221)F_T + D$$

The quantity D is the two-way doppler-shift frequency, and has a maximum value of about 200 kHz at earth escape velocity.

The receiver reference loop is phase-locked to this received frequency, and receiver reference signals containing frequencies coherently related to the received frequency are applied to the doppler extractor.

Similarly, frequencies coherently related to the transmitted frequency are also applied to the extractor. Within

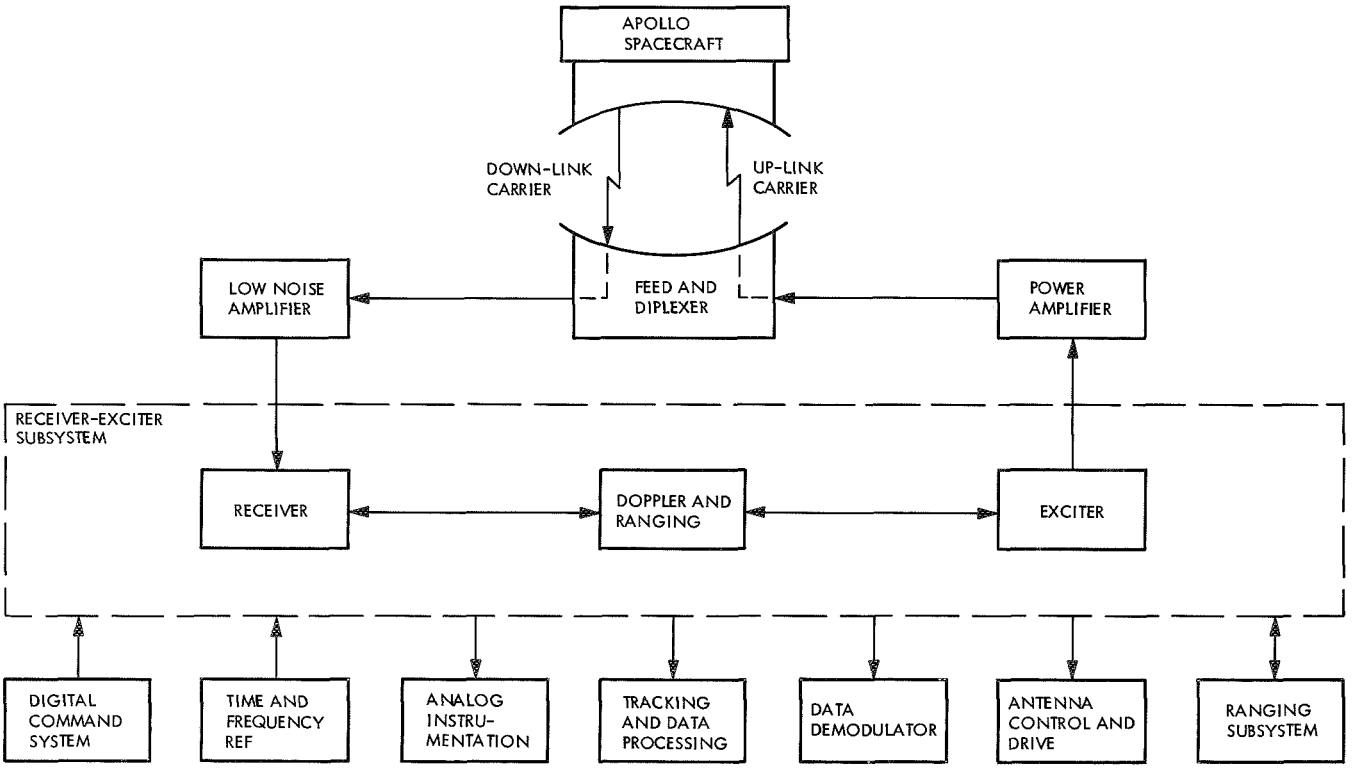

Fig. 50. Unified S-band system functions

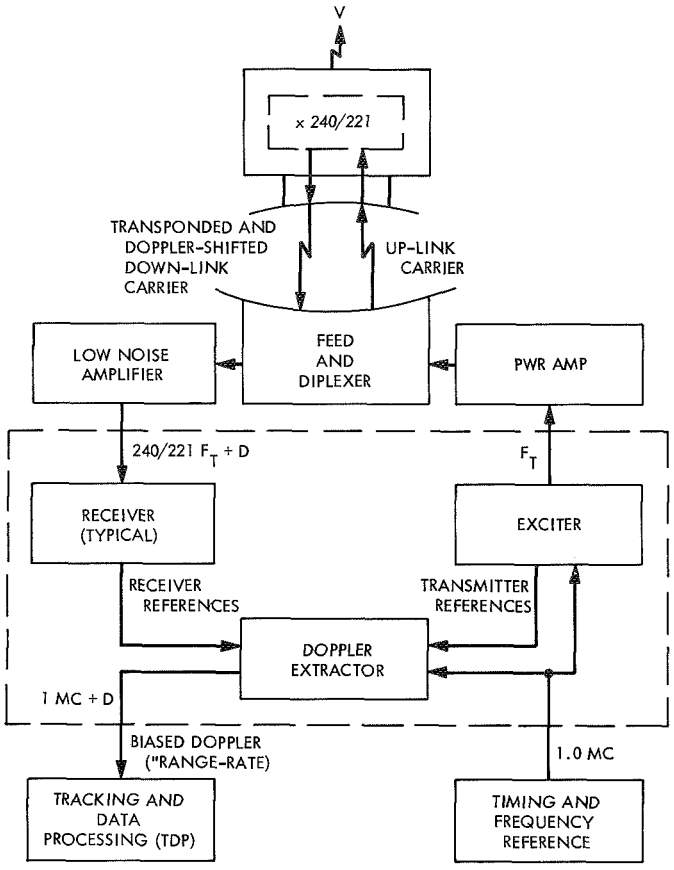

Fig. 51. Doppler extraction function

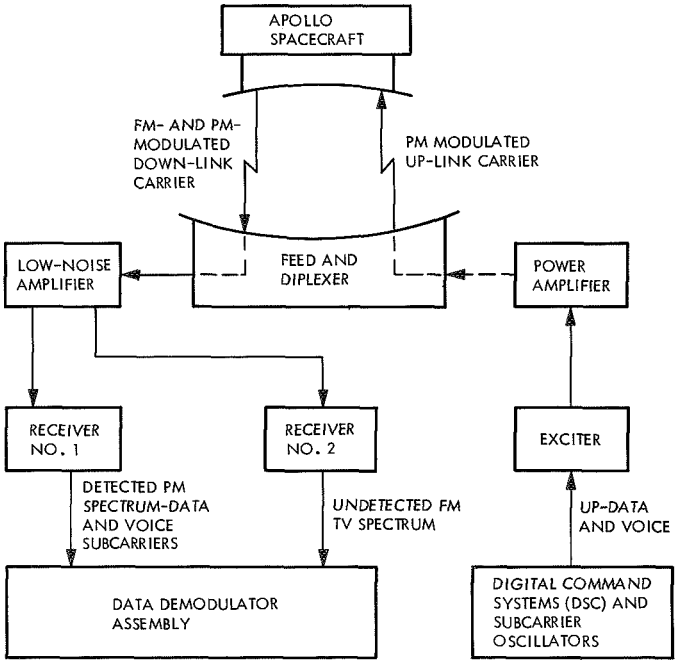

Fig. 52. Two-way communications function

the doppler extractor, the transmitter references are suitably combined and shifted coherently to simulate the 240/221 ratio occurring in the spacecraft. The resulting signal is functionally differenced with the receiver to yield the doppler frequency D. Finally, this frequency is added to a 1.0-MHz bias from the timing and frequency reference assembly, and the resulting biased doppler, or range rate signal, is supplied for further reduction to the tracking and data processing subsystem. The biasing is done to supply the doppler signal in a form convenient for further reduction by a computer.

The frequency D is approximately related to the spacecraft radial velocity vector and transmitter frequency by the expression

$$D \approx \frac{240}{221} \times F_T \times 2\frac{\mathbf{V}}{C}$$

where $\mathbf{V}$ is considered positive when the range is increasing. Thus, if the spacecraft were moving away from the ground station, the biased doppler frequency will be greater than 1 MHz, whereas if the spacecraft were approaching the ground station, the biased doppler frequency will be less than 1 MHz.

3. *Two-way communication functions.* The receiver/exciter subsystem contains an S-band transmitter exciter that processes the up-data and voice modulation for the *Apollo* spacecraft, and also contains two functionally identical receivers that process the modulated received carriers from the *Apollo* spacecraft. The received modulation consists of spacecraft TV and data telemetry, as well as voice information.

A typical operational configuration using both receivers is shown in Fig. 52. Up-data and voice FM subcarriers from the subcarrier oscillators are applied to the exciter phase modulator. The phase-modulated carrier from the exciter drives the power amplifier, which, in turn, feeds the phase-modulated uplink carrier to the spacecraft—lunar excursion module (LEM) or command and service module (CSM)—via the antenna and microwave equipment. Within the spacecraft, the carriers are suitably demodulated to provide uplink information for the inflight equipment and personnel. The frequency- and phase-modulated carriers are generated within the spacecraft (LEM, CSM, or S-IV-B) and transmitted to the ground station. In the configuration shown in Fig. 51, the separate carriers are amplified through the multichannel low noise amplifier and applied to the separate receivers.

Receiver 1 operates as phase-lock, double-conversion equipment, and coherently detects the phase-modulated carrier. The resulting detected spectrum consists of information subcarriers frequency-modulated by voice and data information. This spectrum is supplied to the data demodulator assembly for subcarrier demodulation.

Receiver 2 operates in an open-loop, single conversion, wideband mode. It supplies a gain-controlled FM spectrum (usually TV information) around a center frequency of 50 MHz, the receiver first intermediate frequency. This spectrum is also supplied to the data demodulator assembly for FM demodulation.

Receivers 1 and 2 are not limited to the modes of operation shown in Fig. 51. Either or both receivers can be simultaneously operated in either the open-loop or closed-loop configuration on any one of four received channel frequencies in the 2270- to 2290-MHz band. The receiver internal configurations are identical, except that only one source of reference signals is required, and this is included in receiver 1 for use by both receivers.

4. Angle tracking function. The subsystem contains dual-channel angle receivers that operate in conjunction with the antenna feed and antenna control and drive equipment to form an antenna position tracking servo system.

The received carrier from the spacecraft is split by the antenna feed equipment into three channels, as shown in Fig. 53: the sum channel Σ, the hour angle (HA) channel, and the declination (dec) channel.

The sum channel signal is amplified by the low noise amplifier, and is the main received carrier for the reference loop of the receiver.

The HA and dec channel signals are not preamplified, but are applied directly to the dual-channel angle receiver. Using reference signals generated by the receiver reference loop, the angle channels operate as dual-conversion receivers. They produce dc outputs (E_{HA} and E_{dec}) with magnitude proportional to the amplitude of the channel input signal.

The antenna pattern associated with each channel is such that when the radial axis of the antenna is perpendicular to the plane of the incoming wavefront, the sum channel amplitude is maximum but the angle channel inputs are minimum, or null inputs. Under this condition, the error signal dc outputs E_{HA} and E_{dec} are also at a minimum.

When the antenna is slightly displaced from radial alignment in either the HA or dec tracking planes, as occurs during angular tracking, the angle channel input amplitude increases. The detected error voltages then take on dc values proportional to the angular displacement or tracking error. The polarity of the error voltage is a function of the phase of the channel input signal, which in turn is dependent on the direction of the angular tracking error. The antenna pattern associated with the angle channels is essentially biphase; that is, the phase goes through a 180-deg reversal at the null (alignment) position of the antenna.

The error signals thus contain information as to the direction and magnitude of the angular tracking error, and the angle channels function as the amplifiers and detectors in the antenna tracking servo loop. The other elements of the loop are the antenna feed, which performs the sensing function, and the antenna control and drive equipment, which actuates the motions of the antenna structure.

The standard single configuration contains two complete angle channel receivers, one associated with each of the reference loops. Receiver 1 is ordinarily used with the main (30-ft or 85-ft) antenna, while receiver 2 is ordinarily associated with the small, widebeam acquisition antenna. When the acquisition antenna is not in use, receiver 2 reference loop is ordinarily switched to receive via the large antenna through the multi-channel low noise amplifier.

5. Ranging function. The receiver/exciter subsystem contains a ranging receiver and other associated subassemblies that operate in conjunction with the digital ranging subsystem to provide data which, when properly reduced, yields the instantaneous range between the *Apollo* spacecraft and the ground station. This portion of the receiver/exciter subsystem is described in detail in Section III.

6. The receiver reference loop. The reference loop of a typical receiver is particularly important as an element of the subsystem, as it contains equipment that is operational in all four of the major functions. Figure 54 shows a typical receiver reference loop.

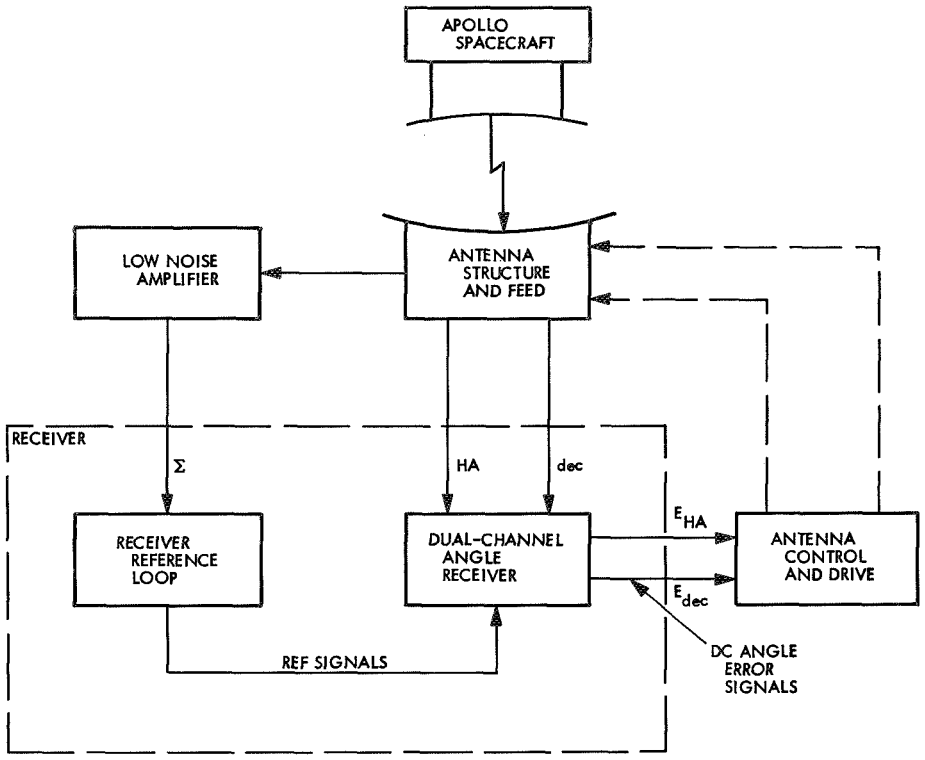

Fig. 53. Angle tracking function

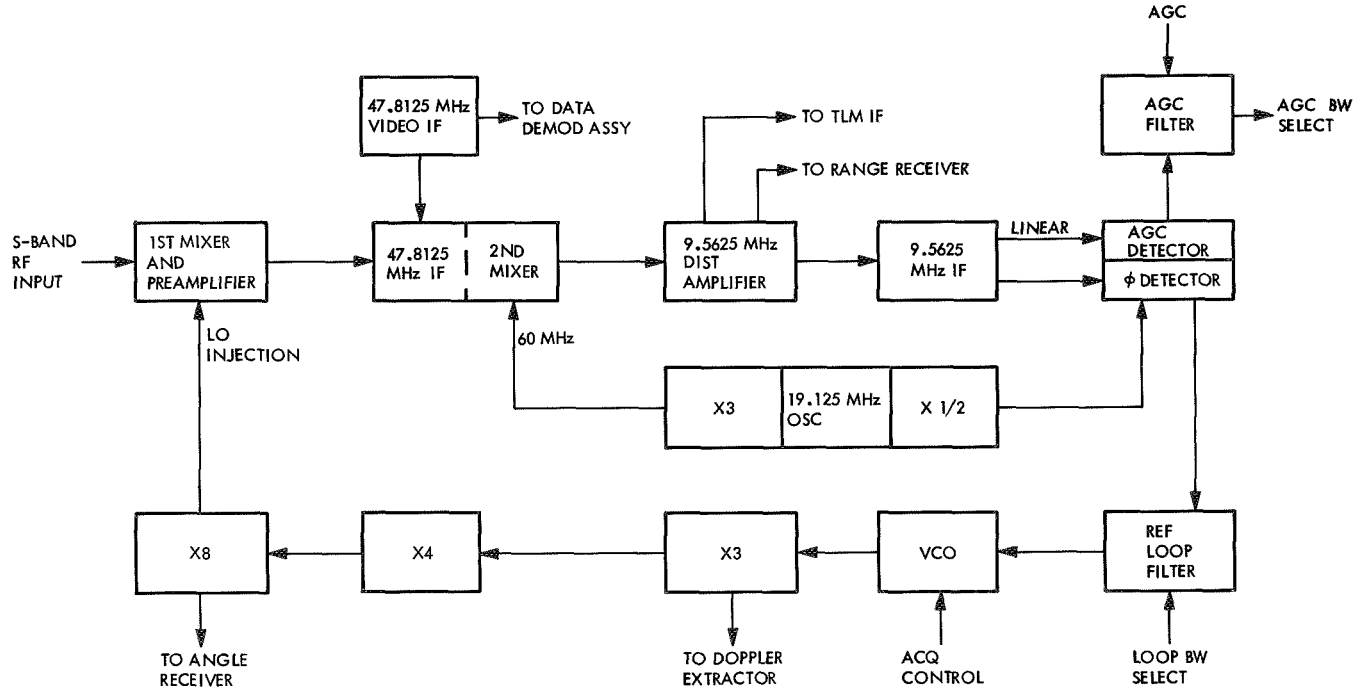

Fig. 54. Receiver reference loop

The S-band RF input, at one of four carrier center frequencies in the 2270- to 2290-MHz range, is applied to the first mixer and preamplifier. At the mixer, the signal is differenced with the local oscillator chain injection signal, which is 50 MHz lower in frequency than the received signal. The resulting 50-MHz IF signal is preamplified and applied to the automatic gain control 50-MHz IF amplifier.

During open-loop operation, when the carrier is frequency-modulated by television information, the 50-MHz spectrum is branched off at this point, passes through a gain-controlled, wideband, 50-MHz IF amplifier, and is supplied as an undetected spectrum to the data demodulator assembly.

In closed-loop operation, the signal is next gain controlled through a series of 50-MHz AGC IF amplifier stages, and then differenced with a 60-MHz reference signal in the second mixer to produce the second IF of 10 MHz. The IF amplifier is capable of a total gain control range of 91 dB, operating at an overall gain between +51 and −40 dB. The phase and gain changes across this range have to be carefully controlled during manufacture to assure compatible operation with parallel units in the angle receiver channels.

The 10-MHz output is applied to a distribution amplifier, where telemetry channel IF and range receiver channel input signals are branched off.

The reference loop signal is next applied to a 10-MHz IF amplifier, where a crystal filter establishes the loop predetection noise bandwidth of about 7.0 kHz. After filtering, the signal is split into two channels. The first operates at high gain and contains a limiter whose output is applied to the loop phase detector. The second channel operates at lower gain without limiting, and this channel output is applied to the loop AGC detector.

Within the loop phase detector, and assuming loop phase lock, the limited output signal frequency is differenced with a 10-MHz reference signal. The resulting output is a small dc voltage proportional to the angular phase error in the loop. This dc output is applied to the reference loop filter, within which time constants are selected manually to control the overall loop-noise bandwidth 2 β_L. Threshold values for this bandwidth 2 β_{LO} of 50, 200, and 700 Hz can be selected.

The loop filter output, known as the loop static phase error, is a small and relatively noise-free dc voltage. This voltage is applied to the VCO where, during phase lock, it automatically adjusts the VCO frequency to maintain lock during input signal frequency variations.

An acquisition input voltage to the VCO is applied manually by the operator to obtain initial lock (acquisition), and then to balance out the residual phase error when acquisition had been accomplished. This latter function is indicated by a reduction of the station phase error to zero. The VCO output is next multiplied by three, and a coherent reference signal for the doppler extractor is branched off from the multiplier.

Finally, the VCO signal is multiplied by the ×4 and ×8 multiplier chain for a total multiplication of 96, and applied as the local oscillator injection signal to the first mixer, thus closing the loop. Local oscillator injection signals for the angle channel receiver are branched off at the ×8 multiplier output.

Returning to the AGC path, the detector output is applied to the AGC loop filter. Within the filter, the AGC loop bandwidth is selected by the control operator for one of three values, grossly designated narrow, medium, or wide. These values are ordinarily paired with the corresponding reference loop 2 β_{LO} settings, although this is not a necessity for proper operation.

The filter output is the dc AGC voltage, with a dynamic range of 10 V. This voltage is applied to the gain-controlled stages in the 50-MHz IF amplifiers in the reference loop, and to the parallel angle receiver channels. It is also displayed and recorded by the analog instrumentation equipment, as it varies with, and is a measure of, the input signal level.

The 60- and 10-MHz reference frequencies are both derived from a 20-MHz crystal oscillator. The 60-MHz signal is obtained through a ×3 multiplier, while the 10-MHz signal is derived from a ×½ multiplier. This reference generation equipment is present in only one of the receivers. Reference signals for the second receiver, the angle channels, the telemetry channels, the range receiver, and the doppler extractor are all branched off of the ×3 and ×½ multiplier outputs.

In summary, the reference phase-lock loop is of second order, with the dual-phase integration occurring through the loop filter and VCO, whereas the AGC loop is of first order with single integration occurring through the AGC filter.

7. Variation in loop noise bandwidth. The reference loop varies with the input signal level, primarily because of the suppression of signal by noise within the limiter preceding the phase detector. The increased loop gain at high signal levels results in an increased damping and widening of the bandwidth. The values of 50, 200, and 700 Hz mentioned earlier are values occurring at the system signal threshold; the strong signal bandwidths are much wider.

This effect is shown in Fig. 55. It should be noted that in the 700-Hz position, the bandwidth rises to about 2 kHz when the signal exceeds the threshold value by about 30 dB. This wide bandwidth is desirable for tracking the high doppler rates encountered during the earth orbital phase of the *Apollo* missions, and will ordinarily be used during these passes. Carrier phase modulation within the loop bandwidth cannot be properly demodulated because the loop "tracks out" these frequencies. This is of little concern for the *Apollo* program, however, as all modulation except the emergency voice information is on subcarriers at frequencies greater than 1.0 MHz, well beyond the low frequency cutoff of the loop.

The 50-Hz position, reaching a maximum bandwidth of 500 Hz, is intended for use during the lunar phases of the mission. Doppler rates will be low during these phases, and the increased sensitivity and narrow bandwidth will assure an adequate communications margin

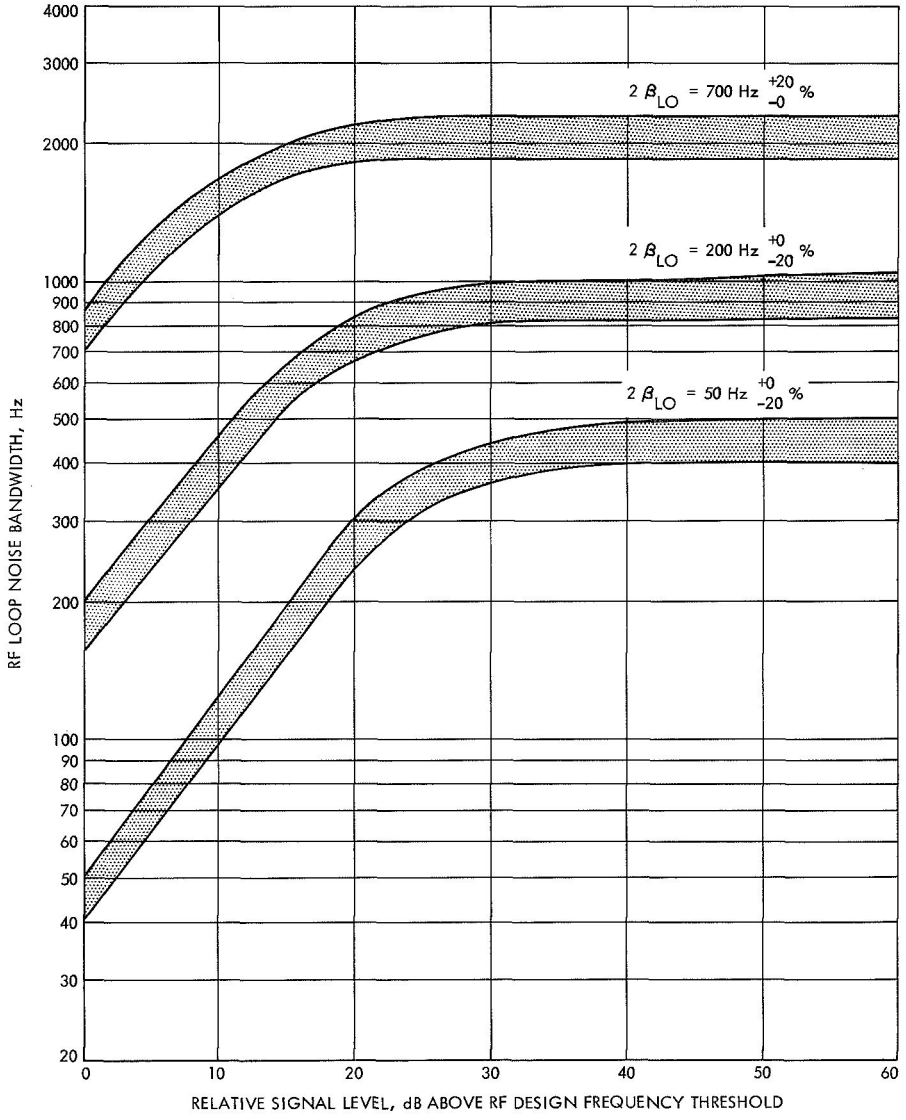

Fig. 55. Radio frequency loop noise bandwidths vs signal level

for the expected received signal levels, even if the emergency modes must be used.

The FM television spectrum will contain energy within the tracking bandwidths shown. However, the receivers are in open-loop condition during FM reception, and no attenuation occurs, as the tracking loop is inoperative.

8. The ranging receiver and detected telemetry channels. The 10-MHz IF distribution amplifier in the receiver channel branches off signals for the ranging receiver and the detected telemetry channel. As these two signal paths are important to the basic functions of the subsystem, they are shown in greater detail in Fig. 56.

The ranging receiver input, from either receiver as selected by the control operator, consists of code x clock modulation on the 10-MHz IF. This modulation occupies a wide spectrum which contains significant sideband components as far as 2 MHz from the carrier. This spectrum is applied to a wideband phase detector which is referenced by code x IF. The code x IF is a modulated spectrum centered at the intermediate frequency of 10 MHz. The spectrum is derived from a phase switch, within which the 10-MHz IF reference signal is periodically switched ± 90 deg by the code signal, also known as the receiver code. This code is supplied by the ranging subsystem.

The phase detector differences the two signals, producing an output spectrum that always contains some energy at the clock frequency. The amplitude of this energy is directly proportional to the degree of correlation between the received code and the receiver code.

The energy at the clock frequency, known as the clock signal, is filtered and amplified through a dual-channel IF amplifier. The channel outputs are applied to a loop phase detector (limited output), and a correlation detector (linear output). The correlation detector develops the dc correlation indication for the ranging subsystem.

The phase detector output drives a loop filter and VCO, which in turn reference the two detectors. These units together define the ranging receiver phase-lock loop. The loop bandwidth, as in the main receiver, is established by manual selection of the time constants in the loop filter. This bandwidth has threshold values of 4, 16, and 40 Hz. These are considerably narrower than the bandwidths of the main loop; therefore, ranging threshold is not ordinarily reached during operation.

The receiver loop acts as a narrowband tracking filter, providing relatively noise-free frequency references at the clock frequency and its second harmonic. These are supplied to the ranging subsystem. The frequencies are used to drive the receiver coder within that subsystem.

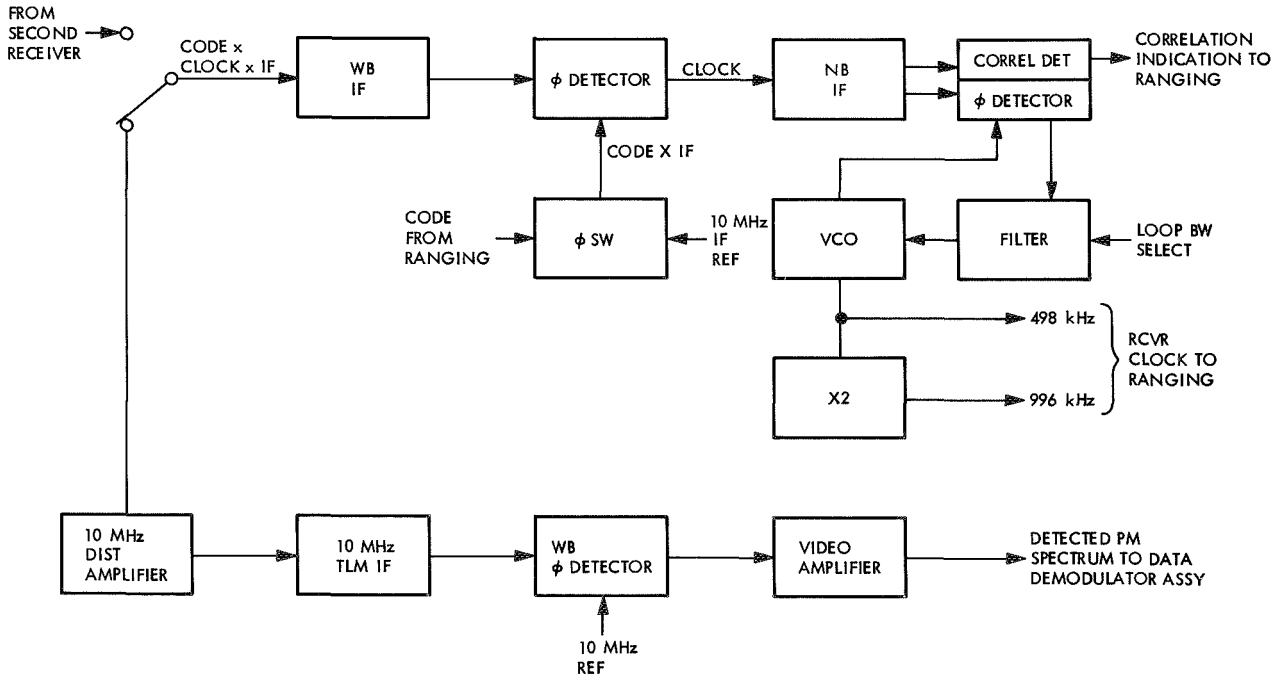

Fig. 56. Detected telemetry channel

The detected telemetry channel is a simple series arrangement of IF amplifier, wideband phase detector, and video amplifier. The phase detector is referenced with a 10-MHz signal from the reference signal generator in the receiver.

The detected signal is supplied at a level of 0 dBmW and a −1 dB bandwidth of 1.25 MHz to the data demodulator assembly.

F. Receiver/Exciter Subsystem Equipment Layout

The control room cabinets that contain the receiver/exciter equipment are shown in Fig. 57. The first three cabinets on the left contain subsystem control panels and monitoring equipment, tilted and arranged for convenience by a seated control operator. Continuing from left to right, the fourth, fifth, and eighth cabinets each contain two roll-out frames which mount subassemblies of the subsystem. More than 80 different types of subassemblies are used, and the total count exceeds 200.

One frame of cabinet 1 is rolled out to show the subassembly packaging and mounting methods. All of the interconnecting coaxial cabling is routed on the outer surface of the mounting plates, while the power, dc, and low-frequency signal paths are all wired with shielded leads on the inner surface of the plates within the frame. Each subassembly is individually removable for quick replacement. Connections to the wiring within the frames are made through multipin connectors

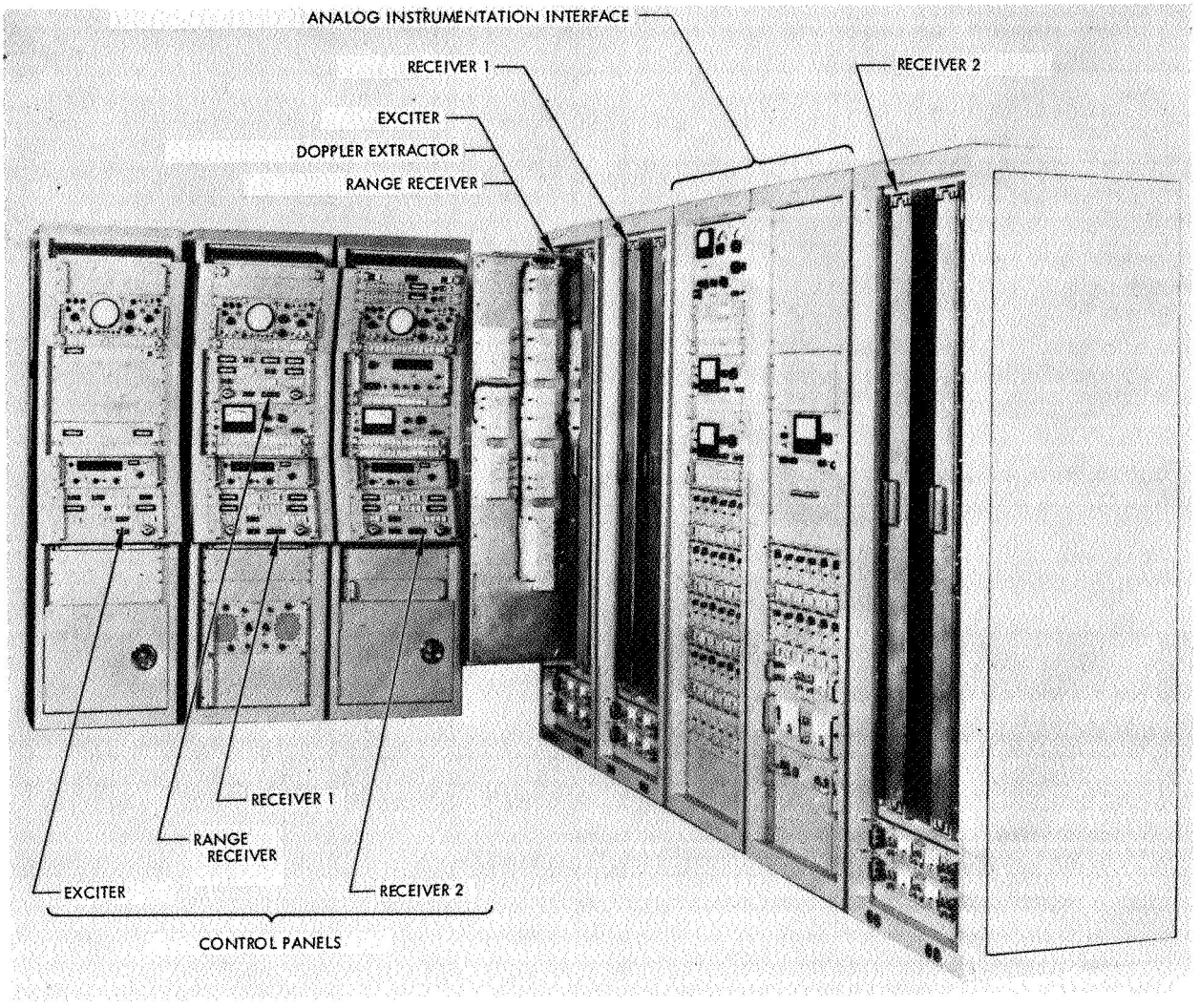

Fig. 57. Receiver/exciter subsystem equipment layout

mounted at the ends of the subassemblies. Intracabinet cabling is routed through floor channels beneath the cabinets, and all connections to these cables are made through connector plates at the base of the cabinets. Subassembly power supplies are rack-mounted beneath the rollout frames, and ac convenience outlets are placed on the cabinet lower lips.

Cabinets 2 and 5 contain the subassemblies for receivers 1 and 2, respectively. Each receiver thus housed consists of the reference loop, the angle channels, and the telemetry channels.

Cabinet 1 contains subassemblies of the exciter, the doppler extractor, and the range receiver, as well as other minor equipment used with the ranging receiver during the ranging program. The exposed plate contains subassemblies of the doppler extractor.

Additional subassemblies containing equipment operable in the S-band region are normally mounted near the antenna, and do not appear in this picture.

Cabinets 3 and 4 of the right-hand group contain the isolation amplifiers and power supplies which preprocess monitoring signals before they are fed to the analog instrumentation subsystem. All of these signals are normalized for a peak-to-peak level of 10 V from the low-impedance output of the isolation amplifiers. The cabinets also contain instrumentation used while testing and evaluating the performance of the subsystem equipment.

The characteristics of the MSFN receiver/exciter subsystem are shown in Table 7. Data cited in the table are shown in Figs. 58–66.

Table 7. Manned Space Flight Network receiver/exciter subsystem characteristics

Item	Characteristic
Overall exciter	
Exciter output frequency range	2100–2110 MHz
Reference output frequencies	
Exciter VCO ×1	21.927 MHz nominal
Exciter VCO ×3	65.781 MHz nominal
Spurious outputs	−30 dB max level
Power output	
Exciter power output	+35 ±1.5 dBmW at nominal center frequency of 2105 MHz into 50-Ω load with a max VSWR[a] of 2.0:1
Test signal power output	+5 ±3 dBmW at nominal center frequency of 2105 MHz into 50-Ω load with a max VSWR of 2.0:1
Bandwidth	Such that the power output does not vary more than 2.0 dB over the frequency range of 2100–2110 MHz
Phase stability	7 deg rms jitter max, in loop noise bandwidth of 50 Hz, exciter and receiver
Automatic frequency control and synthesizer loop	
Frequency coverage	
By VCO selection	21.875–21.979 MHz
By VCO tuning	±2300 Hz min about VCO nominal center frequency
Frequency stability	Same as station standard
Frequency selection	Approximately 0.01-Hz increments from the VCO nominal
Loop transfer function	Such that the frequency response curve falls within limits shown in Fig. 58
Manual frequency control	
Oscillator type	Voltage-controlled quartz crystal
Frequency coverage	
By VCO selection	21.875–21.979 MHz in four channels as follows:

Channel	*S-band frequency, MHz*	*VCO frequency, MHz*	*VCO × 5/221, kHz*
1	2101.802	21.893,772	495.334
2	2106.406	21.941,732	496.419
3	2101.802	21.893,772	495.334
4	2106.406	21.941,732	496.419

By VCO tuning	±2300 Hz min about VCO nominal center frequency
Frequency	3×10^{-6}/10 h
VCO voltage sensitivity	400 Hz/V nominal

[a]VSWR = voltage standing wave ratio.

Table 7 (contd)

Item	Characteristic
Automatic sweep frequency control	
Frequency sweep range	0 to ±2300 Hz min, minus or plus the manual offset from VCO nominal center frequency (adjustable at exciter control panel)
Sweep rate	Adjustable from 0.01 to 10.00 Hz min (at function generator, cabinet 1)
Sweep accuracy	Dial reading accuracy 1 % or better
Sweep symmetry	10% or better
Sweep waveform	Sine, triangular, or square (selectable at function generator)
Modulator	
Overall	
Modulation of command and ranging signals	Simultaneous or separate
Incidental amplitude modulation	Less than ±1 dB relative to the detected carrier
Linearity	The instantaneous sensitivity of any given input voltage (from 10% max deviation to max deviation) equals the overall average sensitivity ±10%
Command phase modulation	
Modulation deviation referred to the RF carrier	3.0 rad peak max
Modulation sensitivity	$\frac{3.0\left(\begin{smallmatrix}+0.3\\-0\end{smallmatrix}\right)\text{ rad peak}}{\text{V peak}}$
Modulation input terminal frequency response (−3 dB)	Direct-coupled to 100 kHz
Modulation input voltage	1.0 V peak max
Modulation signal input VSWR	1.5:1 max (relative to 50 Ω)
Modulation stability (dc to 100 kHz)	3%/10 h
Ranging phase modulation	
Modulation deviation referred to the RF carrier	2.1 rad peak max

Item	Characteristic
Modulator (contd)	
Ranging phase modulation (contd)	
Modulation sensitivity	$\frac{5.0\left(\begin{smallmatrix}+0.5\\-0\end{smallmatrix}\right)\text{ rad peak}}{\text{V peak}}$
Modulation input voltage waveshape	Binary
Modulation input terminal frequency response (−3 dB)	Direct-coupled to 2 MHz
Modulation signal input VSWR	1.5:1 max (relative to 50 Ω)
Modulation output spectra asymmetry with 500-kHz square wave modulation applied and for modulation deviation from 10% of max to max deviation	First order sideband ±1 dB and third order sideband ±2 dB
Modulation stability (dc to 2 MHz)	3%/3 h
Modulation carrier null (S-band output)	Capable of 30-dB (or greater) carrier null when modulated at the proper modulation index
Test translator	
Output frequency range	2280.0–2290.0 MHz by VCO selection
Power output	−20 ±5 dBmW with attenuator set to 10-dB attenuation
Dynamic range	114 dB nominal
Power monitor output	−17 ±5 dBmW
Coherent translation ratio	240/221
Receiver reference channel	
Receiver frequency range (−3 dB max)	
Coherent mode	2280–2290 MHz
Noncoherent mode	2270–2280 MHz
RF input impedance	50 Ω nominal; VSWR = 2.0:1 max (measured at preselector input)
Cable loss	2 dB max (from antenna cabinet input to preselector)

Table 7 (contd)

Item	Characteristic
Receiver reference channel (contd)	
Noise figure	10.6 dB max (measured at input of preselector with 290°K reference)
Spurious responses	40 dB min (measured over frequency range of 2150–2400 MHz)
Loop noise bandwidth and threshold	Threshold defined as the point at which the rms noise error at the phase-locked loop output is equal to 1 rad
Characteristics (at preselector input)	*Noise bandwidth* $2\beta_{LO}$, *Hz* / *Signal suppression factor* α_o, *nominal ratio* / *Sensitivity, dBmW* $50^{+0\%}_{-20\%}$ / 0.0708 / -146.8^{+0}_{-4} $200^{+0\%}_{-20\%}$ / 0.1416 / -140.8^{+0}_{-4} $700^{+20\%}_{-0\%}$ / 0.2834 / -134.5^{+0}_{-4}
Loop transfer function	Such that the strong signal frequency response curves fall within the limits shown in Figs. 60–62
Frequency response overshoot	50% max above unity level shown in Figs. 59–61
RF loop phase error	35 deg max at signal frequencies displaced ±9.0 parts/10^5 from the nominal S-band center frequency
First intermediate frequency	50.000 MHz nominal
Second intermediate frequency	10.000 MHz nominal
Predetection IF bandwidth (for IF and AGC loop filters)	−3 dB bandwidth = 6300 Hz nominal; noise bandwidth = 7010 Hz nominal
Second IF amplifier output	
Limited output level (for RF loop filter)	+4 dBmW nominal
Linear output level (for AGC loop filter)	−22 to −23 dBmW nominal
Noise bias (threshold conditions)	No greater than 46 dB below the strong signal phase detector peak output voltage as measured at the RF loop phase detector error point
RF phase-lock loop coherent interference (spurious signal level relative to receive threshold signal level)	−40 dB min

Item	Characteristic
Receiver reference channel (contd)	
Doppler tracking rate	Equal to or greater than the following values: *Noise bandwidth* $2\beta_{LO}$, *Hz* / *Phase error, deg* / *Minimum doppler rate, Hz* $50^{+0\%}_{-20\%}$ / 30 / 1,500 $200^{+0\%}_{-20\%}$ / 30 / 12,000 $700^{+20\%}_{-0\%}$ / 30 / 115,000
VCO frequency	$F_{VCO} = \frac{\text{Received frequency} - 50\ \text{MHz}}{96}$
VCO channel frequencies	For selectable crystal frequencies in the following order: *Channel* / *S-band frequency, MHz* / *VCO center frequency, MHz* 1 / 2272.500 / 23.151,042 2 / 2277.500 / 23.203,125 3 / 2282.500 / 23.255,208 4 / 2287.500 / 23.307,292
VCO frequency stability	3×10^{-6}/10 h max
VCO manual tuning capability about the center frequency	±2300 Hz min (±220.8 kHz) at received S-band input frequency
VCO automatic acquisition	
Selection	Reference receiver 1, receiver 2, or exciter (at exciter control panel)
Frequency sweep range	0 to ±2300 Hz min minus or plus the manual offset from VCO nominal center frequency (adjustable at exciter control panel)
Sweep rate	Adjustable from 0.01 to 10 Hz min (at function generator, cabinet 1)
Sweep accuracy	Dial reading accuracy 1% or better
Sweep symmetry	10% or better
Sweep waveform	Sine, triangular, or square (selectable at function generator)

Table 7 (contd)

Item	Characteristic
Receiver reference channel (contd)	
AGC characteristics	
AGC loop bandwidth and time constants	The nominal bandwidth and time constants (−3 dB response of relative voltage response at strong signal conditions) are as follows:
AGC bandwidth position	*Time constant, s* / *Frequency response, Hz*
Narrow	150.0 / 0.16 ±0.04
Medium	15.0 / 1.6 ±0.4
Wide	4.0 / 6.0 ±1.5
AGC voltage vs signal level	A plot of AGC voltage vs RF signal input level (at preselector input) is shown in Fig. 62
RF signal level dynamic control range	−60 to −151 dBmW nominal
AGC loop coherent interference (spurious signal level relative to receiver threshold signal level)	−40 dB min
Noise error (−100 dBmW)	0.6 mV rms on the AGC buss, max
Static gain stability (at strong signal conditions)	0.4 dB max/10 h
Maximum noise power before signal suppression occurs at CAD[b] (specified at −23 dBmW signal level input to CAD)	0 dBmW
MGC[c] characteristics	
Control voltage range	0 to −10 Vdc min
Gain control range	−60 to −151 dBmW min
Receiver gain change transients	When the gain control is switched from MGC to AGC, transients appearing on the gain control voltage do not exceed 10% of the existing control potential when the differential input, between the MGC and AGC voltage, is less than 1.0 Vdc
Static gain control change stability	0.4 dB max/10 h

Item	Characteristic
Angle receivers	
Input characteristics	Same as reference channel receivers
Predetection IF bandwidth	−3 dB bandwidth = 2000 Hz nominal; noise bandwidth = 2200 Hz nominal
Output signal level of CAD (to servo, with −22 dBmW signal level at CAD input)	−1.0 to +1.0 Vdc
CAD output linearity (−22 dBmW input)	±5% at 0 or 180 deg phase, relative to reference signal phase
Gain tracking accuracy (between either angle channel and reference channel)	±2 dB max from max signal level to threshold with −105 dBmW reference point
Phase tracking accuracy (between either angle channel and reference channel)	±15 deg max from max signal level to threshold with −105 dBmW reference point
Phase adjustment capability (of each CAD) relative to reference channel signal	0 to 360 deg, continuous, with accuracy of ±7 deg
Amplitude adjustment capability (of each angle channel relative to reference channel)	12 dB total in 1 dB increments (nominal setting = 2 dB)
Maximum noise power before signal suppression occurs at CAD (specified at −23 dBmW signal level input to CAD)	0 dBmW
Signal and spurious signal cross-coupling (each angle channel relative to reference channel)	Greater than 40 dB below the min threshold signal level
Telemetry channel A	
10 MHz IF bandwidth (−3 dB)	6.0 ±0.8 MHz
Signal power output	
AGC operation	−22 ±5 dBmW
MGC operation	0 dBmW nominal

[b]CAD = coherent amplitude detector.

[c]MGC = manual gain control.

Table 7 (contd)

Item	Characteristic
Telemetry channel A (contd)	
Signal-to-noise ratio (−90 dBmW input signal level)	Values as follows:
AGC condition	−0.5 dB nominal
MGC condition	+6 dB nominal
Bandpass phase symmetry (−3 dB)	−30 deg max
Telemetry channel B	
10 MHz IF bandwidth	Selection at receiver control panel, with bandwidths as follows:

Filter select position	*−1 dB bandwidth (min)*	*−3 dB bandwidth (max)*
4.5 kHz	4.5 kHz	7.0 kHz
20.0 kHz	20.0 kHz	30.0 kHz
420.0 kHz	380.0 kHz	700.0 kHz
3.3 MHz	2.2 MHz	4.0 MHz

Signal power output	
AGC operation	−22 ±2 dBmW
MGC operation	0 dBmW nominal
Bandpass phase symmetry (−1 dB)	±10 deg max
Phase demodulated outputs	An ac-coupled (video) output and a dc-coupled (narrowband) output
Detected output bandwidth	Values as follows:

Filter select position	*Video bandwidth (−1 dB min)*[d]	*Narrowband bandwidth (−1 dB min)*[d]
4.5 kHz	to 2.25 kHz	to 2.25 kHz
20.0 kHz	to 10.00 kHz	to 7.00 kHz
420.0 kHz	to 210.00 kHz	to 8.00 kHz
3.3 MHz	to 1.25 MHz	to 8.00 kHz

Power output (during AGC operation for phase modulation index of 1 rad rms and signal-to-noise ratio of 10 dB or better):	
Video output	0 ±2 dBmW
Narrowband output	2.8 V peak to peak nominal

Item	Characteristic
Telemetry channel B (contd)	
Strong signal predetection signal-to-noise ratio	Values with input signal level at −90 dBmW as follows:

Operating mode	*Signal-to-noise ratio (nominal), dB Predetection bandwidth*			
	3.3 MHz	600 kHz	30 kHz	6 kHz
AGC	1.5	9.5	24	31
MGC	8.5	16.5	30	37

50 MC IF bandwidth	
−1 dB	4.0 MHz min
−3 dB	8.0 MHz min
AGC range	Noncoherent AGC maintains total power output (signal plus noise) at −20 ±3 dBmW over the input signal level range of −100 to −60 dBmW
Reference frequency generator	
Reference oscillator	
Type	Quartz crystal frequency-controlled
Frequency	20 MHz nominal
Frequency tuning range	±200 Hz min
Frequency stability	
Short term	1×10^{-7}/20 min
Long term	1×10^{-6}/10 h
Distributed reference frequencies	
Reference and angle channels	10 and 60 MHz
Telemetry channels	10 MHz
Doppler extractor	10 MHz
Ranging section	10 MHz
Distributed power output	+10 dBmW nominal
Noncoherent spurious signals	40 dB min below desired output signal
Doppler extractor	
Input signals	
Reference receiver 1	VCO ×3
Reference receiver 2	VCO ×3
Exciter	VCO ×1
Exciter	VCO ×3

[d]Under closed-loop conditions, the low-frequency response characteristics are determined primarily by the relative voltage response characteristics of the RF carrier phase-locked loop. Under normal coherent conditions, the low-frequency response (−1 dB) of the video output is 50 Hz or less.

Table 7 (contd)

Item	Characteristic
Doppler extractor (contd)	
Input signals (contd)	
Reference frequency	10 MHz nominal
Doppler reference (external input)	1 MHz nominal
Range doppler outputs	
Number and phase	Two phase-related outputs with a phase separation of 90 $\pm$10 deg
Frequency response	dc to 125 kHz min
Output level	5 $^{+3.7}_{-2.2}$ V peak with 5-K load
Output impedance	Nominal 500 Ω max
Total phase jitter at strong signals	5 deg rms max
Doppler shift	The output doppler shift is one-fourth the rate of the S-band carrier doppler shift; the 0-deg output lags the 90-deg output for a receding spacecraft
Biased doppler output	
Bias frequency	1.000 MHz nominal (external reference)
Spacecraft velocity vector	
Vector toward receiver	1 down to 0.5 MHz
Vector away from receiver	1 up to 1.5 MHz
Total phase jitter at strong signals	8 deg rms max
Output level	+13 $^{+4}_{-1}$dBmW
Output impedance	50 Ω nominal
Range clock receiver	
Input center frequency	10.000 MHz nominal
Input bandwidth	4.5 $\pm$0.5 MHz
Input power level	
Sideband power equal to carrier power	-66 to -65 dBmW nominal
Noise input level at threshold	-12 dBmW max
Decode signal input	
Bandwidth	dc to 2.0 MHz min
Level	-0.55 ± 0.1 to -1.35 ± 0.1 V binary waveform, and -1.35 ± 0.1 to -0.55 ± 0.1 V binary waveform (inverted)

Item	Characteristic
Range clock receiver (contd)	
Loop noise bandwidth and threshold	As follows:
	Characteristic noise bandwidth 2 β_{LO}; Hz / ***Signal suppression factor α_o, nominal ratio*** / ***Sensitivity dBmW***
	4 $^{+0\%}_{-20\%}$ / 0.0368 / -157.7 $^{+0}_{-4}$
	16 $^{+0\%}_{-20\%}$ / 0.0734 / -151.7 $^{+0}_{-4}$
	40 $^{+0\%}_{-20\%}$ / 0.1157 / -147.7 $^{+0}_{-4}$
Loop transfer function	Such that the strong signal frequency response curves fall within the limits shown in Figs. 63–65
Loop phase error	The static phase error for strong signal conditions does not exceed 14 deg at signal frequencies displaced $\pm$9.0 parts/10^5 from the nominal ranging VCO center frequencies
Intermediate frequency	495.877 kHz nominal
Predetection IF bandwidth (for RF loop filter and coherent amplitude detector)	-3 dB bandwidth = 2000 Hz nominal; noise bandwidth = 2085 Hz nominal
IF amplifier output	
Limited output level (for RF loop filter)	+14 dBmW nominal
Linear output level (for CAD)	-18 to +18 dBmW nominal
Noise bias	The noise bias produced at threshold conditions is not greater than 46 dB below the strong signal phase detector peak output voltage as measured at the loop phase detector error point
Coherent interference (spurious signal level relative to loop threshold signal level)	-40 dB min
Range clock receiver loop VCO	
Basic VCO center frequency	680 kHz $\pm$0.002%
Injection input center frequency (from mixer in code clock transfer loop)	1.175,877 kHz nominal (5/221 $\times$ exciter VCO + 680 kHz)
Output center frequency	495.877 kHz nominal

Table 7 (contd)

Item	Characteristic
Range clock receiver (contd)	
Range clock receiver loop VCO (contd)	
Frequency stability	1×10^{-5}/3 h max
Tuning capability about the center frequency	±50 Hz min
Phase stability	1 deg rms in a loop bandwidth (2 β_L) of 4.0 Hz ($\alpha = 1$) within a range of ±50 Hz about the nominal VCO center frequency
Range clock receiver loop acquisition characteristics	
Source	Local or remote
Local control	Controls loop bandwidth, filter short, and VCO tuning
Remote control	By external equipment (ranging subsystem); controls filter short and VCO tuning only
Indication	Local = TEST, remote = OPERATE, controlled by external equipment
Acquisition tuning range	±50 Hz min about VCO nominal center frequency
Correlation amplitude detector characteristics	
Linear input range (to CAD)	−18 to + dBmW nominal
Output bandwidth	50 Hz min
Correlation indication (amplitude proportional to correlation of range code components)	0 to 5 Vdc via isolation amplifier
In-lock indication	The CAD indicates loop in-lock conditions for an output level of 0.2 Vdc nominal via an in-lock relay isolation amplifier
Code clock transfer loop	
Input signal	5/221 × exciter VCO frequency or range clock receiver VCO
Loop transfer function	Such that the frequency response curve falls within the limits shown in Fig. 66
CCTL[e] VCO	Loop uses a tracking oscillator with the same characteristics as the range tracking oscillator, except the phase stability is measured in a loop bandwidth 2 β_L of 120 Hz and does not exceed 0.1 deg rms within a range of ±50 Hz about the nominal VCO center frequency
Acquisition tuning range	±50 Hz min about VCO nominal center frequency
Loop phase error	The static phase error does not exceed 27.5 deg at signal frequencies displaced ±9.0 parts/10^5 from the nominal VCO center frequency
Loop in-lock indicator	The CCTL uses a dual phase detector with a 0 deg output for the loop filter input, and a 90 deg output for the in-lock indicator, which is actuated via a relay isolation amplifier
Reference oscillator	The CCTL has a reference oscillator and mixer for distribution of reference frequencies to the CCTL and range clock receiver VCOs
Input frequency	5/221 × exciter VCO frequency
Basic oscillator frequency	680 kHz ±0.002%
Frequency stability of oscillator	1×10^{-5}/3 h max
Output frequency	1.17 MHz nominal (5/221 × exciter VCO + 680 kHz)
Phase stability	1 deg rms in a loop bandwidth (2 β_L) of 4.0 Hz
Output signals (to ranging subsystem)	
Receiver code generator clock (decode)	
Frequency	992 kHz nominal (CCTL VCO output × 2)
Phase	Adjustable 0 to 720 deg, continuous, relative to VCO
Transmitter code clock (encode)	
Frequency	496 kHz nominal (exciter VCO × 5/221) 992 kHz nominal (exciter VCO × 10/221)
Phase	Adjustable 0 to 360 deg, continuous, 992 kHz relative to 496 kHz
Output power	+10 ±3 dBmW
Output impedance	50 Ω nominal

[e]CCTL = clock code transfer loop.

Table 7 (contd)

Item	Characteristic
Clock doppler detector (two outputs)	
Phase separation of signals	90 ±5 deg
Frequency response (−3 dB)	dc to 125 Hz min
Amplitude	5 $^{+3.7}_{-2.2}$ V peak into 5-K load
Phase jitter with strong signal ($\alpha = 1$) applied to receiver and code clock detector	0.75 deg rms max
Output impedance	500 Ω max

V. Role of JPL in the Implementation of Modifications to the DSN Stations for MSFN Support

A. Background Information

Early in 1964, operational and engineering investigation of the *Apollo* mission profiles, data requirements, and equipment circuit margins was conducted by the Manned Space Center, Goddard Space Flight Center, and the Jet Propulsion Laboratory. This investigation suggested that a second 85-ft antenna with a unified S-band RF system was needed in each of the three complexes around the world.

The National Aeronautics and Space Administration faced the choice of building a duplicate 85-ft antenna station at each of its three prime sites or utilizing the co-located DSN stations. The agency decided to utilize the co-located DSN stations in a backup capacity during the translunar and transearth phases of the *Apollo* missions. In addition, a DSN backup station would be capable of acquiring and tracking the combined CSM/LM spacecraft in the event of an equipment failure at the MSFN prime station.

Early in 1965, it was concluded that each of the MSFN 85-ft-antenna prime stations should be configured with a dual S-band RF system to cover those phases of flight in which tracking and data retrieval from both the CSM and LM manned spacecraft was feasible. These findings were a result of studies conducted at the MSC and GSFC.

Finally, the use of the DSN as backup stations was modified to the extent that one 85-ft antenna provided marginal support at the moon for simultaneous tracking and data acquisition retrieval from both the CSM and LM manned spacecraft during the lunar phase of the mission. An 85-ft antenna RF pattern centered on the LM landing site would suffer a loss of from 9 to 12 dB at the lunar horizon; this loss would make acquisition of the CSM almost impossible until its orbit brought it within the limits of the RF pattern.

1. Implementation. Because the *Apollo* project would require extensive full-system tests and tracking simulation over a long period of time and might prevent JPL from supporting unmanned deep space missions, it was decided to use two separate control rooms or wings at each of the three 85-ft-antenna DSN/*Apollo* backup stations. This decision enabled the DSN to continue to fulfill its commitments to unmanned space missions.

Jet Propulsion Laboratory supplied equipment racks in the MSFN control room of the backup stations; an MSFN cassegrain cone with two maser amplifiers and an acquisition aid antenna (for MSFN *Apollo* prime station at Canberra only); two 20-kW DSN S-band power amplifiers, which were to be tuned to the MSFN frequency for the actual missions; and three racks of MSFN receiver/exciter equipment in the cage behind the antenna reflector for each station.

The disposition of equipment in the control room was as follows:

JPL supplied	GSFC supplied
Dual S-band receiver/exciters	Down subcarrier demodulators
Dual 20-kW transmitters	PCM signal conditioner
Maser control and *monitor*	Uplink subcarrier oscillators and auxiliary equipment
Microwave switching	Command verification receiver
Digital ranging equipment	Wideband analog tape recorder
	Intersite microwave links (Goldstone to Houston)
	Frequency and timing *subsystem*
	Tracking data processor
	Antenna programmer

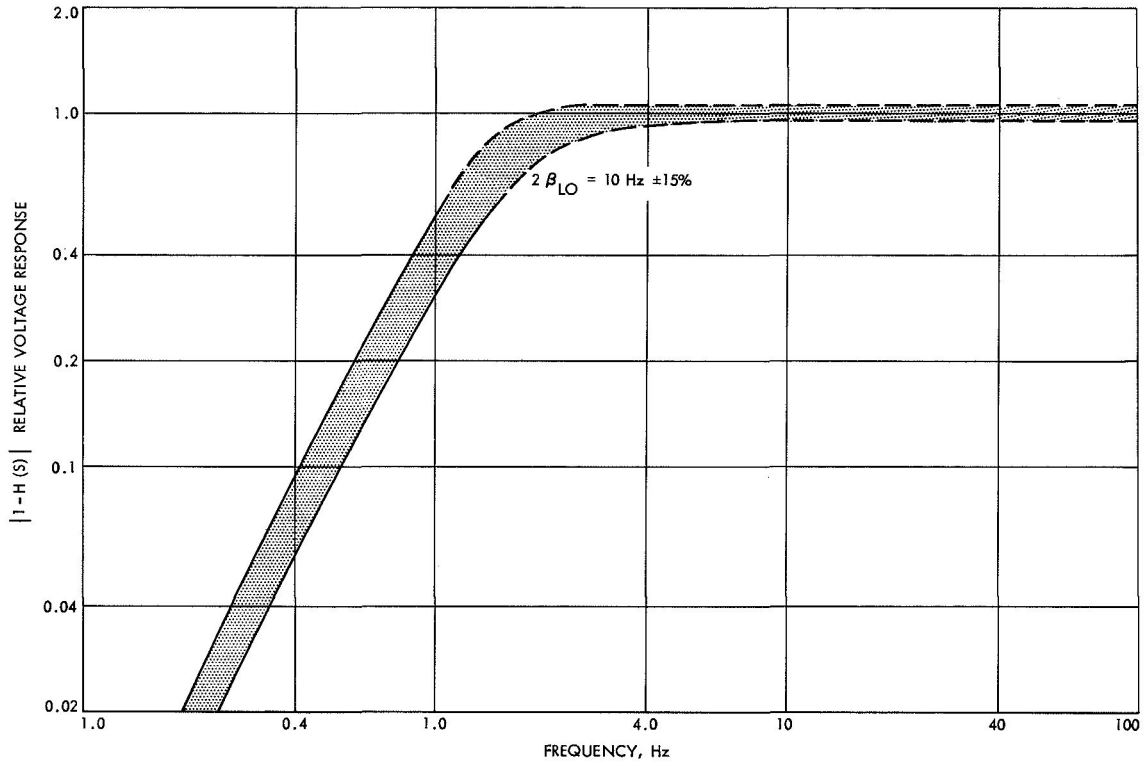

Fig. 58. Synthesizer loop relative voltage response vs frequency

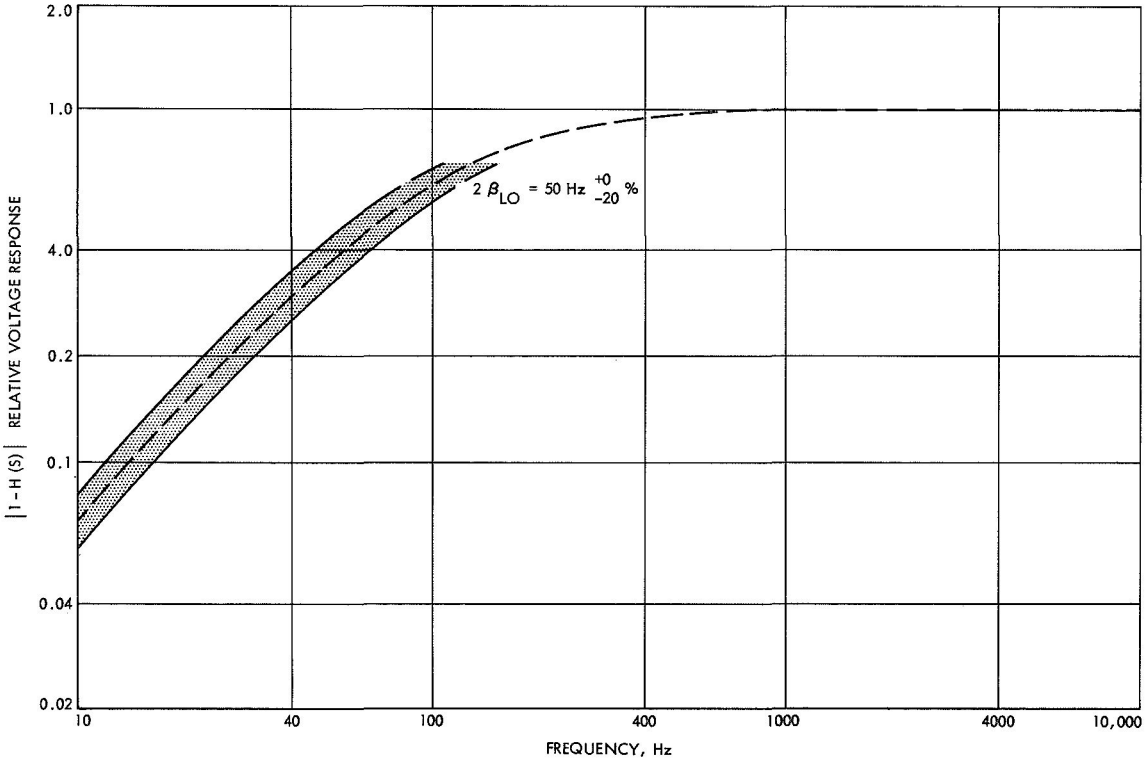

Fig. 59. Radio frequency loop relative voltage response vs frequency (50 Hz)

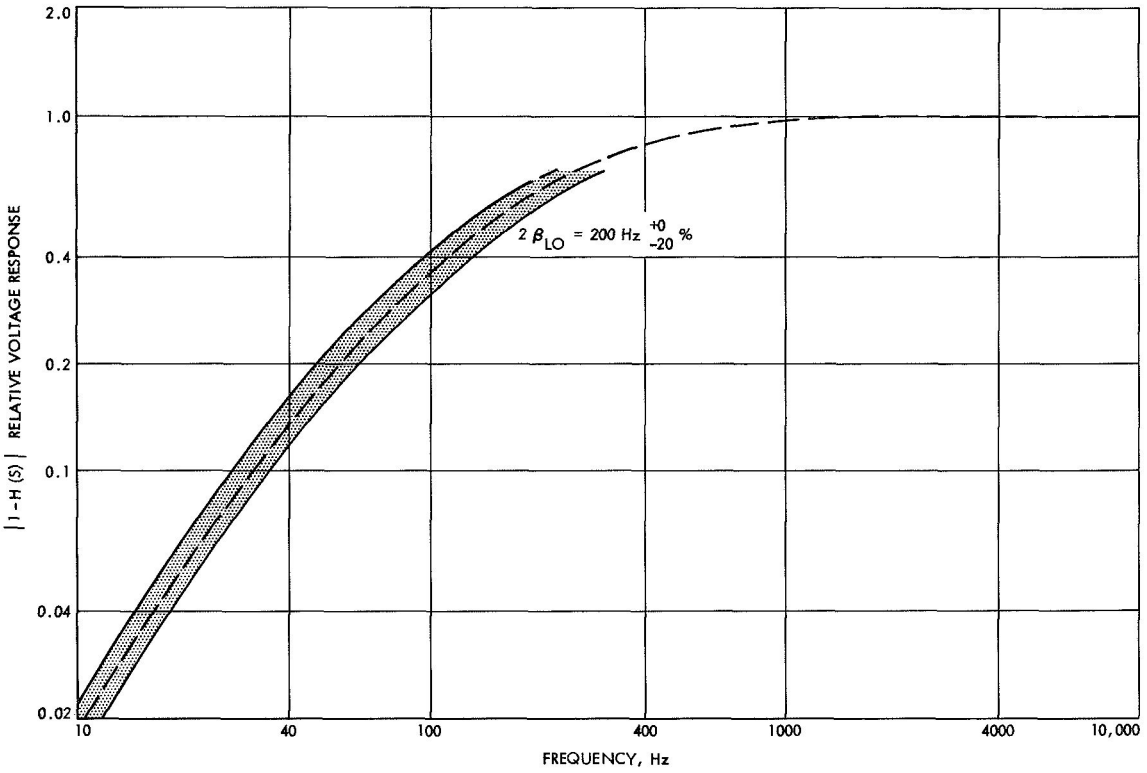

Fig. 60. Radio frequency loop relative voltage response vs frequency (200 Hz)

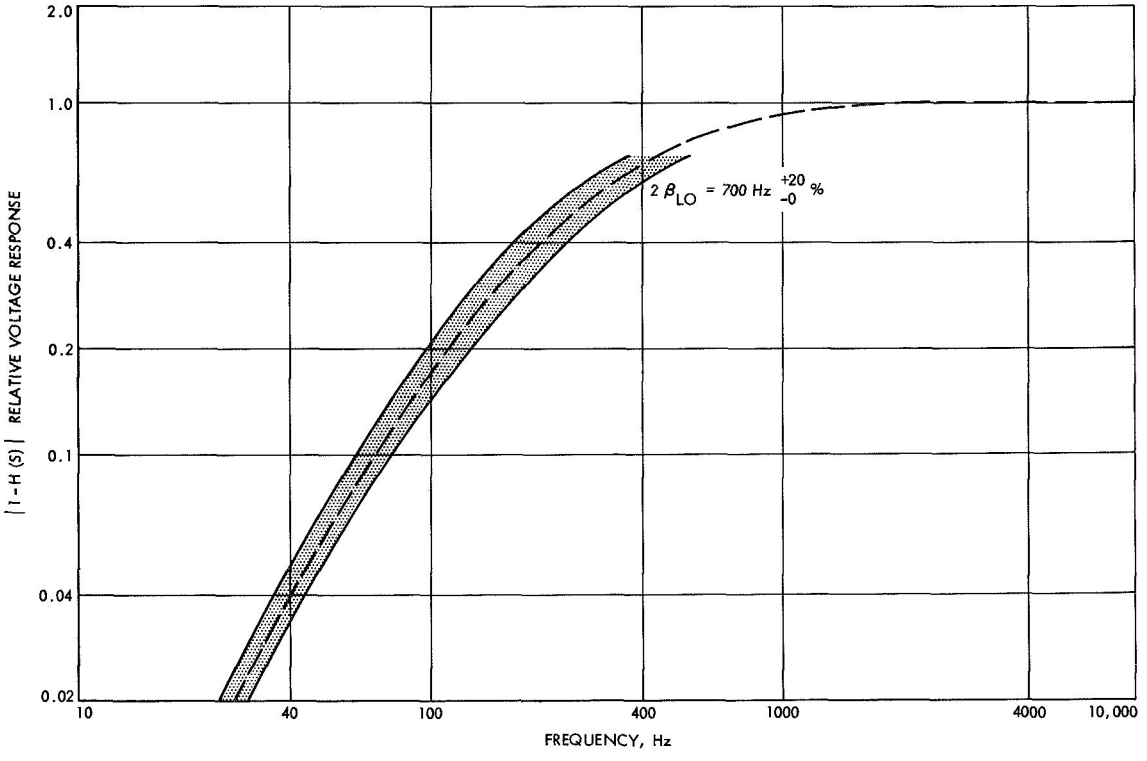

Fig. 61. Radio frequency relative voltage response vs frequency (700 Hz)

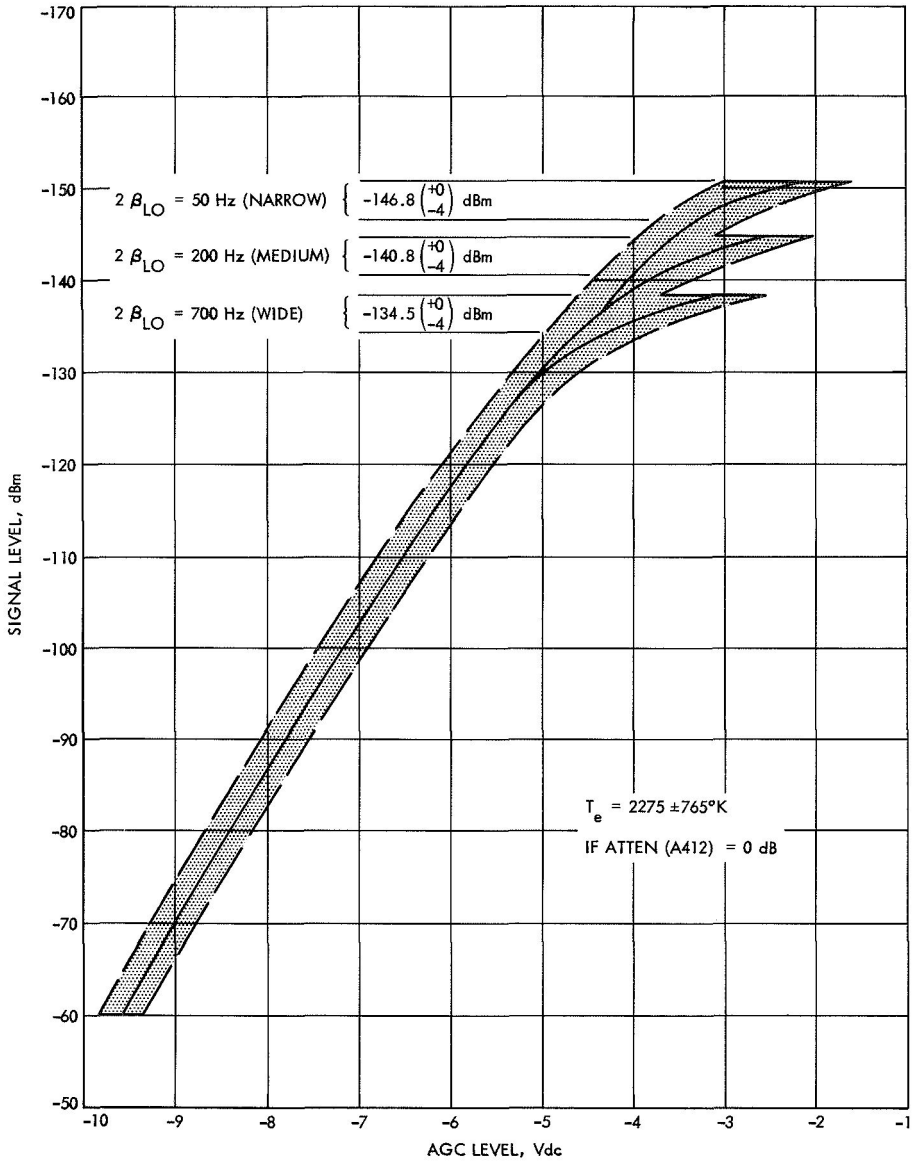

Fig. 62. Automatic gain control voltage vs signal level

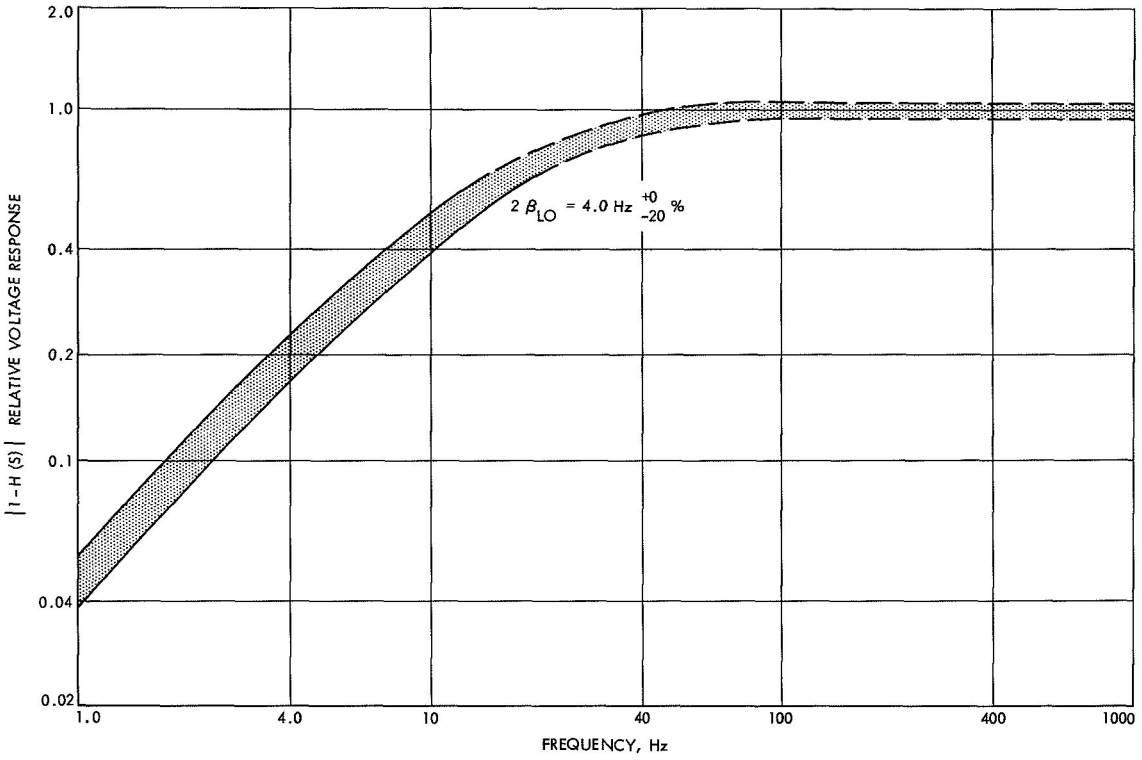

Fig. 63. Range receiver loop relative voltage response vs frequency (4 Hz)

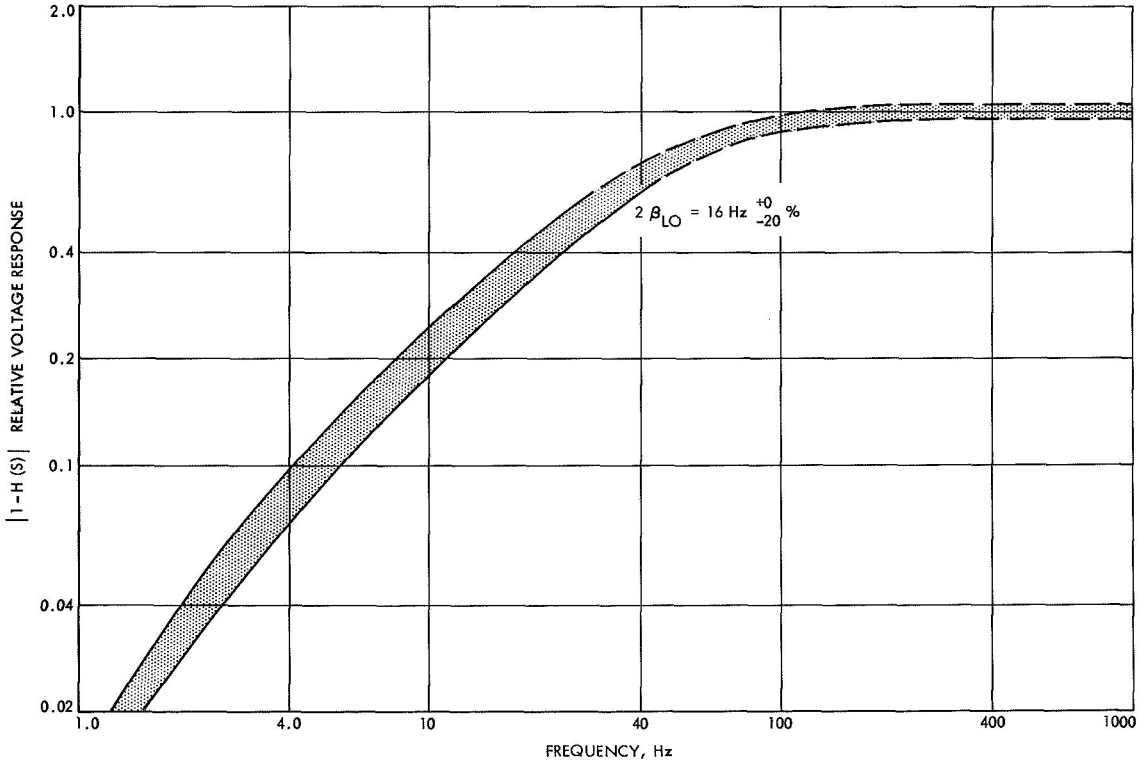

Fig. 64. Range receiver loop relative voltage response vs frequency (16 Hz)

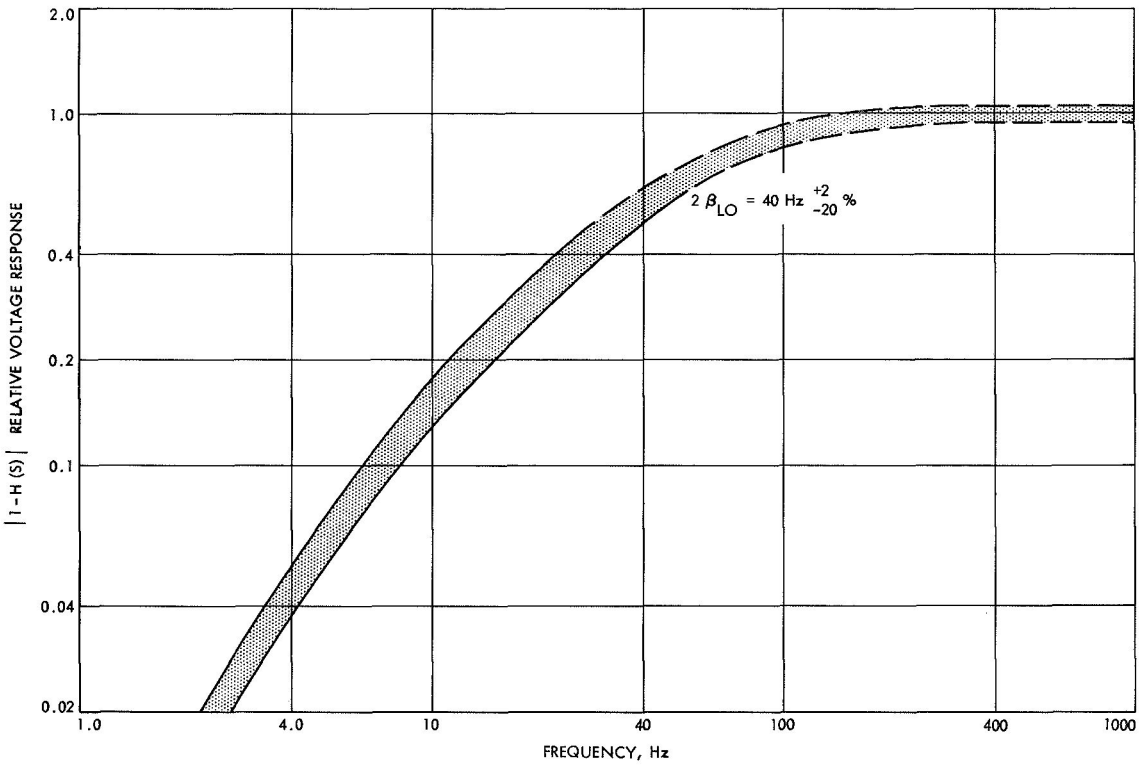

Fig. 65. Range receiver loop relative voltage response vs frequency (40 Hz)

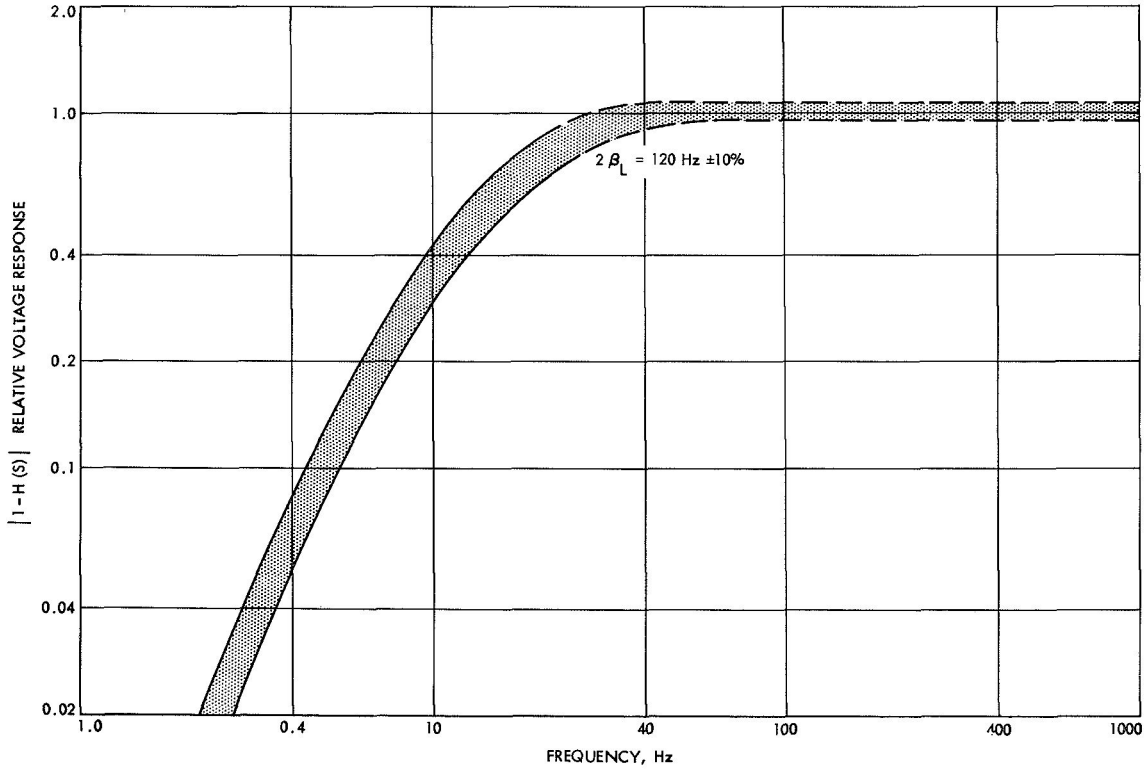

Fig. 66. Code clock transfer loop relative voltage response vs frequency

2. Additional data handling and communications requirements. A broadband data link was installed by GSFC between the JPL/DSN (backup) and GSFC/MSFN (prime) sites. The link carried all the *Apollo* data. The microwave link, which had been proved by years of service in the DSN, was selected as the most dependable method of transmission. One passive microwave repeater located on elevated ground near each site provided the necessary link between the backup stations (DSN/MSFN) and the *Apollo* prime stations.

3. Summary. In summary, the DSN facilities were augmented with sufficient *Apollo* MSFN equipment to permit:

(1) Tracking and two-way data transfer with either the CSM or the LM during the lunar phases.

(2) Tracking and two-way data transfer with the combined CSM/LM during portions of the translunar phase.

(3) Backup for prime site by providing passive track (spacecraft to ground RF links) of the *Apollo* spacecraft during the translunar and transearth phases.

4. Preliminary agreements. Certain specific capabilities and restrictions were stated to define the scope of the data interface required of the backup station to accomplish operational roles and to conform to recognized MSFN practices. These were:

(1) The metric tracking data format originating from the backup site would be identical to the format originating from the primary site.

(2) Metric tracking data would be transmitted directly to Mission Control Center, Houston over the best NASA Communications Network (NASCOM) routing.

(3) *Apollo* mission data would be transmitted from the backup site via the MSFN prime 85-ft antenna station to NASCOM.

(4) Voice and command data would be routed directly to the backup site from the prime site for subsequent transmission to the spacecraft.

5. Policy agreement. A policy for integrating the DSN *Apollo* backup system into the MSFN during *Apollo* mission periods was agreed upon in Dallas, Tex., during November 1965. The role that the JPL sites had fulfilled in other NASA programs was acknowledged. Every effort was made to prevent or reduce to a minimum any conflicts between *Apollo* requirements and those of the other programs in which JPL backup facilities were involved. No scheduling conflicts were expected to occur during the *Apollo* mission periods because of their priority; however, during the periods between *Apollo* missions, conflicts between JPL mission activities and MSFN premission preparation activities would undoubtedly occur. These conflicts were to be arbitrated by mutual agreement between the DSN and MSFN scheduling offices.

6. Operating principles. The mission period was to be initiated by the release of a message from the flight director announcing that the network was on mission status, and end when the individual stations were released from mission support. Normally, this period was to begin at approximately liftoff minus 14 days.

Backup site support was to be provided on a station-to-station rather than DSN-to-MSFN basis. During the *Apollo* mission, the backup sites were considered operating elements of the co-located MSFN prime stations.

Once on mission status, scheduling would be accomplished by the weekly GSFC network control group schedule. The prime sites and backup sites were to be scheduled as a single facility during *Apollo* mission periods.

Operation and maintenance of the common equipment at the DSN backup facilities was to be the responsibility of JPL. However, the procedures and standards used were to be compatible with those employed by the prime stations.

The backup sites were to participate to the maximum extent feasible in MSFN tests, drills, and mission simulations. Evaluations of test results and determination of station readiness to provide mission support would be the responsibility of GSFC.

The need for JPL to monitor and evaluate the activities and performance of the backup stations during MSFN operations was recognized; where any independent test programs were required by JPL for backup station evaluation, they were to be conducted outside the *Apollo* mission periods.

NASA functional requirements placed on the DSN/MSFN *Apollo* backup system were to:

(1) Acquire and track spacecraft signals through an integral acquisition subsystem.

(2) Transmit voice, data, and ranging signals to spacecraft.

(3) Transfer track from the acquisition subsystem to the main receiving subsystem.

(4) Determine range and range rate parameters of spacecraft and transfer this information to recorders and/or NASCOM.

(5) Receive video, voice, and telemetry information from the spacecraft, and transfer this information to recorders and/or NASCOM.

(6) Accept pointing information from specified sources (drive tapes, manual) and utilize this information to drive the antenna.

(7) Maneuver or position the antenna according to any manual drive inputs within the specified maximum rate and acceleration.

(8) Operate in programmed search modes.

(9) Use the antenna in a slaved mode.

(10) Provide slaving signals for driving other antennas.

(11) Provide visual readout of antenna pointing angle, record this information, and/or transfer this information to NASCOM.

7. ***Interfaces.*** Jet Propulsion Laboratory designed, installed, and checked out the necessary interface equipment for the backup stations, and, with GSFC assistance, installed and checked out MSFN supplied antenna mounted electronics at each DSS. In addition, JPL completed the system tests at the DSN *Apollo* backup stations for acceptance by GSFC engineering personnel. The major signal interfaces between DSN and MSFN subsystems at the DSN *Apollo* backup stations existed at the inputs to the MSFN receivers, the DSN transmitter final amplifier, the MSFN tracking data processor, and the servo control. Additional interfaces also existed at the antenna position programmer, intercommunications, optical target aid, status displays, and site utilities. The major equipment added to achieve GSFC (MSFN) and JPL (DSN) interface included two receivers, two masers, one additional 20-kW transmitter, and new subsystem/system switching modifications. The DSN and MSFN control rooms were each supplied with a master mission configuration control switch. Both switches had to be thrown to effect a transfer of the system configuration between the DSN and MSFN configurations. The interfaces are listed in Table 8 and shown in Fig. 67.

8. ***Final configuration.*** The final configuration involved switching the common antenna drive between the two separate DSN and MSFN electronic control systems. These control systems are identical, fully compensated, and so configured that the system not actually controlling the antenna is connected to a dummy load to allow simulation of operation. The selection of the system to be connected to the antenna is made by the DSN/MSFN transfer switch which controls the relays and interlocks needed. This resulted in complete redundancy of the electrical portion of the control system, allowing for immediate takeover by the standby system upon request. It also resulted in minimum conflict between DSN and *Apollo* Projects over technical and personnel problems, and reduced the scheduling problems to assignment of actual antenna time.

9. ***Contingency plan for emergencies.*** Should a failure or serious degradation of performance occur at the *Apollo* prime station, mission requirements commit the co-located DSN/MSFN *Apollo* backup station to be fully capable of substituting for the prime station within a short time. The co-located DSN/MSFN stations normally participate in the *Apollo* lunar missions and their simulations on a full-time basis from launch minus 2 wk until the end of the mission and at other times on a scheduled basis.

Each DSN/MSFN backup station has a dual capability, thereby permitting communication with two *Apollo* spacecraft simultaneously. Different frequencies are assigned to the dual functions; however, only a single DSN 85-ft antenna is used. Dual tracking, including data formatting, is accomplished at the DSN/MSFN site and employs separate NASCOM circuits to the computers at the MSC Mission Control Center, Houston, providing full redundancy to the prime station. Two-way voice is shared between the MSFN prime and the DSN/MSFN backup sites. While the transmitter and receiver are located at the backup site, the downlink voice demodulators are located at the prime station, with the latter's NASCOM circuits used to relay voice to and from Houston. Two-way data (commands, telemetry, TV, etc.) are handled similarly to two-way voice. However, for both of these functions the DSN *Apollo* stations are implemented with subcarrier modulators. Subcarrier demodulation and decommutation are performed at the prime sites using composite spectra from the DSN *Apollo* station's carrier phase demodulators and/or the 50 MHz IF (FM) output. Selected spacecraft telemetry (e.g., transponder phase error and AGC) is routed back to the

Table 8. Implementation interface responsibilities

Design cognizant	Procurement	Installation and test	Subsystem and document
JPL	JPL	JPL	Cassegrain feed, to handle both DSN and MSFN requirements
			Acquisition feed
			Tidbinbilla backup, Pioneer backup[a]: Modify existing JPL antenna to handle both DSN and MSFN requirements
			Robledo backup: No acquisition antenna planned or required
			Antenna, mechanical
			Switch control of antenna equipment for MSFN (within DSN control room)
			1. Microwave switch control
			2. Power amplifier switching
			3. Low noise amplifier switching
			Cassegrain cone
			Low noise amplifier
			Low noise amplifier with 4 output ports and noise figure measurement/indication
JPL	JPL	JPL	Klystron power amplifier sampling coupler to verification receiver
GSFC	GSFC	JPL/ GSFC	Verification receiver (MSFN control room)
			Interconnecting cables
GSFC	GSFC	GSFC	1. Within MSFN control room (MSFN-to-MSFN equipment)
GSFC	GSFC	JPL/ GSFC	2. Between DSN antenna electronics room and MSFN control room. (RF direct run type coaxial cables, MSFN-to-MSFN)
JPL	JPL	JPL	3. DSN antenna electronics room to interface J-box via hydromechanical room (power, control signals and indicator types)
			4. MSFN equipment to DSN interface
			Interface racks, J-boxes, etc.
			Collimation towers
			SCM[b] optical target
	JPL	JPL	SAA[c] optical target
JPL	GSFC	JPL/ GSFC	Spare transponder and test transmitter (in MSFN control room)
GSFC	GSFC	JPL/ GSFC	Collimation tower control equipment from MSFN control room
JPL	JPL	JPL	Antenna boresight TV camera
GSFC	GSFC	JPL/ GSFC	Boresight TV monitor display (MSFN control room)
GSFC	GSFC	GSFC	Racks in collimation tower building
GSFC	GSFC	JPL/ GSFC	Boresight signal source (3 radio frequencies)
JPL	JPL	JPL	Collimation tower remote operation cables (50 pair) and trenching
GSFC	GSFC	JPL/ GSFC	Tactical intercom (MSFN control room)
JPL	JPL	JPL	Interface intercom
			System integration of antenna mounted RER (4 racks)
			Angle encoders interface
			Servo interface
			Tracking data processor interface
JPL	JPL	JPL	Antenna pointing programmer interface
GSFC	GSFC	JPL/ GSFC	System monitor (GSFC) Install: same as entire MSFN

[a]This unit serves as a network spare for the prime acquisition stations, Woomera, Tidbinbilla, and Johannesburg.

[b]SCM = S-band cassegrain-monopulse.

[c]SAA = S-band acquisition aid (subsystem).

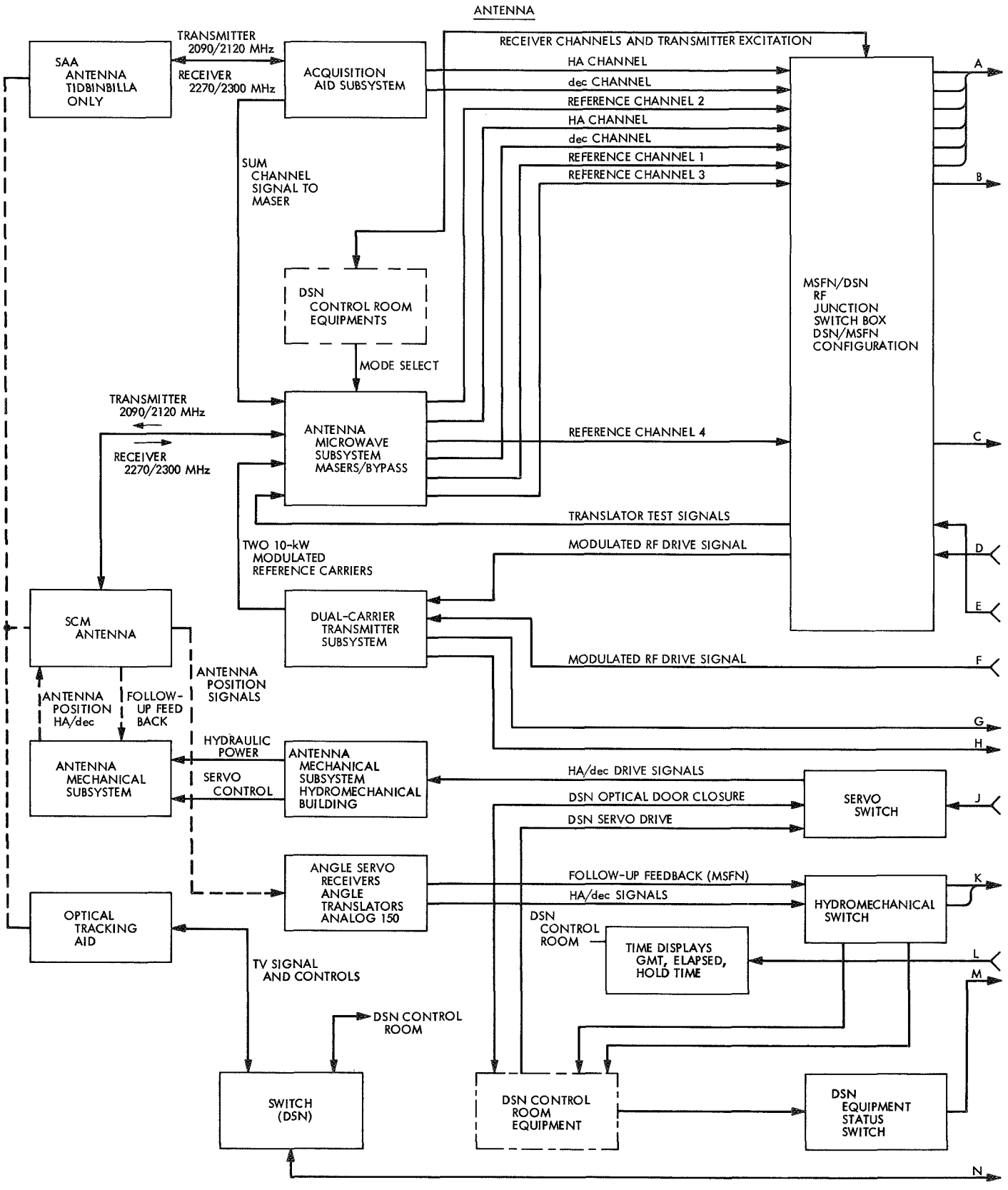

Fig. 67. System interface diagram of MSFN/DSN *Apollo* backup station

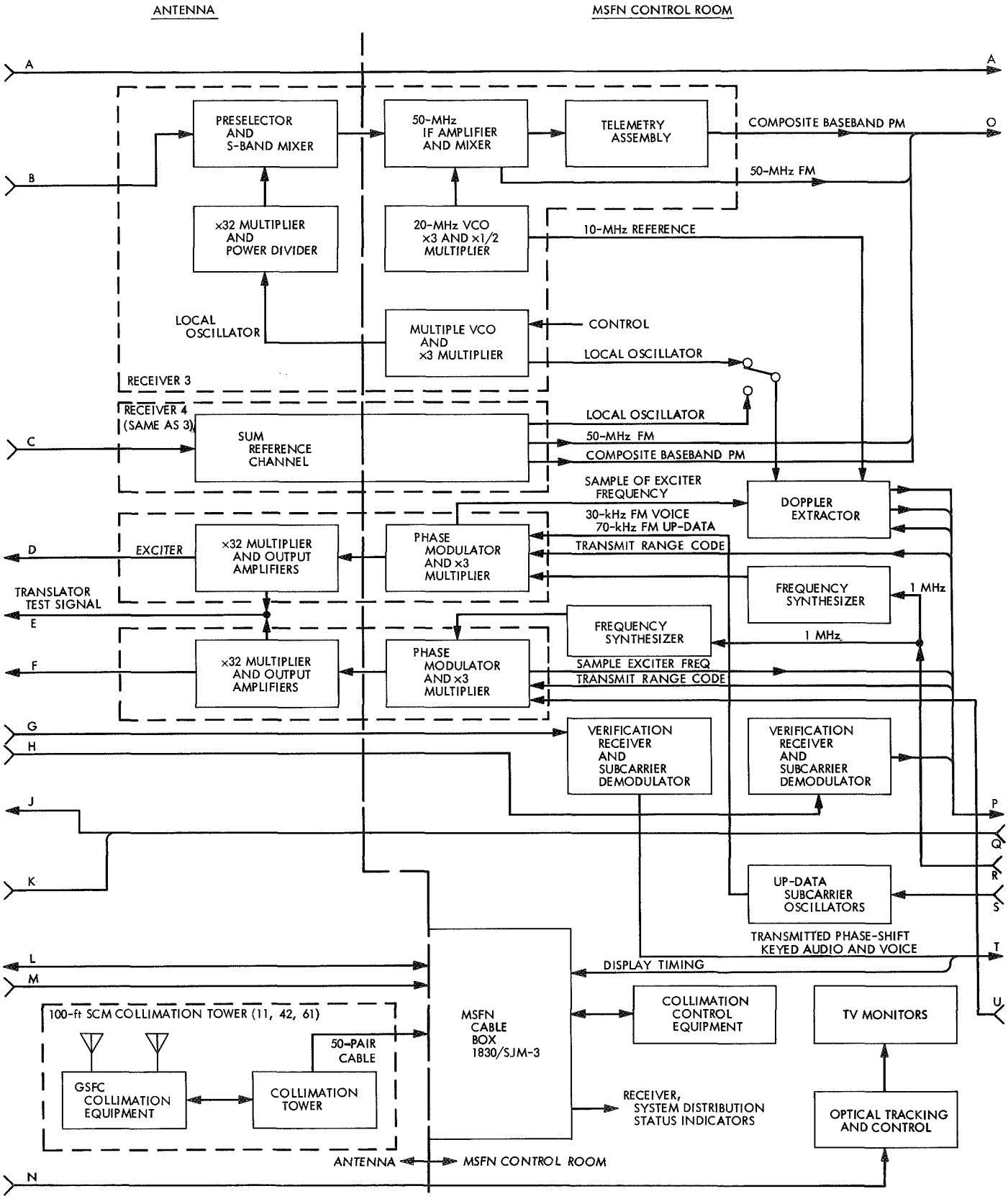
ANTENNA
MSFN CONTROL ROOM
A
A
PRESELECTOR AND S-BAND MIXER
50-MHz IF AMPLIFIER AND MIXER
TELEMETRY ASSEMBLY
COMPOSITE BASEBAND PM
O
B
50-MHz FM
x32 MULTIPLIER AND POWER DIVIDER
20-MHz VCO x3 AND x1/2 MULTIPLIER
10-MHz REFERENCE
LOCAL OSCILLATOR
MULTIPLE VCO AND x3 MULTIPLIER
CONTROL
LOCAL OSCILLATOR
RECEIVER 3
RECEIVER 4 (SAME AS 3)
LOCAL OSCILLATOR
C
SUM REFERENCE CHANNEL
50-MHz FM
COMPOSITE BASEBAND PM
SAMPLE OF EXCITER FREQUENCY
DOPPLER EXTRACTOR
30-kHz FM VOICE
70-kHz FM UP-DATA
D
EXCITER
x32 MULTIPLIER AND OUTPUT AMPLIFIERS
PHASE MODULATOR AND x3 MULTIPLIER
TRANSMIT RANGE CODE
FREQUENCY SYNTHESIZER
1 MHz
TRANSLATOR TEST SIGNAL
E
FREQUENCY SYNTHESIZER
1 MHz
F
x32 MULTIPLIER AND OUTPUT AMPLIFIERS
PHASE MODULATOR AND x3 MULTIPLIER
SAMPLE EXCITER FREQ
TRANSMIT RANGE CODE
G
VERIFICATION RECEIVER AND SUBCARRIER DEMODULATOR
VERIFICATION RECEIVER AND SUBCARRIER DEMODULATOR
H
J
P
Q
K
R
UP-DATA SUBCARRIER OSCILLATORS
S
TRANSMITTED PHASE-SHIFT KEYED AUDIO AND VOICE
T
L
DISPLAY TIMING
M
U
100-ft SCM COLLIMATION TOWER (11, 42, 61)
MSFN CABLE BOX 1830/SJM-3
COLLIMATION CONTROL EQUIPMENT
TV MONITORS
50-PAIR CABLE
GSFC COLLIMATION EQUIPMENT
COLLIMATION TOWER
RECEIVER, SYSTEM DISTRIBUTION STATUS INDICATORS
OPTICAL TRACKING AND CONTROL
ANTENNA
MSFN CONTROL ROOM
N

Fig. 67 (contd)

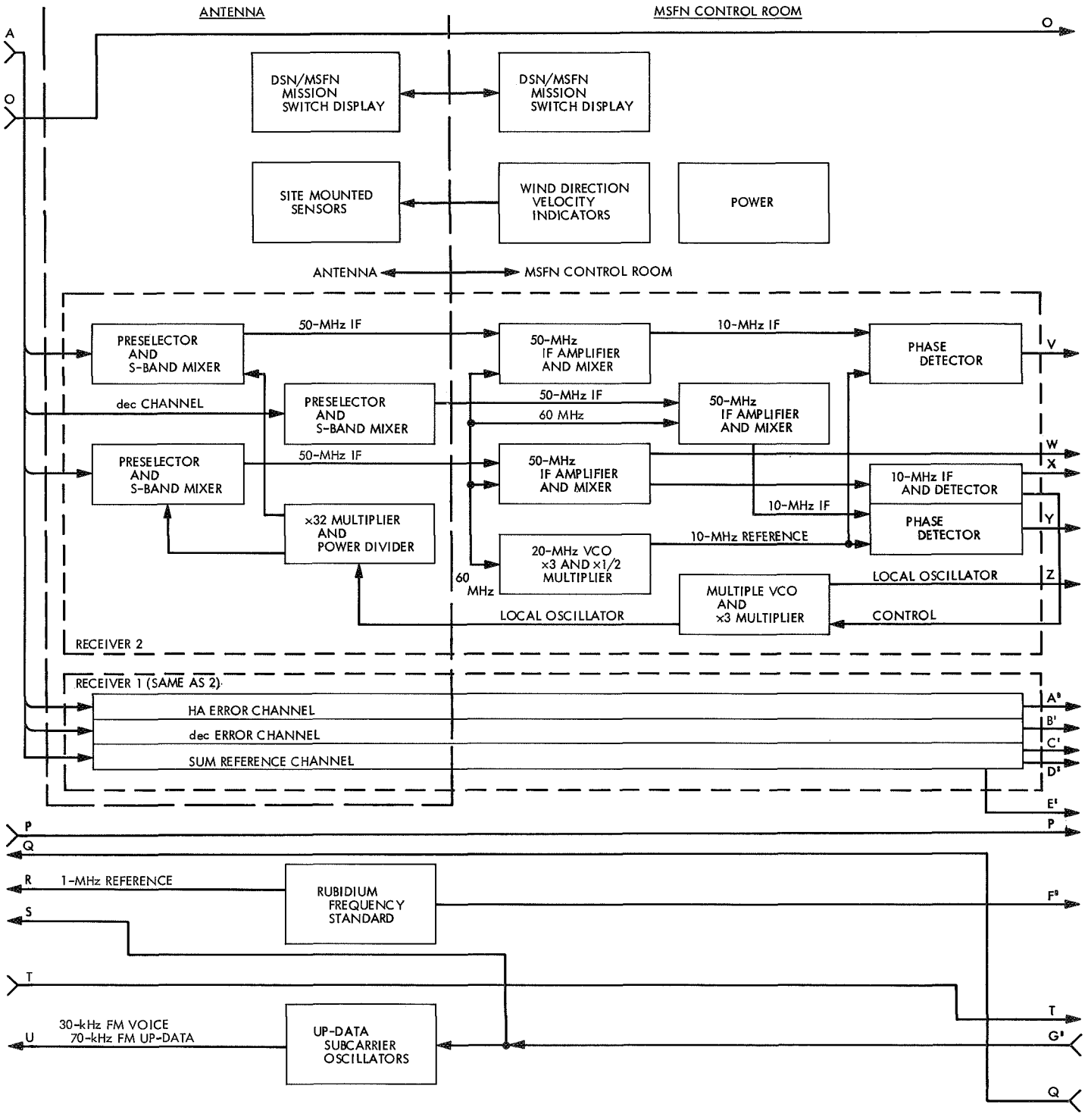
ANTENNA
MSFN CONTROL ROOM
A
O
O
DSN/MSFN MISSION SWITCH DISPLAY
DSN/MSFN MISSION SWITCH DISPLAY
SITE MOUNTED SENSORS
WIND DIRECTION VELOCITY INDICATORS
POWER
ANTENNA
MSFN CONTROL ROOM
PRESELECTOR AND S-BAND MIXER
50-MHz IF
50-MHz IF AMPLIFIER AND MIXER
10-MHz IF
PHASE DETECTOR
V
dec CHANNEL
PRESELECTOR AND S-BAND MIXER
50-MHz IF
60 MHz
50-MHz IF AMPLIFIER AND MIXER
PRESELECTOR AND S-BAND MIXER
50-MHz IF
50-MHz IF AMPLIFIER AND MIXER
W
X
10-MHz IF AND DETECTOR
10-MHz IF
PHASE DETECTOR
Y
×32 MULTIPLIER AND POWER DIVIDER
20-MHz VCO ×3 AND ×1/2 MULTIPLIER
10-MHz REFERENCE
60 MHz
MULTIPLE VCO AND ×3 MULTIPLIER
LOCAL OSCILLATOR
Z
LOCAL OSCILLATOR
CONTROL
RECEIVER 2
RECEIVER 1 (SAME AS 2)
HA ERROR CHANNEL
dec ERROR CHANNEL
SUM REFERENCE CHANNEL
A'
B'
C'
D'
E'
P
P
Q
R
1-MHz REFERENCE
RUBIDIUM FREQUENCY STANDARD
F'
S
T
T
30-kHz FM VOICE
U
70-kHz FM UP-DATA
UP-DATA SUBCARRIER OSCILLATORS
G'
Q

Fig. 67 (contd)

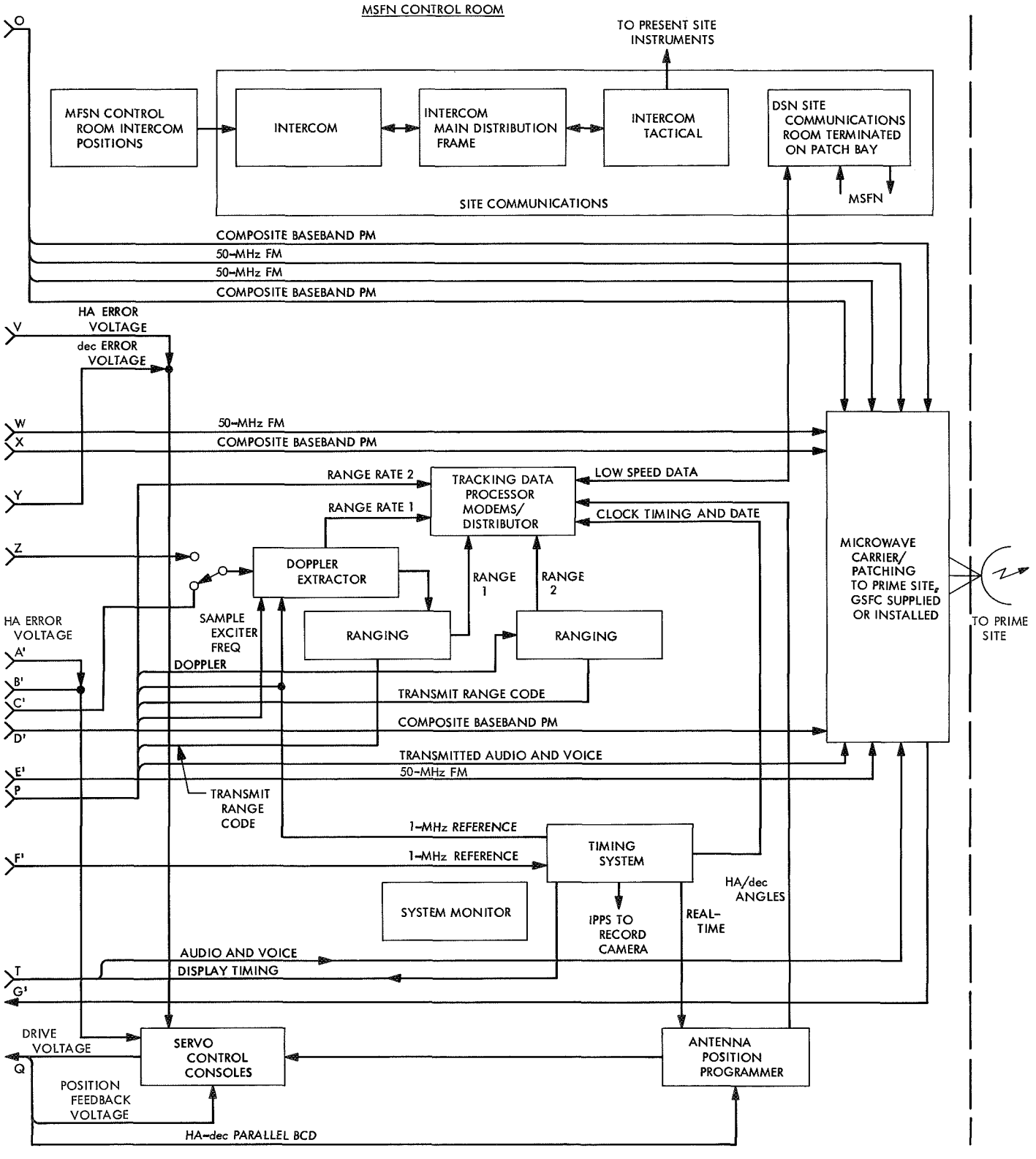
MSFN CONTROL ROOM
TO PRESENT SITE INSTRUMENTS
MFSN CONTROL ROOM INTERCOM POSITIONS
INTERCOM
INTERCOM MAIN DISTRIBUTION FRAME
INTERCOM TACTICAL
DSN SITE COMMUNICATIONS ROOM TERMINATED ON PATCH BAY
MSFN
SITE COMMUNICATIONS
O
COMPOSITE BASEBAND PM
50-MHz FM
50-MHz FM
COMPOSITE BASEBAND PM
V
HA ERROR VOLTAGE
dec ERROR VOLTAGE
W
50-MHz FM
X
COMPOSITE BASEBAND PM
Y
RANGE RATE 2
RANGE RATE 1
TRACKING DATA PROCESSOR MODEMS/ DISTRIBUTOR
LOW SPEED DATA
CLOCK TIMING AND DATE
Z
DOPPLER EXTRACTOR
RANGE 1
RANGE 2
MICROWAVE CARRIER/ PATCHING TO PRIME SITE, GSFC SUPPLIED OR INSTALLED
TO PRIME SITE
HA ERROR VOLTAGE
SAMPLE EXCITER FREQ
RANGING
RANGING
A'
DOPPLER
B'
C'
TRANSMIT RANGE CODE
COMPOSITE BASEBAND PM
D'
TRANSMITTED AUDIO AND VOICE
E'
50-MHz FM
P
TRANSMIT RANGE CODE
1-MHz REFERENCE
F'
1-MHz REFERENCE
TIMING SYSTEM
HA/dec ANGLES
SYSTEM MONITOR
IPPS TO RECORD CAMERA
REAL-TIME
AUDIO AND VOICE
T
DISPLAY TIMING
G'
DRIVE VOLTAGE
SERVO CONTROL CONSOLES
ANTENNA POSITION PROGRAMMER
Q
POSITION FEEDBACK VOLTAGE
HA-dec PARALLEL BCD

Fig. 67 (contd)

DSN site after processing by the prime station. A two-way microwave communication system links the co-located *Apollo* prime and backup stations.

In the event of a system failure at the *Apollo* prime, two DSN/MSFN selector switches, one in each wing, are manually activated to automatically change the DSS equipment configuration to MSFN mission support. Except for the site intercom/communication manual patches and transmitter/master retuning, the DSN/MSFN station is in one configuration or the other, by the activation of these selector switches.

10. Time limits. In July 1963, GSFC released the Data System Development Plan for the *Apollo C-1* program, which required that the unified S-band RER system, for which JPL was responsible, was to be installed and ready for operational qualification prior to the second *Apollo C-1* flight scheduled for the second quarter of 1965. The actual deadlines were Pioneer site by October 15, 1966; Tidbinbilla site by January 15, 1967; and Robledo site by April 1, 1967. The implementation schedule prepared to meet the deadlines established by GSFC is shown in Fig. 68.

B. Implementation of Control Rooms

1. Description. Equipment, facilities, and power requirements of the MSFN control rooms are described in the paragraphs that follow.

a. Equipment. Following the decision on February 4, 1964 to adopt the JPL-developed coherent tracking and telemetry technology for both the *Apollo* earth orbital and lunar missions, the Office of Tracking and Data Acquisition at NASA headquarters directed JPL to provide RER equipment needed by the earth-based tracking stations. This equipment was supplied to both the MSFN and DSN by JPL, which supports the *Apollo* lunar missions by employing three of its 85-ft antennas as backup to three MSFN 85-ft antennas installed during the MSFN's upgrade from the *Gemini* Project to the *Apollo* Project.

b. Facilities. The configuration employed at the DSN 85-ft antenna *Apollo* backup stations was carefully studied. As the *Apollo* lunar mission profile became defined, the term "backup" became something of a misnomer. The beamwidth of an 85-ft antenna at S-band suggested the consideration of two such antennas when *Apollo* was at the moon: one to cover the orbiting CSM and the other the landed LM. En route to and from the moon, however, the second 85-ft antenna would serve as a true, redundant backup.

The projected DSN tracking schedules were also quite full well into the expected *Apollo* time period. For these reasons, it was decided to separate the *Apollo* activity from the other activities at the DSN backup stations as much as possible to maximize the amount of parallel usage of these facilities. This was accomplished through the addition of MSFN control rooms to the operations buildings at the Pioneer, Tidbinbilla, and Robledo sites.

The MSFN control room, connected to the DSN 85-ft antenna and its associated equipment, constitutes a MSFN dual-type tracking station; except that the *Apollo* mission-peculiar telemetry, voice, etc., are sent prior to demodulation via a microwave link to the neighboring MSFN prime 85-ft antenna station. An MSFN dual station contains two complete independent S-band receiving, transmitting, and ranging channels to permit simultaneous tracking and communications with both the *Apollo* CSM and LM whenever they are jointly within the antenna beamwidth. Because the *Apollo* spacecraft have two transmitting frequencies (one for coherent phase modulation and the other for frequency modulation), each MSFN dual station has the capability to simultaneously receive four frequencies (downlinks) and transmit two frequencies (uplinks), the latter with a radiated capacity of 10 kW each at the 85-ft antenna stations.

These *Apollo* operational requirements necessitated addition of considerable MSFN-oriented equipment to the declination-axis wheel house on the DSN backup station's antennas. In addition to a second maser and high-power klystron, four racks of MSFN receiver/exciter equipment and numerous DSN/MSFN transfer switching networks were added to the antenna; the latter was connected to an elaborate key-controlled interlock network that enables the station to be converted rapidly from DSN to MSFN service and vice versa.

The design goal of maximum parallel activity in the two control rooms, except for antenna usage, was, therefore, achieved. During *Apollo* activities, the DSN backup stations are staffed by MSFN personnel, with selected support from a limited number of DSN personnel to operate the common inter-network subsystems, with the MSFN maintenance and operations supervisor in charge. At other times these stations, except for the MSFN control rooms, are under the direction of the DSN station director.

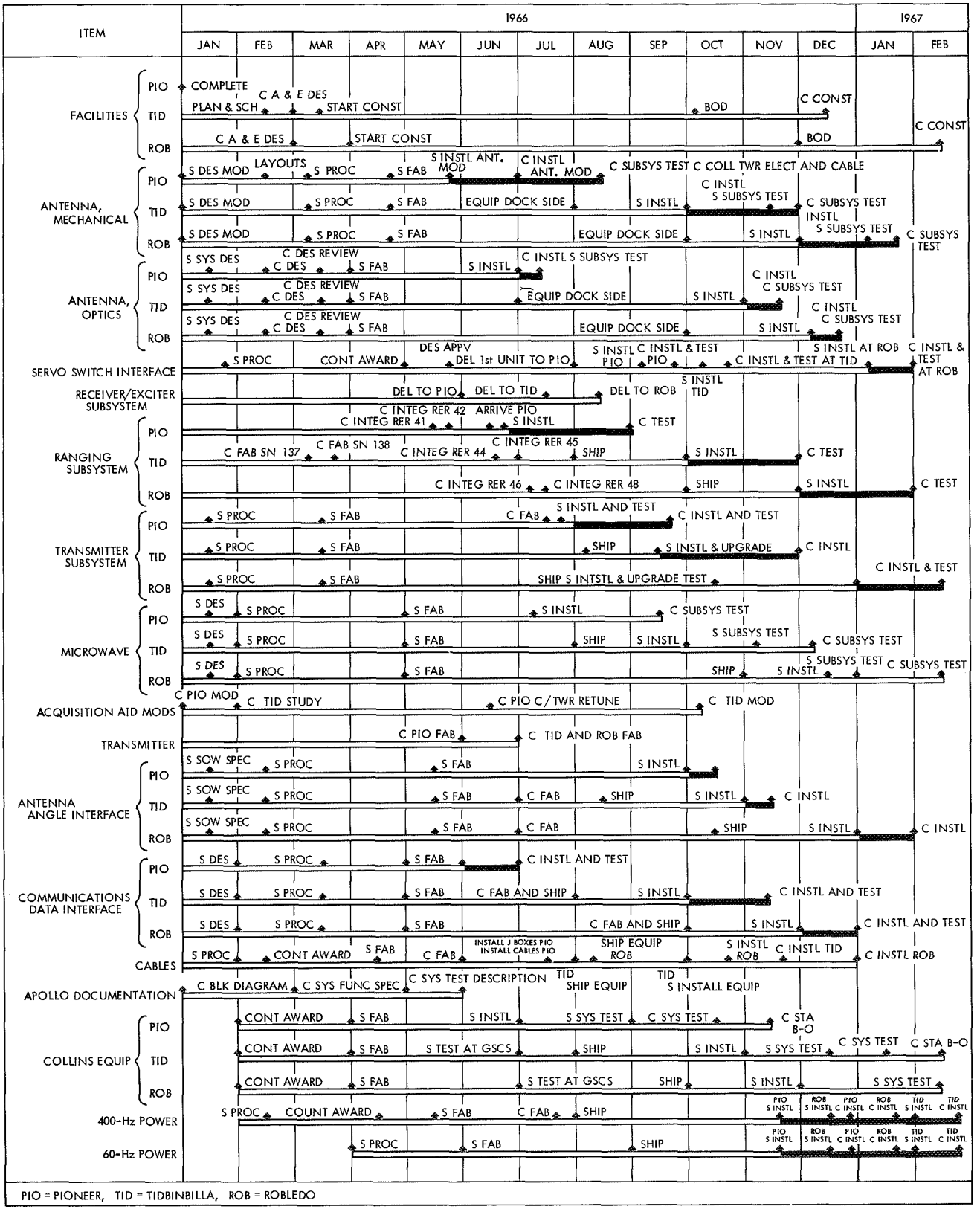

Fig. 68. Deep Space Network/MSFN implementation schedule

c. Power. The power requirements for the DSN *Apollo* backup stations were also carefully studied. Although the power available at each station was sufficient for DSN operation, it was not capable of providing the 100% backup reliability required by the MSFN. The 480 V, 60 Hz, three-phase, three-wire power requirements for each MSFN control room are shown in Table 9.

Pioneer and Tidbinbilla sites. To achieve the full backup power requirement at Pioneer and Tidbinbilla, it was necessary to remove two of four 150-kW generator sets and replace them with two 500-kW generator sets. In addition, two 50-kW generator sets were removed and replaced by two 200-kW generator sets to provide the required 400-Hz transmitter power.

Robledo site. Backup power in the form of an additional 500-kW diesel generator was provided at Robledo. The 400-Hz transmitter power was provided by replacing two 50-kW generator sets with two 200-kW generator sets.

2. *Construction of control room facilities.* Construction of control room facilities is discussed in the paragraphs that follow.

a. Pioneer site. With the selection of Pioneer site as the initial DSN/MSFN *Apollo* backup station, testing facility for all S-band equipment, and training school for local and overseas personnel, it became necessary to increase the size of the original station facilities. An interim prefabricated S-band building annex was erected to house the first S-band RF subsystem (SN 01) equipment and to allow equipment testing to proceed on schedule.

Table 9. Power requirements for MSFN control rooms

Item	Power requirement, kW		
	Pioneer site	Tidbinbilla site	Robledo site
Equipment[a]	38	38	38
Hydromechanical[a]	10	10	10
Collimation tower[a]	3	3	3
400-Hz transmitter power[b]	175	175	170
Antenna drive[b]	150	150	150
Power amplifier[b]	20	20	40
Heat exchanger[b]	60	60	—[c]
Miscellaneous[a]	20	20	20
Miscellaneous[a]	20	20	25

[a]Critical mission, motor equipment, noninterruptable controlled fluctuations.

[b]Critical mission, electronic, noninterruptable, clean, nonfluctuating and regulated.

[c]Not available.

Construction of the DSN and MSFN control rooms (Fig. 69) began in March 1964 and was completed in October of the same year (Fig. 70). An area of 2520 ft² adjoining the station's operation control building was allocated for the MSFN operations control room (Fig. 71). A 2520-ft² airtight basement plenum was provided directly under the control room to contain the 24-in. cable lay-in trays. Entrance into the basement plenum was through an air lock that prevented the 50-deg regulated air temperature, required for equipment cooling, from fluctuating whenever someone entered or left.

A 7-ft-diam corrugated steel tunnel was installed underground from the existing hydromechanical building 81 ft towards the original control building. At this point it branched off to join the basement plenum of the MSFN wing. Twelve-inch cable lay-in trays were attached to the side walls of this tunnel for routing of cables from the basement of the MSFN control room to the hydromechanical building and antenna mountal equipment.

b. Tidbinbilla site. The architectural and engineering design drawings for the MSFN control room at Tidbinbilla were completed in February 1966 by the Australian Department of Works. Construction of the MSFN control room began in late April with a scheduled completion date of December 1966. A building occupancy date was scheduled for October 28, 1966, and met. The MSFN control room (Fig. 72) located at the west end of the station's operations and engineering building and in line with the antenna support building, occupies 3500 ft² of floor space with its operation control room, communications room, and offices. An airtight basement plenum of equal size provides for cable raceways and air conditioning equipment. As at the Pioneer site, entrance into the basement plenum is through an air lock. The control room equipment layout is shown in Fig. 73.

The station's existing 7-ft-diam underground cable tunnel was modified by the addition of new cable trays to handle the MSFN cables leading from the MSFN basement plenum to the station's airtight basement plenum and to the antenna support building and the antenna mounted equipment.

To house the additional MSFN equipment required, the south end of the station's existing antenna support building was enlarged 1092 ft².

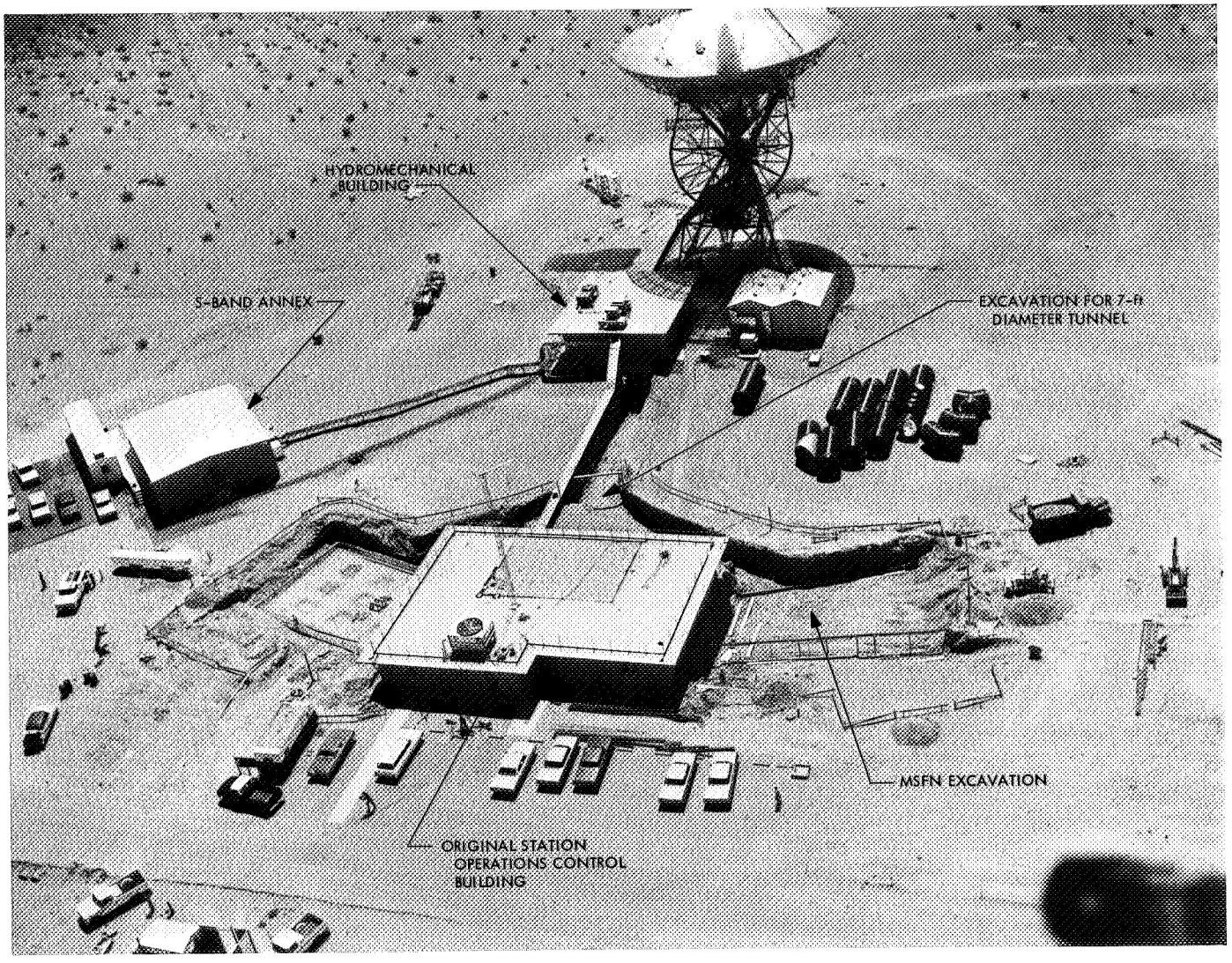

Fig. 69. Construction at Pioneer site

Fig. 70. Aerial view of Pioneer site showing completed buildings

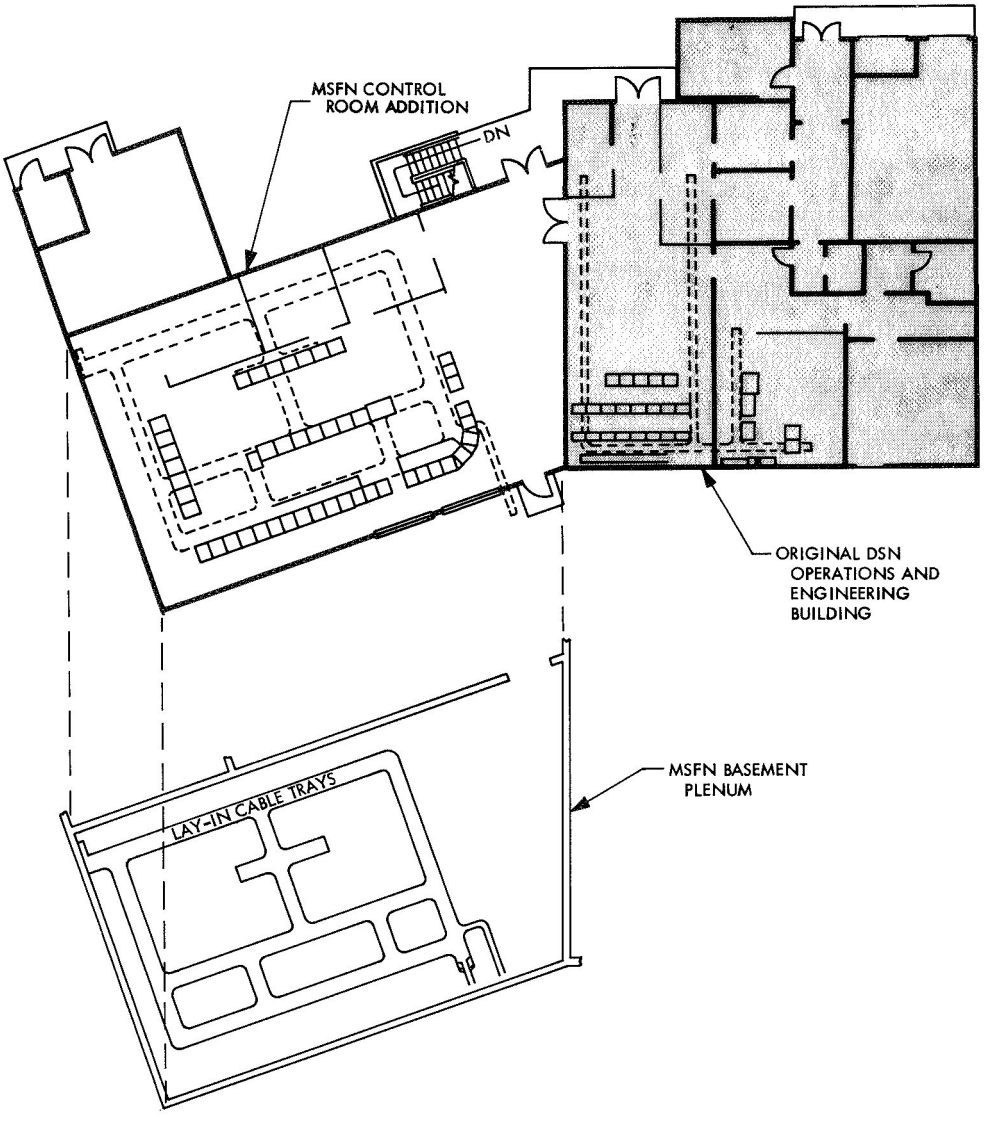

Fig. 71. Manned Space Flight Network control room floor plan at Pioneer site

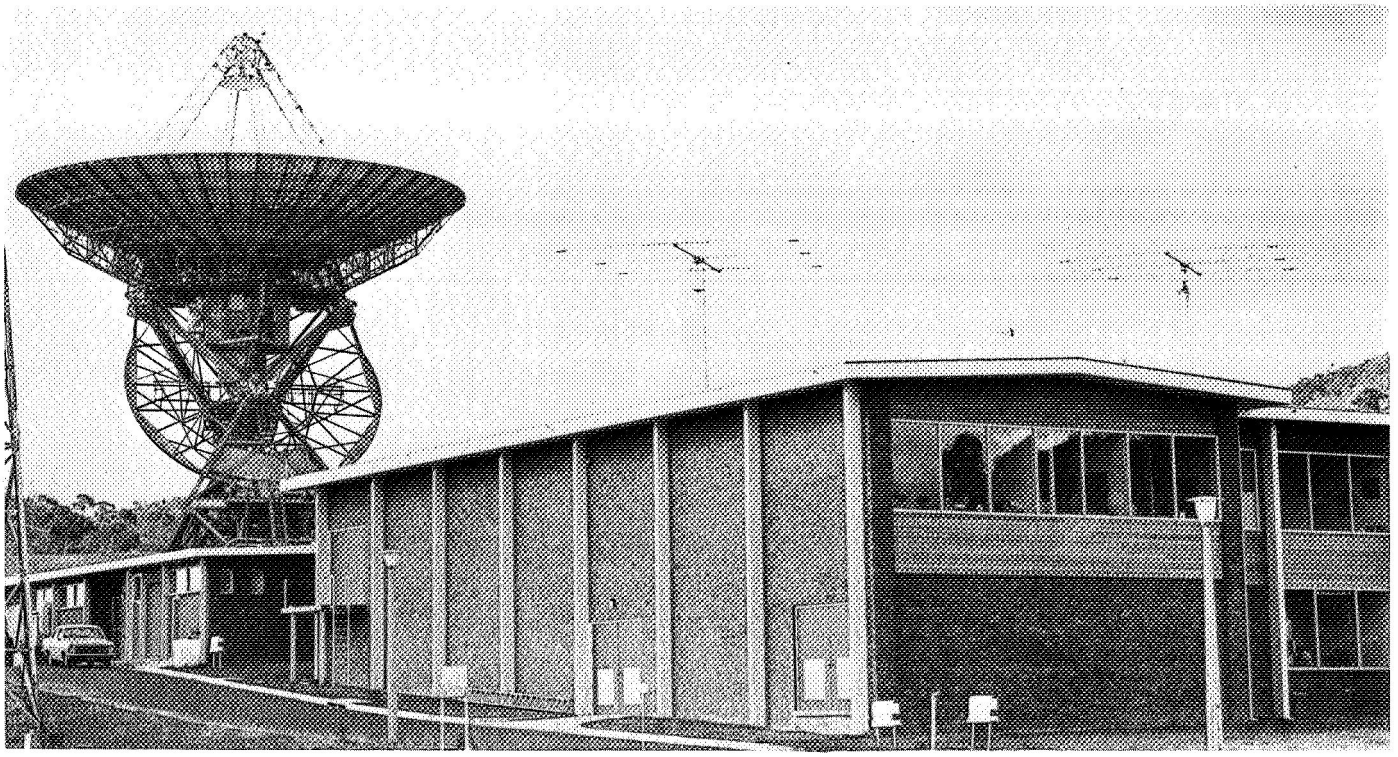

Fig. 72. Manned Space Flight Network control room at Tidbinbilla site

c. Robledo site. The architectural and engineering drawings for the MSFN control room at Robledo were completed in early May 1966 by the U. S. Navy Bureau of Yards and Docks. Construction began in June 1966 and was completed in late February 1967. The control room, like the balance of the station, is unique in that it is constructed entirely of hand-hewn granite blocks (Fig. 74). The precision with which these solid granite blocks fit is a tribute to the skill of today's Spanish stonemasons.

The MSFN control room, located approximately 25 ft east of the station's operations and engineering building, occupies 3167 ft² of floor space with its operations control room, communications room, and offices. An airtight basement plenum of equal size provides room for the cable raceways and the air conditioning equipment required for cooling the operational equipment. As for the other control rooms, entrance into the basement plenum is through an air lock. The control room layout is shown in Fig. 75.

The basement plenum of the control room is connected to the basement plenum of the station's operations and engineering building by a concrete walkthrough cable-tray tunnel. Cables from the control room equipment are routed through this tunnel between the two plenums and out to the hydromechanical building and antenna through a 7-ft-diam underground cable tunnel.

3. Modifications. In March 1964, the existing L-band cassegrain cone and hyperbola at the Pioneer site were replaced with the new S-band cassegrain cone and high-tolerance hyperbola (Fig. 76). The S-band cone and hyperbola were both constructed of 7178-T6 aluminum which provided hailstone protection, reduced weight, and improved surface accuracy from 0.125 to 0.031 in. rms. To support the S-band high-tolerance hyperbola, the tubular-type quadripod was replaced with a new design truss-type for improved strength and stiffness.

The surface area of the 85-ft-diam antenna at the Pioneer site was completely resurfaced. The original expanded aluminum mesh covering was removed and the inner 75% of the radii covered with a 6061-T6 aluminum sheet with a thickness of 0.080 in. and having 0.375-in.-diam drain holes that provided 25% porosity. The outer 25% of the radii was covered with the same material, but provided 50% porosity. In addition to the antenna resurfacing, a new 220-ft² declination wheel/electronics room was constructed in the declination wheel structure (Fig. 77) to accommodate the new MSFN antenna mounted S-band equipment.

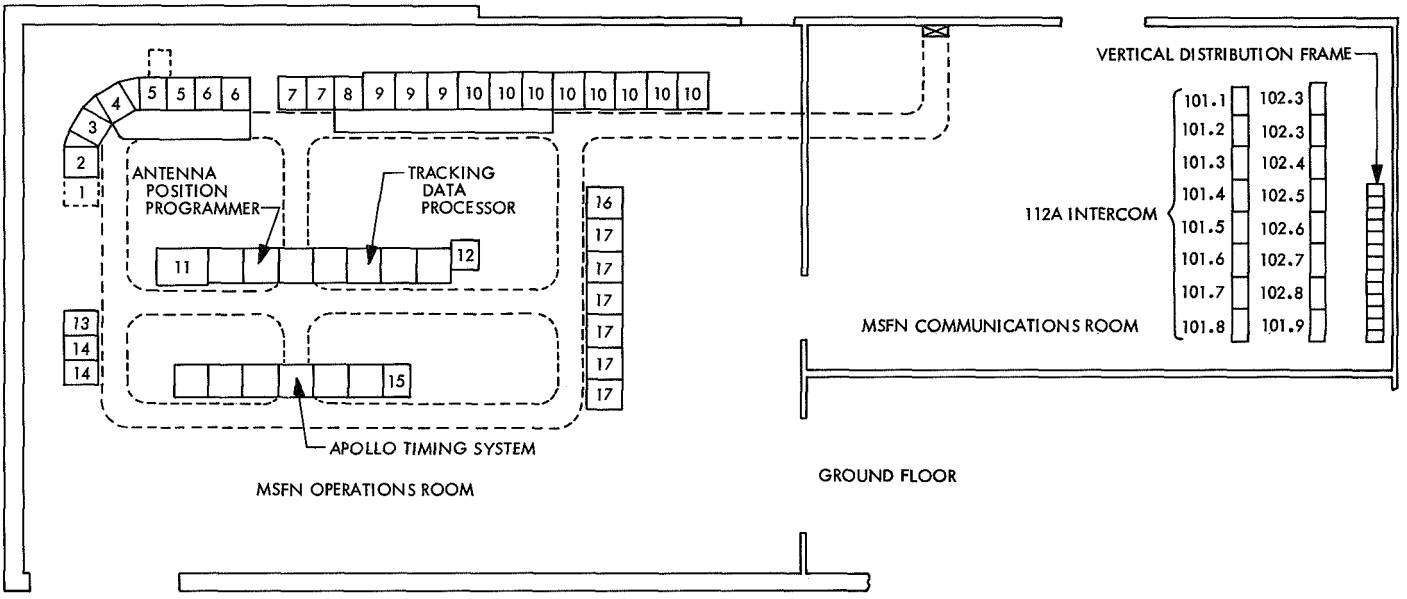

1. MOBILE TEST EQUIPMENT
2. SERVO AMPLIFIER
3. TV RECORD RACK
4. TV MONITOR
5. SERVO CONSOLE
6. DATA CONSOLE
7. SYSTEM MONITOR
8. COLLIMATION TOWER EQUIPMENT CONTROL
9. RANGE AND RANGE RATE RECEIVER/EXCITER CONTROL SYSTEM 2 RACK
10. RANGE AND RANGE RATE RECEIVER/EXCITER CONTROL SYSTEM 1 RACK
11. TAPE PERFORATOR
12. TTY PAGE PRINTER
13. UP-DATA VERIFICATION RECEIVER
14. DATA MULTIPLEX EQUIPMENT PATCH
15. RUBIDIUM FREQUENCY STANDARD TIME RACK
16. RANGE AND RANGE RATE RECEIVER/EXCITER SYSTEM 1 RANGING EQUIPMENT RACK
17. RANGE AND RANGE RATE RECEIVER/EXCITER SYSTEM 2 RANGING EQUIPMENT RACK

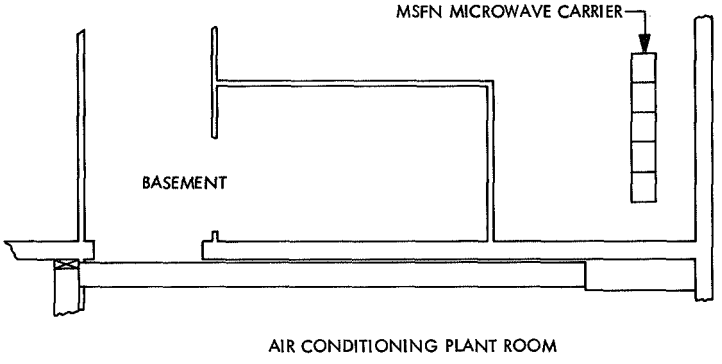

Fig. 73. Manned Space Flight Network control room equipment layout at Tidbinbilla site

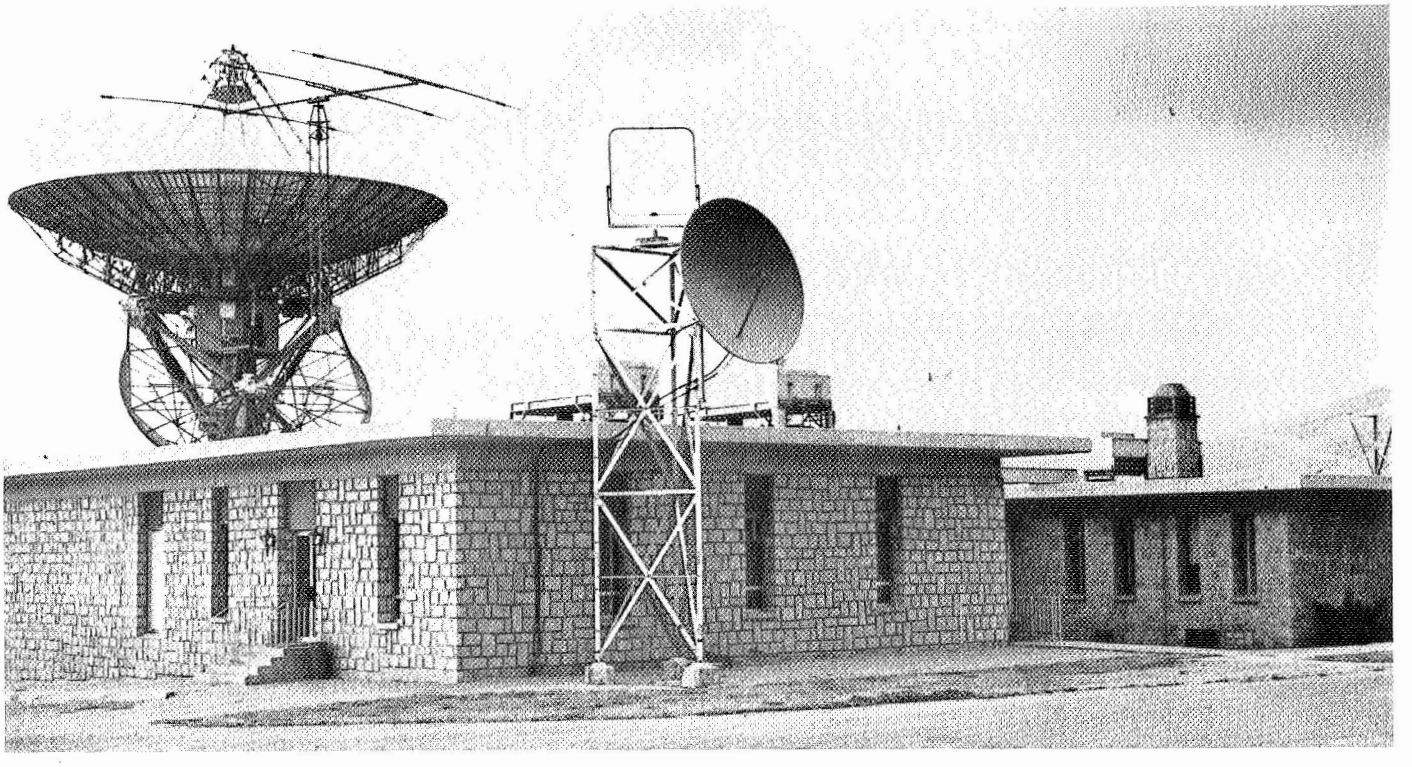

Fig. 74. Manned Space Flight Network control room at Robledo site

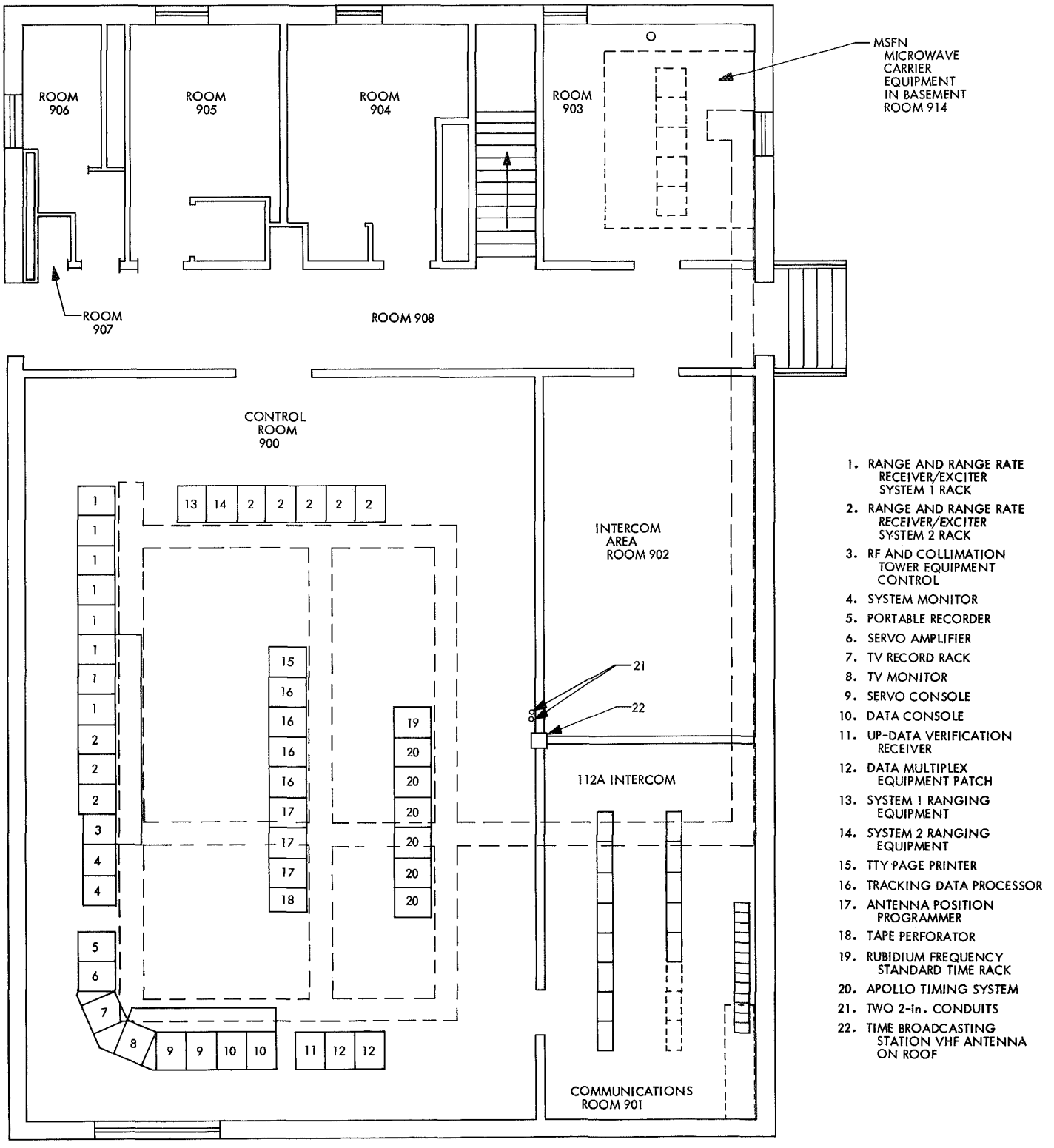

Fig. 75. Manned Space Flight Network control room equipment layout at Robledo site

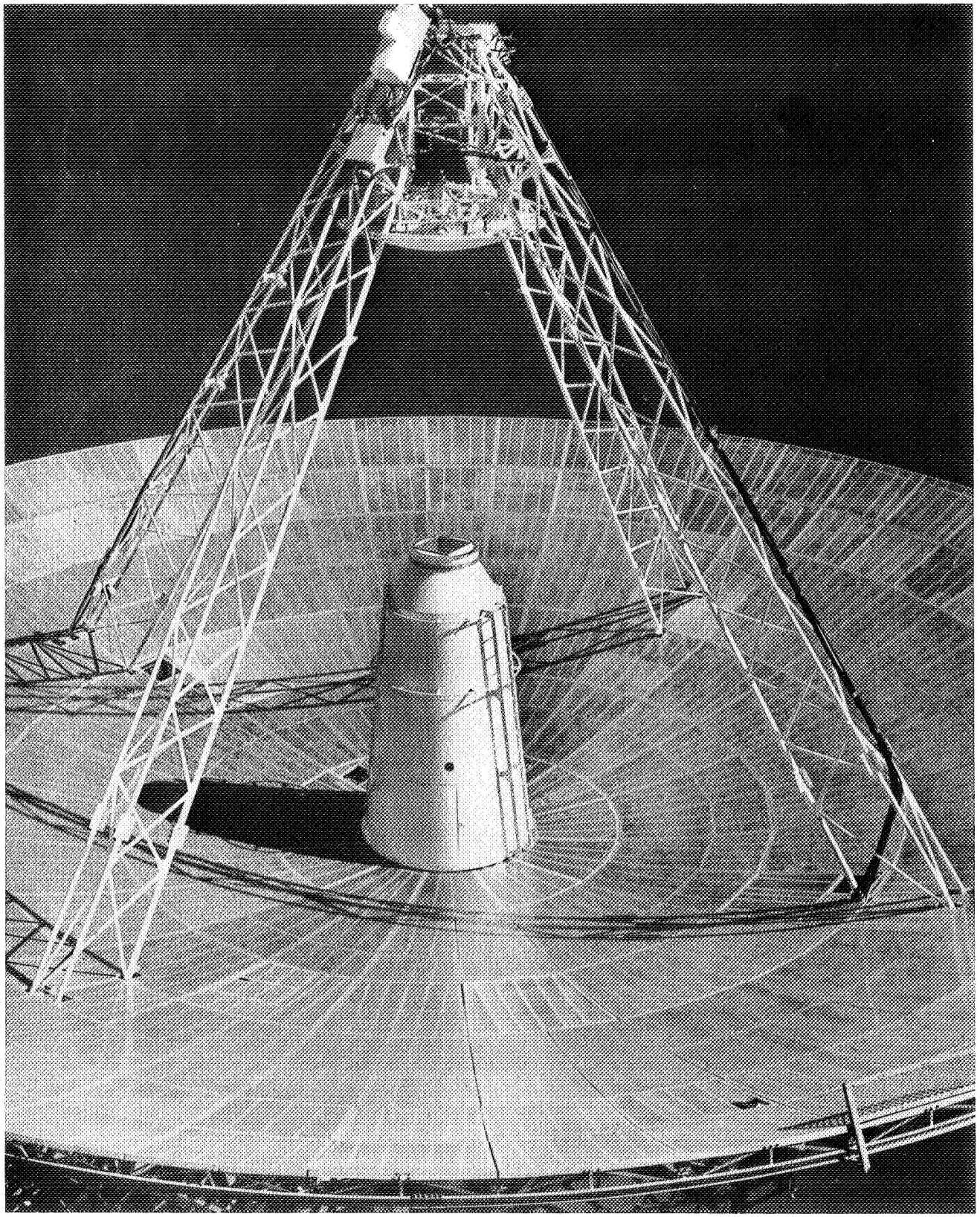

Fig. 76. New S-band cassegrain cone and hyperbola

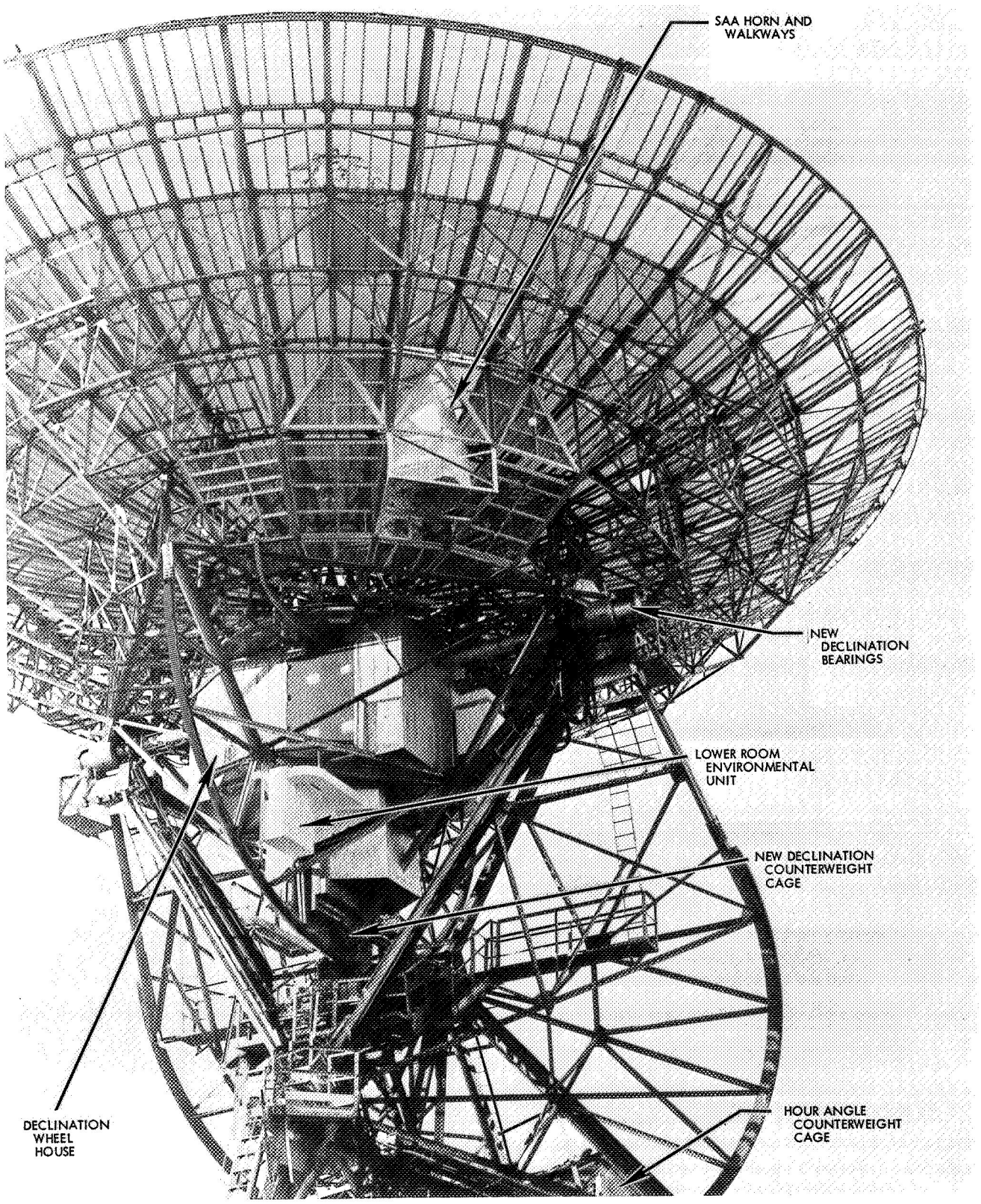

Fig. 77. Antenna structural modifications

To provide operational support to the MSFN and fulfill the DSN commitments, modifications at the Pioneer, Tidbinbilla, and Robledo sites were required to the antenna structure and electronics room.

a. Antenna structure. Modifications to the antenna structure are described in the paragraphs that follow.

Hour angle and declination counterweight modifications. To keep the antennas at Pioneer in balance after addition of the MSFN equipment, it was necessary to remove 1500 lb of lead counterweight from the dec counterweight cage and add 4000 lb of lead to the HA counterweight cage. At Tidbinbilla and Robledo, however, the dec counterweight cage is an integral part of the structure and the required amount of lead could not be removed. Therefore, after the installation of the MSFN equipment in the electronics room, measurements were made of both the HA and dec counterweights. These measurements indicated that, to bring both axes of the antenna to a balanced condition, a maximum 5000 lb of lead was required in the HA counterweight cage.

Hour angle and declination cable wrapup modification. Hour angle and dec cable wrapups were modified to eliminate cables being torn, snagged, or sheared, cable stressing, and the need for a technician to monitor the cables during tracking operations. The HA cable wrapup

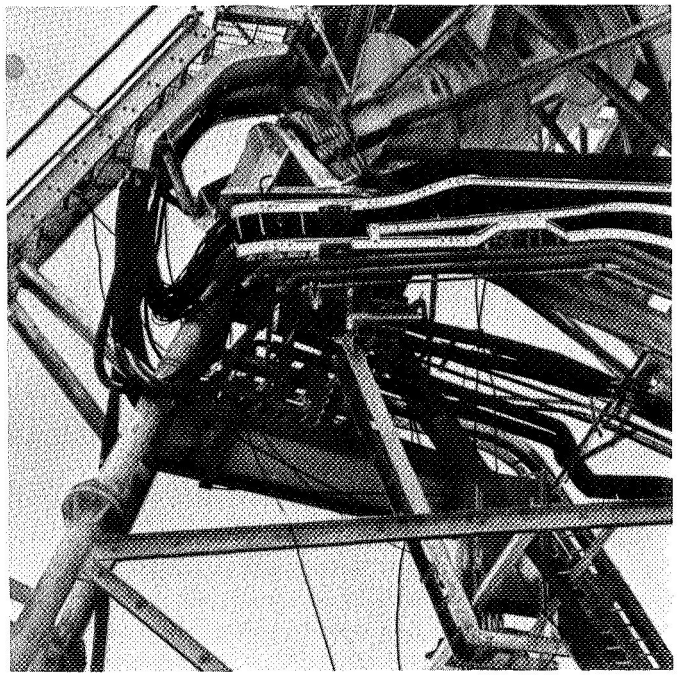

Fig. 78. Hour angle axis cable wrapup modification

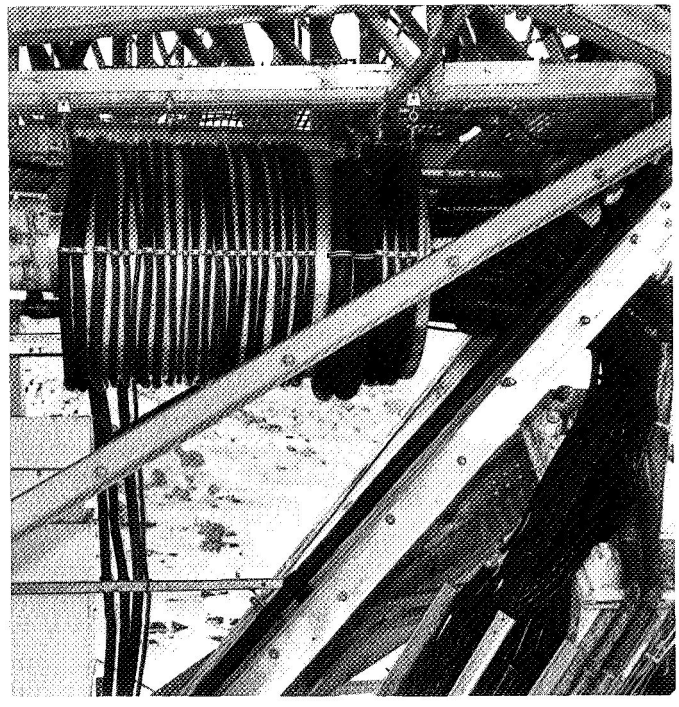

Fig. 79. Declination axis cable wrapup modification

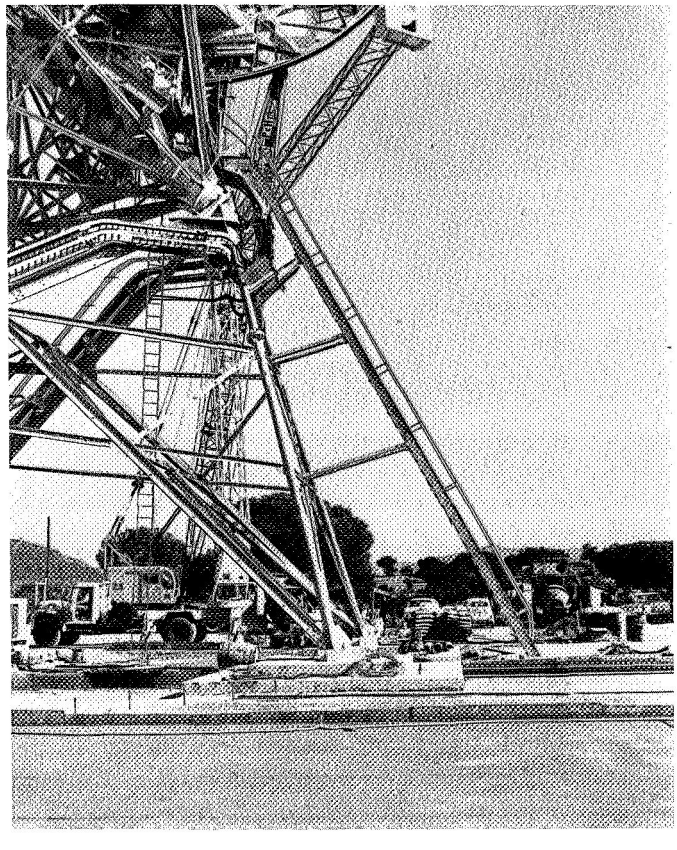

Fig. 80. New ladder and platform

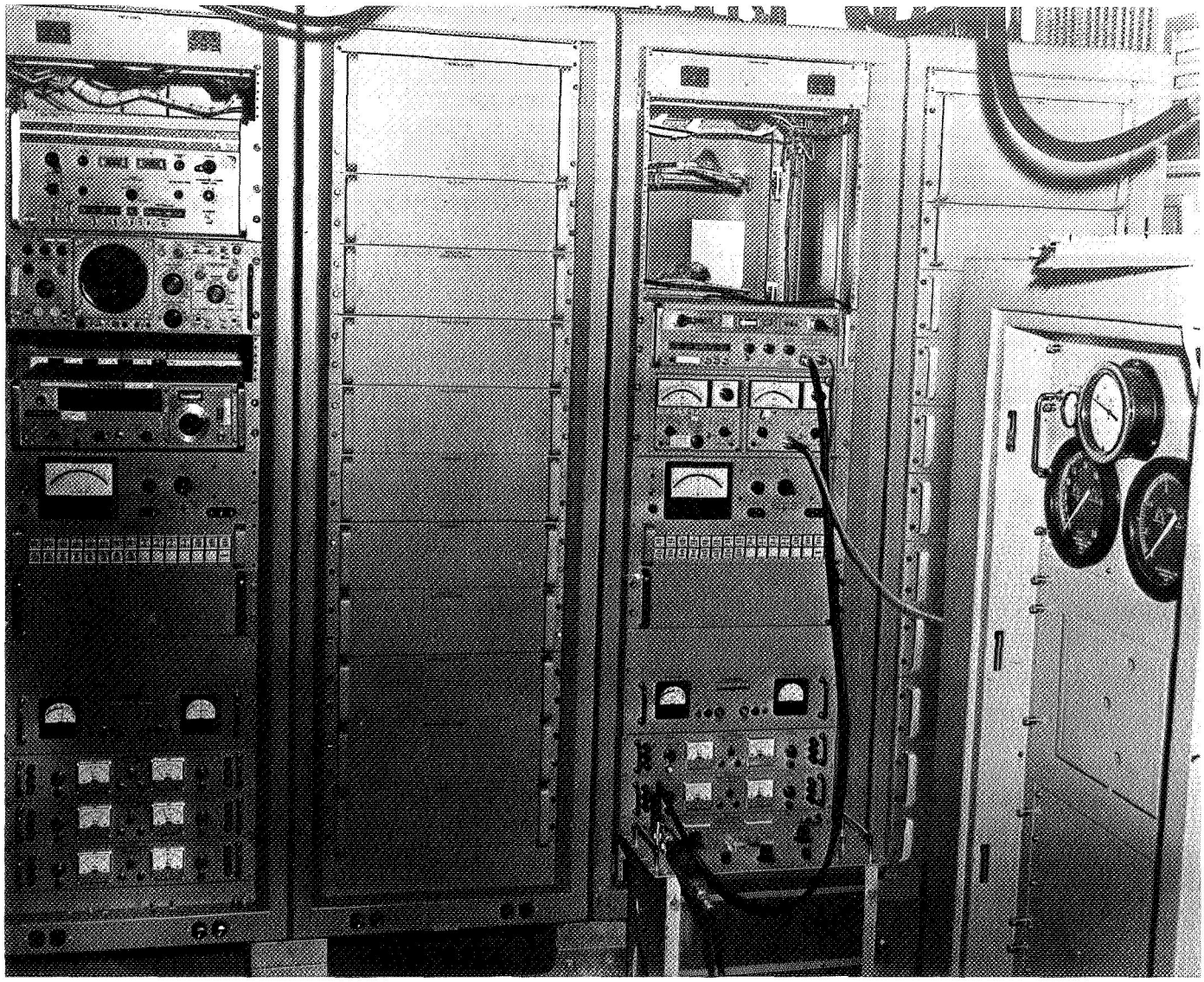

Fig. 81. Receiver and power amplifier racks

modification consisted of a rotating cable tray. The cable tray rotates with the upper antenna structure and is positioned so that the cables leaving the tray rotate on the same axis as the structure. All MSFN cabling is routed on one side and the DSN cabling on the other (Fig. 78).

The dec cable wrapup modification consisted of a stainless steel spiral attached to the rotating declination shaft and the antenna reflector backup structure (Fig. 79). The cables are clamped to the spiral and are reeled on and off the spiral as the declination shaft rotates.

Ladder and platform modification. As a result of the HA cable wrapup modification, the ladder and platform in the area of the new rotating cable tray had to be replaced to provide proper clearance for the cable tray. The new ladder and platform are wider and safety and access to the antenna are improved. (Fig. 80.)

b. Electronics room. Because of the addition of four MSFN receiver racks (Fig. 81), a new maser (Fig. 82), and a 20-kW power amplifier, it was necessary to install the RF switching unit to the outer north wall of the electronics room (Fig. 83). This, of course, required the addition of service platforms. Addition of the MSFN equipment necessitated the addition of MSFN cable trays. To help relieve the congestion, the cargo hoist control storage box was relocated on a ceiling support beam.

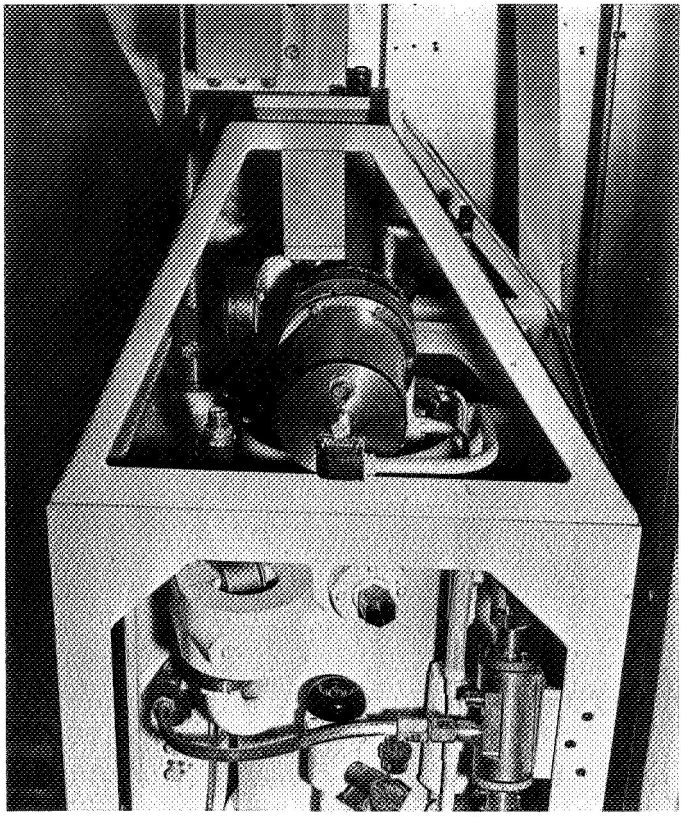

Fig. 82. Maser used at MSFN station

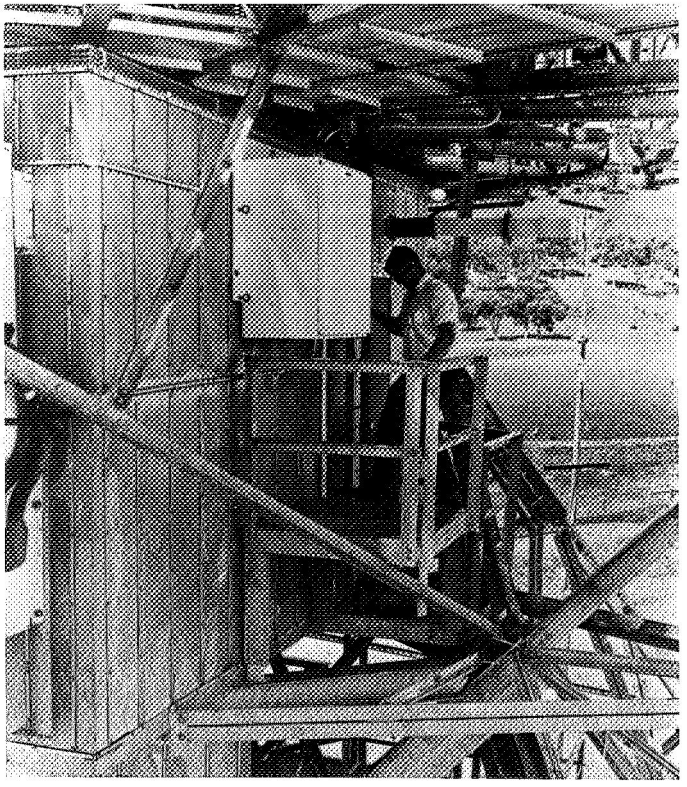

Fig. 83. Antenna-mounted RF switching unit and service platform

VI. Station Test and Evaluation

A. Background Information

System acceptance testing and analysis of the joint DSN/MSFN *Apollo* stations was conducted between November 1, 1966 and April 1, 1967.

The test objectives were to verify the compatibility of the various subsystems, verify the overall operational capability of the system, and compile data necessary for analysis of system errors. The system tests were categorized into the following three general phases:

(1) Static functional tests, consisting of configuration verification, system temperature, dual transmitter/combiner, uplink and downlink data.

(2) Static tracking (stationary target), in determination of angle tracking error gain slope and accumulation of star track data.

(3) Dynamic tracking utilizing aircraft tracking.

A simplified diagram of the overall test configuration is shown in Fig. 84. Table 10 summarizes applicable tests.

B. System Acceptance Testing and Analysis

1. Configuration verification. The objectives of this test (Fig. 84) were to confirm the system configuration of all DSN/MSFN control rooms and to verify equipment operational ability by observing subsystem monitoring displays. As an adjunct to station readiness confirmation, a visual inspection of the site grounding network was accomplished. A 4.0 jacketed cable was installed, tying the antenna structure, hydromechanical/power buildings, and both DSN and MSFN control rooms to the sites' common ground counterpoise. All equipment was grounded directly to this cable.

2. System noise temperature. A quantitative test measuring the system noise temperature of each receiver reference channel was conducted, using the standard Y-factor technique. This measurement technique follows the maser with a receiver that has a precision attenuator in its IF section plus an output detector and a strip-chart recorder. Two well matched sources at temperatures T_N (nitrogen RF load) and T_o (ambient RF load) are alternately connected to the maser input. The measured quantity, or Y-factor, is the addition attenuation that must be introduced with the precision attenuator when

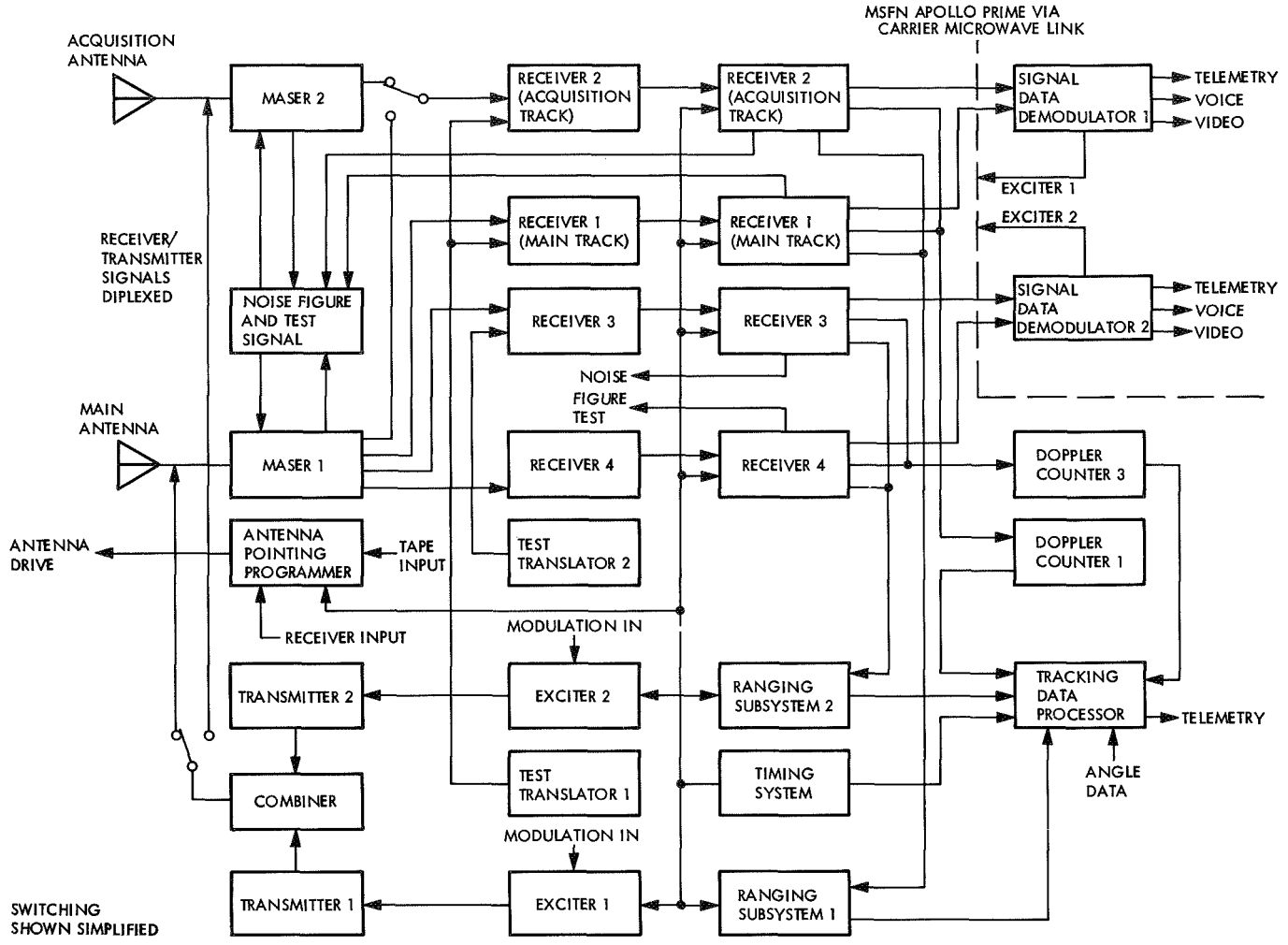

Fig. 84. Test configuration for 85-ft antenna system

the hotter source (ambient) is connected—this to obtain the same chart reading as when the colder source (nitrogen) was connected. This initial measurement determines the equivalent receiver noise temperature contribution T_R. The system noise temperature T_S is then computed by switching between the ambient RF load and the antenna.

Figure 85 illustrates the system noise temperature test configuration. The resulting system temperatures for the respective sites are tabulated in Table 11.

3. *Dual transmitter/combiner test.* Demonstration of the dual transmitter capability and an assessment of system degradation due to the transmitters when radiating into the feed were the primary objectives of this test. The 20-kW klystron used in the 20-kW transmitters was driven across a 14-MHz, −1 dB bandpass, with a maximum of 700-mW drive power to the klystron. Specified bandwidths were readily obtained with the MSFN exciter buffer–amplifiers. Because the dual carrier third-order products were within the 2100 to 2110-MHz MSFN specified bandpass, their levels were required to be 30-dB below either carrier. A 1-h stability test was completed; during the test, the dual 10-kW carriers were diplexed into the antenna, and system noise was monitored on the maser instrumentation recorder; no noticeable increase was observed. The transmitter harmonic filters experienced excessive temperature rises until they were modified by removal of resistive side baffles. Some "spiking" was observed at the Robledo site when the transmitter was activated, but this was attributed to the accumulation of moisture in the waveguide. Maximum voltage standing wave ratio from either transmitter output port through the combiner and into the S-band cassegrain-monopulse or S-band acquisition aid subsystem

Table 10. System tests

Test	Static	Static track	Dynamic track
Configuration verification	X	—	—
System temperature	X	—	—
Dual transmitter/combiner	X	—	—
Uplink data	X	—	—
Downlink data	X	—	—
Error analog	—	X	—
Star tracks	—	X	—
Aircraft tracks	—	—	X

was less than 1.25. The dual transmitter/combiner output test configuration is shown in Fig. 86, and the test results are tabulated in Table 11.

4. Uplink data test. A system demonstration of the interface compatibility and conformance to requirements of the up-data buffer, subcarrier oscillators, exciters, power amplifiers and verification receivers was obtained. This test, and the one that follows, were patterned after the GSFC/Collins Radio Co. acceptance tests that were repeated at the MSFN control rooms with the inclusion of the DSN-supplied subsystems. As indicated in Table 11, frequency response, percent distortion, and test pattern verification were within specifications.

5. Downlink data test. An A and B type substitution test determined the interface compatibility between the signal data demodulator set test unit, exciter, test translator, masers 1 and 2, receivers and demodulators for both PM and FM mode signals. The test unit simulated spacecraft downlink signals which were modulated on phase modulated (PM) and FM carriers, and then sent through the system; the percent of distortion was measured. The PM test signals originated at the MSFN prime site and used the intersite microwave link at the Pioneer site. Distortion measurements, in both the uplink and downlink data tests, were accomplished with the use of the HP 302-A wave analyzer obtaining fundamentals and harmonics of the test tone. In all distortion readings using this method, specifications were met (Table 11).

The FM test at the Robledo site MSFN control room was not completed during system tests because of equipment malfunction and station flight commitments. However, closed-loop FM system tests were completed during subsequent GSFC scheduled aircraft tracks.

6. Static tracking error analog. This test measured the tracking error voltage out of the tracking receiver as a function of target angular error, to determine crossover slopes.

While initial difficulties were experienced, the MSFN and DSN (in concert with their respective contractors) were able to isolate and remedy the problems. Table 11 summarizes the final results.

7. Position accuracy, star tracks. A demonstration of the antenna positioner programmer and servo to work as a unit in positioning the antenna along a pre-selected course was performed at both the Pioneer and Robledo sites. Of singular importance was the determination of the optical to mechanical pointing accuracy of the system.

Collins Radio Co. was contracted by GSFC to reduce and analyze star and aircraft photographic recordings from the MSFN/DSN sites. Collins developed and solved the system tracking error equations. A prepared punched tape containing ephemerides of 12 selected stars was furnished by GSFC as input data to the antenna position programmer.

Essentially, there is one error equation for each antenna axis to describe errors between the optical and encoder or mechanical axes. The first computer program processed the antenna pointing angles and time and film coordinates of each star. Film data showed how far the optical axis was mispointed from the star at the time of recording. These data were used to correct the antenna pointing directions as measured by the encoders. Ephemeris data from the *Nautical Almanac* were used to predict the time coordinates of each star, after adjustment for optical refraction using site weather data. Errors between this true axis and the positioned optical axis were obtained by subtraction. These data were examined for functional relationships resulting in the following two optical-to-encoder star shot error equations:

$$\text{star shot error}_{HA} = S_1 + S_2 - S_3 \sin t \qquad (1)$$

$$\text{star shot error}_{dec} = S_4 + S_5 \cdot \delta + S_6 \cdot t \qquad (2)$$

where

S_1 = HA optical-to-encoder bias error

S_2 = HA optical-to-encoder linearly t (dec)

S_3 = HA optical-to-encoder error sinusoidal t (dec)

S_4 = dec optical-to-encoder bias error

S_5 = dec optical-to-encoder error linearly t (dec)

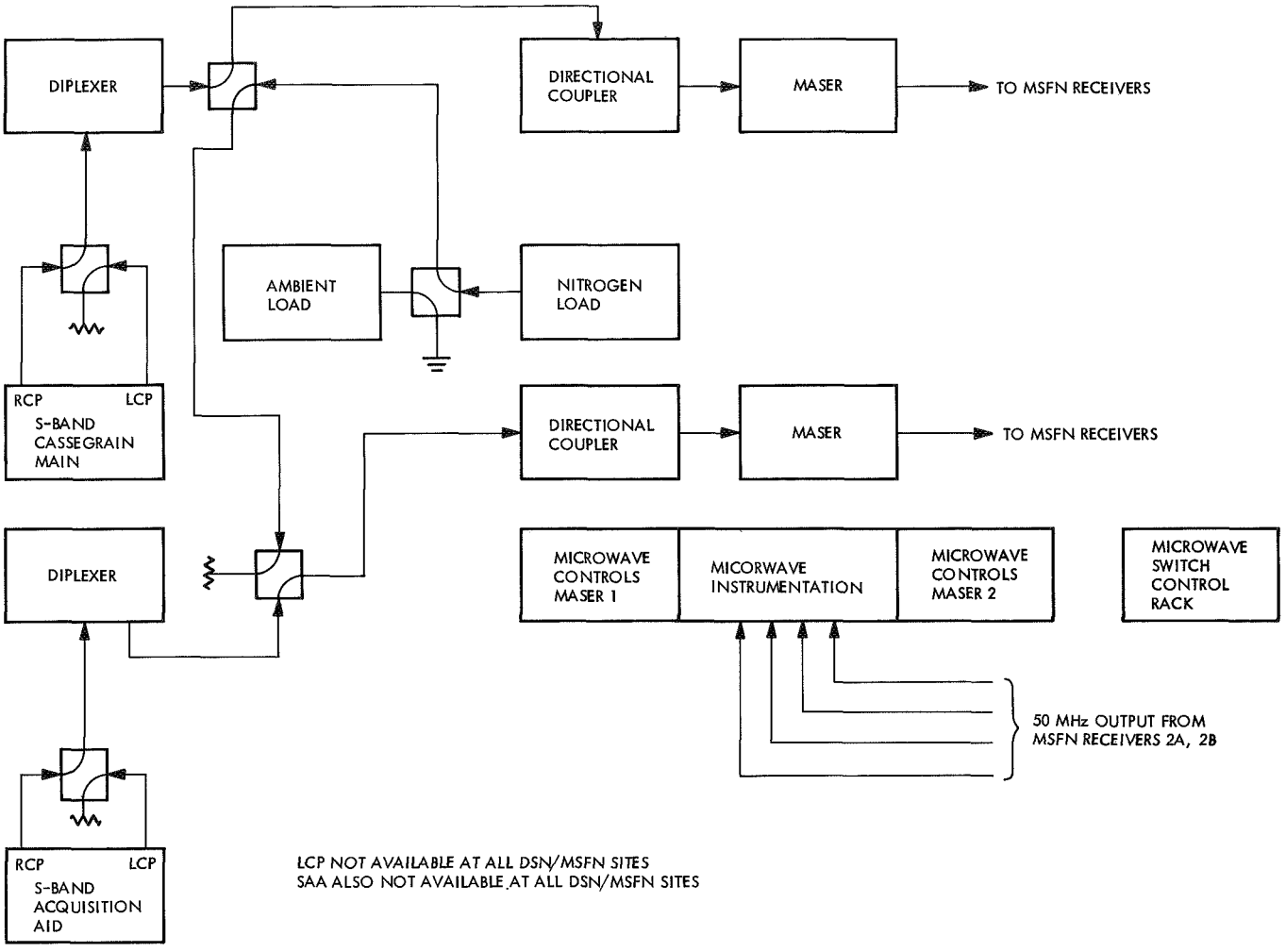

Fig. 85. System noise temperature configuration

S_6 = dec optical-to-encoder error linearly dependent on HA, deg/deg

δ = dec encoder angle, deg

t = HA encoder angle, deg

To prevent the error model from losing continuity at 0 deg dec and 0 deg HA, plus and minus dec and HA must be submitted into the error models (e.g., $t = 330$ deg would be substituted as $t = -30$ deg; $t = 315$ deg would be substituted as $t = -45$ deg).

A second star shot regression computer program was solved for the data in Table 12, using a least-squares-estimate evaluation of the error model coefficients, the coefficients standard errors, and the standard deviation of the residual (random) errors.

A simplified reduction by JPL of the Collins data resulted in a histogram of the frequency distribution of total errors shown in Figs. 87–92. A good statistical grouping of the errors is evident from the Robledo site antenna. Simple linear regression graphs with tick marks indicating standard deviation are shown in Figs. 93–98 for both axes at the subject sites. Again, tighter error tolerances are shown on the Robledo antenna. Allowable errors specified are position repeatability of no more than ± 0.01 deg with position resolution of ± 0.005 deg. Figure 99 shows the test configuration for the star track test.

8. Dynamic aircraft tracks. The ability of the tracking system to acquire and automatically track a moving target was established with a dynamic system test. In particular, after initial acquisition, two-way lock and ranging were demonstrated. Of paramount importance with these aircraft tests was the accumulation of film

Table 11. System test data, Pioneer, Tidbinbilla, and Robledo sites

Static system parameter	Performance			Specification
	MSFN/Pioneer site	MSFN/Tidbinbilla site	MSFN/Robledo site	
Mission system interface	D[a]	D	D	Assume MSFN mission within minutes
System temperature, °K				Signal level 120 dBmW, quiet sky, antenna at zenith, 140°K, +10, −20
SCM[b] maser 1 receiver				
2a1	205	105	142	
2a2	183	114	152	
2b1	83	67	117	
2b2	128	80	104	
SCM maser 2 receiver				
2a1	150	130	118	
2a2	166	—	132	
2b1	90	—	118	
2b2	116	—	94	
Dual transmitter/combiner transmitter 1—20-kW water load bandwidth, MHz				10-MHz 1-dB points, from 2100 to 2110 MHz
1 dB	17.5	16.7	14.0	
3 dB	—	19.7	15.9	
Transmitter 2—20-kW water load bandwidth, MHz				
1 dB	19.0	16.5	12.7	
3 dB	—	20.0	15.6	
Dual transmitter third-order products				Products 30 dB below either carrier
Upper frequency	36 dB below carrier	44 dB below carrier	36 dB below carrier	
Lower frequency	35 dB below carrier	52 dB below carrier	50 dB below carrier	
Uplink data test command channel frequency response				100 to 3000 Hz, +1 dB, −3 dB
System 1	D	D	D	
System 2	D	D	D	
Command channel distortion, %				Less than 5%
System 1	D	D	D	
System 2	D	D	D	
70-kHz up-data pattern verified				
System 1	D	D	D	
System 2	D	D	D	
Downlink data test				Less than 5%
PM[c] telemetry 5.2-kHz tone distortion	D	D	D	
PM voice, telemetry carrier demodulation drop locks	D	D	D	

[a]D = demonstrated. [b]SCM = S-band cassegrain-monopulse. [c]PM = phase modulated.

Table 11 (contd)

Static system parameter	Performance			Specification
	MSFN/Pioneer site	MSFN/Tidbinbilla site	MSFN/Robledo site	
Downlink data test (contd)				
FM[d] system distortion	D	D	D	
FM voice, telemetry carrier demodulator drop locks	D	D	D	
Tracking receiver crossover slope				
SAA[e] hour angle	—	80 mV/deg	—	70 mV/deg
Declination	—	74 mV/deg	—	70 mV/deg
SCM hour angle	154 mV/0.1 deg	258 mV/deg	198 mV/0.1 deg	200 mV/0.1 deg
Declination	190 mV/0.1 deg	214 mV/deg	210 mV/0.1 deg	200 mV/0.1 deg

[d]FM = frequency modulated. [e]SAA = S-band acquisition aid.

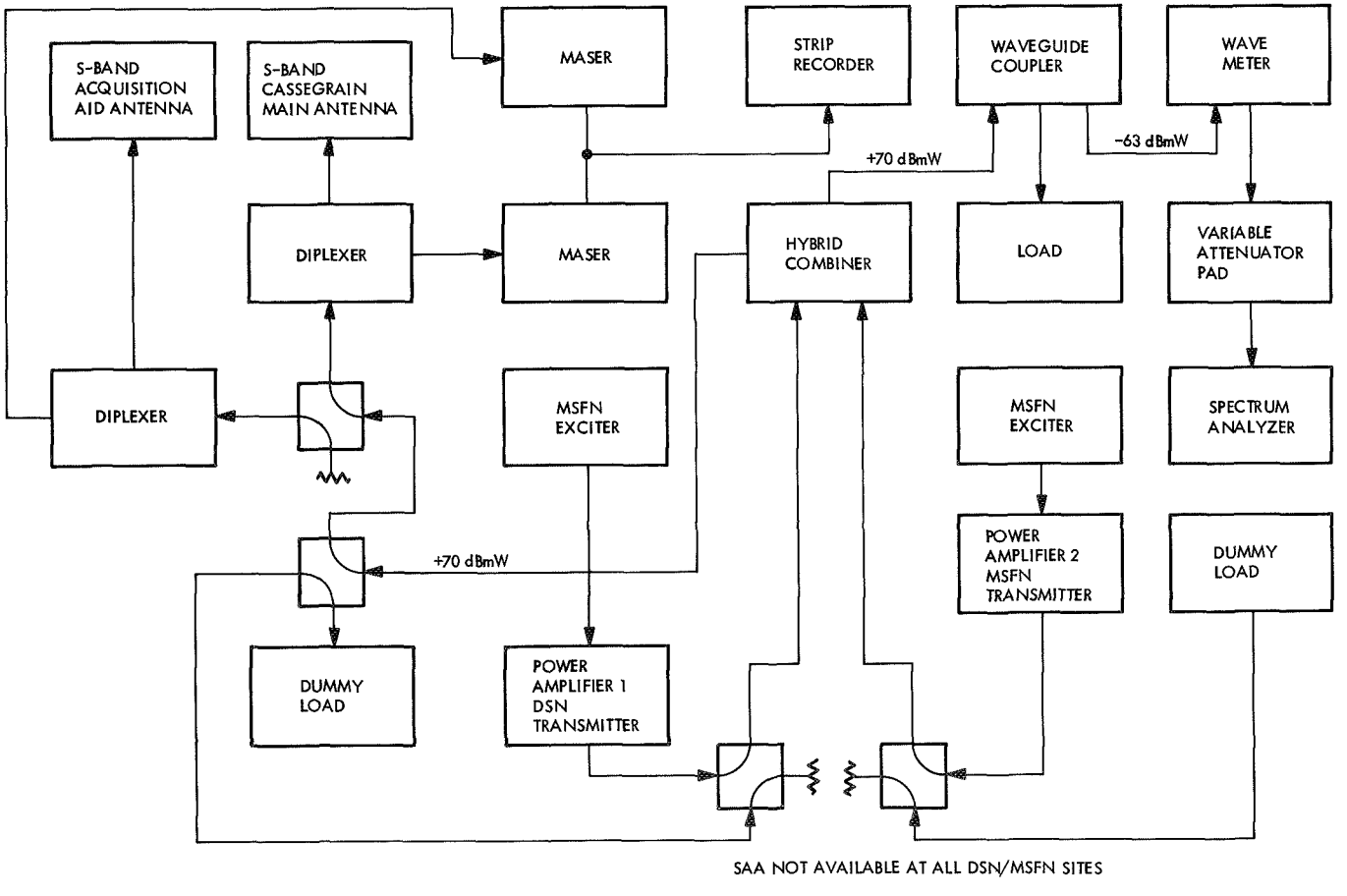

Fig. 86. Dual transmitter/combiner output configuration

Table 12. Star shot data

Symbol	Measurement	Pioneer site	Tidbinbilla site	Robledo site
S_1	HA optical-to-encoder bias error, deg	−0.010 ±0.007	0.002 ±0.003	−0.012 ±0.002
S_2[a]	HA optical-to-encoder error linearly dependent on DEC, deg/deg	±0.0011 ±0.0003	−0.0001 ±0.0001	0.00003 ±0.0002
S_3	HA optical-to-encoder error sinusoidal dependent on HA, deg	+0.040 ±0.010	0.016 ±0.005	0.022 ±0.005
S_4	Declination optical-to-encoder bias error, deg	+0.010 ±0.006	−0.002 ±0.003	0.106 ±0.002
S_5[a]	Declination optical-to-encoder error linearly dependent on dec, deg/deg	0.00036 ±0.00024	0.0009 ±0.0001	0.0007 ±0.0002
S_6[a]	Declination optical-to-encoder error linearly dependent on HA, deg/deg	— —	0.0002 ±0.0001	−0.0004 ±0.00008
HA	HA residual standard deviation	0.013	0.007	0.006
dec	Declination residual standard deviation	0.051	0.019	0.019
δ	Declination encoder angle, deg	—	—	—
t	HA encoder angle, deg	—	—	—

[a]To prevent an error model which is discontinuous at 0-deg dec, plus and minus dec must be submitted into the error models (e.g., 330 deg would be substituted as −30 deg).

data for the determination of system tracking errors between the optical and RF axes.

Figure 100 shows this test configuration. A computer program processed antenna pointing angles and the time and film coordinates of the aircraft light while night tracking. Parallax errors caused by the TV antenna camera offset from the center of the dish and by the displacement of the light from the antenna on the aircraft were corrected. The parallax-corrected errors then became total RF-to-optical tracking errors, which included error contributions from paraboloid and quadripod sag and hyperboloid and feed rotation. The following two RF-to-optical aircraft track error equations were solved by another computer program obtaining least-squares estimates of the error model coefficients:

$$\frac{\text{aircraft track error}_{HA}}{\cos\delta} = \frac{A_1}{\cos\delta} + A_2\ddot{t} \qquad (3)$$

$$\text{aircraft track error}_{dec} = A_3 + A_4 \cdot \ddot{\delta} \qquad (4)$$

where

A_1 = RF-to-dec axis lack of orthogonality

A_2 = HA acceleration lag coefficient

A_3 = dec RF-to-optical bias error

A_4 = dec acceleration lag coefficient

$\ddot{\delta}$ = dec encoder angle, deg

$\ddot{t}$ = HA encoder angle, deg

These equations are based on a type II servo system where the principal errors are bias and lag errors proportionate to antenna acceleration. Antenna encoder accelerations which were computed as more than 0.01 deg/s/s were discarded.

Because the MSFN control room at Robledo had no acquisition aid antenna, successful aircraft tracks were accomplished by using a modified optical acquisition aid with a 3-deg field of view to acquire the aircraft. With the aid of the MSFN servo ball-tracker, the aircraft was then "walked" into the optical acquisition aid 0.5-deg field of view where RF carrier lock was possible.

9. Data analysis and reduction. Two steps are necessary to develop expressions for the random and systematic errors in the measurement of RF axis position as determined by the digital shaft encoders.

The total instantaneous system tracking error per axis is represented by the angle α; it is determined by measurement of the error angles δ and β, which are subsequently summed linearly to yield the total error.

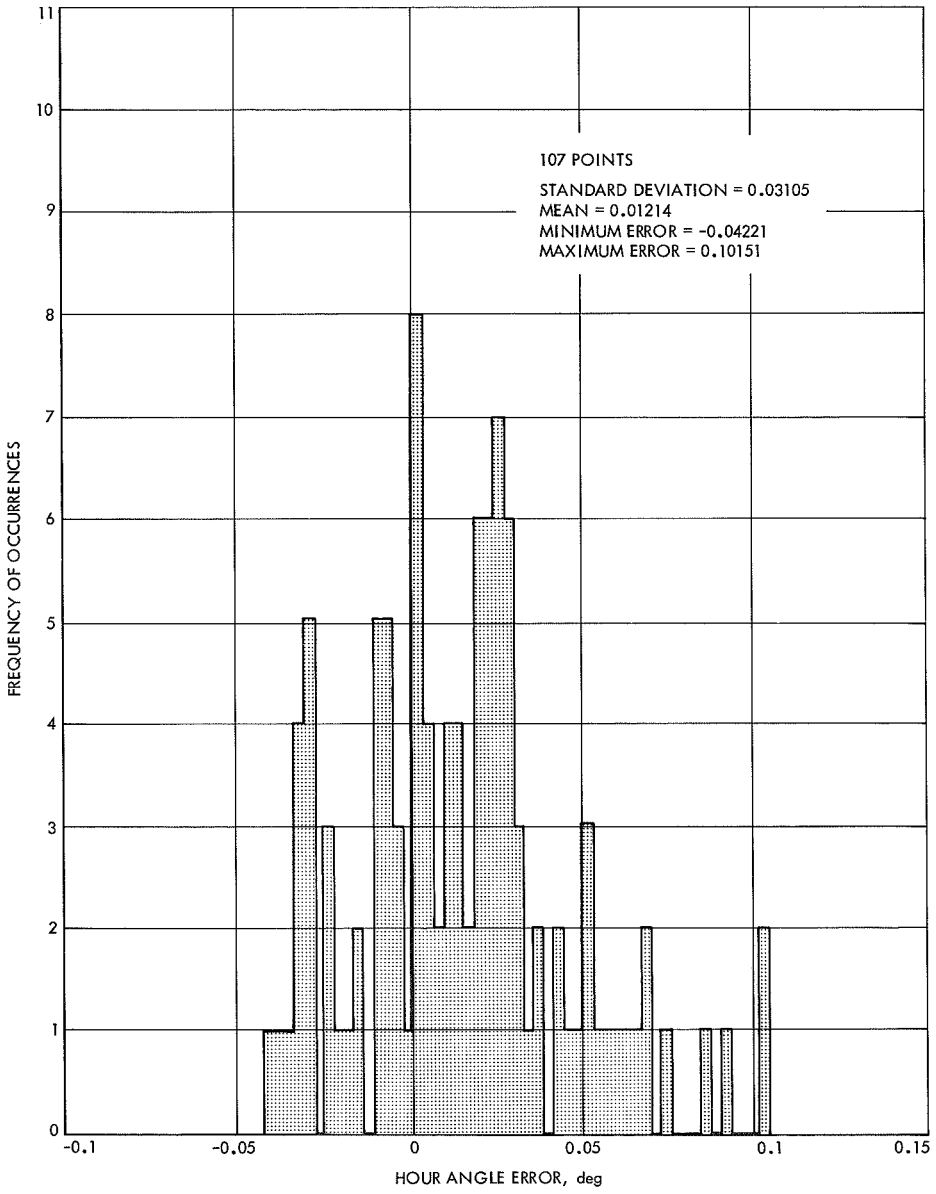

Fig. 87. Pioneer site optical star track data frequency diagram for HA error

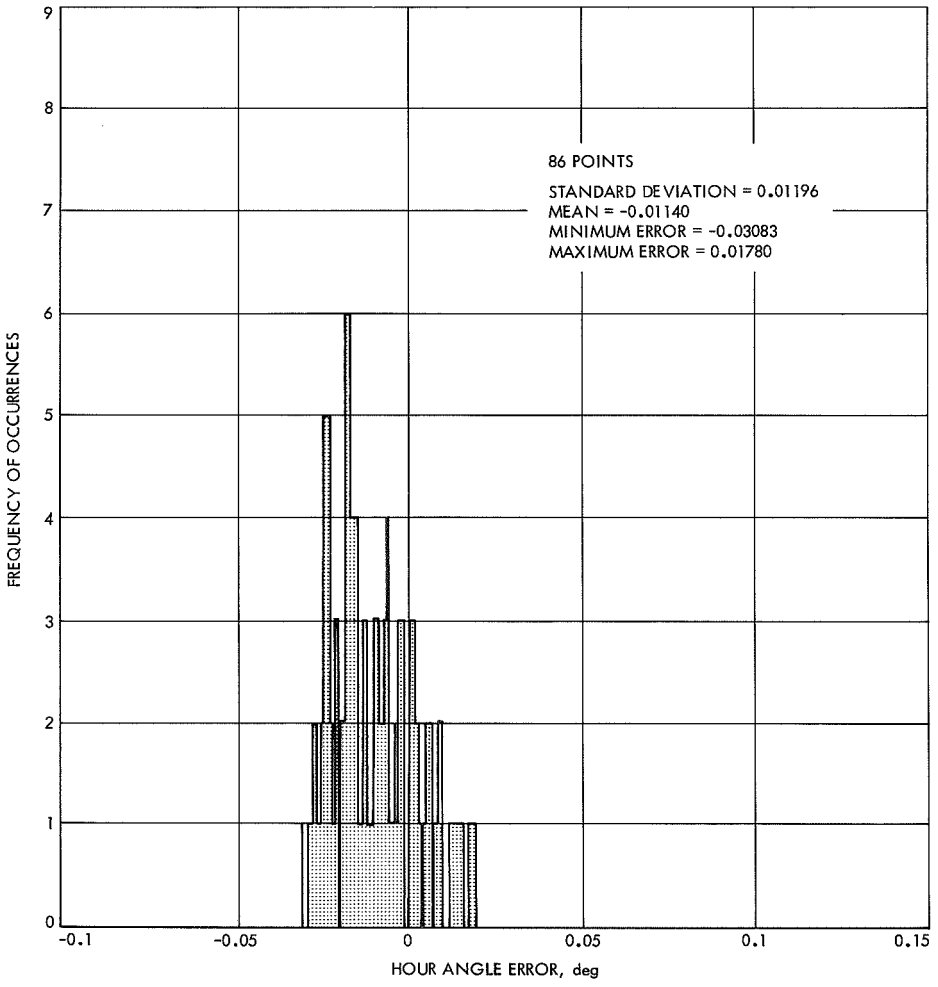

Fig. 88. Tidbinbilla site optical star shot data frequency diagram for HA error

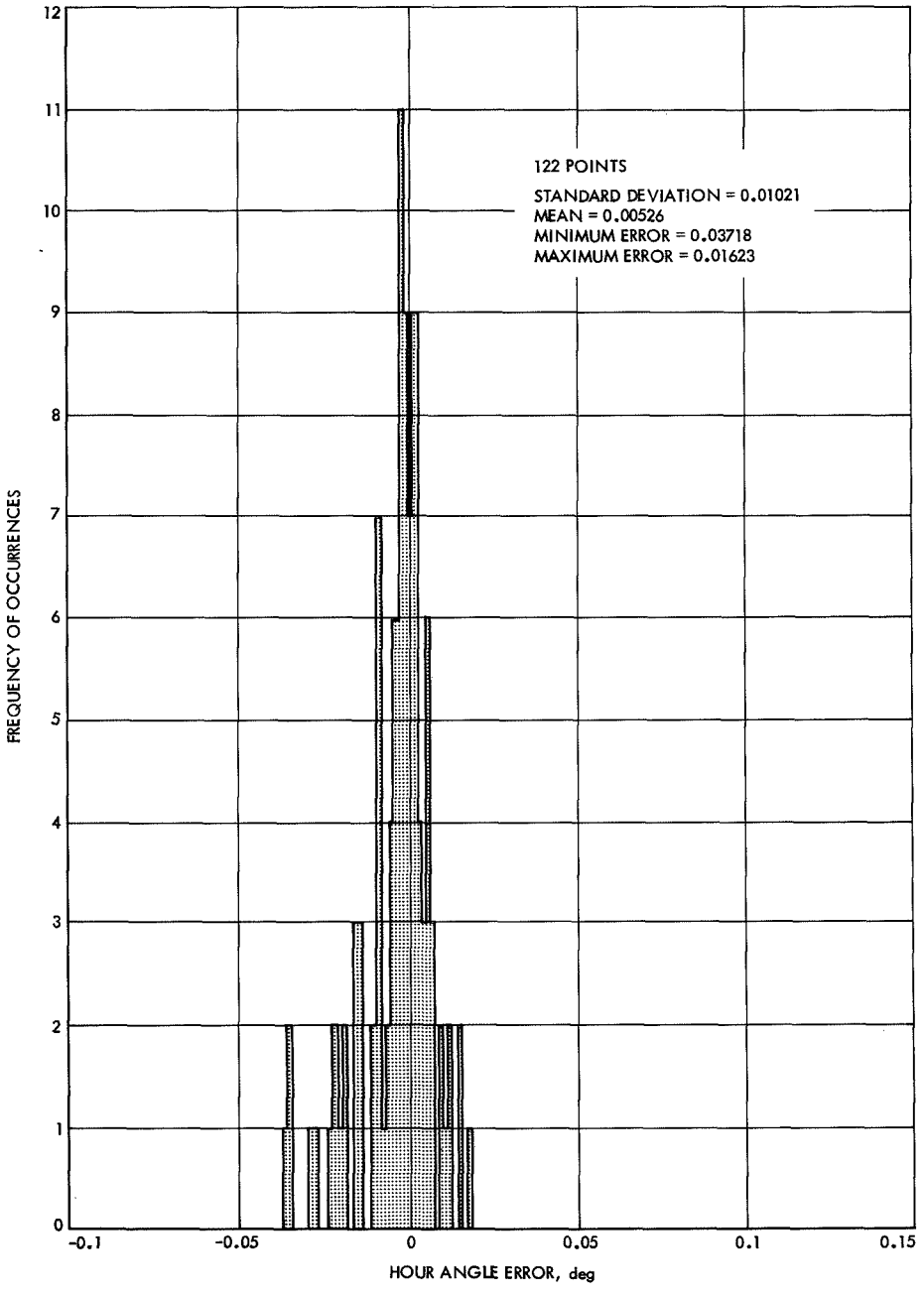

Fig. 89. Robledo site optical star track data frequency diagram for HA error

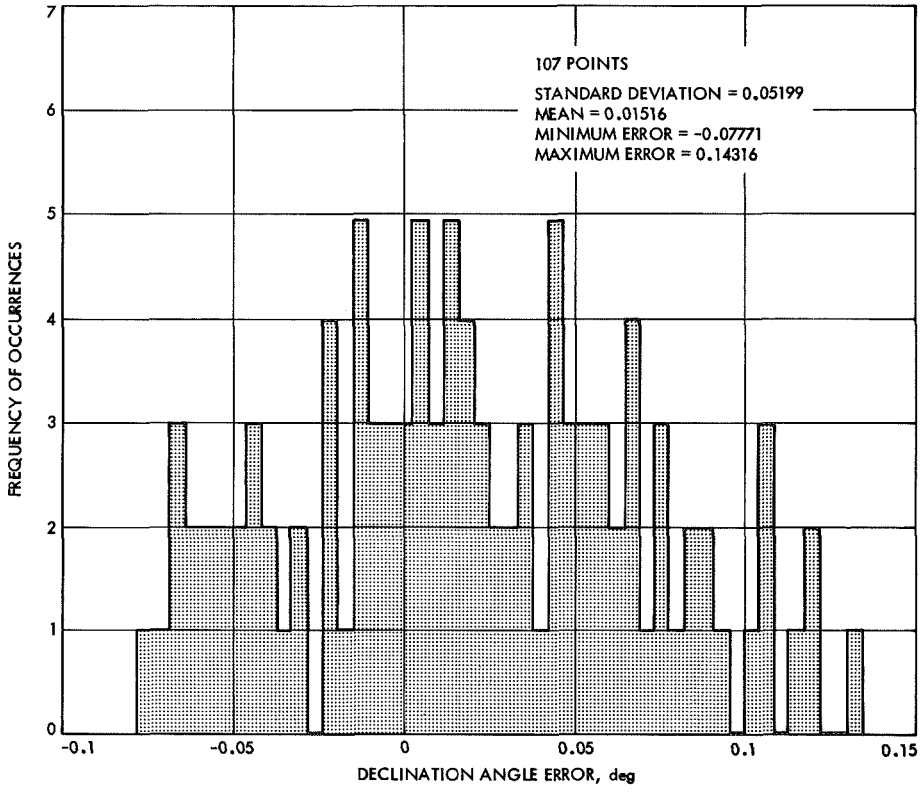

Fig. 90. Pioneer site optical star track data frequency diagram for dec angle error

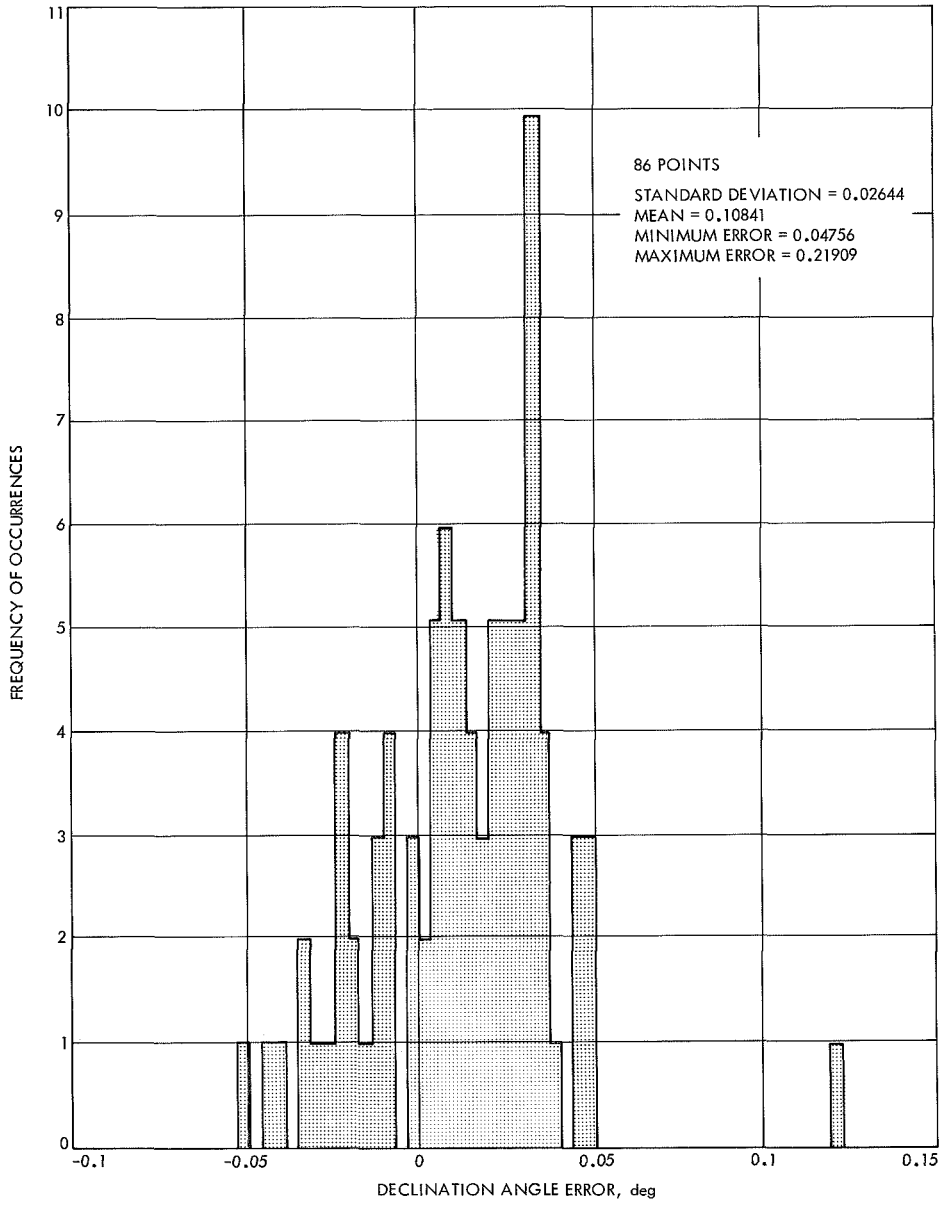

Fig. 91. Tidbinbilla site optical star shot data frequency diagram for dec angle error

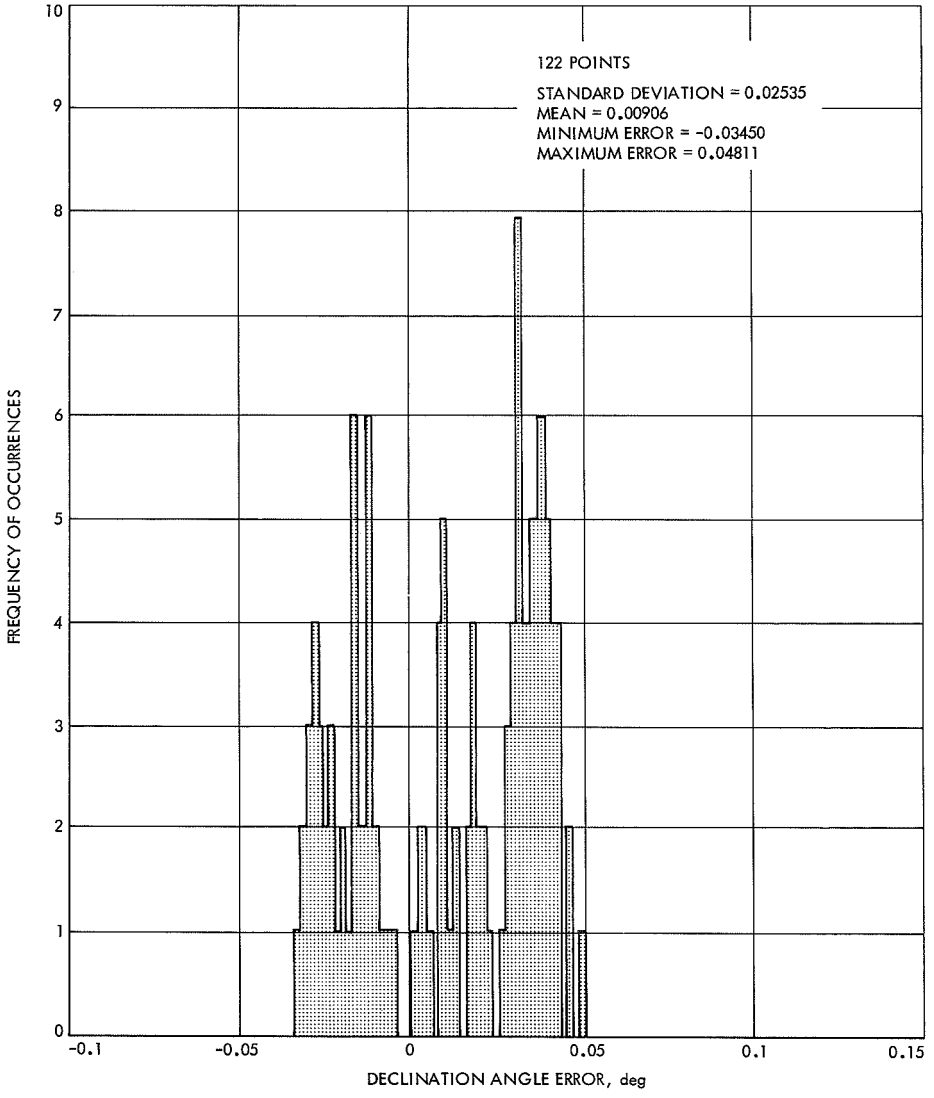

Fig. 92. Robledo site optical star track data frequency diagram for dec angle error

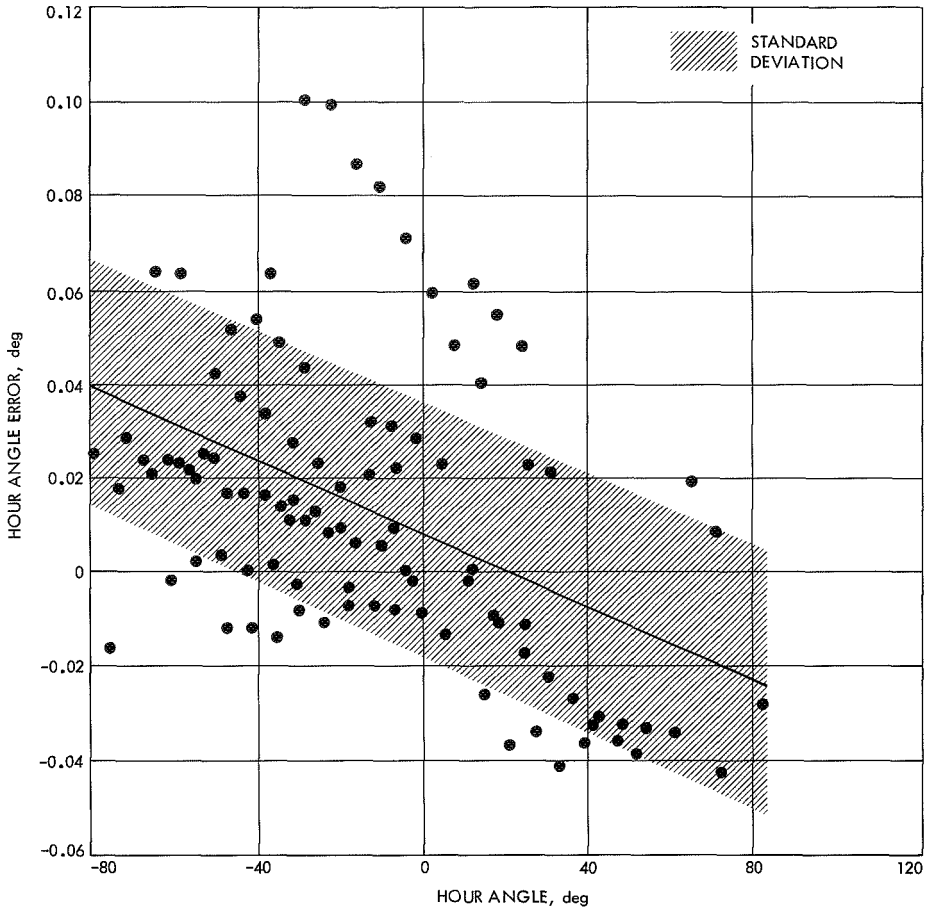

Fig. 93. Pioneer site optical star track data HA error vs HA

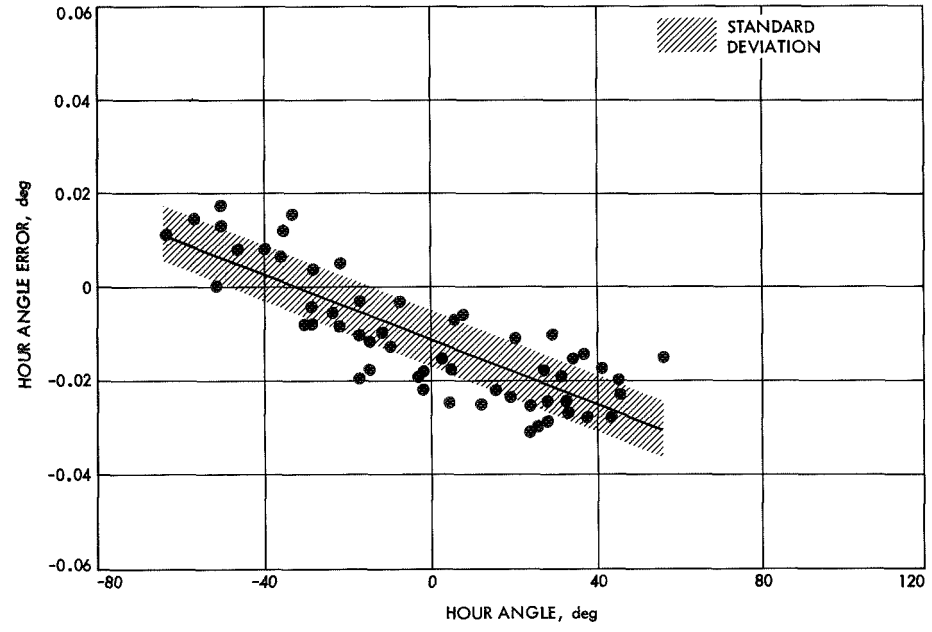

Fig. 94. Tidbinbilla site optical shot data HA error vs HA

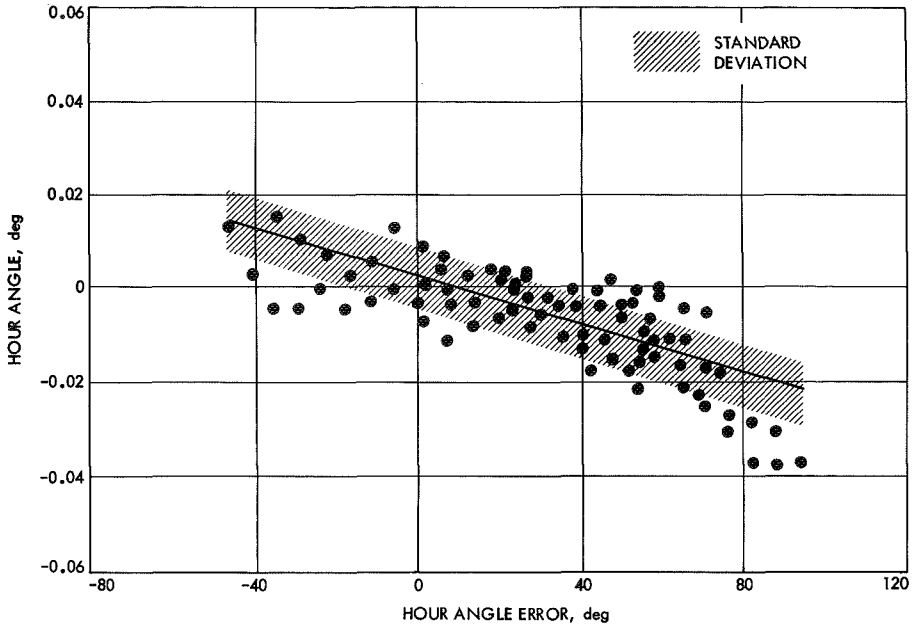

Fig. 95. Robledo site optical star track data HA error vs HA

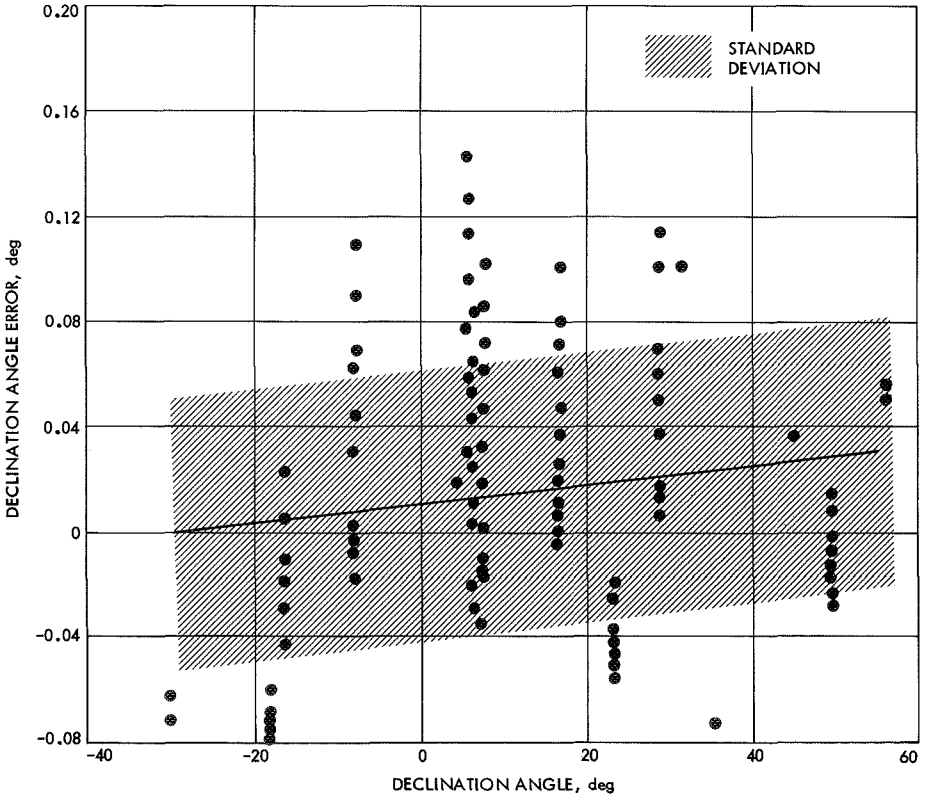

Fig. 96. Pioneer site optical star track data dec angle error vs dec angle

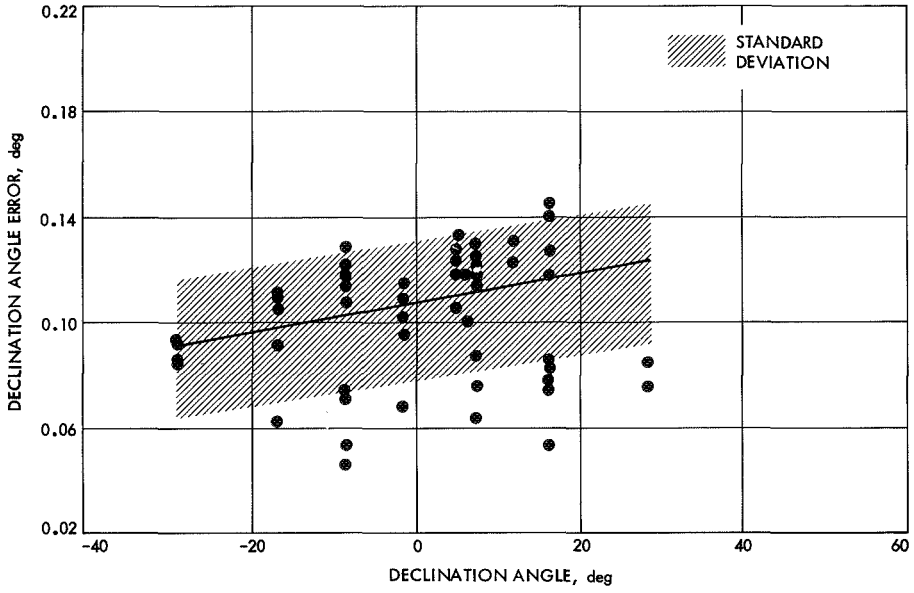

Fig. 97. Tidbinbilla site optical star shot data dec angle error vs dec angle

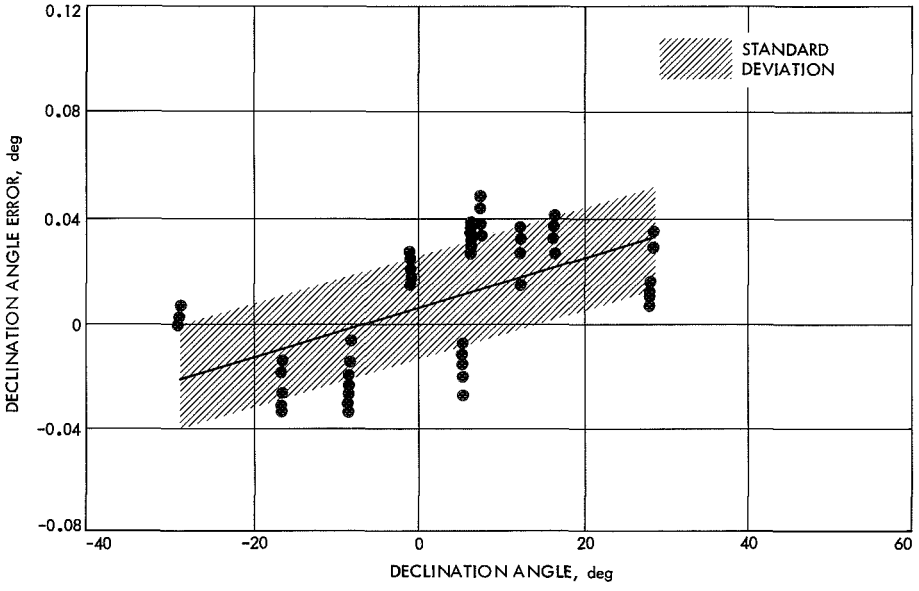

Fig. 98. Robledo site optical star track data dec angle error vs dec angle

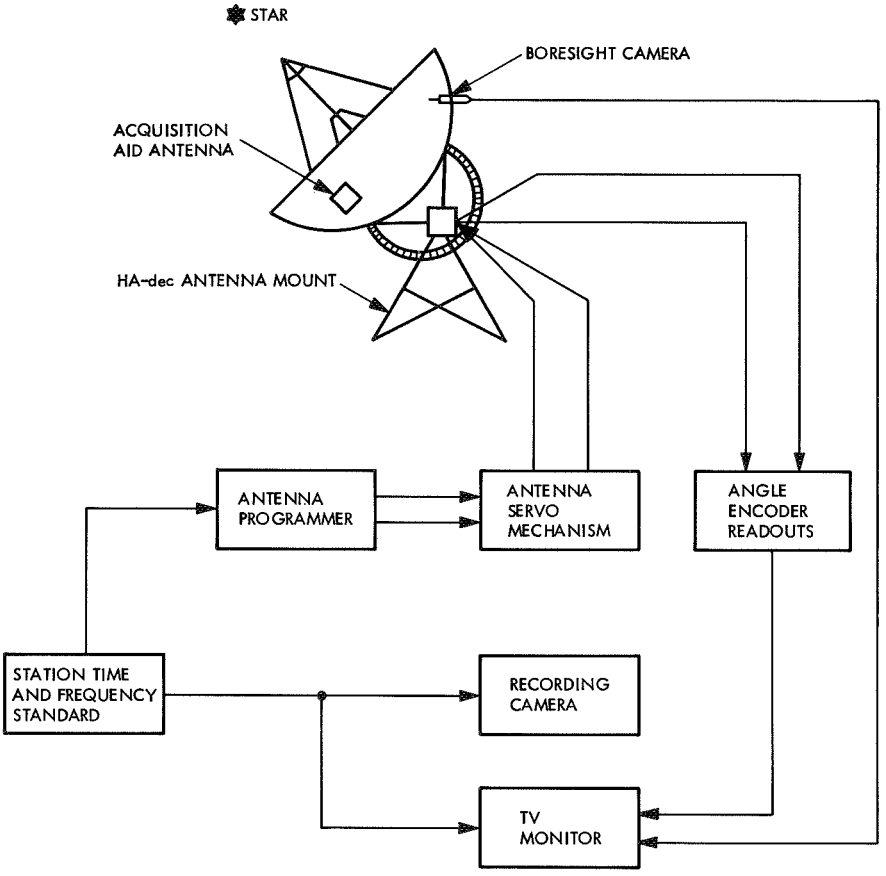

Fig. 99. Block diagram of programmed star track

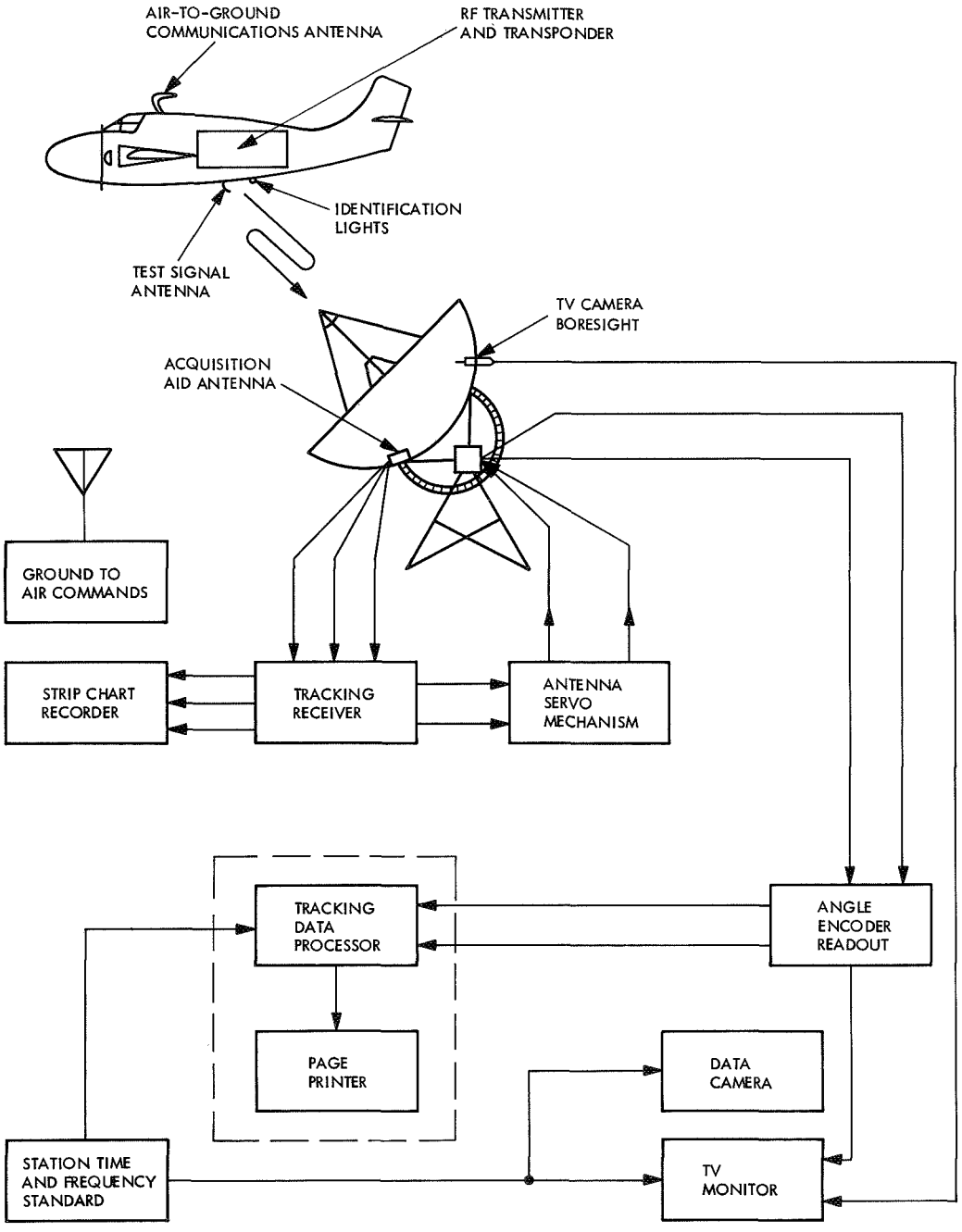

Fig. 100. Dynamic tracking test configuration

The β error contribution is measured by a series of optical star shots randomly covering the celestial hemisphere, while the δ error contribution is determined from aircraft autotrack/optical tests. The raw data are processed statistically through linear regression analysis to yield the best-fit coefficients (in the least-squares sense) of the system error model and the residual errors (random) after best-fitting the data in accordance with the equations of the error model.

When the system error equations are evaluated at any chosen value of HA and dec angles, velocities, and accelerations, the resulting pointing error estimates are the best least-squares estimates of the systematic errors for the chosen conditions.

a. Star shot total errors. To produce star shot errors, the first computer program processes antenna pointing angles, time, and film coordinates F of each star, HA, dec, T, F_{HA}, and F_{dec}, respectively. The 35-mm camera film data coordinates of the star show how far the optical axis is mispointed from the star at the recorded time. These coordinates are used to correct the antenna pointing directions HA and dec as measured by the encoders. These adjusted coordinates state where the antenna records that the star is located. As previously mentioned, ephemeris data from the *Nautical Almanac* are used to predict the true coordinates of each particular star. Predicted HA and dec coordinates are adjusted for optical refraction, using recorded temperature and pressure data. Errors in HA and dec angles between the optical axis (as positioned by the measured encoder axis) and the true axis (refraction adjusted) were obtained by subtracting true values from the measured values. Two optical-to-encoder star error equations were established by a second computer program which evaluated the trends of the two plots: the two plots consisted of antenna encoder angles and total error (dividing the opposite encoder angle into 20-deg intervals), as produced by the first computer program and established the values for Eqs. (1) and (2).

The HA and dec errors and encoder angles for each star from the first program are then entered into a second program (star shot regression) which obtains the least-squares estimates of the error model coefficients in Eqs. (1) and (2). This program solves for the unknown coefficients S_1 to S_6, their standard errors, and the standard deviation of the residual (random) errors. The residual randomness with respect to encoder angles and dependent variable variance reduction indicates a successful solution for the predominant trends in the star shot error data.

b. Aircraft track total errors. To obtain aircraft track total errors, the first computer program processes antenna pointing angles, time, and film coordinates of the aircraft light, HA, dec, T, F_{HA}, and F_{dec}, respectively. F_{HA} and F_{dec} are corrected for two parallax effects in a third computer program. Parallax is caused by the TV camera offset from the center of the dish and by the displacement of the light from the antenna on the aircraft. The parallax-corrected errors thus become total RF-to-optical errors.

Aircraft data points that have antenna encoder accelerations computed as more than 0.01 deg/s/s are not processed in the regression program. This permits automatic rejection of data reduction errors caused by noisy accelerations that occur when one antenna axis is stationary, and to key punch errors.

On the basis of past antenna tracking error experience, there are two predominant factors which contribute to RF-to-optical aircraft track errors. These are bias errors and lag errors proportional to antenna acceleration for a type II servo system. Therefore, the following two RF-to-optical aircraft track error equations are solved from the aircraft track data (using a fourth computer program):

$$\frac{\text{aircraft track error}_{HA}}{\cos\delta} = \frac{A_1}{\cos\delta} + A_2\ddot{t} \tag{5}$$

$$\text{aircraft track error}_{dec} = A_3 + A_4 \cdot \ddot{\delta} \tag{6}$$

To prevent an error model which is discontinuous at 0 deg dec and 0 deg HA, plus and minus dec and HA must be submitted into the error models.

All the information listed in the third computer program is entered into another program (aircraft track regression) that obtains the least-squares estimates of the error model coefficients in Eqs. (5) and (6). This program solves for the unknown coefficients A_1 through A_4, the standard errors, and the standard deviation of the residual (random) errors, for each aircraft track run.

c. Combined star shot and aircraft error equations. The coefficient and variance results of the aircraft track regression equation solutions were processed through a weighted-average and probable-error program that weighted each coefficient inversely as its variance (index of precision). The coefficient averages and probable errors were computed according to Eqs. (7) and (8); the results are listed in Table 13. All the variances were assigned equal weights in order to average them.

Table 13. Radio frequency-to-true-encoder error equation results (combined aircraft and star shot error equations)[a]

Symbol	Measurement	Tidbinbilla site	Robledo site
A_1	RF-to-dec axis lack of orthogonality, deg	0.070 ±0.001	−0.006 ±0.0002
S^1	HA encoder bias, deg	−0.012 ±0.002	0.002 ±0.003
A_2	HA acceleration lag coefficient, deg/deg/s^2	−0.228 ±0.001	−2.331 ±0.014
S_2[b]	HA optical-to-encoder error linearly dependent on dec, deg/deg	0.00003 ±0.0002	−0.0001 ±0.0001
S_4	Declination optical-to-encoder bias error, deg	0.106 ±0.002	−0.002 ±0.003
C_1	Declination RF-to-encoder bias, deg	−0.201 ±0.005	−0.002 ±0.019
A_4	Declination acceleration lag coefficient, deg/deg/s^2	−1.287 ±0.030	−0.277 ±0.009
S_5[b]	Declination optical-to-encoder error linearly dependent on dec, deg/deg	0.0007 ±0.00002	0.0009 ±0.0001
S_6[b]	Declination optical-to-encoder error linearly dependent on HA, deg/deg	−0.0004 ±0.00008	0.0002 ±0.0001
α_t(C)	HA RF-to-encoder residual standard deviation	0.008	0.015
α_δ(C)	Declination RF-to-encoder residual standard deviation	0.021	0.023

[a]Data for the Pioneer site are not available.

[b]To prevent an error model which is discontinuous at 0 deg dec, plus and minus dec must be submitted into the error models (e.g., 330 deg would be substituted as −30 deg).

Letting b_{ij} signify the jth coefficient from the ith aircraft run, the weighted average of the jth coefficient B_j is

$$B_j = \frac{\sum_{i=1}^{n} \frac{b_{ij}}{\sigma_{ij}^2}}{\sum_{i=1}^{n} \frac{1}{\sigma_{ij}^2}} \tag{7}$$

where

$i = 1, 2, \cdots, n$

$j = 1, 2, \cdots, 4$

n = number of aircraft track data groups

σ_{ij} = variance of the ith value of the jth coefficient

The probable error pe in the jth weighted coefficient average is

$$pe = 0.6745 \frac{\frac{\Sigma(b_{ij} - B_j)^2}{\sigma_{ij}^2}}{n(n-1)\frac{1}{\sigma_{ij}^2}} \tag{8}$$

Table 13 lists the symbols, definitions, and values for the combined aircraft coefficients and standard deviations of Eqs. (7) and (8). Probable errors are listed for each coefficient.

VII. Unified S-Band Qualification Tests During *Apollo* Flight Tests

A. Background Information

A thorough test of the USB system was conducted during the unmanned *Apollo 4, 5,* and *6* flights to evaluate the quality and performance of the USB ground systems, individually and as a network. The results of these tests demonstrated that the USB system was capable of providing adequate communications support for *Apollo 7,* the first manned *Apollo* mission. The DSN/MSFN earth-based USB stations employed during these tests are shown in Fig. 101 along with other JPL/DSN and MSFN earth-based stations.

Goddard Space Flight Center conducted a thorough performance evaluation of the MSFN USB system during these three *Apollo* flights also; however, this report will discuss only the special support provided by the DSN during these early *Apollo* flights.

B. The *Apollo 4* Flight

1. Plan and objectives. In June 1966, JPL was informed by NASA that the scheduled launch of *Apollo 4* in October 1967 would be the first flight test of the 7.5×10^6-lb-thrust *Saturn V* launch vehicle and would afford the MSFN and DSN their first opportunity for an extended flight test of the USB.

The planned trajectory of this flight required that the prototype CSM separate from the S-IVB stage just after the second burn. The CSM and S-IVB were both programmed to reach apogee while in view of Ascension Island, and just prior to the re-entry test of the CSM heat shield. During the apogee pass, the two spacecraft would be sufficiently separated as to require the use of both the MSFN and DSN 30-ft antennas located on Ascension Island.

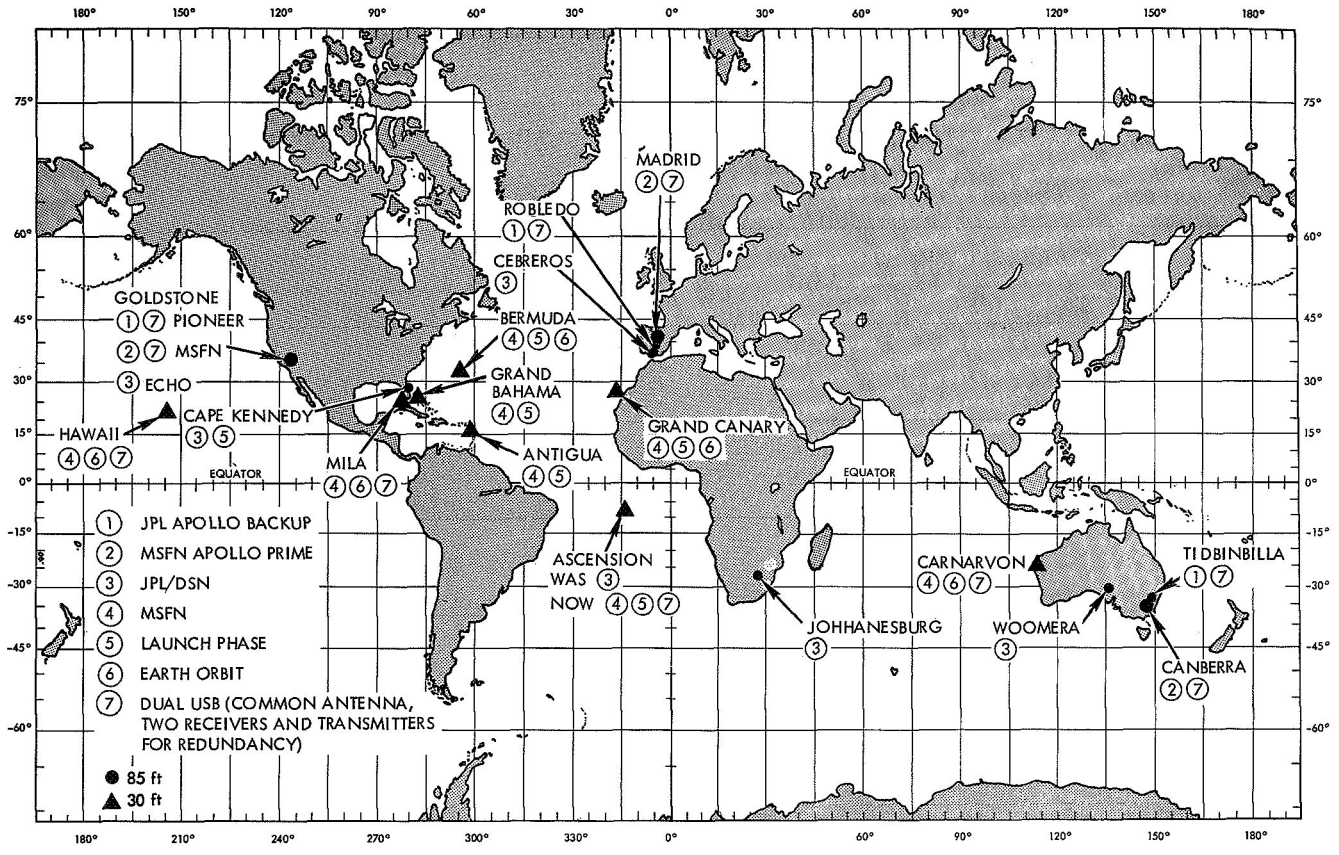

Fig. 101. Deep Space Network/MSFN earth-based USB stations

The requirement for the DSN Ascension Island site and the MSFN Ascension station to jointly support *Apollo 4* necessitated the addition of special interface equipment and the development of compatible operating procedures.

The primary objective of the DSN support was to receive telemetry from and transmit commands to the S-IVB instrumentation unit after separation from the CSM. Considerable engineering effort was spent by both GSFC and JPL in designing the telemetry and command interface required between the MSFN and the DSN Ascension stations. Both the MSFN station and the DSN station were completely separate when originally implemented and contained equipment complements specific to each of the respective networks. For *Apollo,* however, both stations were required to operate as a single facility. After several iterations, a configuration was established that utilized equipment that was available within the respective networks. This was an important factor because at that time there was insufficient leadtime to design and procure new equipment before the planned *Apollo 4* launch date of October 17. A delay in the launch schedule to November 1967 provided the additional time required to develop and perfect the joint MSFN/DSN operational procedures. This task was not as simple as it might seem because the MSFN operational procedures and techniques were tailored specifically for manned orbital and lunar flights, whereas those for the DSN were tailored specifically for unmanned lunar and planetary flights. However, after considerable effort by both the DSN and MSFN, the task of preparing joint operational procedures and techniques was successfully completed. For the first time in the experience of either network, the MSFN network operations directive and its mission supplement heavily cross-referenced the DSN tracking instruction manuals, and vice-versa.

2. ***Testing.*** The first integrated tests in which the MSFN and DSN Ascension Island stations simultaneously tracked an instrumented aircraft were performed in July 1967. In early October 1967, the DSN tracked *Lunar Orbiter V,* which at the time was in orbit about the moon, in an exercise of the station ranging system. This was followed by a second instrumented aircraft test.

Besides providing additional training, the second instrumented aircraft test provided experience in the rapid conversion from a DSN configuration into an MSFN configuration. On October 16, 1967, the station began configuration verification testing, which in this case was a DSN procedure adapted to an MSFN configuration. During and following configuration testing, the station followed a series of MSFN checkout and training procedures, which had been adapted specifically for the DSN in a special section of the network operations directive mission supplement for *Apollo 4*. These procedures included system tests, integrated system tests, station readiness tests, and countdown demonstration tests (CDDT). These tests were scheduled by the MSFN, and DSN took operational instructions from the MSFN Ascension station maintenance and operations supervisor.

On October 24, 1967, the DSN placed the Ascension Island site under configuration control; this was followed by a configuration freeze on October 28, 1967. Also on October 28, the MSFN placed Ascension on mission status, which meant that throughout the mission, Ascension would receive its operational directives from the Mission Control Center, Houston, which had project responsibility for the *Apollo 4* flight.

During the countdown demonstration tests, a suspected multipath problem developed between the MSFN station located on Merritt Island (referred to as MILA) and the *Saturn V* vehicle on launch pad 39A at the Kennedy Space Center. The DSN was requested to convert the Cape Kennedy station to the *Apollo* frequency band and measure the stability of the *Apollo 4* S-band signals from a different vantage point. The station responded to the MSFN request and, through a makeshift arrangement, was able to receive strong, stable signals from the *Apollo 4* spacecraft, providing confidence that the MILA system was in proper working order and that the launch preparations could continue.

3. ***Tracking operations.*** Tracking operations are discussed in the paragraphs that follow.

a. Cape Kennedy site. During the terminal countdown, Cape Kennedy provided CSM telemetry and periodic signal strength and stability measurements to the MSFN MILA station. This support started at 14:00 GMT on November 8, 1967 and continued until *Apollo 4* was successfully launched at 12:00:01 GMT on November 9, 1967. The *Apollo 4* CSM was manually tracked with the Cape Kennedy 4-ft-diam antenna to the local horizon for 9 min, 7 s, during which time the received signal strength varied between −72 dBmW at $T-0$ and −141 dBmW at loss of signal.[2] At $T+00:02:02$ ground elapsed time, one momentary out-of-lock occurred due to spacecraft antenna null. Although they were not requested to do so by GSFC, the personnel at Cape Kennedy station maintained operational status and passively tracked the *Apollo 4* CSM for 6 min, 44 s at the end of its first earth orbital revolution. The received signal strengths were in the range of −104 to −110 dBmW. Again, Cape Kennedy passively tracked the CSM at the end of its second earth orbital revolution. Toward the end of this pass, the S-IVB stage ignited a second time to place the CSM in a high, earth-intersecting elliptical orbit with an apogee of 9,800 nmi above the earth (Fig. 102). During this pass, Cape Kennedy tracked the CSM for 11 min, 46 s; loss of signal occurred at 15:20:02 GMT. A log of the Cape Kennedy site activities, reflecting the major events that occurred from beginning of the countdown until end of track, is shown in Table 14.

b. Ascension Island site. At 15:22:37 GMT, the Ascension Island site had acquisition of signal on the S-IVB/instrumentation unit. While the vehicle was near the station's horizon, multipath effects and spacecraft antenna pattern variations caused signal fluctuations.

During the early minutes of the pass, Ascension Island experienced several receiver out-of-lock conditions (Table 15), which were later attributed to MSFN stations uprange that were sweeping the transponder of the S-IVB/instrumentation unit. However, once the Ascension Island site elevation angle reached approximately 10 deg, the received signal stabilized in the vicinity of −100 dBmW, and the preprogrammed sequence of ranging measurements and commands was followed without any apparent anomaly.

Because of the high apogee of the S-IVB/instrumentation unit stage, which was roughly 1000 mi less than for the CSM, the station track lasted 3 h, 36.5 min. Interestingly, the received signal was very strong at the end of the pass, and Ascension Island reported −99 dBmW at loss of signal at 0 deg el angle.

Table 16 shows a log of Ascension Island site activities and reflects the major events that occurred from beginning of the countdown until end of track.

[2] "*T*-minus" time differs from "launch-minus" *L* time because the latter must account for the built-in holds (*L* time displays a larger negative number). During a countdown, the *T* clock stops during the holds, while the *L* clock continues to count down toward launch. The *T* and *L* clocks are in step after the last hold.

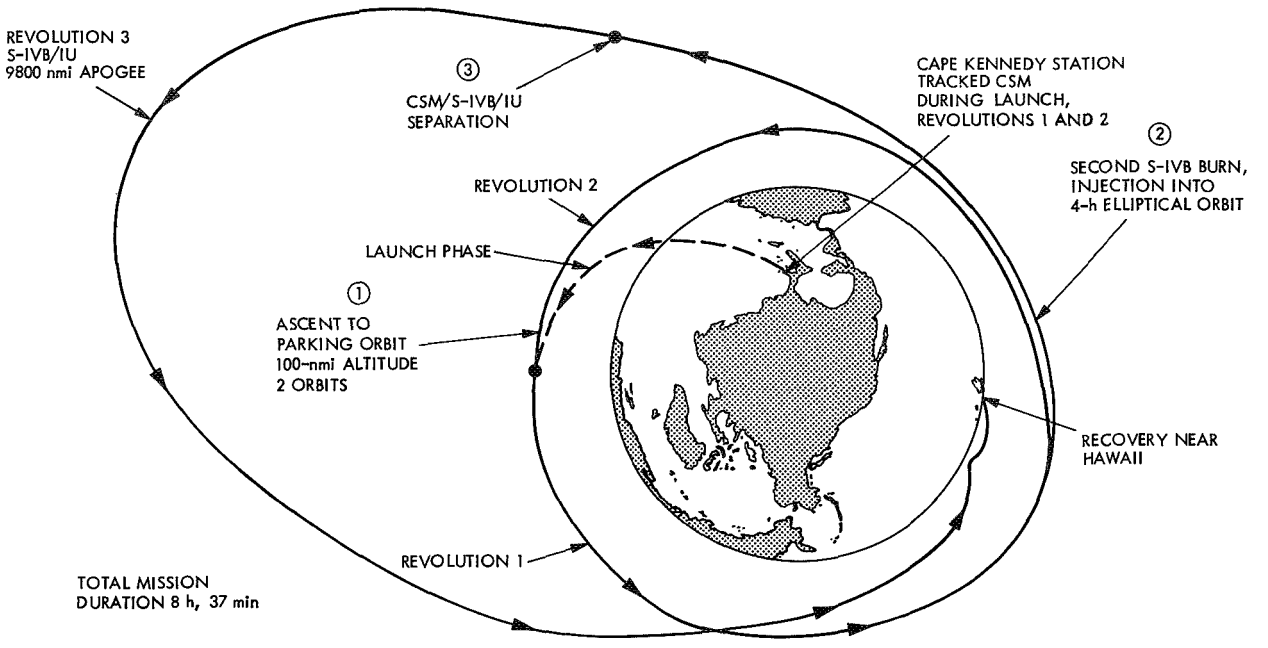

Fig. 102. Apollo 4 mission profile

c. Summary. Postflight analysis indicated that both the Cape Kennedy and Ascension Island sites achieved their primary mission objectives of providing reliable telemetry data to their counterpart MSFN stations. The only major anomaly occurred at Ascension Island where a balky 100ths digit in the doppler counter resulted in a considerable number of bad data points. However, the Ascension angle and range data appeared to be good. Difficulties were experienced with the teletype circuit from the Goldstone systems data analysis (SDA) facility to Ascension, which prevented the station from getting the planned real-time evaluation of its tracking data. It is doubtful, however, that the station could have corrected the doppler counter problem during the pass since it was an intermittent defect in the counter. The joint operating procedures developed for the MSFN and DSN Ascension stations worked very well; as expected, however, experience with *Apollo 4* did disclose areas where relatively minor improvements could be made. It should be recognized, nevertheless, that *Apollo 4* was truly a perfect mission, and as such was an easy test of the new MSFN/DSN procedures and cross-support capabilities. For this reason, joint training exercises continued after the *Apollo 4* mission.

C. The Apollo 5 Flight

1. Plan and objectives. The primary objectives of the *Apollo 5* flight were to test the fully configured LM, with all its systems and subsystems, under flight conditions which simulated those of a lunar mission, and to check the compatibility of its tracking and communications subsystems with the MSFN. A secondary objective of this flight was to check and evaluate the performance of the USB ground systems, individually and as a network.

The *Apollo 5* flight plan called for the LM to be placed in an earth orbit by an uprated *Saturn I* launch vehicle comprised of an S-1B first stage and an S-IVB second stage. After several earth orbits, a series of engine firings (Fig. 103) were scheduled to alter the LM orbital parameters. Ascension Island, according to the flight plan, would have spacecraft visibility starting on the third earth orbital revolution and lasting through to the sixth.

At the request of GSFC, the Cape Kennedy site was required to support *Apollo 5* during the CDDT. There was no requirement, however, for Ascension Island to support *Apollo 5*, but, since it would provide additional station training, the DSN obtained permission from the MSFN for Ascension to passively track the LM. The operational improvements which resulted from *Apollo 4* were quickly introduced into the procedures so they could be flight-tested on *Apollo 5*.

2. Testing. Premission testing for *Apollo 5* closely paralleled that for *Apollo 4*. On December 15, 1967,

Table 14. Cape Kennedy site operations log for *Apollo 4*

Time, GMT	Events/remarks
	Day 312, November 8, 1967
14:00	Started station countdown
14:30	FTS[a] checks completed. FTS set for propagation delay time of 8.8 ms. Time code generator is delayed from the PC-141 clock by 739 μs
14:55	DIS[b] checks completed
15:07	Performed first motion check of AIS[c] CEC[d] recorder
15:11	Receiver subsystem checks completed
15:12	AIS checks completed
15:30	*Receiver switch position checks completed*
16:43	Completed receiver 1 AGC calibration. Receiver 1 is on the track antenna and paramp mode. Receiver 1 threshold at −158 dBmW
18:00	Checked and adjusted no-break power system
18:34	Completed receiver 2 AGC calibrations. Receiver 2 threshold at −155 dBmW. Receiver 2 is connected to the calibrate antenna and preamplifier
19:00	Completed station countdown
20:24	Receiver 1 locked to CSM frequency. Tape recorder 1A and CEC recorder are ON
20:28	CSM downlink carrier is ON. On the CSM spectrum, the B antenna has bouncing subcarriers. The A antenna is symmetrical
20:48	Tape recorder 1A and CEC recorder are OFF. MILA Station unable to lock to Cape Kennedy data on the A2A line during the time that receiver 1 was locked up
21:07	Test SCO[e] connected to the test transmitter through receiver 1 with sidebands of 1.024 MHz and a bit rate of 72 and 51.5 bits/s. MILA reported that the signals were satisfactory
22:30	Checked and adjusted no-break power system
	Day 313, November 9, 1967
02:00	Count is at $T-390$ min and holding for 2 h. Understand this is a built-in 2-h hold.
02:15	No-break power system checked at this time; all satisfactory
03:15	Made a satisfactory voice check with MILA. Still holding at $T-390$. Expect to resume the count at 04:00 GMT
04:00	*Resumed the count at $T-390$ min*

Time, GMT	Events/remarks
	Day 313, November 9, 1967 (contd)
04:05	Downlink from the CSM is ON in the noncoherent mode, but the uplink has not been acquired. This signal is impossible to lock to since it is very erratic and spurious. Taking polaroid pictures of this. Have the FR-1400 and the CEC recorder ON
04:10	MILA reports good solid lock on Cape Kennedy data. Downlink signal strength is about −104 dBmW. Downlink frequency is 23.307340 MHz at VCO
04:15	Spacecraft is in two-way lock. The signal level is a −74 dBmW. Downlink frequency is 2287.500032 MHz
04:19	MILA downlink at receiver VCO correlates exactly to the cycle with that of the Cape Kennedy receiver VCO, which is 23.307292 MHz. MILA data personnel say that the uplink exciter frequency is 21.941732 MHz. This correlates exactly to the 240/221 ratio from receive to transmit
04:28	Signal level from the spacecraft has dropped from −74 to −113 dBmW. SDDS[f] personnel at MILA have still got demodulator lock but their word sync is gone. This is due to the fact that Cape Kennedy is below telemetry threshold at this time. There is no word as to what is going on with the spacecraft
04:29	Spacecraft is back to −74 dBmW
04:36:30	Downlink has been terminated
04:39	Tape reel 1A and CEC recorder stopped
08:09	$T-231$ min and counting
09:05	HF Ascension line was just brought up. In contact with Ascension Island, and voice communication is good
10:20	*$T-100$ and counting. No problems up to this point.* The count is going as per schedule
11:15	CSM downlink is ON in a one-way configuration at a signal level of about a −74 dBmW. The S-band frequency is 2287.504736 MHz
11:24:30	Cape Kennedy is in a three-way condition with the spacecraft and processing good data to the SDDS at MILA. Signal strength of the signal received is a −71 dBmW. Frequency at S-band is 2287.500032 MHz. The VCO frequency is 23.307292 MHz
11:47	Switched to receiver 2 so that MILA can verify good data off the receiver 2 as well as receiver 1
11:49:25	Back on receiver 1. SDDS at MILA confirms good data off both receivers

[a]FTS = frequency timing subsystem.
[b]DIS = digital instrumentation subsystem.
[c]AIS = analog instrumentation subsystem.
[d]CEC = Consolidated Electrodynamics Corp.
[e]SCO = subcarrier oscillator.
[f]SDDS = signal data demodulator set.

Table 14 (contd)

Time, GMT	Events/remarks
Day 313, November 9, 1967 (contd)	
12:02	MILA dropped uplink lock. Cape Kennedy receiver operators are maintaining one-way lock
12:02:20	Dropped lock momentarily; back in lock
12:05	At $T+5$ min, 30 s into the flight, signal strength at −133 dBmW
12:06:30	At $T+6$ min, 30 s into the flight, −141 dBmW
12:07	At $T+7$ min, 30 s into the flight, −134 dBmW
12:08:25	At $T+8$ min, 28 s, signal level on receiver 1 is −131 dBmW
12:09:15	At $T+9$ min, 18 s, signal level on receiver 1 is −156 dBmW. Out of lock
12:10	Stopped the tape recorders and the CEC recorder and are reconfiguring for postcalibrations
12:20	Checked and adjusted no-break power system
12:21	MILA reported official liftoff time as 12:00:01.392 GMT
12:58	DSS 71 loss of signal at 12:09:08 GMT
13:00	Polaroid camera jammed right before $T-0$. The last good polaroid picture was at $T-2$ min
13:21	Completed postcalibrations on receivers 1 and 2 AGC. Receiver 1 threshold is −158 dBmW. Receiver 2 threshold is −155 dBmW
13:25	Preparing for the first pass of AS-501 which has a nominal rise time at station of 13:35 GMT. The station has just completed postcalibrations and standing by for the rise of the AS-501

Time, GMT	Events/remarks
Day 313, November 9, 1967 (contd)	
13:35:41	Receiver 1 is in lock for the first pass. The signal level is −110 dBmW
13:36:19	Lost lock temporarily
13:39	Cape Kennedy continues to maintain a strong signal level of −104 dBmW. Tracking is nominal
13:40	Back in lock after dropping momentarily. Signal level was −108 dBmW
13:42:25	Receiver out of lock
13:44	CEC recorder OFF. Tape recorder 3A and 3B OFF
15:07	Tape recorder 3A and 3B are ON. CEC recorder ON. This is for pass 2 of *Apollo 4* CSM
15:08:16	Receiver 2 acquired the CSM at a signal level of −113 dBmW
15:08:25	Receiver 1 acquired the CSM at a signal level of −113 dBmW
15:19:55	Receiver 2 dropped lock at a signal level of −145 dBmW
15:20:02	Receiver 1 dropped lock with a signal level of −149 dBmW
15:21	Tape recorders 3A and 3B and CEC recorder OFF at this time for pass 2
15:46	MILA reported that Cape Kennedy data were intermittent to good during second pass

Ascension Island participated with the MSFN station in the final network readiness test prior to the MSFN going into mission status. From then until launch, Ascension passively participated in every MSFN scheduled premission test, with special emphasis on the integrated system tests, during which time both the MSFN and DSN stations acted as a single facility. Configuration control was established upon Ascension Island on January 3, and a configuration freeze was established on January 10.

Three special training exercises were performed, on January 12, 15, and 17, using the *Test and Training Satellite 1* (*TETR-1*). During the first two exercises, the MSFN station established two-way lock and performed ranging measurements, with Ascension Island tracking passively in the three-way mode. On the last exercise the two stations reversed roles.

The Cape Kennedy site participated in the CDDTs, using essentially the same configuration as that employed for *Apollo 4*. The only significant difference was that the LM S-band transponder was activated only at specific times during the countdown (i.e., at $T-76$ h and $T-20$ h, when the gantry was in place and a cable connection could be made to the S-band system). During launch, the LM was inside the S-IVB shroud, which did not contain an S-band parasitic coupler antenna; thus, launch coverage was restricted to VHF. During launch, Cape Kennedy was on "stand-by" in the event that an abort caused a premature separation of the LM, at which time an S-band signal would become accessible.

3. Tracking operations. *Apollo 5* was launched at 22:48:09 GMT on January 22, 1968, and was successfully inserted into earth orbit by its launch vehicle. The first

Table 15. Ascension Island site receiver out-of-lock times

Time (Nov 9, 1967), GMT		Out-of-lock interval, min:s		Remarks
From	To	Instant	Total	
15:26:50	15:26:52	00:02	00:02	Results of *Vanguard* transmitter off at 15:26:49.5 GMT
15:30:29	15:30:54	00:25	00:27	Intermittent out of lock; reason unknown
15:32:12	15:32:29	00:17	00:44	Reason unknown
17:33:00	17:36:06	03:06	03:50	Result of Carnarvon sweeping uplink
18:15:04	18:15:15	00:11	04:01	Result of Ascension Island transmitter turnon at 18:15:02 GMT

pass over Ascension Island occurred on the third revolution 2 h, 19 min into the mission. The DSN station passively tracked the LM in a three-way mode with the MSFN station for a period of 4 min, 17 s. Composite telemetry provided by the DSN station to the MSFN station was not used since that station had a good signal lock on the spacecraft. The DSN station tracking data were successfully transmitted to and processed by the systems data analysis group at Goldstone, which performs the tracking data validation function. Between the third and fourth revolutions over Ascension Island, the LM was programmed to initiate the first descent propulsion system burn. An on-board system malfunction, however, caused the descent propulsion system engines to shut down after only a few seconds burn time, with the result that the LM was placed on a nonstandard trajectory. As a result, neither the DSN nor the MSFN station at Ascension was able to obtain solid signal lock on the fourth revolution.[3] By the time Ascension was ready for

[3] *MSFN Postmission Report on the AS-204 LM Mission*, p. 2-1. Goddard Space Flight Center, Greenbelt, Md., May 1968.

Table 16. Ascension Island site operations log for *Apollo 4*

Time, GMT	Events/remarks
Day 312, November 8, 1967	
18:30	DSN equipment checks/countdown started
20:30	All subsystems ready for phase I SRT[a]
20:36	Started phase I SRT
20:49	Completed phase I SRT
20:50	Started phase II SRT and 2.7.3 AGC curves
20:55:30	Time check between Ascension Island MSFN station and DSN station
21:15	AGC calibrations complete
21:17	Standing by for power amplifier configuration indentification index
21:19	Began configuration identification index 2.7.2
21:20	Configuration identification index complete
21:26	RF command interface 2.6 also conducted with 642B computer. Completion estimate of 21:50 GMT for BER[b] test
22:10	Began 2.8.4 MILA/PCM BER test
22:35	2.6 command test complete
23:17	2.8.4 MILA/PCM BER test complete
23:20	Set up for phase III SRT
Day 313, November 9, 1967	
00:16	Completed phase III SRT
03:25	At T−7:35:00
04:05	Maintenance and operations advised to configure for RF boresight; called for tracking data format II[c]
04:28	Maintenance and operations called for tracking data format 14
04:36	TDH[d] equipment off line; data good
04:40	Maintenance and operations approved release from computation and data flow integrated subsystem test
04:45	MILA called for Ascension Island to radiate collimation tower at 10 kW to assist in locating problem
04:50	MILA checks complete. Antenna to "stow" (transmitter) OFF
05:30	Reported to maintenance and operations that doppler counter in TDH equipment marginal; count incorrect
09:30	Message from JPL communications relayed by Cape Kennedy instructs use of "JSDA" teletype address header on tracking data; no preamble required

[a] SRT = station readiness test.
[b] BER = bit error rate.
[c] Format numbers refer to the use of particular prewired patch panels that allow transmission of specific types of metric data.
[d] TDH = tracking data handling.

Table 16 (contd)

Time, GMT	Events/remarks
	Day 313, November 9, 1967 (contd)
09:45	Combined reference frequency message received
15:30:29	Receivers in and out of lock
15:32:12	Receivers out of lock
15:32:29	Two-way lock
15:34	Ready for commanding
15:35:40	Reset TDH to ×1 doppler
15:36:30	Receiver 1 at −105 dBmW; receiver 2 at ×131 dBmW
15:41:40	Receiver 1 at −90 dBmW; receiver 2 at −131 dBmW
15:43:45	Receiver 1 at −108 dBmW; receiver 2 at −134 dBmW
15:45:30	Receiver 1 at −90 dBmW; receiver 2 at −117 dBmW
15:47:20	Receiver 1 at −92 dBmW; receiver 2 at −119 dBmW
15:50	Advised by Ascension Island MSFN station mission operations that no more IRVs[e] available
16:20:20	Receiver 1 at −96 dBmW; receiver 2 at −123 dBmW
16:23:29	Receiver 1 at −117 dBmW; receiver 2 at −140 dBmW
16:28	Receiver 1 at −92 dBmW; receiver 2 at −120 dBmW
16:36	Ranging modulation OFF
16:38	Receiver 1 at −92 dBmW; receiver 2 at −121 dBmW
16:39:02	Command sequence stopped
16:42	Command sequence started
16:42:20	Receiver 1 at −94 dBmW; receiver 2 at −122 dBmW
16:45	Ranging modulation ON
16:45:30	Acquired ranging code
16:46	Receiver 1 at −95 dBmW; receiver 2 at −124 dBmW
16:48	Command sequence stopped
16:51	Ranging modulation OFF
16:52	Receiver 1 at −94 dBmW; receiver 2 at −126 dBmW
16:54	Command sequence started
16:57	Ranging modulation ON
16:57:22	Acquired ranging code
17:00	Command sequence stopped; receiver 1 at −95 dBmW; receiver 2 at −124 dBmW
17:02	Ranging modulation OFF
	Day 314, November 10, 1967
11:30	TDH test started; data sent to Goldstone using teletype address header "JVLA"
11:35	TDH test completed; data satisfactory
11:45	Combined reference frequency message received (no change in frequencies)
12:13	Doppler counter is GO
12:15	Predicts an IAPS[f] tape generated based on liftoff time and combined reference frequency information
13:04	54.3.5.15S-IVB receiver AGC started
14:52	$L-30$ min
14:54	IRV received
14:57	Acquisition messages confirmed
15:00	Predicts and IAPS tape generated from $L-30$ IRV
15:07	IAPS confirmed
15:13	Antenna to point
15:15	Recorders ON
15:18	$L-5$ IRV received; same as one at $L-30$
15:19	Time check completed
15:21	TDH off line to change format
15:22	TDH on line
15:22:37	Receiver 2 in lock
15:22:49	Receiver 1 in lock at −104 dBmW
15:23:11	Receiver 1 at −117 dBmW
15:23:39	Receiver 2 at −132 dBmW
15:24:30	S-band acquisition aid auto track
15:25:01	Transmitter on 10 kW (30-ft antenna)
15:25:09	30-ft antenna auto track
15:25:40	Servo to good data
15:26	On exciter VCO "nominal" frequency
15:26:25	Ranging modulation ON
15:26:50	TDH off line to change to ranging format 11. Ranging code acquired. Receivers dropped lock

[e]IRVs = inter-range vectors.

[f]IAPS = interim antenna pointing subsystem.

Table 16 (contd)

Time, GMT	Events/remarks
Day 314, November 10, 1967 (contd)	
15:26:52	Receivers in lock
15:28:16	Receiver 2 at −128 dBmW
17:06	Command sequence started
17:09	Ranging modulation ON
17:09:19	Acquired ranging code
17:09:50	Receiver 1 at −96 dBmW; receiver 2 at −125 dBmW
17:12	Command sequence stopped
17:15	Ranging modulation OFF
17:18	Ranging modulation ON
17:18:19	Ranging code acquired
17:20	Ranging modulation OFF. Tracking data monitor data being received from Goldstone
17:24:50	Receiver 1 at −100 dBmW; receiver 2 at −126 dBmW
17:28	Transmitter OFF; selected bad data; changed to TDH format 14; small receiver malfunction
17:28:01	On IAPS for driving antenna
17:28:02	Selected good data; tracking in three-way mode
17:28:10	Auto track on main antenna
17:33	Receivers dropped lock
17:33:12	On IAPS
17:36:06	Receivers in lock
17:36:17	Auto tracking on main antenna
17:37	Receiver 1 at −100 dBmW; receiver 2 at −128 dBmW
17:39:32	Changed TDH format 14
17:41	Receiver 1 at −101 dBmW; receiver 2 at −128 dBmW
17:41:20	Tracking data going to Goldstone advanced to real-time
17:42	TDH on line
17:47	Receiver 1 at −100 dBmW; receiver 2 at −126 dBmW
18:00	Receiver 1 at −101 dBmW; receiver 2 at −127 dBmW
18:04	Receiver 1 at −102 dBmW; receiver 2 at −128 dBmW

Time, GMT	Events/remarks
Day 314, November 10, 1967 (contd)	
18:07	Receiver 1 at −100 dBmW; receiver 2 at −126 dBmW
18:10:40	Receiver 1 at −99 dBmW; receiver 2 at −125 dBmW
18:14:45	Selected bad data; change to TDH format 11
18:15:02	Transmitter on 10 kW
18:15:04	Receivers out of lock
18:15 08	TDH on line
18:15:10	Ranging modulation ON
18:15:15	Receivers in two-way lock
18:15:50	Ranging code acquired
18:18:30	Receiver 1 at −99 dBmW; receiver 2 at −128 dBmW
18:21	Receiver 1 at −99 dBmW; receiver 2 at −127 dBmW
18:26	Receiver 1 at −99 dBmW; receiver 2 at −126 dBmW
18:35	Receiver 1 at −99 dBmW; receiver 2 at −127 dBmW
18:40	Receiver 1 at −99 dBmW; receiver 2 at −126 dBmW
18:44	End of IAPS drive tape
18:45	Receiver 1 at −99 dBmW; receiver 2 at −126 dBmW
18:50	Receiver 1 at −99 dBmW; receiver 2 at −126 dBmW
18:52	Receiver 1 at −99 dBmW; receiver 2 at −126 dBmW
18:52:30	Transmitter OFF
18:53	Changed to TDH format 14
18:56	Receiver 1 at −99 dBmW; receiver 2 at −126 dBmW
18:56:40	Antenna at 0 deg el
18:56:55	Aided track
18:58:14	Antenna at pre-limits (−0.488 deg el)
18:58:58	Receiver 1 out of lock
18:58:10	Receiver 2 out of lock. End of track

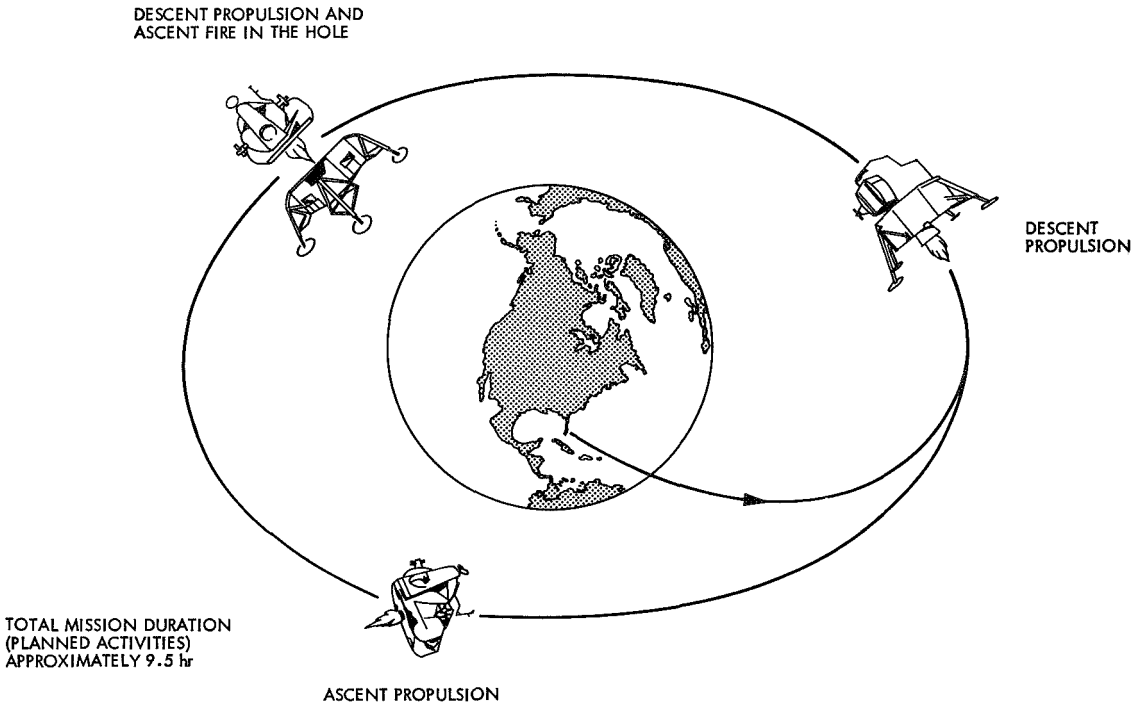

Fig. 103. *Apollo* 5 flight profile

the fifth revolution, the MSFN had been able to process the postburn tracking data from enough stations to permit the generation of a new acquisition message prior to the pass. This time both stations had successful tracks, and the data were handled as during the third revolution. Following the fifth revolution pass over Ascension Island, the LM was commanded to execute the final ascent propulsion system burn to fuel depletion. However, at this time, the LM attitude control system's fuel supply was also depleted, which resulted in spacecraft tumbling. The mission was declared completed shortly thereafter.

A postflight analysis of the Ascension Island site activity during the *Apollo 5* flight showed that both the station and the upgraded procedures performed very well and that the experience gained should prove valuable for the *Apollo 6* flight commitment. With the relaxation of the configuration freeze and control after the *Apollo 5* flight, a thorough investigation of the doppler counter problem was started, because this problem had recurred. The investigation disclosed a wiring error, made during the installation of the doppler resolver kit, had created a logic problem in the counter, causing the 100ths digit to malfunction. Although no further doppler counter difficulties were encountered after correction of the wiring error, this potential problem area was watched carefully during the preparations for *Apollo 6*.

D. The *Apollo* 6 Flight

1. Flight description. The *Apollo 6* flight was the second unmanned test of the *Saturn V* launch vehicle, which for this mission carried an instrumented, developmental spacecraft and an inert lunar module test article. The nominal *Apollo 6* flight profile was to be very similar to that of the highly successful *Apollo 4*. The significant difference between the two mission profiles was that the *Apollo 6* third stage, the S-IVB, was to burn to full lunar injection velocity and target for a theoretical moon. The spacecraft (i.e., the CSM) was to separate shortly after injection and perform a braking maneuver to limit its apogee to approximately 12,000 nmi. The CSM was programmed to burn its propulsion system on the downward leg so as to reenter the earth's atmosphere at a simulated lunar return velocity in a final test of the spacecraft's heat shield. However, two significant anomalies occurred that prevented the accomplishment of all of the mission objectives and affected the support provided by both the MSFN and the DSN. While these anomalies, which are discussed in the paragraphs that follow, were not related, their combined effect was to greatly alter the combined MSFN/DSN post-lunar-injection test plan for this mission.

a. Premature shutdown of the S-II second stage during the launch phase. In itself, this first anomaly had

minimal effect upon the network's ability to acquire the spacecraft in earth orbit, because the S-IVB stage's first burn compensated for the velocity deficiencies created by the second-stage engine failure.[4] The resulting earth orbit was somewhat elliptical (96 by 198 nmi) but within the network's acquisition capabilities.

b. Failure of the S-IVB third stage to restart for the lunar injection burn. The second anomaly had the more significant effect upon the combined MSFN/DSN support plans. As a result of the S-IVB restart failure, an alternate mission plan was put into execution. The CSM was immediately separated from the S-IVB third stage, and the spacecraft's propulsion system was ignited to drive the CSM to near its intended apogee (Fig. 104). In so doing, its fuel was depleted to such an extent that the CSM could not accelerate to lunar return velocity on the downward leg and was forced to land in a secondary recovery area. There it was successfully recovered by the aircraft carrier *USS Okinawa*. In the meantime, the S-IVB remained in its 96 × 196-nmi elliptical earth orbit, invalidating the preflight nominal acquisition information at the stations until new acquisition messages were received.

[4]*Apollo 6 Mission Report*, MSC-PA-R-68-9, pp. 1-1 and 1-2. Manned Spacecraft Center, Houston, Tex., May 1968.

Deep Space Network support for *Apollo 6* differed from that provided for *Apollos 4* and *5* in that the MSFN control rooms at the 85-ft antenna backup stations (the Pioneer, Tidbinbilla, and Robledo sites) were involved for the first time.

The planned S-IVB/instrumentation unit postinjection trajectory of *Apollo 6* provided an excellent opportunity to exercise both the prime MSFN 85-ft antenna stations and the backup 85-ft antenna stations with MSFN control rooms in a simulated *Apollo* lunar-mission-type trajectory. The MSFN requested, and the DSN concurred in the request, that the DSN stations with MSFN control rooms be scheduled to track *Apollo 6* on a "best-effort" basis, consistent with the DSN commitments to other flight projects. Also, it was mutually recognized that the angular-tracking-rate limitation of the DSN 85-ft antennas might preclude continuous coverage on certain preinjection earth-orbital passes; however, it was considered a worthwhile experiment to determine how well the DSN stations with MSFN control rooms could handle such a pass. Consequently, the MSFN developed a special "wing–prime evaluation plan" to:

(1) Evaluate the performance of the 85-ft antenna stations.

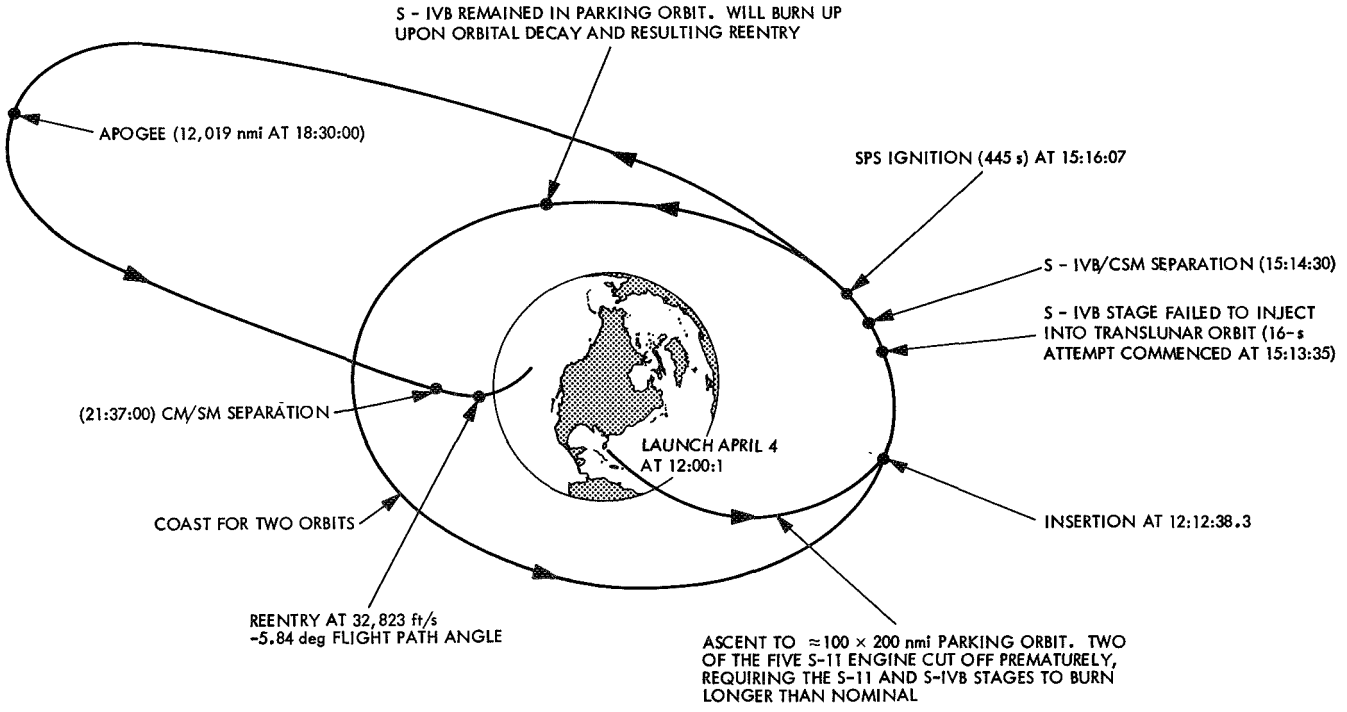

Fig. 104. *Apollo 6* flight profile

(2) Evaluate the current operational procedures at the 85-ft antenna stations.

(3) Provide valuable training for the 85-ft antenna station crews.

The wing–prime evaluation plan, however, produced relatively little data because of the *Apollo 6* mission anomalies.

c. Deep Space Network commitments. The Pioneer, Tidbinbilla, and Robledo sites were committed to provide the 85-ft antenna and common subsystems required to achieve the desired wing (control room) support configuration and capability. This commitment of the antennas and associated common subsystems such as the dual masers, antenna microwave, and dual 20-kW power amplifiers included a commitment for the Deep Space Stations to assure that the DSN systems fully met the required performance specifications. This was accomplished through completion of tests prior to the time the control rooms would be conducting overall site verification tests.

The MSFN was responsible for overall performance of the control rooms and was, therefore, responsible for developing test procedures required to demonstrate that the station was fully operational. However, the DSN was responsible for maintaining the common subsystems and for providing minor operations support even when the stations were in the MSFN configuration. Therefore, the DSN was responsible for producing and maintaining procedures pertinent to the performance of the subsystems.

Switchover from DSN to MSFN was accomplished to obtain the required configuration as defined in the *Apollo 6* network operations directive supplement and the MSFN station configuration message. The MSFN-prepared wing–prime evaluation plan covered the reasons for desiring control room participation, methods for accomplishing objectives, operational control policies, and control room flight support activities such as tracking, handovers, and commands.

Data validation. The DSN was responsible for validating the metric tracking data received by the Ascension Island site. The Goldstone computer facility received metric tracking data from the Ascension Island site and inter-range vectors from GSFC. Real-time comparison and evaluation of data received provided rapid identification of problems and recommendations for corrective action.

Technical direction and monitoring. The net control area at the SFOF in Pasadena, Calif., was required to act as the central and single point of contact between the Cape Kennedy and Ascension Island sites and other DSN agencies for status reporting, monitoring, and technical assistance purposes. To meet these requirements, the DSN established the voice and teletype circuits shown in Fig. 105.

Table 17 provides a summary of testing performed by the Cape Kennedy and Ascension Island sites and the MSFN control rooms at the Pioneer, Tidbinbilla, and Robledo sites.

2. Tracking operations. Tracking activities are discussed in the paragraphs that follow.

a. Cape Kennedy site. As was the case with *Apollos 4* and *5*, Cape Kennedy provided informal assistance to the MSFN MILA station during the countdown and launch of *Apollo 6*. The station was configured in a manner identical to that for the *Apollo 4* mission; i.e., the CSM S-band downlink would be received at Cape Kennedy, and the detected phase-modulated telemetry baseband would be relayed to the MSFN MILA station for processing should multipath or flame attenuation cause reception difficulties at MILA that possibly might not be experienced at Cape Kennedy. Activities started with a countdown demonstration test 96 h before liftoff and proceeded through the terminal count and subsequent launch of *Apollo 6* at 12:00:01 GMT on April 4, 1968. During this period, Cape Kennedy observed the received signal on a spectrum analyzer, took Polaroid pictures, and reported signal strength data to the MSFN MILA station. The received signal at Cape Kennedy was nominal, based on *Apollo 4* countdown experience: −74 dBmW at 40 s after liftoff. A momentary dropout occurred 2 min, 31 s after liftoff, but the signal was immediately recovered at a signal strength of −116 dBmW. Signals in the range of −106 to −124 dBmW were then received until 8 min after liftoff, when signal strength dropped to −140 dBmW. Loss of signal occurred 9 min, 14 s after liftoff on the launch pass.

A log of Cape Kennedy activities, reflecting the major events that occurred until end of track, is shown in Table 18.

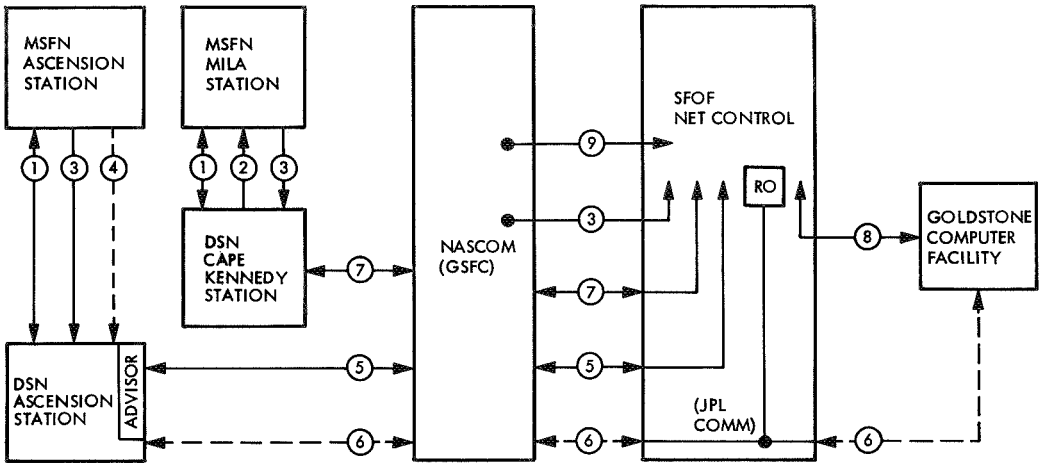

Fig. 105. Communications circuits for DSN support of *Apollo 6*

b. Ascension Island site. Preparations for the *Apollo 6* mission at Ascension Island officially started at 00:00 GMT on February 29, 1968, with the establishment of configuration control of the station in the MSFN configuration. In reality, the station had remained in the MSFN configuration since the *Apollo 4* mission and had participated in a practice exercise with *Apollo 5*. During the time between the *Apollo 5* tracking and the launch of *Apollo 6*, the station participated in all requested MSFN prelaunch tests, network simulations, and *TETR* tracks. A configuration freeze was established on March 12, at which time the DSN station went on "mission status," thereby joining the MSFN Ascension Island station in responding to the *Apollo* Project scheduling requests. From this time through launch, the DSN station reported "status GREEN."

The DSN station was formally committed to the MSFN for *Apollo 6* mission support, since the nominal mission profile required two antennas at Ascension Island after the planned lunar injection: one to cover the CSM and the other to cover the S-IVB stage. The MSFN Ascension Island station was assigned to the former vehicle, whereas the DSN station was assigned to the latter vehicle. Had the S-IVB injection burn been nominal, the DSN station would have experienced a 12-h pass, tracking the S-IVB/instrumentation unit stage starting with the third orbital revolution. (The first and second orbital revolutions were not visible to the DSN station.) Because the S-IVB did not restart for the lunar-injection engine burn at the end of the second orbital revolution, its subsequent passes over Ascension Island were all earth-orbital-type tracks.

The restart anomaly occurred at the beginning of the third orbital revolution, just minutes before the expected CSM and S-IVB acquisition-of-signal times for the two Ascension Island stations. Because the CSM propulsion

Table 17. Formal MSFN tests

Date (1968)	Test	Station
Jan 8, 11	Network simulation	Cape Kennedy and Ascension Island
Jan 12, 17	*TETR-1* tracking	Ascension Island
Mar 12	USB range receiver normalization test	Ascension Island, Pioneer/MSFN control room, Tidbinbilla/MSFN control room, and Robledo/MSFN control room
Mar 13	USB bit error rate test	Ascension Island
Mar 14, 15	Network simulation (long count)	Ascension Island, Pioneer/MSFN control room, Tidbinbilla/MSFN control room, and Robledo/MSFN control room
Mar 20	System tests and integrated system tests	Robledo/MSFN control room
Mar 21	Network simulation (short count)	Ascension Island, Pioneer/MSFN control room, Tidbinbilla/MSFN control room, and Robledo/MSFN control room
Mar 22	System tests and integrated system tests	Tidbinbilla/MSFN control room and Robledo/MSFN control room
Mar 25	Network simulation (short count)	Ascension Island, Pioneer/MSFN control room, Tidbinbilla/MSFN control room, and Robledo/MSFN control room
Mar 28, 29	CDDT and terminal count	
Apr 1	USB ranging delay test	
Apr 3	Terminal count	
Apr 4	Launch	Ascension Island, Pioneer/MSFN control room, Tidbinbilla/MSFN control room, and Robledo/MSFN control room

system was ignited to place the spacecraft in a near-standard, high-apogee elliptical orbit, the MSFN Ascension Island station was able to acquire the CSM at almost the expected time. The DSN station searched for the S-IVB/instrumentation unit at its preflight nominal arrival azimuth bearing until well after its predicted arrival time (Fig. 106). Having failed to detect the S-IVB/instrumentation unit, the DSN station next searched in the vicinity of the CSM, using verbally reported look angles from the MSFN Ascension Island station, again without success. After an estimated 2 min into the pass, the VHF telemetry antenna at the MSFN Ascension Island station acquired the S-IVB/instrumentation unit VHF telemetry signals and relayed the vehicle's position to the DSN station. The late "arrival" of the S-IVB, which was caused by the restart anomaly, had created an almost 180-deg azimuth bearing difference in station look angles between the CSM and S-IVB/instrumentation unit by the time the latter's signals were acquired.

Despite this confused start, the DSN station successfully completed 6 min, 9 s of main beam autotrack on the S-IVB/instrumentation unit in the third orbital revolution. The DSN station first acquired the S-IVB/instrumentation unit at 15:32:30 GMT on its acquisition antenna system and then transferred to the main-beam autotrack mode 6 s later. The signal strength at the acquisition-of-signal time was −85 dBmW, a strong signal. The DSN station was successful in sending several commands and performing several ranging measurements, even though the third orbital revolution was a short earth-orbital pass. The signal strength at the loss-of-signal time was −120 dBmW.

Using verbal acquisition data provided by the MSFN station, the DSN station rapidly acquired the S-IVB/instrumentation unit on the fourth orbital revolution at 17:07:41 GMT, and transferred to the main beam at 17:09:20 GMT. The signal strength at that time was −100 dBmW. The track was successful during the entire pass, which terminated at 17:15:17 GMT with loss of signal. An attempt was made to track the S-IVB/instrumentation unit again on the fifth revolution, but the vehicle's orbit progression caused the track to follow the station's horizon, with the result that the DSN station had only intermittent signal lock.

During the foregoing time period, the DSN station metric tracking data were sent in real-time to the SFOF, where they were inspected and manually checked for accuracy. Metric tracking data were also forwarded to Goldstone Deep Space Communication Complex for processing through the SDA computers which had been set up to perform a real-time evaluation. However, the accurate set of injection conditions required by the SDA program to perform an analysis was not available in time due to the anomalies in the mission. Therefore, the SDA-accumulated raw data were retained for postflight analysis. The manual analysis of the metric tracking data did not disclose any particular problem areas, and the

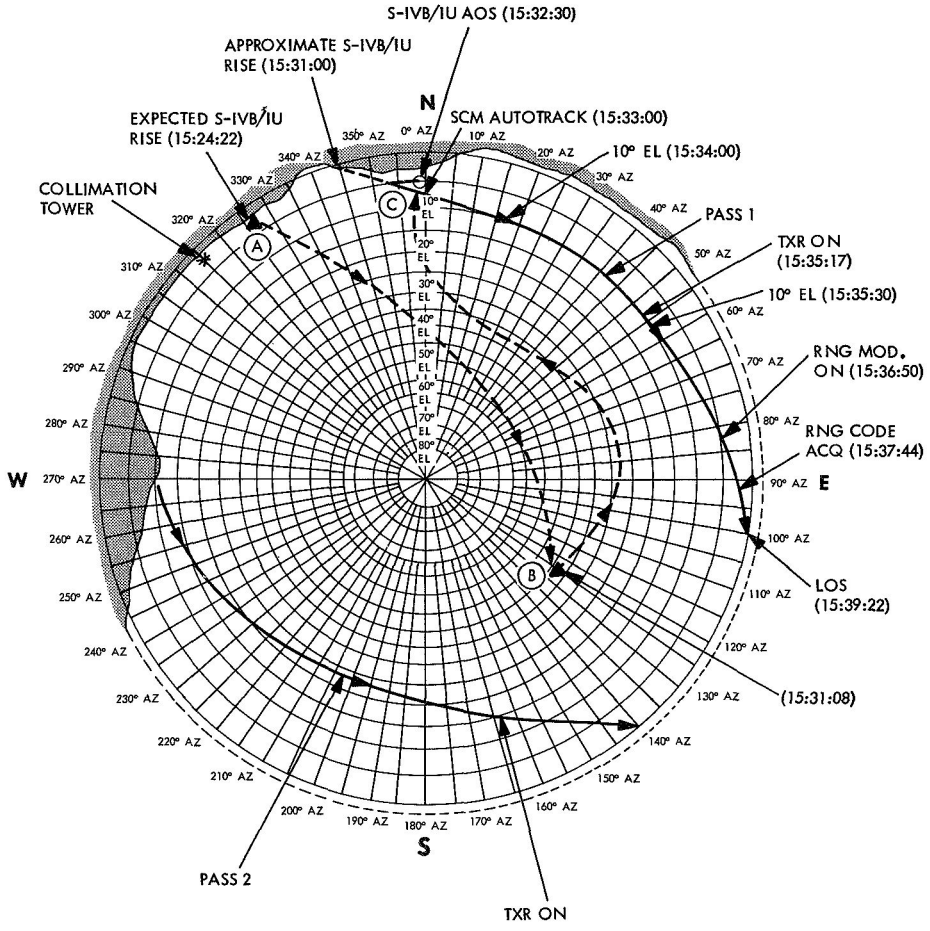

LEGEND:

A to B APPROX. CSM ANGLES ABOUT WHICH SEARCH FOR S-IVB/IU WAS CONDUCTED.

B to C APPROX. MOVEMENT OF ANTENNA IN GOING TO ACQUISITION POINT (AOS).

- - → RCV'S NOT IN LOCK.

——→ RCV'S IN LOCK.

PLOTS OF S-IVB/IU AND PASSES 1 & 2 (REVS 3 & 4)

DEVIL'S ASHPIT
ASCENSION ISLAND
AZ-EL COORDINATES
STEREOGRAPHIC PROJECTION

--- ANTENNA LIMIT (-1°)

Fig. 106. Ascension Island site stereographic projection of S-IVB/instrumentation unit track

Table 18. Cape Kennedy site operations log for *Apollo 6*

Time (Apr 4, 1968), GMT	Events/remarks
03:30	At $T-8$ and holding. Anticipating S-band to come on at $T-8$, at which time will process demodulated S-band video to MILA station
04:03	Downlink is on from the spacecraft. Cape Kennedy receivers 1 and 2 are both in lock. However, since the station has no uplink, the downlink is very erratic, and cannot hold a solid lock. The demodulation from MILA advises they are locked up on Cape Kennedy data; however, they are experiencing a few dropouts
04:04:30	MILA station has brought up their uplink. The downlink is very stable. Processing good data to the MILA station. MILA experiencing dropouts. They have a good solid lock on Cape Kennedy data. Continuing to take polaroid pictures. Received frequency is 2287.5 MHz at a signal level of −78 dBmW
04:29:37	S-band signal has been terminated. This is the end of the readout session. This is the end of this sequence of events
11:00	Station standing by with 15 min from CSM RF carrier on. A check with MILA indicates that the count is still on time. Spectrum analyzer indicates that the *Saturn VI* stage RF is up
11:10:35	Locked up to CSM spacecraft. VCO frequency 23.307340 MHz. Downlink signal strength is −74 dBmW on receiver 2
11:15:30	MILA has locked up two-way with the spacecraft. Receiver 2 VCO is 23.307292 MHz. Locked up in a three-way condition with the spacecraft
11:48	At $T-13$ min and counting. Signal level is −76 dBmW. Countdown is progressing well at this time
11:56:01	At $T-4$ min and counting. Everything looks good. Signal level is −76 dBmW. Countdown is progressing well at this time
11:59:31	At $T-30$ s and counting. Everything looks good
11:59:58	Ignition
12:00	Liftoff
12:00:40	signal level −74 dBmW
12:02:00	Signal −95 dBmW
12:02:10	Have dropped lock momentarily; now are back in with a signal level of −116 dBmW
12:02:31	Spacecraft staging. Second-stage ignition
12:03	Signal level −106 dBmW
12:03:12	Signal level is varying: −113 to −124 dBmW
12:03:30	Signal level is steady at −106 dBmW
12:04	Signal level −106 dBmW
12:08	Signal level −140 dBmW
12:09:14	Dropped lock
12:10:15	CEC recorder and FR-1400 recorder stopped

doppler counter problem appeared to have been corrected.

Concurrently with the DSN station S-IVB activity, the MSFN Ascension Island station tracked the CSM in its high-apogee orbit, thereby fulfilling the Project's requirement for two-antenna coverage from Ascension Island. The high-apogee CSM pass (third orbital revolution) lasted 4 h, 11.5 min, which meant that the MSFN station's loss-of-signal time on the CSM was after the fifth orbital revolution of the S-IVB stage; this was the last revolution visible until the orbit precessed sufficiently to reappear over Ascension Island. Because the latter would occur well after the CSM loss of signal, the Manned Spacecraft Center released the DSN station from further support to *Apollo 6* at 19:00 GMT on April 4.

A log of the Ascension Island DSN station activities, reflecting the major events that occurred until end of track, is shown in Table 19.

c. Pioneer site MSFN control room. Like the Goldstone prime MSFN (85-ft antenna) station, the MSFN control room at Pioneer contains two complete receiving and transmitting systems to simultaneously communicate with the CSM and the S-IVB whenever they are mutually within the beam. The *Apollo* spacecraft are acquired by pointing the antenna at the expected horizon bearing angle, while the transmitter/exciter operator sweeps the uplink frequency in such a manner as to "capture" the spacecraft transponder, which in turn causes the downlink to be similarly swept in frequency. The station's receiver operators tune to a frequency offset from the nominal by the expected doppler shift and await capture by the sweeping downlink. Two-way capture is detected by the resulting sweep of the station receiver, which is nearly synchronous with the exciter sweep. (The offset is proportional to the signal round-trip time.) After two-way capture, the exciter sweep is decayed to the nominal uplink frequency, and the transmitter is locked to the rubidium frequency standard.

Table 19. Ascension Island site operations log for *Apollo 6*

Time (Apr 4, 1968), GMT	Events/remarks
10:25	Voice line activated and station reported "green" for support
10:55	TDH[a] transmission test started
11:00	TDH transmission test completed
12:20	Predicts being generated for S-IVB and CSM from IRV[b]
12:37	Trajectory program completed for S-IVB
13:08	Trajectory program completed for CSM
13:15	TDH data sent from Ascension Island to DSN computer at Goldstone to check communications circuit
15:02	IRV received and WTRAJ started
15:06	IRV cannot be loaded into computer. Getting a new IRV from GSFC
15:10	Generating predicts
15:30	MILA unable to acquire S-IVB and requested permission from Mission Control Center, Houston to try VHF acquisition of S-IVB using SAA.[c] Permission granted
15:32:20	Ascension on auto track on S-IVB
15:32:30	Acquisition of signal on receiver 2 for revolution 3
15:33:13	On SCM[d] auto track
15:33:30	Receiving good data. Signal level −85 dBmW
15:36:03	Transmitter on and in two-way lock, transmitter VCO frequency 21.893772 MHz
15:36:20	Command modulation on, go for commanding
15:36:50	Ranging modulation on. Antenna at 4.6 deg and decreasing rapidly
15:37:44	Range code acquired
15:38:55	Antenna at prelimits. Signal level −120 dBmW
15:39:22	Loss of signal
15:41:25	Transmitter off
17:07:41	Acquisition of signal for revolution 4. Signal level −100 dBmW
17:09:20	On auto track
17:11	Signal level −91 dBmW
17:12:28	Transmitter turned on at VCO frequency of 21.893772 MHz
17:13:28	Signal level −88 dBmW. Range code acquired. Good data. Antenna at 1 deg elevation
17:15:17	Antenna at prelimits and receivers dropped lock
17:16:42	Transmitter off
18:43 to 18:46	Receiver 2 in lock intermittently on revolution 5
19:00	End of track; station released from Apollo support MSC

[a]TDH = tracking data handling.
[b]IRV = inter-range vector.
[c]SAA = S-band acquisition aid.
[d]SCM = S-band cassegrain-monopulse.

Good-quality two-way metric tracking data are then obtained.

Although the premission nominal trajectory predicted that the first orbital revolution pass over the Goldstone prime MSFN station and the Pioneer site would be quite close to the station horizon, it was felt that the second orbital revolution would be sufficiently high to afford a reasonable time to execute part of the wing–prime evaluation plan, yet not so high as to create overly excessive antenna rates. The *Apollo 6* earth-orbital insertion anomaly caused the first orbital revolution pass to be near-perigee, with the result that the track was within the Pioneer antenna's predicted limits for most of the pass. The Pioneer site/MSFN control room passively tracked (three-way with the Goldstone prime MSFN station) during the second orbital revolution, although some metric tracking data were lost around the time *Apollo 6* crossed the station's meridian because of the higher-than-anticipated angular rates. The evaluation activity scheduled for the postinjection S-IVB trajectory was cancelled when the engine did not restart. Pioneer site did, however, passively track the S-IVB, which was still in earth orbit on the third revolution.

With the cancellation of the wing–prime evaluation plan, the Pioneer site/MSFN control room was released from further *Apollo 6* support, and the configuration freeze (established at 00:00 GMT on March 31) was terminated at 18:40 GMT on April 4.

d. Tidbinbilla site/MSFN control room. In contrast to the Pioneer site/MSFN control room, the Tidbinbilla site/MSFN control room was expected to experience a reasonable view of *Apollo 6* on the first orbital revolution, but not on the second. Because of the insertion anomaly that placed the earth-orbital-phase apogee (196 nmi) near Australia, both revolutions were tracked, with neither exceeding the station antenna's angular-rate capability. All scheduled wing–prime evaluation plan "handovers" between the Tidbinbilla site/MSFN control room and the prime Honeysuckle (Canberra) MSFN station were accomplished during the first orbital revolution. Since the stations had not been expected to have good visibility of *Apollo 6* on the second revolution, no handovers were scheduled. The prime MSFN station maintained two-way lock and Tidbinbilla/MSFN control room maintained three-way lock throughout the second-orbital-revolution pass.

The MSFN reported no problems on either pass, and preliminary indications were that the evaluation-plan data would be satisfactory. The injection-burn *Apollo 6* anomaly cancelled further evaluation tests at the Tidbinbilla/MSFN control room, and the station was released from "mission status." The configuration freeze (established at 00:00 GMT on March 31) was terminated at 18:40 GMT on April 4.

e. Robledo site/MSFN control room. If the *Apollo 6* mission had been nominal, the prime Madrid MSFN station and Robledo site/MSFN control room would have had an 8.5-h view period of the injected S-IVB; hence, the wing–prime evaluation plan tests were concentrated heavily at these stations. Because of its northerly latitude, Madrid was not scheduled to see either the first or the second earth-orbital passes. Even so, both stations were staffed and ready during the countdown and launch of *Apollo 6* and remained in a ready condition throughout the mission.

Because the injection burn did not occur, neither station had visibility of either the S-IVB/instrumentation unit or the CSM, even on the high-apogee pass, and with the cancellation of the evaluation plan, the Robledo/MSFN control room was released from "mission status." The configuration freeze (established at 00:00 GMT on March 31) was terminated at 18:40 GMT on April 4.

E. The *Apollo 7* Mission

1. Mission description. The *Apollo 7* spacecraft, the first manned *Apollo* spacecraft, was launched at 15:02:45 GMT on October 11, 1968, from pad 34 at Cape Kennedy. It carried astronauts W. M. Schirra, Jr., D. F. Eisele, and W. Cunningham into a slightly elliptical earth orbit with an initial altitude of 123–153 nmi. The mission, lasting approximately 10 days, 20 h, 9 min, was designed primarily to check out the spacecraft in its entirety and to provide crew training for rendezvous with the S-IVB third-stage vehicle. Included was a complete checkout of the entire communications system, including real-time TV transmission to earth while the spacecraft was over the United States. All mission objectives were met with the successful splashdown of *Apollo 7* at 11:11:48 GMT on October 22.

As was the case with *Apollos 4*, *5*, and *6*, the Cape Kennedy site provided informal assistance to the MSFN MILA station during the countdown and launch. The station was configured in a manner identical to that for the *Apollo 4* mission (i.e., the CSM S-band downlink signal was received at Cape Kennedy, and the detected phase modulation telemetry baseband was relayed to MILA station for processing in the event that multipath or flame attenuation caused reception difficulties that might possibly not be experienced at Cape Kennedy).

The significant difference between the *Apollo 4* and *Apollo 7* launches was that the *Apollo 7* launch was from pad 34, just a few miles almost directly north of the Cape Kennedy site, and the *Apollo 4* launch was from pad 39, several miles distant. The Cape Kennedy site was in a very strategic location for providing cross-support to MILA. The prelaunch and postlaunch tracking by Cape Kennedy was accomplished using the manually steerable 4-ft antenna (Fig. 107).

Although the MSFN wings at the DSN stations were not committed to support the earth-orbital *Apollo* missions, a need existed for operational training of personnel to prepare them for support of the forthcoming lunar missions. With the successful participation in *Apollo 7* support on a "best-effort" basis by the Tidbinbilla and Robledo sites/MSFN control rooms, personnel at each of the three DSN/MSFN control rooms received this required preliminary training. A major structural upgrade, however, of the Pioneer site 85-ft antenna precluded participation of the MSFN control room in *Apollo 7* support.

The *Apollo 7* mission occurred at the time that the Tidbinbilla control room was undergoing a major reconfiguration in preparation for the early November

Fig. 107. Manually operated 4-ft antenna at Cape Kennedy site

Pioneer IX launch and the subsequent *Mariner Mars 1969* spacecraft launch in early 1969. Because the equipment in the MSFN control room was not affected by the reconfiguration work, arrangements were made with the MSFN to provide *Pioneer VIII* tracking cross-support utilizing the antenna with the MSFN control room equipment. The station continued *Pioneer VIII* tracks intermixed with the essential *Apollo* premission test activities up to time of the *Apollo 7* launch.

2. Testing. The countdown demonstration test was started on September 11, 1968 at the $T-96$ h point in the countdown. Support of the countdown by Cape Kennedy also started at $T-96$ h when the CSM S-band signal was turned on. The Cape Kennedy site received the S-band signal, transmitted the telemetry from the S-band receiver to MILA for processing, photographed the RF spectrum, and reported the relative sideband amplitudes to MILA. This support was provided from 08:55 until 10:02 GMT, when the S-band signal was turned off; MILA reported that good telemetry was received during this period.

The terminal portion of the countdown demonstration test started on September 15 with the reactivation of the S-band signal at $T-6$ h, 50 min. The Cape Kennedy site was requested by the Manned Spacecraft Center at Houston to provide an RF spectrum analysis utilizing a technique devised at Cape Kennedy. During the terminal count, Cape Kennedy ran the RF spectrum analysis program and found the following spurious signals on the S-band RF carrier spectrum:

Frequency from carrier, kHz	Relative amplitude from carrier, dB
±30	−12
±51.2	−29
±70.0	−12

The 30- and 70-kHz signals from MILA which were the uplink command and voice subcarriers, were turned around in the spacecraft transponder.

The Tidbinbilla site/MSFN control room participated with the Canberra (Honeysuckle) prime MSFN station in the MSFN station readiness tests conducted October 3 and again October 9 and 10. On October 10, the station completed a *Pioneer VIII* pass and the associate post-tracking calibration at 15:00 GMT. The station was reconfigured and checked out in the MSFN configuration at 22:00 GMT on October 10. The terminal count and launch support preparations were then initiated on October 11 at 04:30 GMT.

3. Tracking operations. Tracking activities are discussed in the paragraphs that follow.

a. Cape Kennedy site. The Cape Kennedy site participation in the launch countdown began at 20:05 GMT on October 6 for the S-band signal test at $T-98$ h. The command service module S-band signal turned off at 00:00 GMT on October 7.

The next participation was at $T-6$ h, 50 min in the count at 02:42 GMT on October 11. The Cape Kennedy site provided the same support as before, and good data were received at MILA. At liftoff, at 15:02:45 GMT, Cape Kennedy had a received signal level of -63 dBmW and had manually tracked the spacecraft until 15:02:21 GMT, except for a momentary drop of lock at 15:04:43 GMT. The spacecraft was manually tracked using prelaunch predicted look angles. Automatic gain control meters from the receiver to the antennas also helped the antenna operator follow the spacecraft after loss of visual sighting.

The data from the countdown and launch were distributed to MILA and the Marshall Space Flight Center in Huntsville, Ala., for evaluation.

b. Tidbinbilla site/MSFN control room. The first acquisition of *Apollo 7* on revolution 1 was at 15:04 GMT. During revolutions 14–16, a leak occurred in the hydraulic system at the Tidbinbilla/MSFN control room that reduced the tracking-rate capability of the station and limited its coverage during these revolutions. The leak was repaired, and normal operations were resumed during the next visibility period on revolution 27.

With the exception of two minor anomalies, the Tidbinbilla/MSFN control room tracked *Apollo 7* on each available orbit (total of 32 passes) until the end of revolution 105 on October 17, at which time the station was relieved of further *Apollo 7* support to prepare for the *Pioneer IX* launch.

c. Robledo site/MSFN control room. The *Apollo 7* mission was the first in which the Robledo/MSFN control room participated. The restart anomaly of the S-IVB third-stage vehicle had prevented its scheduled participation in the *Apollo 6* mission. Preparations for *Apollo 7* support at the MSFN control room started at 23:00 GMT on October 10, and a class A countdown was completed at 08:30 GMT on October 11. Although the station maintained a standby condition for the launch, the *Apollo 7* trajectory was such that the station could not track until revolution 12.

On October 16, during revolution 87, the Robledo/MSFN control room received a handover from the MSFN Canary Island station and went into a two-way track. This was the first *Apollo* two-way track experienced by the Robledo site in the MSFN configuration.

With the exception of an October 14 search for the *Mariner V* spacecraft, the Robledo/MSFN control room participated in the daily *Apollo 7* tracks through October 22 (total of 32 passes) and revolution 161 (the final pass over the station). However, at the request of the MSFN, the station remained on standby status until the actual spacecraft splashdown, to be used if an anomaly had occurred during the retromaneuver over the Hawaiian Islands.

F. The *Apollo 8* Mission

1. Mission description. While *Apollo 8* was the second manned *Apollo* mission, it was the first manned *Apollo* mission flown aboard the three-stage *Saturn V* launch vehicle. It carried astronauts Frank Borman (spacecraft commander), James A. Lovell, Jr. (command module pilot), and lunar module pilot William A. Anders on an historic flight to the vicinity of the moon and 10 lunar orbits before returning to a successful splashdown in the Pacific Ocean 147 h, 11 s later.

Apollo 8 was launched from pad 39-A at Cape Kennedy at 12:51:00.92 GMT on December 21, 1968, on a launch azimuth of 72.12 deg. It was inserted into a 103-nmi circular earth orbit by a complete burn of the S-IC booster stage, followed by a complete burn of the S-II second stage, and a partial burn of the S-IVB third-stage vehicle. During the second revolution, the S-IVB stage was reignited over the Pacific Ocean and *Apollo 8* was injected into a lunar transfer orbit. After injection into lunar transfer orbit, the CSM separated from the S-IVB third stage and performed a practice transposition maneuver with the S-IVB stage that would be required on later missions when the lunar module would be carried aboard the interstage adapter between the S-IVB third stage and the CSM. The lunar module was not carried aboard *Apollo 8*.

Following a separation maneuver and two small midcourse corrections, *Apollo 8* deboosted into an elliptical lunar orbit measuring approximately 60 by 170 nmi. After two such elliptical orbits around the moon, the *Apollo 8* service propulsion system was burned again to place it into a circular lunar orbit of about 60 nmi.

This was followed by eight additional orbits around the moon, then an additional burn of the service propulsion system aboard the CSM for injection into an earth tranfer orbit. The trajectory was so precise that only one midcourse correction was required on the return flight.

Prior to reentering the earth's atmosphere, the command module portion of the CSM separated from the service module portion and assumed a proper attitude for entering the earth's atmosphere in the planned aerodynamic skip profile, which was so precise that the command module splashed down a mere 5000 yards from the carrier *USS Yorktown,* southwest of Hawaii. The separated service module portion entered the atmosphere on a ballistic trajectory and was consumed by heat. Upon arrival of the three astronauts aboard the carrier *Yorktown* on December 28, 1968, the first attempt to reach the vicinity of the moon by manned flight was successfully completed. A listing of the significant events of this journey is shown in Table 20, expressed as ground-elapsed time or time from launch. Figure 108 illustrates the flight profile of *Apollo 8* with significant events expressed in Greenwich Mean Time.

Table 20. *Apollo* 8 sequence of events

Time from liftoff, h:m:s	Event
00:00:00	Liftoff
00:01:17	Maximum dynamic pressure
00:02:06	S-IC center engine cutoff
00:02:31	S-IC outboard engine cutoff
00:02:32	S-IC/S-II separation
00:02:33	S-II ignition
00:02:55	Camera capsule ejection
00:03:07	Launch escape tower jettison
	Mode I/mode II abort changeover
00:08:40	S-II cutoff
00:08:41	S-II/S-IVB separation
00:08:44	S-IVB ignition
00:10:06	Mode IV capability begins
00:10:18	Mode II/mode III abort changeover
00:11:32	Insertion into earth parking orbit
02:50:31	TLI[a] ignition
02:55:43	TLI cutoff
	Translunar coast begins
03:09:14	S-IVB/CSM separation
04:44:54	Begin maneuver to slingshot attitude
05:07:54	Liquid oxygen dump begins
05:12:54	Liquid oxygen dump ends
TLI + 6 h	Midcourse correction 1
TLI + 25 h	Midcourse correction 2
69:07:29	LOI initiation[b]
69:11:35	LOI termination
73:30:53	LOI initiation
73:31:03	LOI termination
89:15:07	TEI initiate[c]
89:18:33	TEI terminate
TEI + 15 h	Midcourse correction
146:49:00	Entry interface
147:00:00	Splashdown

[a]TLI = translunar injection.
[b]LOI = lunar orbit insertion.
[c]TEI = transearth injection.

2. ***Requirements for DSN support of Apollo 8.*** The successful checkout of the *Apollo* CSM during the *Apollo 7* mission created confidence that the *Apollo 8* mission could be upgraded from an earth-orbital mission to a lunar-orbital mission. There was, however, one item aboard the CSM that had not been previously checked out in space—the spacecraft's multiple beamwidth high-gain antenna system. Should this system fail while the *Apollo* spacecraft was near the moon, there would be insufficient signal strength received by the 85-ft-diam antenna MSFN/DSN ground stations to detect the *Apollo* high-bit-rate telemetry signal. Because such a situation was considered undesirable, NASA headquarters decided to guard against this possibility by requesting support from the DSN Goldstone 210-ft-diam antenna at the Mars site during the *Apollo 8* mission (Fig. 109).

When the DSN received the *Apollo* requirement in late October, the Mars site control room equipment was being moved from the antenna pedestal to a new control room. To support *Apollo 8,* it became necessary to accelerate portions of this move as well as to improvise temporary arrangements. In addition, a workable interface between the Mars site and the MSFN *Apollo* prime station at Goldstone had to be developed to deliver the signals received by the Mars site to the MSFN for processing and subsequent remoting to the Mission Control Center at Houston. Since there was insufficient time to install a new microwave link for this purpose, it was necessary to use existing facilities.

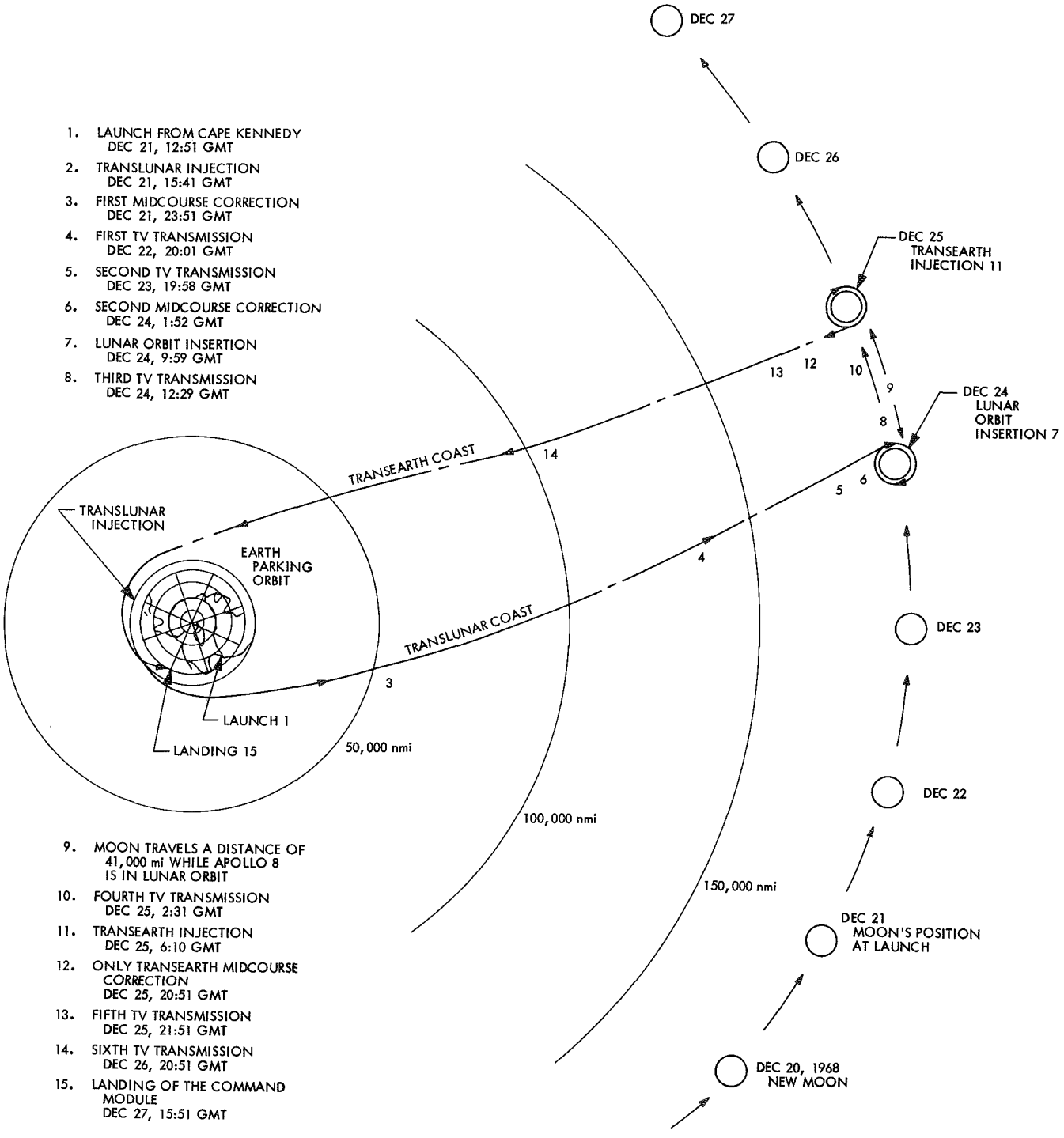

Fig. 108. *Apollo 8* flight profile

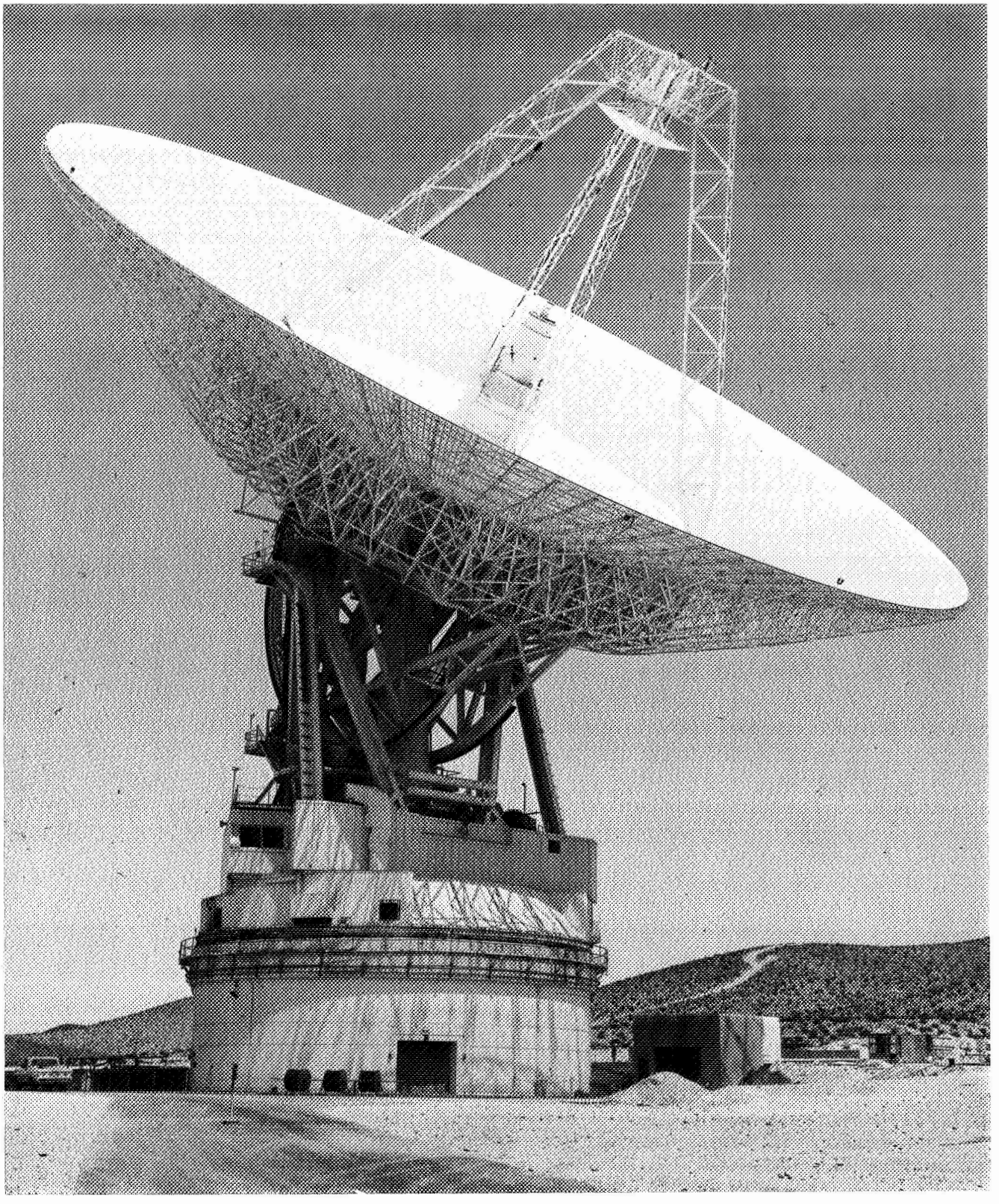

Fig. 109. Mars site 210-ft antenna

Unfortunately, the existing DSN intersite microwave system at Goldstone did not have passband characteristics to enable the raw *Apollo* signals to be simply remoted to the MSFN *Apollo* prime station for demodulation and decommutation. A cooperative effort was then undertaken wherein the MSFN and the DSN pooled their resources and efforts in an attempt to find a prompt solution to the problem. A signal data demodulator subsystem was borrowed from the MSFN *Apollo* prime station and placed in the communications room in the basement of the new control building at the Mars site (Fig. 110). The subsystem provided a suitable interface between the Mars site receivers and the DSIF Goldstone intersite microwave system. This interface, together with the microwave routing employed for *Apollo 8*, is shown in block diagram form in Fig. 111. Table 21 lists the major activities that occurred at the Mars site between the final planning meeting on November 18, 1968 and the station countdown for launch, which began on December 20, 1968.

The *Apollo 8* requirement also imposed two new operational interfaces. First, the Mars site antenna feed system does not have auto-track capability. It was, therefore, necessary to make arrangements to have the MSFN and/or the Manned Spacecraft Center provide timely

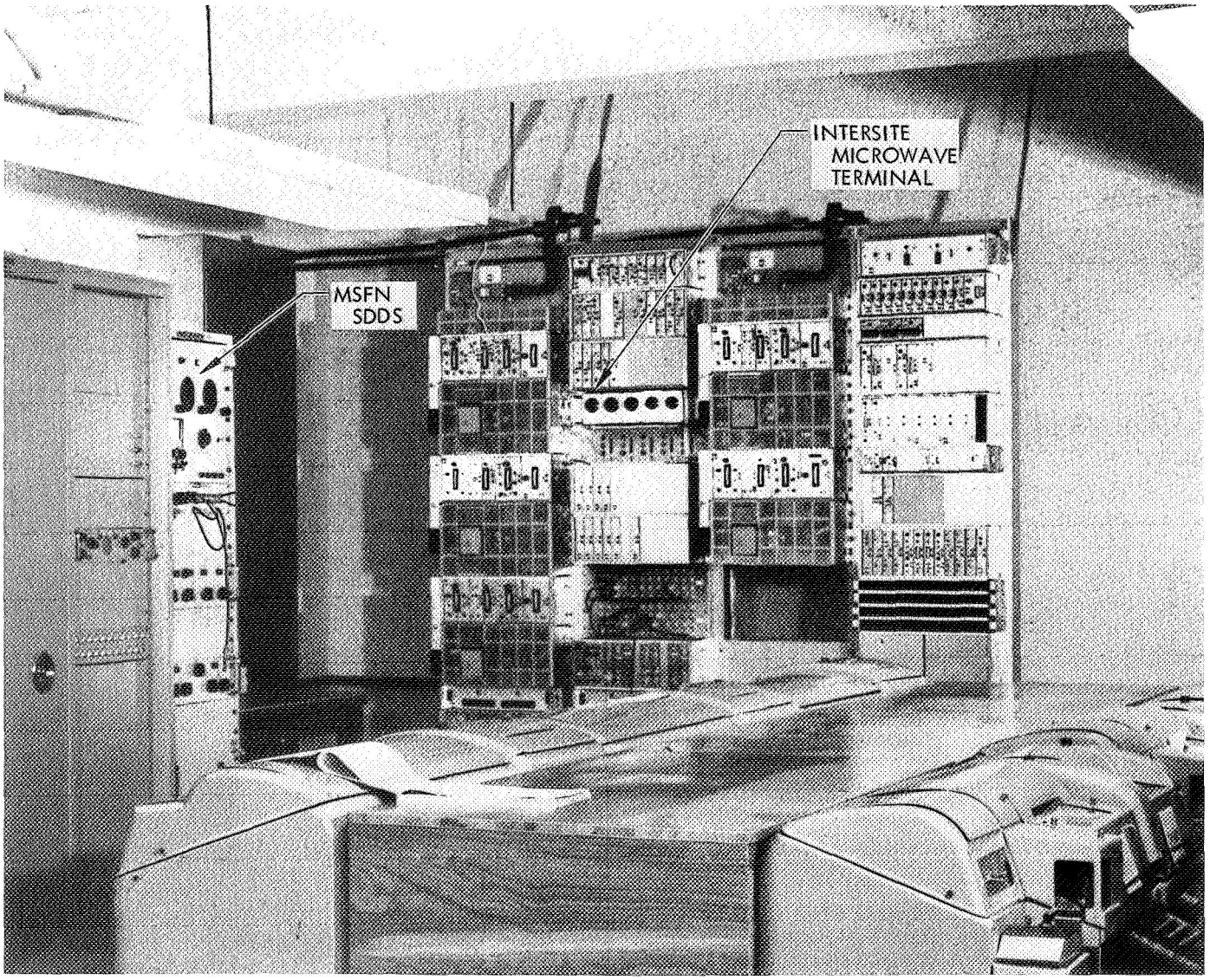

Fig. 110. Manned Space Flight Network signal data demodulator subsystem installed in communications room of Mars station

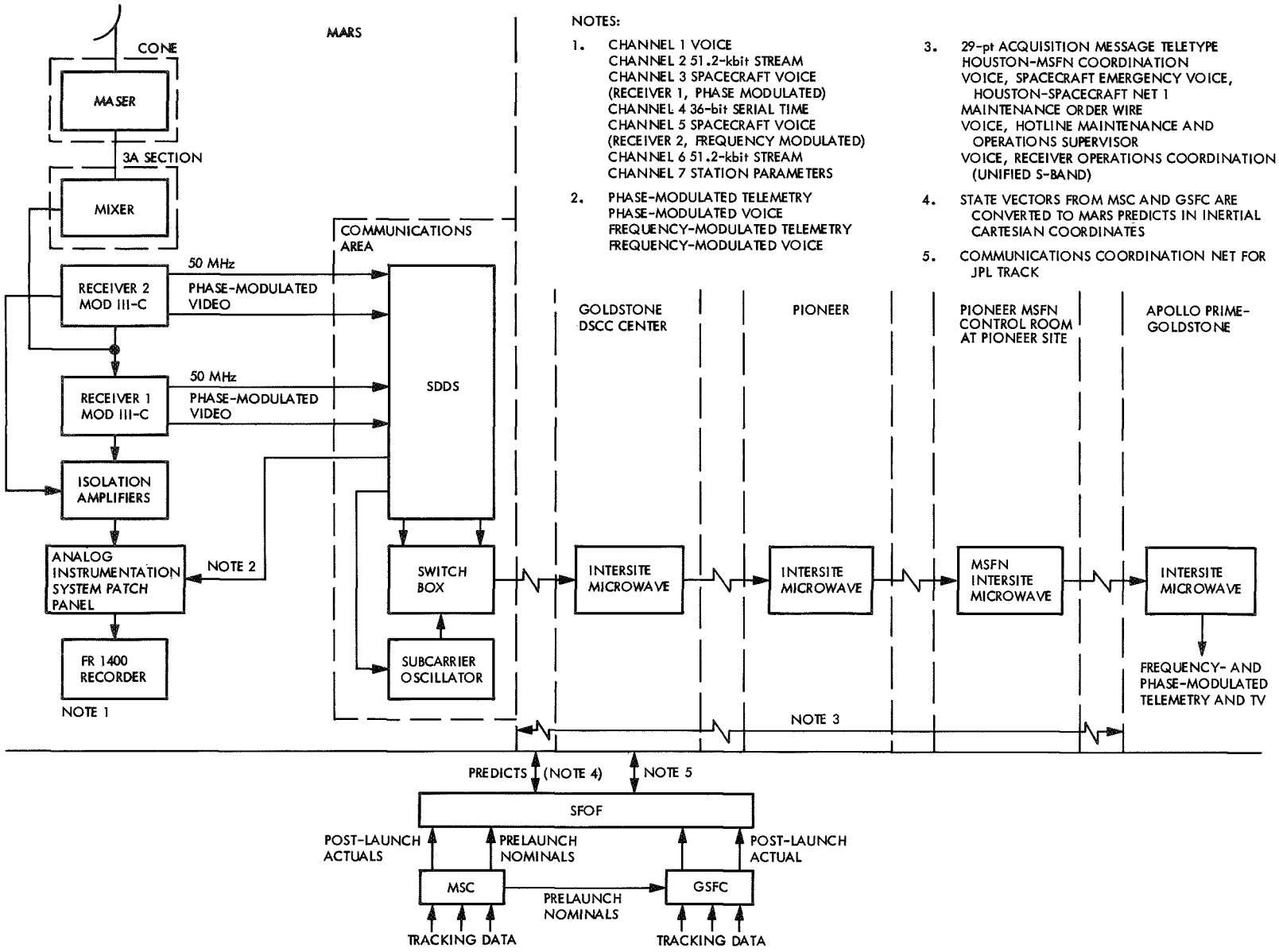

Fig. 111. Special Mars site configuration for *Apollo 8*

Table 21. Mars site major premission activities

Date (1968)	Activity
Nov 18–22	Resolved Mars site specific cabling configuration for *Apollo*
Nov 20	Removed dual frequency pump package from maser 1 assembly and replaced with MSFN 2295/2388 MHz package
	Installed an oscilloscope and sweep circuitry for maser 1 visual tuning instrumentation and checked for proper operation
Nov 27	Installed MSFN VCOs
Nov 29	Conducted maser/receiver interface tests at MSFN parameters
Nov 30	Moved tactical intercommunications bay from the pedestal to the new operations support building communications room and reinstalled it
Dec 2–3	Moved the recorder from the pedestal control room to the operations support building control room and reinstalled it
Dec 2	Conducted system temperature measurements at MSFN frequencies
	Installed teletype lines and machines
Dec 4–6	Installed recorder cabling to the *Apollo* SDDS[a]
Dec 4–8	Alignment and test of teletype and voice communications equipment
	Installed station instrumentation cabling
Dec 4–5	Modified maser 1 by adding dc amplifier to the video circuit
	Warmed up and cleaned CCR[b] 1. Replaced seals in maser 1 refrigerator. Replaced CCR 1 absorber. Cooled down CCR 1
	Installed a new Joule-Thompson flow metering system for CCR 1
	Installed a modified S-band converter in section of the cone to provide a swept output of maser 2 for visual tuning instrumentation
	Installed an oscilloscope in maser 2 instrumentation rack (UWV-2) as a part of the visual tuning instrumentation
	Installed a signal generator (HP-8614A) and counter (HP-5254L) in place of the existing signal generator (816)
Dec 5	Received center of the moon predicts
	Received MSFN control room 1218 computer antenna drive tape output. First attempt to use as a backup antenna pointing data source by converting it to a Mars site drive tape was unsuccessful because the conversion program did not operate properly
Dec 6	Conducted system temperature measurements
	Maser tuning and verification
	Checked out receiver interface cabling
	Three Mars site personnel went to the *Apollo* prime station for training by participating in a TETR-2 track
	Pioneer VI solar occultation support using open loop receiver continued through December 6
	Met with DSN project engineer and Deep Space Station operations planning project engineer to discuss internal operations and predict sources
Dec 9	Connected the block IIIC receiver to the system and tuned for MSFN parameters
	Patched *Apollo* communications lines to station communication circuits
	Set up recorder communication lines for voice annotation, in-house communication and *Apollo* maintenance and operations voice
	Installed tunable discriminator
	Set up recorder in accordance with DSN standard operating procedures
	Started CVT[c]
	Aligned microwave from Pioneer site to MSFN prime station
	Interfaced receiver with the MSFN SDDS, and microwave data loop to prime station was completely closed
Dec 10	Four station personnel went to the prime station for training by tracking the *TETR-2*
	Started training of communications personnel for the *Apollo 8* mission
	Set signal level from MSFN SDDS to the recorder
	Set VCOs
	CVT completed
	FR-1400 recorder inspected by Ampex representative for speed, and signal-to-noise ratio
	Second check on MSFN control room drive tape conversion run and DSS 14 drive tape made
Dec 11	Conducted system temperature measurements at zenith and on the moon in microwave modes 1, 5, and 7
	Interfaced with MSFN prime station
	Checked signal level, at the recorder, from the prime station
	Bit error checks started

[a]SDDS = signal data demodulator set. [b]CCR = closed-cycle refrigerator. [c]CVT = configuration verification test.

Table 21 (contd)

Date (1968)	Activity
Dec 11 (contd)	Set up for *Apollo* FM check with *Apollo* power splitters installed in the receiver
Dec 12	Completed system temperature measurements
	Checked drive tapes, generated on December 10, on ascent propulsion system driving master equatorial. Checkout was good
Dec 13	Conducted training of communication personnel
	Performed FM and TV checks on the receiver
Dec 14	Participated in DSN ORT[d]
Dec 14–15	Tracked *Pioneers VI* and *VII* (two-way)
Dec 16	Completed receiver FM and PM checks
Dec 17	Participated in second DSN ORT. Recorded one tape on each FR 1400, at 30 in./s, of *Apollo* FM and PM 51,200-bit/s telemetry
Dec 17 (contd)	Took data tapes to prime station for playback on the MSFN recording subsystems to ascertain if their decommutator could lock to Mars site recorded data. Test was very successful
	Conducted star track to align master equatorial
Dec 18	Contingency drill for *Apollo 8* countdown
	Tracked *Pioneers VI* and *VII*
Dec 19	Contingency drill for *Apollo 8* countdown
	Tracked *Pioneers VI* and *VII*
Dec 20	Ran ORT for recorders
	Made equipment check and ran precalibrations for the *Apollo 8* mission
	Tracked *Pioneers VI* and *VII*
	System implementation complete and in state of operational readiness for *Apollo 8*

[d]ORT = operational readiness test.

spacecraft state vectors so that the SFOF might generate station predictions and/or drive tapes for each phase of the *Apollo 8* mission that required Mars site support. This support was required whenever the *Apollo 8* spacecraft was at a range of 50,000 mi or more from the earth. New state vectors would be needed after every engine burn by the *Apollo* spacecraft. Both preflight nominal and inflight actual state vectors were received during the *Apollo 8* mission via the interface routing indicated in Fig. 111.

The other operational interface requirement resulted from the fact that Mars site personnel had no previous operational experience in a manned mission and there was insufficient time for them to undergo formal training prior to launch. The Mars site and the *Apollo* prime station exchanged selected personnel who conducted accelerated briefings on the operational use and techniques of their respective networks. Also, arrangements were made to exchange high-level "interpreters" who would be stationed at the other's facility during the mission to explain proceedings and coordinate combined efforts.

3. Deep Space Network operations support for Apollo 8. *Apollo 8* was the first mission wherein all of the supporting DSN Deep Space Stations were fully committed to the mission. In the previous *Apollo* missions, this support was on a best-efforts basis and used for training purposes. When *Apollo 8* became a lunar-orbital mission, support from the Deep Space Stations became a first requirement and a formal commitment was made to support the mission. This support is best described by the phases of the *Apollo* mission.

a. Launch phase. The Cape Kennedy site supported the *Apollo 8* prelaunch and launch activities in a manner identical with the support previously provided for *Apollos 4, 5, 6,* and *7,* and was configured in a manner identical to that for the *Apollo 4* mission (i.e., the CSM S-band downlink was received and the detected phase-modulated telemetry baseband was relayed to the MILA station for processing). This arrangement provided back-up during launch in case the MILA station experienced signal-level difficulties due to either multipath propagation phenomena or flame attenuation phenomenon from liftoff to horizon loss of signal.

The Cape Kennedy site participated in the prelaunch countdown demonstration test and proceeded to provide support through the terminal count and subsequent launch of *Apollo 8* at 12:51:00.92 GMT on December 21, 1968. The received signal strength at Cape Kennedy from launch to horizon loss is shown in Table 22. No anomalies were experienced and the mission support was terminated at loss of signal.

Table 22. Cape Kennedy site launch support for *Apollo 8*

Time (Dec 21, 1968), GMT	Receiver 1 automatic gain control, −dBmW	Time (Dec 21, 1968), GMT	Receiver 1 automatic gain control, −dBmW
12:51:00	68.8	12:56:00	121.0
12:51:30	65.4	12:56:30	122.6
12:52:00	66.9	12:57:00	125.1
12:52:30	69.2	12:57:30	128.7
12:53:00	83.9	12:58:00	135.0
12:53:30	97.5	12:58:30	141.6
12:54:00	111.6	12:58:33	—[a]
12:54:30	118.4	12:58:42	—[b]
12:55:00	121.2	12:59:00	136.0
12:55:30	120.9	12:59:10	—[a]

[a]Receiver 1 out of lock.

[b]Receiver 1 in lock.

b. Earth-orbital phase. The subearth tracks of the first two revolutions of *Apollo 8* were such that the spacecraft was seen briefly by Pioneer and Tidbinbilla, but not by Robledo. Although these stations are not formally committed to support the earth-orbital phase of *Apollo* missions, the stations do participate in the terminal count and attempt to acquire the spacecraft during those earth-orbital passes that are within view of the station.

Experience on previous *Apollo* flights has shown that the angular rates while in earth orbit frequently exceed the rate capability of these antennas. Such was the case during *Apollo 8* revolution 1 over the Tidbinbilla site. In addition, that station simultaneously experienced an overloading of the receiver front end because of a combination of: (1) strong received signal strength from the spacecraft, and (2) a gain saturation created by the installation, just prior to the mission, of a transistor follow-on amplifier behind the maser. The combination of these two effects gave rise to an unstable antenna angular track, which was more severe than had been experienced on previous earth-orbital tracks. This phenomenon was self-correcting in that Tidbinbilla did not have a view period for revolution 2 so that, when the station reacquired the spacecraft after translunar injection, the signal strengths had decreased to a tolerable level and the high-rate dynamic instability had disappeared. Remedial action was, therefore, deferred until after the mission.

The high angular tracking rate problem was not experienced at Pioneer because the spacecraft elevation angles were sufficiently low to avoid the problem. However, the Pioneer site did experience two minor anomalies: (1) During revolution 1, extreme weather conditions caused a nylon chain on the pre- and final-limit control boxes of the antenna servo system to break. No loss of data resulted and the chains were repaired prior to revolution 2. (2) During revolution 2, the low-speed clutch on the hour-angle axis became inoperative and it was necessary to switch to the high-speed mode. However, no degradation in tracking or data acquisition resulted.

c. Translunar phase. The *Apollo 8* mission was designed to have injection into a lunar transfer trajectory occur over Hawaii in the Pacific Ocean. As a result, the stations in the Goldstone Deep Space Communication Complex were the first to acquire *Apollo 8* after translunar injection. The Pioneer site acquired *Apollo 8* at horizon rise of the spacecraft; the Mars site acquired *Apollo 8* some 8 min later using preflight nominal predictions and drive tapes. However, the received signal was so strong as to overload the receiver, with the result that it was 3 to 4 h before the correct angle offsets could be punched into the servo control unit to accurately peak the 0.15-deg beamwidth of the 210-ft-diam antenna onto the spacecraft and obtain a meaningful signal-strength reading. When obtained, the reading was found to agree with the expected 8- to 10-dB improvement over the 85-ft-diam antenna stations.

The earth track of *Apollo 8* carried it eastward over the United States until it reached its synchronous altitude

point approximately over Bermuda where the earth track reversed direction, starting in a westerly direction (with respect to Goldstone) back across the United States to final set over the Pacific. The Goldstone stations, therefore, experienced the same long postinjection track as is normally experienced by the Johannesburg, South Africa, site on unmanned launches with Atlantic injections.

During this time, and on subsequent Goldstone passes, the MSFN *Apollo* prime station had a choice of "the best of three" data sources to process and remote to Mission Control Center at Houston: (1) *Apollo* prime station data, (2) Pioneer/MSFN control room data, or (3) Mars site data. Much of this was automatically selected by computers, so an accurate time history of which data were used is difficult to ascertain. However, as the spacecraft distance from earth increased, the Mars site high-bit-rate telemetry reception data became more and more useful due to what is known as the "rotisserie" or "barbecue" effect: To keep thermal balance throughout the spacecraft, the *Apollo* mission was designed so that the spacecraft rotated slowly about its roll axis to keep illumination from the sun uniform. This made it necessary for the astronauts to select between the four omniantennas as the rotation proceeded. A typical received signal-strength pattern at the Mars site would show the signal strength dropping slowly some 30 to 35 dB and then reinstating itself suddenly as the antennas on the spacecraft were switched. As the spacecraft neared the moon, this drop in signal strength would cause the signal to fall below the 51,200-bit/s high-bit-rate telemetry threshold at the 85-ft-diam antenna stations but not below the threshold at the 210-ft-diam antenna. By selecting the Mars site telemetry data for processing and remoting to Houston, many unnecessary commands to change to low-bit-rate telemetry were avoided while the *Apollo 8* spacecraft was in view of Goldstone.

Fortunately for the TV viewers throughout Europe, the United States, and Japan, the *Apollo 8* multi-beamwidth, high-gain antenna performed successfully during the mission. This permitted TV transmission from the spacecraft to be obtained at the 85-ft-diam antenna stations in Madrid and Goldstone for relay to Houston and subsequent distribution through commercial TV channels. The TV transmission signal strengths were in the vicinity of −95 dBmW, which produced a very acceptable signal into the 85-ft-diam antennas. Because of this, and also because of a very slight degradation of TV picture quality over the Goldstone intersite microwave link, *Apollo 8* TV signals from the Mars site were not used during the mission.

During the translunar midcourse maneuver and coast phases, the MSFN control rooms at the Pioneer, Tidbinbilla, and Robledo sites provided continuous coverage of the *Apollo 8* spacecraft in both the two-way and three-way mode of operation. Scheduled commands and voice were successfully uplinked through these facilities to the *Apollo 8* spacecraft during portions of this period, which ended with the successful arrival of *Apollo 8* in the vicinity of the moon on Christmas Eve while the spacecraft was in view of the Tidbinbilla site.

d. Lunar phase. The beginning of the *Apollo 8* lunar-orbital phase started on December 24 at 09:49:08 GMT with spacecraft occultation behind the moon as viewed from Tidbinbilla. *Apollo 8* exited occultation from behind the moon at 10:23 GMT, at which time Tidbinbilla tracked lunar orbit 1, which ended at 11:47 GMT, with the second lunar occultation. The beginning of the second lunar orbit was viewed simultaneously by the Tidbinbilla and Robledo sites. *Apollo 8* set on the Tidbinbilla horizon at 12:41 GMT. The coverage was continued at Robledo through lunar orbits 2–6, which were tracked without anomaly and reported signal-strength readings in the range of −102 to −126 dBmW. *Apollo 8* lunar orbit coverage continued during the Goldstone visibility and on into the Tidbinbilla visibility for orbits 8, 9, and 10. *Apollo 8* experienced its last lunar occultation on orbit 10 on December 25 at 05:42 GMT. The *Apollo 8* service propulsion system transearth injection burn occurred while the spacecraft was occulted behind the moon during orbit 10.

e. Transearth phase. The transearth phase of *Apollo 8* began on December 25 with acquisition by Tidbinbilla at 06:19:46 GMT and continued at this station until loss of signal because of horizon set at 12:42 GMT that day. However, Robledo had acquired *Apollo 8* at 12:03 GMT in a three-way mode so there was no loss of data during the handover. The Robledo view period extended to 22:54 GMT on December 25; the entire pass was in the three-way mode. The Robledo view period overlapped that of the Goldstone stations supporting *Apollo.*

The Pioneer site view period was from December 25 at 19:41 GMT through December 26 at 06:25 GMT. During this time, the station reported both one-way and three-way tracks without anomalies. The Goldstone tracks

Table 23. Deep Space Network tracking support summary[a]

Station	Day of year (1968)	Orbit/pass/ revolution	Acquisition of signal	Loss of signal	Tracking mode[b]	Remarks
Cape Kennedy	356	Launch	12:51:00	56:59:10	1	8-min, 10-s track
Pioneer	356/357	Revolutions 1, 2; pass 1	14:20	05:10:24	1	Tracking time includes start of orbit 1, orbit 2, and end of first translunar pass
	357/358	Pass 2	18:50:55	05:30:20	1, 3	Translunar pass
	358/359	Pass 3	19:10:58	05:30:20	1, 3	Translunar pass
	359/360	Pass 4	19:25:50	06:24:15	1, 3	Lunar orbit pass
	360/361	Pass 5	19:41:00	06:25:25	1, 3	Transearth pass
	361/362	Pass 6	19:51:04	07:06:37	1, 3	Transearth pass to end of Pioneer support
Tidbinbilla	356	Revolution 1	13:51:30	13:55:09	3	
	357	Pass 1	00:31:08	11:52:04	2	Both commands and voice were first successfully uplinked through the wing station
	358	Pass 2	00:46:50	12:22:03	2, 3	
	359	Pass 3; orbits 1, 2	00:46:40	12:40:50	2, 3	Last transearth pass and first two lunar orbits
	360	Pass 4; orbits 8, 9, 10	01:21:57	12:52:00	2, 3	Lunar orbits 8, 9, 10 and first transearth pass
	361	Pass 5	01:38:30	12:54:27	2, 3	
	362	Pass 6	02:18:18	13:04:40	2, 3	End of Tidbinbilla support
Robledo	356	Pass 1	16:10:10	20:49:06	3	Average signal level −105 dBmW
	357	Pass 2	11:08:01	21:23:00	2, 3	Average signal level −123.8 dBmW
	358	Pass 3	11:30:45	21:36:52	3	Average signal level −105 dBmW
	359	Orbits 2–6	12:30:57	21:48:00	3	Average signal level during lunar orbit −117.2 dBmW
	360	Pass 4	12:00:36	22:23:28	3	Signal level at acquisition −137 dBmW
	361	Pass 5	12:03:21	22:54:50	3	Signal level at acquisition −133 dBmW
	362	Pass 6	12:58:02	14:53:53	2, 3	Average signal level −101.0 dBmW; end of Robledo support
Mars	356/357	Pass 1	15:59:32	04:47:34	3	Average signal level −102 dBmW
	357/358	Pass 2	18:58:16	05:07:18	3	Average signal level −111.5 dBmW
	358/359	Pass 3	19:15:42	05:09:12	3	Average signal level −103.5 dBmW
	359/360	Lunar orbit	19:30:09	05:42:37	3	Average signal level −117 dBmW
	360/361	Pass 4	19:40:00	06:05:00	3	Average signal level −110 dBmW; end of Mars support

[a]All dates and times are GMT.

[b]Number indicates mode: 1 = one-way, 2 = two-way, etc.

overlapped those of Tidbinbilla, which acquired *Apollo 8* in a three-way mode on December 26 at 01:38 GMT. Tidbinbilla alternated between three-way and two-way modes of operation over this pass, which ended at 12:54 GMT with no anomalies being reported. This was followed by an overlapping view period with Robledo, which remained in the three-way mode for the entire pass; the pass ended at 22:54 GMT on December 26.

Overlap with Goldstone began at 19:51 GMT on December 26. The Pioneer site operated in both one-way and three-way modes throughout the entire pass, which ended on December 27 at 07:06 GMT without anomaly. Since the *Apollo* return trajectory was such that Goldstone would not have another view period, Pioneer was relieved of further *Apollo* support at the end of this pass.

The succeeding December 27 tracks by Tidbinbilla and Robledo similarly concluded participation in the *Apollo 8* mission because these tracks were the last for these stations before spacecraft splashdown. The end of track occurred at 13:04 GMT for Tidbinbilla, and at 14:53 GMT for Robledo. No problems were reported by either station on this final track in support of the *Apollo 8* mission. A summary of the DSN tracking support provided is shown in Table 23.

f. Conclusion. The support provided to *Apollo 8* by all participating stations in the MSFN and in the DSN was excellent throughout the mission. Messages congratulating all participating stations on their fine performance during the mission were sent by the Manned Spacecraft Center at Houston and by the Manned Flight Support Directorate at the Goddard Space Flight Center.

Glossary

AGC	automatic gain control
AIS	analog instrumentation subsystem
AM	amplitude modulation
ARPA	Advanced Research Project Agency
BER	bit error rate
CAD	coherent amplitude detector
CCR	closed-cycle refrigerator
CCTL	code clock transfer loop
CDDT	countdown demonstration test
CEC	Consolidated Electrodynamics Corp.
COLL	collimation tower equipment
CSM	command service module
CVT	configuration verification test
dec	declination angle
DIS	digital instrumentation subsystem
DSIF	Deep Space Instrumentation Facility
DSN	Deep Space Network
DSS	Deep Space Station
FM	frequency modulation
FTS	frequency and timing subsystem
GSFC	Goddard Space Flight Center
HA	hour angle
HF	high frequency
IAPS	interim antenna pointing subsystem
IF	intermediate frequency
IRV	inter-range vector
IU	instrumentation unit
JPL	Jet Propulsion Laboratory
LEM	lunar excursion module
LM	lunar module
LOI	lunar orbit insertion
MCC	Mercury Control Center
MGC	manual gain control
MILA	Merritt Island launch area
MSC	Manned Spacecraft Center
MSFN	Manned Space Flight Network
NACA	National Advisory Committee on Aeronautics
NASA	National Aeronautics and Space Administration

Glossary (contd)

NASCOM	NASA Communications Network
ORT	operational readiness test
OTDA	Office of Tracking and Data Acquisition
PCM	pulse code modulation
PM	phase modulation
RER	receiver/exciter/ranging
RF	radio frequency
R&RR	range and range rate receiver/exciter
RU	range unit
RUB	rubidium frequency standard
SAA	S-band acquisition aid
SCM	S-band cassegrain-monopulse
SCO	subcarrier oscillator
SDA	systems data analysis
SDDS	signal data demodulator set
SFOF	Space Flight Operations Facility
SRT	station readiness test
STG	Space Task Group
TAGIU	tracking and ground instrumentation unit
TDH	tracking data handling
TETR	*Test and Training Satellite*
TWM	traveling-wave maser
UHF	ultra-high frequency
USB	unified S-band
UWV	microwave subsystem
VCO	voltage-controlled oscillator
VSWR	voltage standing wave ratio
WWV	National Bureau of Standards time broadcasting station

Bibliography[12]

Anderson, J. D., *Determination of the Masses of the Moon and Venus and the Astronomical Unit from Radio Tracking Data of the Mariner II Spacecraft,* Technical Report 32-816, July 1, 1967.

Berman, A. L., *ABTRAJ-on-Site Tracking Prediction Program for Planetary Spacecraft,* Technical Memorandum 33-391, Aug. 15, 1968.

Berman, A. L., *Tracking System Data Analysis Report: Ranger VII Final Report,* Technical Report 32-719, June 1, 1965.

Cain, D. L., and Hamilton, T. W., *Determination of Tracking Station Locations by Doppler and Range Measurements to an Earth Satellite,* Technical Report 32-534, Feb. 1, 1964.

Hamilton, T. W., et al., *The Ranger IV Flight Path and Its Determination from Tracking Data,* Technical Report 32-345, Sept. 15, 1962.

Labrum, R. G., Wong, S. K., and Reynolds, G. W., *The Surveyor V, VI, and VII Flight Paths and Their Determination from Tracking Data,* Technical Report 32-1302, Dec. 1, 1968.

Lorell, J., and Sjogren, W. L., *Lunar Orbiter Data Analysis,* Technical Report 32-1220, Nov. 15, 1967.

[12]All of the documents listed herein are publications of the Jet Propulsion Laboratory, Pasadena, Calif.

Bibliography (contd)

McNeal, C. E., *Ranger V Tracking Systems Data Analysis Final Report,* Technical Report 32-702, Apr. 15, 1965.

Melbourne, W. G., et al., *Constants and Related Information for Astrodynamical Calculations,* Technical Report 32-1306, July 15, 1968.

Miller, L., *The Atlas Centaur VI Flight Path and Its Determination from Tracking Data,* Technical Report 32-911, Apr. 15, 1966.

Mulholland, J. D., and Sjogren, W. L., *Lunar Orbiter Ranging Data: Initial Results,* Technical Report 32-1087, Jan. 6, 1967.

Muller, P. M., and Sjogren, W. L., *Consistency of Lunar Orbiter Residuals with Trajectory and Local Gravity Effects,* Technical Report 32-1307, Sept. 1, 1968.

Muller, P. M., and Sjogren, W. L., *MASCONS: Lunar Mass Concentrations,* Technical Report 32-1339, Aug. 16, 1968.

Null, G. W., Gordon, H. J., and Tito, D. A., *Mariner IV Flight Path and Its Determination from Tracking Data,* Technical Report 32-1108, Aug. 1, 1967.

O'Neil, W. J., et al., *The Surveyor III and Surveyor IV Flight Paths and Their Determination from Tracking Data,* Technical Report 32-1292, Aug. 15, 1968.

Pease, G. E., et al., *The Mariner V Flight Path and Its Determination from Tracking Data,* Technical Report 32-1363, Feb. 1969.

Renzetti, N. A., *Tracking and Data Acquisition for Ranger Missions 1–5,* Technical Memorandum 33-174, July 1, 1964.

Renzetti, N. A., *Tracking and Data Acquisition for Ranger Missions 6–9,* Technical Memorandum 33-275, Sept. 1966.

Renzetti, N. A., *Tracking and Data Acquisition Report: Mariner Mars 1964 Mission: Volume I. Near-Earth-Trajectory Phase,* Technical Memorandum 33-239, Jan. 1, 1965.

Renzetti, N. A., *Tracking and Data Acquisition Report: Mariner Mars 1964 Mission: Volume II. Cruise to Post-Encounter Phase,* Technical Memorandum 33-239, Oct. 1, 1967.

Renzetti, N. A., *Tracking and Data Acquisition Report: Mariner Mars 1964 Mission: Volume III. Extended Mission,* Technical Memorandum 33-239, Dec. 1, 1968.

Renzetti, N. A., *Tracking and Data Acquisition Support for the Mariner Venus 1962 Mission,* Technical Memorandum 33-212, July 1, 1965.

Renzetti, N. A., *Tracking and Data System Report for Mariner Venus 1967: Volume I. Planning Phase through Midcourse,* Technical Memorandum 33-385, Oct. 1969.

Renzetti, N. A., *Tracking and Data System Report for Mariner Venus 1967: Volume II. Midcourse through End of Mission,* Technical Memorandum 33-385, Oct. 1969.

Bibliography (contd)

Renzetti, N. A., *Tracking and Data System Support for the Pioneer Project: Prelaunch to End of Nominal Mission: Volume I. Pioneer VI; Volume II. Pioneer VII; Volume III. Pioneer VIII,* Technical Memorandum 33-426 (in publication).

Renzetti, N. A., *Tracking and Data System Support for Surveyor: Volume I. Missions I and II; Volume II. Missions III and IV; Volume III. Mission V; Volume IV. Mission VI; Volume V. Mission VII,* Technical Memorandum 33-301, 1969.

Sjogren, W. L., et al., *Physical Constants as Determined from Radio Tracking of the Ranger Lunar Probes,* Technical Report 32-1057, Dec. 30, 1966.

Sjogren, W. L., *Proceedings of the JPL Seminar on Uncertainties in the Lunar Ephemeris,* Technical Report 32-1247, May 1, 1968.

Sjogren, W. L., *The Ranger III Flight Path and Its Determination from Tracking Data,* Technical Report 32-563, Sept. 15, 1965.

Sjogren, W. L., et al., *The Ranger V Flight Path and Its Determination from Tracking Data,* Technical Report 32-562, Dec. 6, 1963.

Sjogren, W. L., et al., *The Ranger VI Flight Path and Its Determination from Tracking Data,* Technical Report 32-605, Dec. 15, 1964.

Vegos, C. J., et al., *The Ranger VIII Flight Path and Its Determination from Tracking Data,* Technical Report 32-766 (in publication).

Vegos, C. J., et al., *The Ranger IX Flight Path and Its Determination from Tracking Data,* Technical Report 32-767, Nov. 1, 1968.

Winn, F. B., *Post Landing Tracking Data Analysis, Surveyor VII Mission Report: Part II. Science Results,* Technical Report 32-1264, Mar. 15, 1968.

Winn, F. B., *Post Lunar Touchdown Tracking Data Analysis, Surveyor Project Report: Part II. Science Results,* Technical Report 32-1265, June 15, 1968.

Winn, F. B., *Selenographic Location of Surveyor VI, Surveyor VI Mission Report: Part II. Science Results,* Technical Report 32-1262, Jan. 10, 1968.

Wollenhaupt, W. R., et al., *Ranger VII Flight Path and Its Determination from Tracking Data,* Technical Report 32-694, Dec. 15, 1964.

NASA — JPL — Coml., L.A., Calif.